MICROBIOTAL IMPACTS ON C. ELEGANS MODELS OF PARKINSON'S

EXPLORING THE IMPACTS OF THE HUMAN MICROBIOTA IN *C. ELEGANS* MODELS OF PARKINSON'S DISEASE

By:

GERMAIN SOPHIE NGANA

A Thesis Submitted to the School of Graduate Studies in Partial Fulfilment of the Requirements for the Degree

Doctor of Philosophy

McMaster University DOCTOR OF PHILOSOPHY (2023)
Hamilton, Ontario (Biochemistry and Biomedical Sciences)

TITLE: Exploring the impacts of the human microbiota in *C. elegans* models of Parkinson's Disease

AUTHOR: Germain Sophie Ngana (McMaster University)

SUPERVISOR: Dr. Lesley MacNeil

NUMBER OF PAGES: xvi, 197

Lay abstract

Thousands of bacteria which inhabit our bodies are collectively referred to as the microbiota and play important roles in human health. Changes in the bacterial makeup of the microbiota have been observed in Parkinson's Disease (PD), the second most common neurodegenerative disorder worldwide. We focused on determining if and what microbiota bacteria protect against PD. We used *Caenorhabditis elegans* worms displaying traits of PD to model the disease and identified bacteria from the human gut microbiota able to improve neuron health. Looking at changes in gene expression in worms fed the bacteria, we identified that aspartic cathepsins were increased. Removal of these genes from *C. elegans* worsened the health of neurons. Having observed an increase in aspartic cathepsins in response to the microbiota and the adverse impact on neuron health when these cathepsins are lost, we have uncovered additional proof supporting the microbiota's potential in promoting nervous system health.

Abstract

The human gastrointestinal tract is home to a community of trillions of microorganisms, predominantly bacteria, collectively known as the gut microbiota. The role of the gut microbiota in human health and disease has become increasingly apparent, with microbiotal dysbiosis being linked to many disorders, including Parkinson's Disease (PD). PD is a common complex neurodegenerative disorder characterized by selective degeneration of dopaminergic neurons in the substantia nigra pars compacta and accumulation of alpha-synuclein enriched protein aggregates within neurons. Obvious genetic causes are detected in only 5-10% of cases, suggesting that environmental factors, like the microbiota, play a major role in its development. However, despite accumulating evidence linking the gut microbiota to PD, minimal work has successfully identified causal mechanisms between bacterial molecules and the neurodegenerative process. In order to identify the relationship between human gut commensals and PD pathophysiology, we applied a single-bacterium approach, using the nematode *Caenorhabditis elegans* as a gnotobiotic model. Animals expressing disease-associated G2019S mutant human leucine-rich repeat kinase (LRRK2) protein in dopaminergic neurons were employed as a model of neurodegeneration to systematically test 57 bacteria representative of the human gut microbiota to identify gut commensals able to modulate PD pathophysiology. We identified a microbiotal isolate, *Actinomyces viscosus*, able to reduce *LRRK2*-mediated neurodegeneration and alpha-synuclein aggregation in a synucleinopathy model. Global gene expression analysis via RNA sequencing revealed increased expression of *C. elegans* aspartic cathepsins in response to neuroprotective *A.*

viscosus. Monitoring autophagic markers confirmed that *A. viscosus* suppresses autophagic dysfunction associated with pathogenic LRRK2 expression. RNAi-mediated and genetic knockdown of identified aspartic cathepsins induced neurodegeneration in the *LRRK2* transgenic model, confirming their implication in neuronal health. Our findings contribute to the current understanding of how the gut microbiota can influence host physiology in the context of PD, elucidating a potential mechanism of microbiota-mediated neuroprotection.

Acknowledgements

I would like to express my sincere gratitude to the following individuals and groups, without whom the completion of this PhD thesis would not have been possible:
First and foremost, I extend my deepest appreciation to my supervisor, Dr. Lesley MacNeil, for her unwavering support, guidance, and patience throughout this journey. Her invaluable mentorship and dedication to my academic and personal growth have been instrumental in shaping this thesis and my overall research experience.

I am also profoundly grateful to my thesis committee members, Dr. Ray Truant and Dr. Jane Foster, for their insightful feedback, constructive criticism, and valuable suggestions. Their expertise and commitment to my research significantly enhanced the quality of this work.

To Dr. James Rutka, Dr. Suneil Kalia, and Dr. Lorraine Kalia for taking a chance on a high school student. Those experiences early on were pivotal in shaping the path I find myself on now, and for that, I am forever grateful.

To Mercedes, Kim, Sommer, and Hiva, my lab mates and dear friends, I don't have the words to explain how grateful I am for you all. Your friendship, encouragement, and shared experiences have made the often-challenging research process not only bearable but genuinely enjoyable. I can say with all my heart my journey through this degree was more fun, more joyful, and more fulfilling because I had the opportunity to be your friend.

To Usman, thank you for the love and the balance you bring to my life. Your unwavering support, patience, and understanding are the gifts you give me daily, and for that, I am grateful. To Odelle, Rebecca, and Anastasia, thank you for making Hamilton feel like home for a girl moving out on her own for the first time. To Beatrix, there is no one else I would want to be "productive" or productive with. And to all my dear friends from the many chapters of my life, I am grateful for the countless ways you've shown me support; your friendship is a deeply cherished gift.

My family deserves a special mention for their unconditional love and support. To my parents, your unwavering belief in my abilities and your sacrifices have been my greatest source of strength. Thank you for always reminding me that *je suis une valeur ajoutée à la vie.* To Yannick, my oldest brother and my third parent, I am profoundly grateful for your specific brand of encouragement and support throughout this process and in life. To William, my brother and my friend, your belief in my abilities and your camaraderie are some of my most cherished constants. To Henry-Charles, one of the best things to have happened to me, being your older sister, has been one of the greatest joys of my life and a much-needed respite throughout my academic journey.

To my ancestors and those who came before me, your enduring legacy and resilience paved the way for my pursuit of knowledge. Your wisdom, values, and strength, passed down through generations, continue to guide and inspire me.

This thesis is the result of collective efforts and the support of numerous individuals, and I am genuinely thankful for each of you. Your contributions, whether big or small, have left an indelible mark on my academic journey and personal growth.

TABLE OF CONTENTS

LIST OF FIGURES

CHAPTER ONE – Introduction

CHAPTER TWO – Assessing the impact of anaerobic gut microbiotal bacteria on dopaminergic neurodegeneration in a *C. elegans* model of Parkinson's Disease

CHAPTER THREE – Elucidating Mechanisms of *Actinomyces* Mediated Neuroprotection in *C. elegans* Models of Parkinson's Disease

LIST OF TABLES

CHAPTER ONE – Introduction

CHAPTER TWO – Assessing the impact of anaerobic gut microbiotal bacteria on dopaminergic neurodegeneration in a C. elegans model of Parkinson's Disease

CHAPTER THREE – Elucidating Mechanisms of *Actinomyces* Mediated Neuroprotection in *C. elegans* Models of Parkinson's Disease

LIST OF ABBREVIATIONS

6-OHDA	6-hydroxydopamine
ADP	Adenosine diphosphate
AMP	Adenosine monophosphate
AMPK	Adenosine monophosphate-activated protein kinase
ATG10	Autophagy-related 10
ATG12	Autophagy-related 12
ATG16L	Autophagy-related 16L
ATG3	Autophagy-related 3
ATG5	Autophagy-related 5
ATG7	Autophagy-related 7
ATG9A	Autophagy-related 9
ATP	Adenosine triphosphate
ATP13A2	ATPase Cation Transporting 13A1
BHI	Brain Heart Infusion Broth
CCL5	C-C Motif Chemokine Ligand 5
CEP	Cephalic
CGC	Caenorhabditis Genetics Centre
CHCHD2	Coiled-coil-helix-coiled-coil-helix domain containing 2
CI-MPR	Cation-independent mannose-6-phosphate receptor
CLIP-Seq	Cross-linking and immunoprecipitation sequencing
CMA	Chaperone-mediated autophagy

CNS	Central nervous system
CRP	C-reactive protein
DJ-1	Protein deglycase
DNAJC6	Putative tyrosine-protein phosphatase auxilin
DR	Dietary restriction
EIF4G1	Eukaryotic translation initiation factor 4 gamma 1
ER	Endoplasmic reticulum
FBS	Fetal Bovine Serum
FBX07	F-box protein 7
FOXO	Forkhead box transcription factor class O
FUDR	5-Fluoro-2′-deoxyuridine
GABARAP	GABA type A receptor-associated protein
GBA	Glucocerebrosidase enzyme
GFP	Green fluorescent protein
GIGYF2	GRB10 interacting GYF protein 2
GST	Glutathione S-Transferase
HIP	Heat shock protein 70 interacting protein
HOP	Heat shock protein 70/ Heat shock protein 90 organizing protein
HSC70	Heat shock cognate protein 70
HSP70	Heat shock protein 70
HSP90	Heat shock protein 90
HTRA2	HtrA serine peptidase 2

IL-10	Interleukin 10
IL-1β	Interleukin 1β
IL-2	Interleukin 2
IL-6	Interleukin 6
LAMP2A	Lysosome-associated membrane protein type 2A
LB	Luria-Bertani
LC3	Microtubule-associated protein 1A/1B-light chain 3
LC3B	Microtubule-associated protein 1A/1B-light chain 3
LPS	Lipopolysaccharide
LRRK2	Leucine-rich repeat kinase 2
MAPK	Mitogen-activated protein kinase
miRNA	MicroRNA
MPTP	1-methyl-4-phenyl- 1,2,3,6-tetrahydropyridine
mRNA	Messenger RNA
mTORC1	Target of rapamycin complex 1
NCBI	National Center for Biotechnology Information
NEB	New England Biolabs
NGM	Nematode Growth Media
ORF	Open reading frame
PCR	Polymerase chain reaction
PD	Parkinson's Disease
PI3KC3	Class III phosphatidylinositol 3-kinase

PI3P	Phosphatidylinositol-3-phosphate
PINK1	PTEN-induced kinase 1
PLA2G6	Phospholipase A2 Group VI
PRKN	Parkin
PSAP	Prosaposin
RAPTOR	Regulatory association protein of TOR
RICTOR	Rapamycin-insensitive companion of TOR
RME8	Receptor-mediated endocytosis 8
RNAi	RNA interference
RocCOR	Ras of complex proteins/C-terminal of Roc
SCF	Skp-1-Cul1-F-box protein
SD	Standard D
SNARE	Soluble N-ethylmaleimide-sensitive-factor attachment receptor
SNCA	Alpha-synuclein
SQSTM1	Sequestosome 1
SWI/SNF	SWItch/Sucrose Non-Fermentable
SYNJ1	Synpatojanin-1
TAAR	Trace amin-associated receptor
TNF-α	Tumor necrosis factor α
TOR	Target of rapamycin
TORC2	Target of rapamycin complex 2
UCHL1	Ubiquitin C-terminal hydrolase

UGT	UDP-Glucuronosyl Transferases
ULK1	Unc-51-like kinase 1
UV	Ultraviolet
VPS13C	Vacuolar protein sorting-associated protein 13C
VPS26	Vacuolar protein sorting 26
VPS29	Vacuolar protein sorting 29
VPS35	Vacuolar protein sorting 35
WT	Wild type
YFP	Yellow fluorescent protein

CHAPTER ONE - Introduction

Parkinson's Disease

Parkinson's disease (PD) is a complex progressive neurodegenerative disease affecting millions of elderly individuals globally. PD is the second most common neurodegenerative disorder after Alzheimer's Disease, with a prevalence of approximately 0.3% globally, increasing to greater than 3% among persons 80 years of age and older (Pringsheim et al. 2014). Clinically, PD is marked by the presence of motor deficits, including tremor, rigidity, bradykinesia and postural instability. The primary neuropathological hallmark of PD, underlying these characteristic motor phenotypes, is the selective degeneration of dopaminergic neurons, primarily in the substantia nigra pars compacta (Dickson et al. 2009). Loss of these neurons results in the depletion of striatal dopamine and the impairment of the nigrostriatal system that is otherwise required for the execution of coordinated voluntary movement. Additionally, PD is characterized by the accumulation of abnormal alpha-synuclein enriched cytoplasmic deposits within neuronal cell bodies and neurites known as Lewy bodies and Lewy neurites, respectively (Spillantini et al. 1998).

PD is a largely idiopathic disorder; however, a small fraction of cases (~10%), known as familial PD, can be linked to a causative genetic mutation (Migliore and Coppedè 2009). Genetic research over the past two decades has greatly advanced the current understanding of familial PD. Following the discovery of alpha-synuclein's presence in Lewy pathology, the A53T missense mutation in alpha-synuclein, encoded by the *SNCA* gene, was the first disease-causing genetic mutation identified in PD

(Polymeropoulos et al. 1997). Later studies identified other genes linked to both autosomal dominant and recessive modes of inheritance (Lesage and Brice 2009). To date, over 20 genes or genetic loci have been linked to PD development with varying degrees of replication and functional validation (Blauwendraat, Nalls, and Singleton 2020; Funayama et al. 2023). Despite the infrequency of causative genetic mutations among the PD patient population, the functions of these gene products provide insight into the underlying disease pathogenesis.

The role of autophagy in Parkinson's Disease

Protein homeostasis, or proteostasis, is the mechanism by which cells regulate the proteome by controlling protein expression, folding, localization, and elimination (Gregersen et al. 2006). A major component of eukaryotic proteostasis required for the promotion of cellular function and viability is the degradation of aberrant proteins by the evolutionarily conserved autophagy lysosomal pathway (Nixon, Yang, and Lee 2008; Perera and Zoncu 2016). The autophagy lysosomal pathway consists of multiple distinct autophagic pathways that culminate in the degradation of cellular components via the lysosome. The three primary autophagic pathways are macroautophagy, microautophagy, and chaperone-mediated autophagy (CMA) (Mizushima et al. 2008). The majority of autophagy-related research has focused on macroautophagy and CMA; however, microautophagy can be briefly described as the selective or nonselective direct sequestration of autophagic cargo by the lysosome for degradation (Marzella, Ahlberg, and Glaumann 1981).

The process of macroautophagy is comprised of four main steps: phagophore initiation and nucleation, phagophore expansion and closure (forming the autophagosome), autophagosome, and lysosome fusion and degradation of the autophagic cargo (Yang and Klionsky 2009). Initiation of the autophagic process in mammals begins with activation of the Unc-51-like kinase 1 (ULK1) complex (Jung et al. 2009; P.-M. Wong et al. 2013). ULK1 complex activation is dependent on various upstream signals, including nutrient and energy availability. A major regulator of ULK1 activity, a component of the ULK1 complex, is the mammalian target of rapamycin complex 1 (TORC1). TORC1 functions in response to growth factor signalling and nutrient abundance (e.g. amino acids and glucose). Under nutrient-rich conditions, TORC1 binds to ULK1, in turn phosphorylating the protein and inhibiting its kinase activity. However, upon starvation, TORC1 dissociates from ULK1, allowing for ULK1 complex assembly and activation (Hosokawa et al. 2009; J. Kim et al. 2011; Ganley et al. 2009). An alternative regulator of ULK1 activity is adenosine monophosphate-activated protein kinase (AMPK). AMPK is activated by a decline in cellular energy status when the ADP/ATP or AMP/ATP ratios increase (Ke et al. 2018). AMPK activity can directly and indirectly facilitate ULK1 complex activation by phosphorylating ULK1 at sites promoting ULK1 complex assembly and inhibiting TORC1 activity, respectively (J. Kim et al. 2011; Rabinowitz and White 2010). Activation of the ULK1 complex, in turn, phosphorylates and activates the class III phosphatidylinositol 3-kinase (PI3KC3) complex. Activation of the PI3KC3 complex phosphorylates phosphatidylinositol to synthesize phosphatidylinositol-3-phosphate (PI3P) enriched structures at the

endoplasmic reticulum, known as omegasomes, defining the site for phagophore assembly (Nascimbeni, Codogno, and Morel 2017; Tooze 2013). PI3P facilitates the nucleation process, mobilizing effector proteins to the phagophore assembly site to allow for phagophore expansion (Obara et al. 2008). Expansion of the phagophore is facilitated by two ubiquitin-like systems. Autophagy-related (ATG) 12, a ubiquitin-like protein, is conjugated with ATG5 through the activity of ATG7 and ATG10. ATG12 and ATG5 then form a complex with ATG16L, creating the E3-like ATG12-ATG5-ATG16L1 complex (Ohsumi 2001; Mizushima et al. 2003). ATG4 processes and the ATG12-ATG5-ATG16L1 complex, together with ATG7 and ATG3, facilitate the conjugation of the ubiquitin-like LC3 (microtubule-associated protein 1A/1B-light chain 3) and GABARAP (GABA type A receptor-associated protein) family proteins with membrane-resident phosphatidylethanolamine, in a process called lipidation. The LC3/GABARAP protein family consists of seven proteins of high sequence similarity, with LC3B being the most well-studied (Geng and Klionsky 2008; Weidberg et al. 2010; Sugawara et al. 2004; Yin et al. 2020). During the process of expansion, transmembrane protein ATG9A acts as a lipid carrier, enabling growth of the phagophore (Maeda et al. 2020). During phagophore expansion, autophagic substrates may be sequestered randomly or selectively. The selective autophagic degradation of ubiquitinated cargo can be facilitated by autophagy receptor sequestosome 1 (SQSTM1/p62). SQSTM1 contains a ubiquitin-associated domain which interacts with ubiquitinated cargo and an LC3 interacting region to target said cargo to the autophagic membrane (Pankiv et al. 2007; Ichimura et al. 2013; Isogai et al. 2011). The elongating phagophore eventually closes to form a sealed autophagosome.

Fusion of the autophagosome requires the activity of various proteins, including Rab GTPases, tethering factors, and soluble N-ethylmaleimide-sensitive-factor attachment receptor (SNARE) proteins (Kriegenburg, Ungermann, and Reggiori 2018).

CMA, an exclusively selective pathway, involves the identification of protein targets via chaperones and their subsequent delivery to and translocation across lysosomal membranes for degradation (Chiang et al. 1989; Dice 1988). CMA is activated in response to stressors that can cause protein damage, including hypoxic stress (Dohi et al. 2012), and mild oxidative stress and in response to starvation (Mizushima et al. 2004). Recognition of CMA protein targets is facilitated by the chaperone protein heat shock cognate protein 70 (HSC70). HSC70 is able to recognize and bind proteins containing the highly conserved KFERQ-like motif. This recognition sequence is flanked on one side by a glutamine (Q) residue and must contain one or two positive residues (K or R), one or two hydrophobic residues (F, L, I, or V), and one negatively charged residue (E or D) (Dice 1990). Additionally, the recognition sequence can be generated via phosphorylation of an S, T or Y amino acid in an otherwise complete motif missing the negatively charged residue (Kaushik and Cuervo 2016; C. Park, Suh, and Cuervo 2015; Quintavalle et al. 2014). Once recognized by the CMA chaperone protein, the autophagic substrate is then transported to the lysosomal membrane, where HSC70 interacts with the lysosome-associated membrane protein type 2A (LAMP2A). Co-chaperone proteins heat shock protein (HSP) 90, HSP70, HSP70/HSP90 organizing protein (HOP), and HSP70 interacting protein (HIP) are proposed to facilitate requisite substrate unfolding prior to lysosomal translocation (Agarraberes and Dice 2001; Salvador et al. 2000). LAMP2A

oligomerization allows unfolded proteins to be translocated into the lysosome for degradation (Bandyopadhyay et al. 2008).

The degradative capacity of the lysosome is dependent on the activity of two main protein classes: lysosomal membrane proteins and lysosomal hydrolases (Saftig and Klumperman 2009; Schröder et al. 2010). Lysosomal membrane proteins operate at the interface of the lysosome and cytosol to fulfill essential roles for lysosomal function, including the acidification of the lysosomal lumen, the fusion with other cellular compartments (e.g., autophagosomes) and the translocation of degradation products (Eskelinen, Tanaka, and Saftig 2003). Within the lysosomal lumen, individual lysosomal hydrolases facilitate the degradation of specific substrates, with the most abundant family of hydrolases being the cathepsin proteases (Saftig and Klumperman 2009; Schröder et al. 2010).

Malfunction of the autophagy lysosomal pathway, an important clearance mechanism for alpha-synuclein, is an early disease feature thought to contribute to the pathogenesis of PD (Kulkarni et al. 2023; T. Moors et al. 2016). Both dysfunctional lysosomes and the accumulation of autophagosomes have been observed in the post-mortem brain samples of PD patients (Anglade et al. 1997; J.-H. Zhu et al. 2003). Additionally, ultrastructural examination of the autophagosomes in PD brains revealed accumulation of mitochondria suggesting abnormal mitochondrial degradation (i.e., mitophagy) (J.-H. Zhu et al. 2003). LC3, required for autophagosome formation, colocalizes with alpha-synuclein positive Lewy bodies and neurites. Specifically, the lipidated form of LC3, required for macroautophagy, is markedly elevated in the nigral

samples of PD patients (Alvarez-Erviti et al. 2010; Dehay et al. 2010; Tanji et al. 2011). Lysosomal dysfunction has also been identified in nigral samples from PD patients with lysosomal hydrolases, including cathepsin D, having reduced levels and activity (T. E. Moors et al. 2019). Finally, HSC70 and its receptor LAMP2A were significantly decreased in the substantia nigra of PD patients compared to control individuals (Alvarez-Erviti et al. 2010; Murphy et al. 2015).

In addition to the pathological evidence suggesting a role of autophagy in the pathogenesis of PD, the existing understanding of PD genetics has also established this link. Mutations in leucine-rich repeat kinase 2 (*LRRK2*) are the most common genetic risk factor in both familial and sporadic PD, accounting for 4% of familial and 1% of sporadic PD cases across all populations (Healy et al. 2008). LRRK2 is a large multidomain protein with a catalytic core conferring GTPase and kinase activity via a RocCOR domain and a serine/threonine kinase domain, respectively. Seven PD-associated pathogenic missense mutations (N1437H, R1441G/C/H, Y1699C, G2019S, I2020T), localized to the two enzymatic domains, have been identified to date, with the G2019S mutation being the most common (Bardien et al. 2011; Alessi and Sammler 2018; Taymans et al. 2023). Physiologically, the LRRK2 protein has been implicated in the regulation of lysosomal function via its ability to phosphorylate several Rab GTPases. *In vitro* chloroquine-induced lysosomal overload recruits endogenous LRRK2 to lysosomes, which results in the stabilization of its substrates Rab8a and Rab10 via phosphorylation, allowing these Rab GTPases to further recruit effectors involved in regulating lysosomal homeostasis (Eguchi et al. 2018). Pathogenic *LRRK2* mutations reportedly increase kinase activity,

showing enhanced LRRK2-mediated Rab10 phosphorylation *in vitro* when compared to wildtype *LRRK2* (Kalogeropulou et al. 2022). However, a precise understanding of how these variants perturb the protein's ability to modulate the lysosomal pathway is not well understood beyond the identification of specific physiological phenotypes (Taymans et al. 2023). Notably, overexpression of pathological G2019S LRRK2 protein results in dendritic shortening and neuronal autophagosome accumulation (Plowey et al. 2008). G2019S knock-in mice also demonstrate decreased lysosomal acidification (MacLeod et al. 2013). Additionally, expression of pathological *LRRK2* mutants in mice and human iPSC-derived dopaminergic neurons inhibits assembly of the lysosomal translocation complex, impairing CMA, and in *C. elegans* results in accumulation of autophagosomes and reduced autophagic flux (Ho et al. 2020; Orenstein et al. 2013; Saha et al. 2015).

Homozygous or compound heterozygous loss of function mutations in PTEN-induced kinase 1 (*PINK1*) and Parkin (*PRKN)* have been identified as autosomal recessive forms of PD, linking the development of PD to dysfunction of the autophagy lysosomal pathway (Kitada et al. 1998; Valente et al. 2004). Physiologically, Parkin, and PINK1 function to jointly regulate mitophagy. Specifically, mitochondrial depolarization results in the accumulation of PINK1 on the outer mitochondrial membrane, where it phosphorylates ubiquitin and recruits Parkin (Narendra et al. 2008; Youle and Narendra 2011). In turn, the activated Parkin ubiquitinates outer membrane proteins, which are subsequently phosphorylated by PINK1, tagging the mitochondria for recognition by autophagic receptors (Kazlauskaite et al. 2014; Koyano et al. 2014; Ordureau et al. 2014; Y. C. Wong and Holzbaur 2015). Research in i*n vitro* and *in vivo* contexts has shown that

mutations in *PRKN* and/or *PINK1* facilitate mitochondrial aggregation, reduce mitochondrial turnover and, specifically in mammalian cells and *Drosophila,* are sufficient in inducing PD-like phenotypes (Clark et al. 2006; J. Park et al. 2006; Puschmann et al. 2017; Seibler et al. 2011; Song et al. 2013).

Mutations in vacuolar protein sorting 35 (*VPS35*) are associated with the development of autosomal dominant PD, once again linking autophagy and lysosomal function to the pathogenesis of PD (Zimprich et al. 2011). VPS35 is a component of the retromer complex, which is responsible for the retrograde transport of several cargo proteins from the endosomal network to either the *trans*-Golgi network or the plasma membrane. VPS35, along with VPS26 and VPS29, sits at the endosomal membrane and recognizes cargo (transmembrane proteins), including the cation-independent mannose-6-phosphate receptor (CI-MPR), which is responsible for delivering lysosomal hydrolases to the endosome for eventual delivery to the lysosome, LAMP2A, and ATG9A (Arighi et al. 2004; Williams et al. 2022; Tang et al. 2015). Additionally, VPS35 is hypothesized to function upstream of LRRK2, playing a role in regulating LRRK2 kinase activity (Mir et al. 2018). A single missense mutation in VPS35, D620N, has confirmed pathogenicity segregating with late-onset disease (Vilariño-Güell et al. 2011; Zimprich et al. 2011; Sharma et al. 2012); however, other variants (P316S, R524W, I560T, H599R, M607V) may be linked to PD (Deng, Gao, and Jankovic 2013). Notably, the mechanism by which the D620N mutation contributes to neurodegeneration is largely uncharacterized; however, various studies have identified dysfunction in the lysosomal autophagy pathway resulting from expression of the pathogenic mutation in various contexts (Williams et al.

2022). *In vitro* overexpression of pathological D620N VPS35 protein resulted in decreased autophagosome formation, abnormal trafficking of ATG9A and autophagic impairment (Zavodszky et al. 2014). Abnormal trafficking of the LAMP2A receptor was observed in mice with VPS35–D620N mutations, with these animals showing alterations in lysosomal morphology and a reduction in LAMP2A-positive vesicles (Tang et al. 2015). Pathogenic VPS35 has also been shown to stimulate LRRK2-mediated phosphorylation of Rab GTPases in mouse models (Mir et al. 2018). Additionally, a limited sample of VPS35-associated PD patient-derived peripheral blood cells showed increased LRRK2 activity compared to idiopathic PD and healthy controls (Mir et al. 2018). Finally, pathogenic VPS35 impaired processing of cathepsin D, a major lysosomal protease involved in alpha-synuclein degradation, in model cell lines and PD patient-derived fibroblasts and increased alpha-synuclein aggregation in both *in vitro* and *in vivo* contexts (Follett et al. 2014; Tang et al. 2015).

Beyond the genes identified to cause monogenic forms of PD, genetic risk factors for PD have been established that further link autophagy and lysosomal dysfunction to PD development. A prominent example of this link is heterozygous loss of function mutations in glucocerebrosidase enzyme (*GBA*), functioning as a common risk factor for sporadic PD. This lysosomal hydrolase is mainly involved in sphingolipid metabolism and is required for the degradative capacity of the lysosome (Indellicato and Trinchera 2019). Mixed cultures of *GBA* knockout murine cortical neurons and astrocytes showed impaired autophagic flux (Osellame et al. 2013). Additionally, mice carrying heterozygous mutations in *GBA* exhibited increased accumulation of autophagosomes and

impaired lysosomal degradation (H. Li et al. 2019). Given the plurality of evidence relating the dysfunction of autophagy and the lysosome to the development of PD, autophagic pathways present a promising disease-modifying target for PD therapeutics.

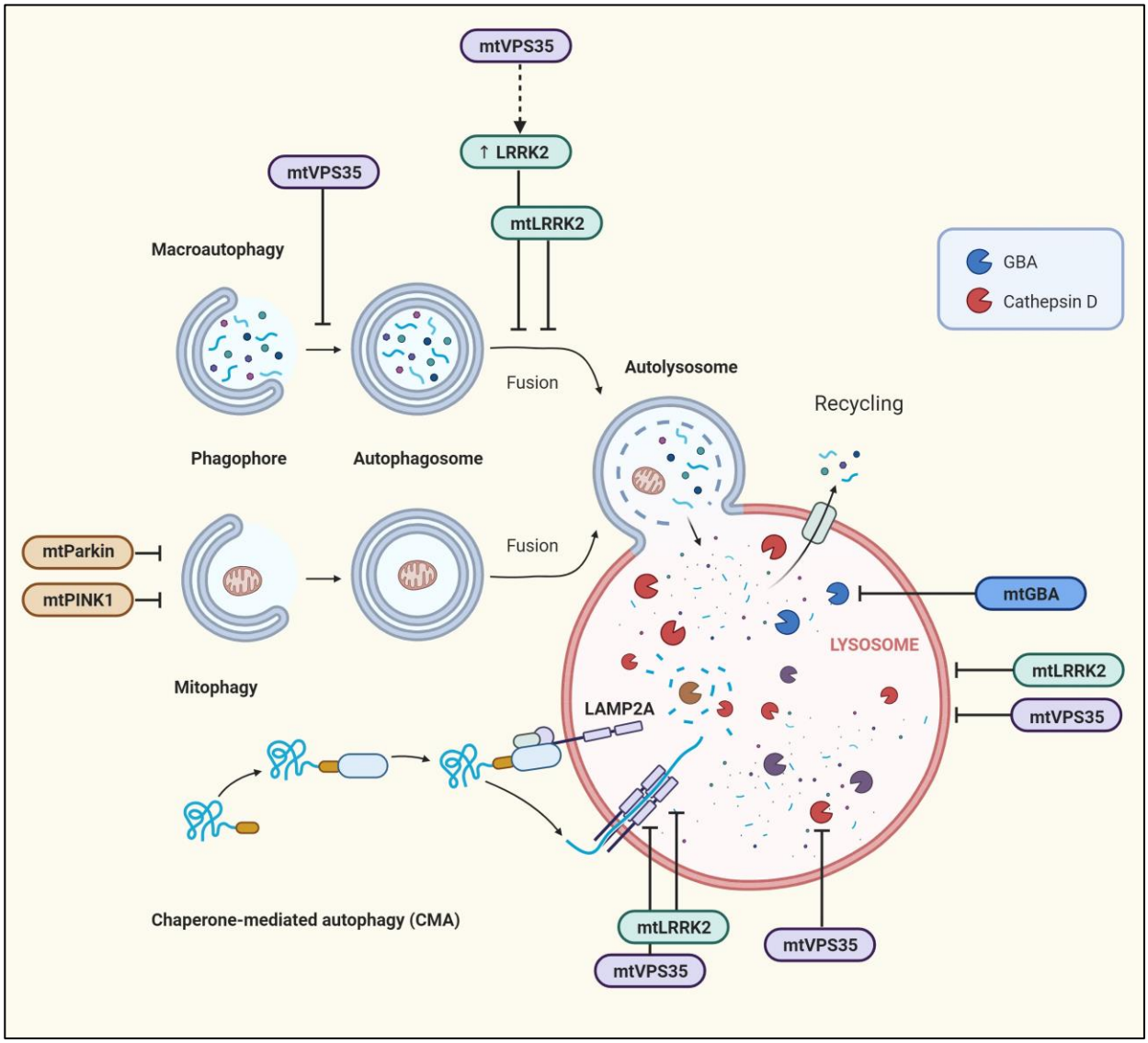

Figure 1. Schematic summarizing impact of pathogenic VPS35, LRRK2, GBA, Parkin and PINK1 mutations of macro- and chaperone-mediated autophagy. Pathogenic LRRK2 mutations result in autophagosome accumulation, impaired lysosomal degradation capacity and inhibition of the lysosomal translocation complex. Pathogenic VPS35 increases the kinase activity of LRRK2, inhibits phagophore expansion, impairs lysosomal degradation capacity and disrupts trafficking of cathepsin D and LAMP2A.

Mutations in Parkin and PINK1 impair the mitochondrial degradation process mitophagy. Mutations in GBA result in decreased lysosomal degradation capacity. mtLRRK2; mutant leucine rich repeat kinase, mtVPS35; mutant vacuolar protein sorting 35, mtGBA; mutant glucocerebrosidase, mtParkin; mutant parkin, mtPINK1; mutant PTEN-induced kinase 1, LAMP2A; lysosome-associated membrane protein type 2A, Hsc70; heat shock cognate protein 70. *Figure adapted from "Three Main Types of Autophagy" by BioRender.com (2023). Retrieved from https://app.biorender.com/biorender-templates.*

The human gut microbiota and the gut-brain axis

The human gut microbiota consists of a complex community of over 30 trillion microorganisms, including eukaryotes, archaea and predominantly bacteria, within the gastrointestinal tract (Sender, Fuchs, and Milo 2016; Turnbaugh et al. 2007). An estimated 500-1000 bacterial species reside in the gut, with their collective genes outnumbering the human genome by at least one order of magnitude (Turnbaugh et al. 2007). Human gut colonization begins at birth, reaching a relatively stable composition after two to three years of life (Mueller et al. 2015). The composition of the gut microbiota differs significantly between individuals and may fluctuate over an individual's lifespan based on a variety of factors, including host genetics, diet, antibiotic exposure, and lifestyle (Human Microbiome Project Consortium 2012; Gilbert et al. 2018).

The role of the gut microbiota in the context of human health and disease is a domain of active investigation. Specifically, the gut microbiota has been identified as functioning in nutrient metabolism (Vyas and Ranganathan 2012; Cummings et al. 1987; Guarner and Malagelada 2003), immune system development (Guarner and Malagelada 2003; Björkstén et al. 2001), and maintenance of the gut mucosal barrier integrity (Guarner and Malagelada 2003). Conversely, dysbiosis, the change in the presence or

relative abundance of individual microbes, has been linked to gastrointestinal diseases (Carroll et al. 2010; Frank et al. 2007; Marasco et al. 2016; T. Wang et al. 2012) and many extra-intestinal disorders including neurological and neuropsychiatric conditions (Vogt et al. 2017; Keshavarzian et al. 2015; Lv Wang et al. 2011). Research has begun to characterize the influence of the gut microbiota on the nervous system via the gut-brain axis, a bi-directional communication network of metabolic, immunological, neural, and hormonal signals linking the enteric nervous system and bacteria to the central nervous system (CNS). This communication network enables the gut microbiota and its metabolites to influence brain function and activity (Collins, Surette, and Bercik 2012; Mayer 2011). Characterizing mechanisms of interaction between the gut microbiota and nervous system in both healthy and disease contexts may have far-reaching implications for the understanding of and treatment of neurological and neuropsychiatric conditions.

Linking the human microbiota and Parkinson's Disease

Historically, studies of neurological disorders have been restricted to the central nervous system; however, the gastrointestinal tract and the gut microbiota have been linked to the onset and/or progression of diseases, including PD, via the gut-brain axis. The concept that chronic gut aggravation contributes to the onset of PD has gathered momentum in the previous decade, with emerging research identifying links between alterations of intestinal integrity and activity of the microbiota on PD progression and pathogenesis (Q. Li et al. 2023). Decreased gut motility is an early sign of PD, with up to 80% of PD patients experiencing constipation and delayed gastric emptying, often years before the onset of motor symptoms (Cersosimo et al. 2013). Additionally, increased

intestinal permeability has been observed in PD patients, with markers of intestinal barrier permeability being elevated even in the absence of gastrointestinal symptoms (Salat-Foix et al. 2012; Dumitrescu et al. 2021; Schwiertz et al. 2018). Researchers have also identified decreased expression of tight junction protein occludin in colon biopsies of PD patients, potentially linked to increased gut permeability (Clairembault et al. 2015). Lipopolysaccharide (LPS), a gram-negative bacterial product increased in PD patients, has been found to increase alpha-synuclein oligomerization and reduce expression of tight junction proteins in intestinal epithelial cells (Brown 2019). In aged alpha-synuclein transgenic mice, increased gut permeability increased neurodegeneration by triggering the aggregation of alpha-synuclein in the enteric nervous system and in the dopaminergic neurons of the substantia nigra (Fang et al. 2020). Interestingly, alpha-synuclein aggregates have been identified in the gut before any CNS involvement (Bloch et al. 2006; Heiko Braak et al. 2006; Wakabayashi et al. 1988). Braak and colleagues were the first to identify Lewy pathology in the dorsal motor nucleus of the vagus nerve and olfactory bulb prior to the appearance of classic motor symptoms in PD by post-mortem histopathological studies. These findings led to the hypothesis that PD begins in the gut, more specifically the enteric nervous system, and spreads to the CNS through prion-like propagation via the vagus nerve (Hawkes, Del Tredici, and Braak 2007; H. Braak et al. 2003). Further supporting this hypothesis, a full truncal vagotomy decreases the risk of developing PD later in life (Svensson et al. 2015). Intestinal inflammation has also been linked to PD, with many studies identifying elevation of fecal calprotectin, a marker of intestinal inflammation, in PD patient samples compared to control individuals

(Schwiertz et al. 2018; Mulak et al. 2019). Increased fecal calprotectin has also been correlated with increased gut dysbiosis (Klingberg et al. 2019). Additionally, inflammatory bowel disease, a condition associated with increased fecal calprotectin, has been linked to an increased risk of PD development in various populations (F. Zhu et al. 2019). Several inflammatory molecules are also elevated in the brain and cerebrospinal fluid of PD patients, including IL-1β, IL-2, IL-6, IL-10, TNF-α, CCL5 and CRP (X. Chen et al. 2018; Lin et al. 2019) with recent studies linking gut dysbiosis to microglial activation and neuroinflammation (Sampson and Mazmanian 2015; de Theije et al. 2014). Altogether, there is accumulating evidence supporting a link between gut microbiota dysbiosis and increased intestinal and neuroinflammation, intestinal permeability and alpha-synuclein pathology, which are understood to play a crucial role in the pathogenesis of PD.

Several studies have examined differences in microbiotal composition between PD patients and healthy control individuals with varied success. One meta-analysis of fifteen case-control studies observed a significantly decreased abundance of *Prevotellaceae*, *Lachnospiraceae*, and *Faecalibacterium* in patients with PD compared to healthy controls. The same study also identified enrichment of *Verrucomicrobiaceae*, *Bifidobacteriaceae*, *Christensenellaceae*, and *Ruminococcaceae* in PD patients (Shen et al. 2021). Another meta-analysis of ten relevant studies found an enrichment of *Megasphaera* and *Akkermansia*, and a reduced abundance of *Roseburia* in PD patients (Toh et al. 2022). A recent systematic review of twenty-six studies found that a minimum of two studies demonstrated an increased abundance of *Bifidobacterium*, *Alistipes*,

Christensenella, *Enterococcus*, *Oscillospira*, *Bilophila*, *Desulfovibrio*, *Escherichia/Shigella*, and *Akkermansia*, and a decreased abundance of *Prevotella*, *Blautia*, *Faecalibacterium*, *Fusicatenibacter*, and *Haemophilus* in PD patients. However, independent studies produced contradictory findings on the abundance of *Bacteroides*, *Odoribacter*, *Parabacteroides*, *Butyricicoccus*, *Butyrivibrio*, *Clostridium*, *Coprococcus*, *Lachnospira*, *Lactobacillus*, *Megasphaera*, *Phascolarctobacterium*, *Roseburia*, *Ruminococcus*, *Streptococcus*, and *Klebsiella* in individuals with PD (Z. Li et al. 2023). It is important to note that many of the existing comparative studies used in these meta-analyses and systematic reviews fail to account for the impacts of decreased transit time (constipation), a common PD symptom and known modifier of the gut microbiota, on microbiotal composition (Vandeputte et al. 2016; Roager et al. 2016; Haikal, Chen, and Li 2019). In addition to the existing taxonomic analyses of the microbiome of PD patients, a few studies have focused on a functional analysis identifying novel changes in the fecal metabolomic profile of PD patients (Tan et al. 2021; Unger et al. 2016; P. Li et al. 2021). Reduced levels of short-chain fatty acids, a class of metabolites with putative neuroprotective effects, were found in PD patients, which correlated with worse motor and cognitive symptoms (Tan et al. 2021), constipation (Unger et al. 2016), increased intestinal permeability, and colonic inflammation (Bullich et al. 2019; Long-Smith et al. 2020). These existing comparative studies linking the microbiome and PD are correlative, largely failing to resolve the effects of confounding factors on microbiotal composition and failing to establish causative relations between bacterial species and the neurodegenerative process.

Given the clinical evidence of gut dysbiosis in the context of PD patients versus healthy individuals, emerging research has focused on determining the therapeutic potential of gut microbiome modification. Recently, probiotic bacteria have been identified as improving PD-associated phenotypes in various models of PD. *L. plantarum* DP189 supplementation was able to decrease alpha-synuclein aggregation in the substantia nigra of mice and reshaped the microbiota of the animals by reducing the relative abundance of pathogenic bacteria, *Proteobacteria* and *Actinobacteria,* while increasing the relative abundance of probiotics, *Lactobacillus* and *Prevotella* (Lei Wang et al. 2022). Supplementation with probiotic SLAB51, a formulation of nine live bacteria strains (*Streptococcus thermophilus, B. longum, B. breve, B. infantis, L. acidophilus, L. plantarum, L. paracasei, L. delbrueckii subsp. bulgaricus, and L. brevis*) resulted in a reduction of dopaminergic neurodegeneration in both *in vitro* and murine models of PD (Castelli et al. 2020). Some studies have validated the preclinical benefits of probiotics in PD patients, concluding that probiotic supplementation improved both the motor and non-motor symptoms of PD (Lei Wang et al. 2022; Tamtaji et al. 2019; Zhao et al. 2022). In addition to viewing the microbiome as a therapeutic target for PD treatment, research has focused on isolating bacterial taxa most relevant to PD pathophysiology. Recently, an exploratory study of 25 early untreated PD patients found that a lower abundance of *Rosburia* was associated with worse motor and cognitive systems after three years (Cilia et al. 2021). Another study of 74 PD patients found that a lower abundance of *Barnesiella* correlated to faster progression of the disease (Lubomski et al. 2022). However, few studies have been able to identify mechanisms by which specific gut

microbiotal bacteria facilitate PD pathogenesis with the expectation of curli-producing bacteria. Curli is an extracellular bacterial amyloid produced by a variety of bacteria, including *E. coli.* Aged rats exposed to curli-producing *E. coli* had increased alpha-synuclein deposition in the brain and gut compared to control rats fed non-curli-producing *E. coli* (S. G. Chen et al. 2016). Similarly, in *C. elegans,* alpha-synuclein aggregation increased when worms were fed the curli-producing bacteria compared to the non-curli producing control, suggesting that the bacterial amyloid is able to enhance alpha-synuclein aggregation (S. G. Chen et al. 2016). The current body of research clearly demonstrates the ability of individual bacteria species to influence the pathophysiology of PD; however, as an emerging field of study, further investigation is required to identify which specific gut bacteria are able to facilitate or impede disease mechanisms and the pathways underlying these effects.

C. elegans as a model for Parkinson's Disease

Caenorhabditis elegans is a free-living, transparent nematode first proposed by Dr. Sydney Brenner in 1963 as a conduit for exploring questions of development and neurobiology (Brenner 1974). The nematode, found naturally among rotting vegetal matter, reaches a maximal length of approximately 1-2 mm in adulthood, has a reproductive cycle of only 3.5 days at room temperature and an average lifespan of approximately three weeks (Brenner 1974; Barrière and Félix 2006). *C. elegans* exists primarily as a self-fertilizing hermaphrodite able to produce up to 300 self-progeny. Additionally, *C. elegans* are capable of cross-fertilization with males arising naturally in populations at a frequency of <0.2%. In laboratory contexts, worms are easily grown and

maintained at ambient temperatures on agar plates seeded with *E. coli* OP50, a uracil auxotroph with limited growth ideal for visualization of animals (Corsi, Wightman, and Chalfie 2015).

Several features of *C. elegans* make it a powerful tool for modelling human disease and, more specifically, PD. The short generation time of *C. elegans* allows researchers to monitor disease states throughout the animal's lifespan, which is invaluable in the context of age-related disease. Their small size allows for large-scale screening of over a hundred animals in a single assay, and their transparency enables the use of fluorescent markers to study biological processes *in vivo,* including neurodegeneration. 60-80% of human genes and over 40% of genes known to be associated with human disease have identified orthologs in the *C. elegans* genome, suggesting a high conservation of underlying molecular pathways implicated in disease pathogenesis (Culetto and Sattelle 2000; Kaletta and Hengartner 2006). Specifically, *C. elegans* has orthologs to many of the genes implicated in PD, including *LRRK2/lrk-1, PINK1/pink-1* and *PRKN/pdr-1* (Table 2). Additionally, the invariant number of somatic cells in *C. elegans* has allowed researchers to generate reconstructions of the animal, including a complete map of the 300-neuron nervous system of the adult hermaphrodite (White et al. 1986). *C. elegans* was the first multicellular organism to have its entire genome sequenced, and currently, its genetic information is not only accessible but easily manipulated via a variety of established techniques (*C. elegans* Sequencing Consortium 1998; Boulin and Hobert 2012). DNA transformation via microinjection has facilitated the generation of numerous transgenic strains of *C. elegans* and has allowed for the

expression of both wild-type and pathogenic forms of human genes in the animal. Additionally, RNA interference (RNAi), first discovered in *C. elegans,* exists as an easy and inexpensive tool for modifying gene expression *in vivo* (Fire et al. 1998). Finally, despite their inability to recapitulate complete disease phenotypes, a variety of assays have been developed that emulate specific human disease phenotypes and pathologies, including those seen in PD (Maulik et al. 2017).

Table 1. OMIM registered PD-associated genes with their respective *C. elegans* orthologs. List of PD-associated genes registered in the Online Mendelian Inheritance in Man (OMIM) and their respective *C. elegans* ortholog(s) when applicable. *C. elegans* orthologs were compiled using OrthoList 2 (W. Kim et al. 2018).

Gene	**Protein**	***C. elegans* Ortholog(s)**
SNCA	Alpha-synuclein	N/A
PRKN	Parkin	*pdr-1*
UCHL1	Ubiquitin C-terminal hydrolase L1	*ubh-1, ubh-2, ubh-3*
PINK1	PTEN-induced putative kinase 1	*pink-1*
DJ-1	Protein deglycase	N/A
LRRK2	Leucine-rich repeat kinase 2	*lrk-1*
ATP13A2	ATPase Cation Transporting 13A2	*catp-5, catp-6, catp-7*
GIGYF2	GRB10 interacting GYF protein 2	C18H9.3
HTRA2	HtrA serine peptidase 2	N/A
PLA2G6	Phospholipase A2 Group VI	*ipla-2, ipla-3, ipla-4, ipla-5 ipla-7,* C45B2.6
FBX07	F-Box Protein 7	N/A
VPS35	Vacuolar protein sorting-associated protein 35	*vps-35*

EIF4G1	Eukaryotic translation initiation factor 4 gamma 1	*ifg-1*
DNAJC6	Putative tyrosine-protein phosphatase auxilin	*dnj-25*
SYNJ1	Synaptojanin-1	*unc-26*
DNAJC13/RME8	Receptor-mediated endocytosis 8	*rme-8*
CHCHD2	Coiled-Coil-Helix-Coiled-Coil-Helix Domain Containing 2	*har-1*
VPS13C	Vacuolar protein sorting-associated protein 13C	T08G11.1
PSAP	Prosaposin	*spp-8, spp-10*

Current *C. elegans* models of PD fall into two major categories: neurotoxin models and genetic models. Prior to the advent of genetic models, neurotoxin models were frequently used to replicate dopaminergic neurodegeneration within the organism via *in vivo* administration of neurotoxins such as 6-hydroxydopamine (6-OHDA), 1-methyl-4-phenyl- 1,2,3,6-tetrahydropyridine (MPTP), rotenone, and paraquat (Nass and Blakely 2003; Zhou, Wang, and Klaunig 2013; Nass et al. 2002). However, these models generally fail to recapitulate other aspects of PD pathophysiology and also fail to capture the slowly progressive nature of the neurodegenerative process given the acute neurotoxicity elicited from neurotoxin exposure. The development of genetic models of PD has allowed for further exploration of the cellular mechanisms underlying the major pathological hallmarks of PD: protein aggregation and neurodegeneration. Protein aggregation has been modelled in *C. elegans* via the expression of an alpha-synuclein GFP or YFP fusion protein in the body wall muscle (*unc-54* promoter), allowing

researchers to monitor alpha-synuclein aggregation *in vivo* (Hamamichi et al. 2008; van Ham et al. 2008). To model neurodegeneration in *C. elegans,* a variety of strains have been developed, exhibiting age-dependent neuronal loss, including alpha-synuclein and *LRRK2* transgenic animals. These worms express wildtype or pathogenic forms of alpha-synuclein or LRRK2 protein either pan-neuronally (*aex-3 or snb-1* promoter) or in dopaminergic neurons (*dat-1* promoter) with a fluorescent neuronal marker to allow monitoring of neuronal integrity *in vivo.* The expression of these human proteins in *C. elegans* provides a simple and relevant system to study the genetic and environmental factors impacting the major pathologies of PD (Lakso et al. 2003; Cao et al. 2005; Kuwahara et al. 2006; Saha et al. 2009; Yao et al. 2010).

C. elegans as a model for the gut-brain axis

Accumulating evidence has led to the recognition of the link between the gut microbiota and nervous system; however, much remains to be discovered regarding the mechanisms underlying this bidirectional communication system. Researchers have primarily used gnotobiotic mice to study host-microbe interactions, yielding critical insights in the field. However, this model is limited in its ability to resolve molecular-level mechanisms, given the complexity of the mammalian host's physiology. The intricacy of the murine nervous system, made up of billions of neurons, makes it infeasible to monitor how microbial signals facilitate neural function *in vivo* (Ortiz de Ora and Bess 2021). In addition to its stated benefits as a model system, C. *elegans* is a practical alternative to gnotobiotic mice given its simpler and fully characterized nervous

system, the ease of maintenance of germ-free worms via hypochlorite treatment (isolates bleach-resistant embryos only), and their bacterivorous nature, allowing for the manipulation, control and monitoring of their microbiota. Moreover, as seen in humans, communication between the gut and nervous system in *C. elegans* is facilitated by neuroendocrine signals with conservation of major neurotransmitters, including dopamine and serotonin (Chase and Koelle 2007; Cook et al. 2019).

Currently, there is a paucity of studies using *C. elegans* as a model organism to examine the role of the gut microbiota in PD. One such study identified that bacterial protein curli is able to enhance alpha-synuclein aggregation in both *C. elegans* and aged rats (S. G. Chen et al. 2016), demonstrating the translational potential of findings made in *C. elegans.* Similarly, another group identified the ability of the major subunit of the curli protein to enter *C. elegans* neurons, facilitating alpha-synuclein aggregation and neurodegeneration in animals neuronally expressing alpha-synuclein. Additionally, by screening the entire *E. coli* genome, using single-gene knockout strains from the Keio library, they identified 38 *E. coli* genes that enhance alpha-synuclein mediated neurodegeneration, involved in converging bacteria pathways including curli formation, LPS production, lysozyme inhibition, oxidative stress response, and metabolism (C. Wang et al. 2021). Another group identified that probiotic *Bacillus subtilis* PXN21 decreased alpha-synuclein aggregation and facilitated clearance of preformed aggregates in young and aging animals in a DAF-16/FOXO-dependent manner (Goya et al. 2020). At a bacterial level, the protective effect was partially mediated by biofilm formation and metabolite production. Additionally, transcriptomic analysis of animals fed *B. subtilis*

found that the probiotic's effect is partially facilitated by alterations in sphingolipid metabolism (Goya et al. 2020). A different study found that a bacterial metabolite produced by *Streptomyces venezuelae* enhanced neurodegeneration in both *LRRK2* and alpha-synuclein transgenic animals. Mechanistically, metabolite exposure increased the production of free oxygen radicals and impaired mitochondrial complex I activity, resulting in neurotoxicity (Ray et al. 2014). These studies together demonstrate the viability of *C. elegans* as a model organism in resolving specific mechanisms underlying host-microbe interactions in the context of neurodegenerative disease.

Thesis rationale and summary of aims

The cellular mechanisms underlying the connection between the gastrointestinal environment and the CNS, and more specifically, the role it plays in PD, are largely uncharacterized. The purpose of this project was to identify bacterial strains isolated from the human microbiota that influence neurodegeneration in *C. elegans* models of PD and to determine cellular mechanisms mediating these effects. The project focused primarily on characterizing changes in host gene expression and signalling pathways to determine processes that are regulated by the microbiota and to understand how these genes and pathways may influence neurodegeneration. We anticipate that identification of such environment-responsive elements will lead to a better understanding of how environment influences PD pathogenesis and may help to identify better targets for intervention in developing treatments for the disease. Additionally, bioactive molecules from bacteria have yielded important therapeutics in the treatment of other diseases (e.g., erythromycin, daunorubicin, rapamycin) (Pham et al. 2019), and so the identification of neuroprotective

microbiotal bacteria may lead to the development of novel drugs.

Summary of studies

1) Developed a novel protocol to assess the influence of individual strains of anaerobic human microbiotal bacteria on neurodegeneration in *LRRK2* transgenic animals (Chapter 2)
2) Identified and characterized host gene expression changes in response to neuroprotective bacteria via RNA sequencing in both wild-type and *LRRK2* transgenic animals (Chapter 3)

References

Agarraberes, F. A., and J. F. Dice. 2001. "A Molecular Chaperone Complex at the Lysosomal Membrane Is Required for Protein Translocation." *Journal of Cell Science* 114 (Pt 13): 2491–99.

Alessi, Dario R., and Esther Sammler. 2018. "LRRK2 Kinase in Parkinson's Disease." *Science* 360 (6384): 36–37.

Alvarez-Erviti, Lydia, Maria C. Rodriguez-Oroz, J. Mark Cooper, Cristina Caballero, Isidro Ferrer, Jose A. Obeso, and Anthony H. V. Schapira. 2010. "Chaperone-Mediated Autophagy Markers in Parkinson Disease Brains." *Archives of Neurology* 67 (12): 1464–72.

Anglade, P., S. Vyas, F. Javoy-Agid, M. T. Herrero, P. P. Michel, J. Marquez, A. Mouatt-Prigent, M. Ruberg, E. C. Hirsch, and Y. Agid. 1997. "Apoptosis and Autophagy in Nigral Neurons of Patients with Parkinson's Disease." *Histology and Histopathology* 12 (1): 25–31.

Arighi, Cecilia N., Lisa M. Hartnell, Ruben C. Aguilar, Carol R. Haft, and Juan S. Bonifacino. 2004. "Role of the Mammalian Retromer in Sorting of the Cation-Independent Mannose 6-Phosphate Receptor." *The Journal of Cell Biology* 165 (1): 123–33.

Bandyopadhyay, Urmi, Susmita Kaushik, Lyuba Varticovski, and Ana Maria Cuervo. 2008. "The Chaperone-Mediated Autophagy Receptor Organizes in Dynamic Protein Complexes at the Lysosomal Membrane." *Molecular and Cellular Biology* 28 (18): 5747–63.

Bardien, Soraya, Suzanne Lesage, Alexis Brice, and Jonathan Carr. 2011. "Genetic Characteristics of Leucine-Rich Repeat Kinase 2 (LRRK2) Associated Parkinson's Disease." *Parkinsonism & Related Disorders* 17 (7): 501–8.

Barrière, Antoine, and Marie-Anne Félix. 2006. "Isolation of C. Elegans and Related Nematodes." *WormBook: The Online Review of C. Elegans Biology*, July, 1–9.

Björkstén, B., E. Sepp, K. Julge, T. Voor, and M. Mikelsaar. 2001. "Allergy Development and the Intestinal Microflora during the First Year of Life." *The Journal of Allergy and Clinical Immunology* 108 (4): 516–20.

Blauwendraat, Cornelis, Mike A. Nalls, and Andrew B. Singleton. 2020. "The Genetic Architecture of Parkinson's Disease." *Lancet Neurology* 19 (2): 170–78.

Bloch, A., A. Probst, H. Bissig, H. Adams, and M. Tolnay. 2006. "Alpha-Synuclein Pathology of the Spinal and Peripheral Autonomic Nervous System in Neurologically Unimpaired Elderly Subjects." *Neuropathology and Applied Neurobiology* 32 (3):

284–95.

Boulin, Thomas, and Oliver Hobert. 2012. “From Genes to Function: The C. Elegans Genetic Toolbox.” Wiley Interdisciplinary Reviews. Developmental Biology 1 (1): 114–37.

Braak, Heiko, Rob A. I. de Vos, Jürgen Bohl, and Kelly Del Tredici. 2006. “Gastric Alpha-Synuclein Immunoreactive Inclusions in Meissner’s and Auerbach's Plexuses in Cases Staged for Parkinson's Disease-Related Brain Pathology.” Neuroscience Letters 396 (1): 67–72.

Braak, H., U. Rüb, W. P. Gai, and K. Del Tredici. 2003. “Idiopathic Parkinson’s Disease: Possible Routes by Which Vulnerable Neuronal Types May Be Subject to Neuroinvasion by an Unknown Pathogen.” Journal of Neural Transmission 110 (5): 517–36.

Brenner, S. 1974. “The Genetics of Caenorhabditis Elegans.” Genetics 77 (1): 71–94.

Brown, Guy C. 2019. “The Endotoxin Hypothesis of Neurodegeneration.” Journal of Neuroinflammation 16 (1): 180.

Bullich, Clara, Ali Keshavarzian, Johan Garssen, Aletta Kraneveld, and Paula Perez-Pardo. 2019. “Gut Vibes in Parkinson’s Disease: The Microbiota-Gut-Brain Axis.” Movement Disorders Clinical Practice 6 (8): 639–51.

Cao, Songsong, Christopher C. Gelwix, Kim A. Caldwell, and Guy A. Caldwell. 2005. “Torsin-Mediated Protection from Cellular Stress in the Dopaminergic Neurons of Caenorhabditis Elegans.” The Journal of Neuroscience: The Official Journal of the Society for Neuroscience 25 (15): 3801–12.

Carroll, Ian M., Young-Hyo Chang, Jiwon Park, R. Balfour Sartor, and Yehuda Ringel. 2010. “Luminal and Mucosal-Associated Intestinal Microbiota in Patients with Diarrhea-Predominant Irritable Bowel Syndrome.” Gut Pathogens 2 (1): 19.

Castelli, Vanessa, Michele d’Angelo, Francesca Lombardi, Margherita Alfonsetti, Andrea Antonosante, Mariano Catanesi, Elisabetta Benedetti, et al. 2020. “Effects of the Probiotic Formulation SLAB51 in in Vitro and in Vivo Parkinson’s Disease Models.” Aging 12 (5): 4641–59.

C. elegans Sequencing Consortium. 1998. “Genome Sequence of the Nematode C. Elegans: A Platform for Investigating Biology.” Science 282 (5396): 2012–18.

Cersosimo, Maria G., Gabriela B. Raina, Cristina Pecci, Alejandro Pellene, Cristian R. Calandra, Cristiam Gutiérrez, Federico E. Micheli, and Eduardo E. Benarroch. 2013. “Gastrointestinal Manifestations in Parkinson’s Disease: Prevalence and Occurrence before Motor Symptoms.” Journal of Neurology 260 (5): 1332–38.

Chase, Daniel L., and Michael R. Koelle. 2007. “Biogenic Amine Neurotransmitters in C. Elegans.” WormBook: The Online Review of C. Elegans Biology, February, 1–15.

Chen, Shu G., Vilius Stribinskis, Madhavi J. Rane, Donald R. Demuth, Evelyne Gozal, Andrew M. Roberts, Rekha Jagadapillai, et al. 2016. “Exposure to the Functional Bacterial Amyloid Protein Curli Enhances Alpha-Synuclein Aggregation in Aged Fischer 344 Rats and Caenorhabditis Elegans.” Scientific Reports 6 (October): 34477.

Chen, Xi, Yang Hu, Zongze Cao, Qingshan Liu, and Yong Cheng. 2018. “Cerebrospinal Fluid Inflammatory Cytokine Aberrations in Alzheimer’s Disease, Parkinson's Disease and Amyotrophic Lateral Sclerosis: A Systematic Review and Meta-Analysis.” Frontiers in Immunology 9 (September): 2122.

Chiang, H. L., S. R. Terlecky, C. P. Plant, and J. F. Dice. 1989. “A Role for a 70-Kilodalton Heat Shock Protein in Lysosomal Degradation of Intracellular Proteins.” Science 246 (4928): 382–85.

Cilia, Roberto, Marco Piatti, Emanuele Cereda, Carlotta Bolliri, Serena Caronni, Valentina Ferri, Erica Cassani, et al. 2021. “Does Gut Microbiota Influence the Course of Parkinson’s Disease? A 3-Year Prospective Exploratory Study in de Novo Patients.” Journal of Parkinson’s Disease 11 (1): 159–70.

Clairembault, Thomas, Laurène Leclair-Visonneau, Emmanuel Coron, Arnaud Bourreille, Séverine Le Dily, Fabienne Vavasseur, Marie-Françoise Heymann, Michel Neunlist, and Pascal Derkinderen. 2015. “Structural Alterations of the Intestinal Epithelial Barrier in Parkinson’s Disease.” Acta Neuropathologica Communications 3 (March): 12.

Clark, Ira E., Mark W. Dodson, Changan Jiang, Joseph H. Cao, Jun R. Huh, Jae Hong Seol, Soon Ji Yoo, Bruce A. Hay, and Ming Guo. 2006. “Drosophila pink1 Is Required for Mitochondrial Function and Interacts Genetically with Parkin.” Nature 441 (7097): 1162–66.

Collins, Stephen M., Michael Surette, and Premysl Bercik. 2012. “The Interplay between the Intestinal Microbiota and the Brain.” Nature Reviews. Microbiology 10 (11): 735–42.

Cook, Steven J., Travis A. Jarrell, Christopher A. Brittin, Yi Wang, Adam E. Bloniarz, Maksim A. Yakovlev, Ken C. Q. Nguyen, et al. 2019. “Whole-Animal Connectomes of Both Caenorhabditis Elegans Sexes.” Nature 571 (7763): 63–71.

Corsi, Ann K., Bruce Wightman, and Martin Chalfie. 2015. “A Transparent Window into Biology: A Primer on Caenorhabditis Elegans.” Genetics 200 (2): 387–407.

Culetto, E., and D. B. Sattelle. 2000. “A Role for Caenorhabditis Elegans in Understanding the Function and Interactions of Human Disease Genes.” Human

Molecular Genetics 9 (6): 869–77.

Cummings, J. H., E. W. Pomare, W. J. Branch, C. P. Naylor, and G. T. Macfarlane. 1987. "Short Chain Fatty Acids in Human Large Intestine, Portal, Hepatic and Venous Blood." Gut 28 (10): 1221–27.

Dehay, Benjamin, Jordi Bové, Natalia Rodríguez-Muela, Celine Perier, Ariadna Recasens, Patricia Boya, and Miquel Vila. 2010. "Pathogenic Lysosomal Depletion in Parkinson's Disease." The Journal of Neuroscience: The Official Journal of the Society for Neuroscience 30 (37): 12535–44.

Deng, Hao, Kai Gao, and Joseph Jankovic. 2013. "The VPS35 Gene and Parkinson's Disease." Movement Disorders: Official Journal of the Movement Disorder Society 28 (5): 569–75.

Dice, J. F. 1988. "Microinjected Ribonuclease A as a Probe for Lysosomal Pathways of Intracellular Protein Degradation." Journal of Protein Chemistry 7 (2): 115–27.

———. 1990. "Peptide Sequences That Target Cytosolic Proteins for Lysosomal Proteolysis." Trends in Biochemical Sciences 15 (8): 305–9.

Dickson, Dennis W., Heiko Braak, John E. Duda, Charles Duyckaerts, Thomas Gasser, Glenda M. Halliday, John Hardy, et al. 2009. "Neuropathological Assessment of Parkinson's Disease: Refining the Diagnostic Criteria." Lancet Neurology 8 (12): 1150–57.

Dohi, Eisuke, Shigeru Tanaka, Takahiro Seki, Tatsuhiro Miyagi, Izumi Hide, Tetsuya Takahashi, Masayasu Matsumoto, and Norio Sakai. 2012. "Hypoxic Stress Activates Chaperone-Mediated Autophagy and Modulates Neuronal Cell Survival." Neurochemistry International 60 (4): 431–42.

Dumitrescu, Laura, Daciana Marta, Adela Dănău, Antonia Lefter, Delia Tulbă, Liviu Cozma, Emilia Manole, Mihaela Gherghiceanu, Laura Cristina Ceafalan, and Bogdan Ovidiu Popescu. 2021. "Serum and Fecal Markers of Intestinal Inflammation and Intestinal Barrier Permeability Are Elevated in Parkinson's Disease." Frontiers in Neuroscience 15 (June): 689723.

Eguchi, Tomoya, Tomoki Kuwahara, Maria Sakurai, Tadayuki Komori, Tetta Fujimoto, Genta Ito, Shin-Ichiro Yoshimura, et al. 2018. "LRRK2 and Its Substrate Rab GTPases Are Sequentially Targeted onto Stressed Lysosomes and Maintain Their Homeostasis." Proceedings of the National Academy of Sciences of the United States of America 115 (39): E9115–24.

Eskelinen, Eeva-Liisa, Yoshitaka Tanaka, and Paul Saftig. 2003. "At the Acidic Edge: Emerging Functions for Lysosomal Membrane Proteins." Trends in Cell Biology 13 (3): 137–45.

Fang, P., S. A. Kazmi, K. G. Jameson, and E. Y. Hsiao. 2020. “The Microbiome as a Modifier of Neurodegenerative Disease Risk.” Cell Host & Microbe 28 (2): 201–22.

Fire, A., S. Xu, M. K. Montgomery, S. A. Kostas, S. E. Driver, and C. C. Mello. 1998. “Potent and Specific Genetic Interference by Double-Stranded RNA in Caenorhabditis Elegans.” Nature 391 (6669): 806–11.

Follett, Jordan, Suzanne J. Norwood, Nicholas A. Hamilton, Megha Mohan, Oleksiy Kovtun, Stephanie Tay, Yang Zhe, et al. 2014. “The Vps35 D620N Mutation Linked to Parkinson’s Disease Disrupts the Cargo Sorting Function of Retromer.” Traffic 15 (2): 230–44.

Frank, Daniel N., Allison L. St Amand, Robert A. Feldman, Edgar C. Boedeker, Noam Harpaz, and Norman R. Pace. 2007. “Molecular-Phylogenetic Characterization of Microbial Community Imbalances in Human Inflammatory Bowel Diseases.” Proceedings of the National Academy of Sciences of the United States of America 104 (34): 13780–85.

Funayama, Manabu, Kenya Nishioka, Yuanzhe Li, and Nobutaka Hattori. 2023. “Molecular Genetics of Parkinson’s Disease: Contributions and Global Trends.” Journal of Human Genetics 68 (3): 125–30.

Ganley, I. G., D. H. Lam, J. Wang, X. Ding, and S. Chen. 2009. “ULK1· ATG13· FIP200 Complex Mediates mTOR Signaling and Is Essential for Autophagy.” Journal of Biological. https://www.jbc.org/article/S0021-9258(20)58389-0/abstract.

Geng, Jiefei, and Daniel J. Klionsky. 2008. “The Atg8 and Atg12 Ubiquitin-like Conjugation Systems in Macroautophagy. ‘Protein Modifications: Beyond the Usual Suspects’ Review Series.” EMBO Reports 9 (9): 859–64.

Gilbert, Jack A., Martin J. Blaser, J. Gregory Caporaso, Janet K. Jansson, Susan V. Lynch, and Rob Knight. 2018. “Current Understanding of the Human Microbiome.” Nature Medicine 24 (4): 392–400.

Goya, María Eugenia, Feng Xue, Cristina Sampedro-Torres-Quevedo, Sofia Arnaouteli, Lourdes Riquelme-Dominguez, Andrés Romanowski, Jack Brydon, Kathryn L. Ball, Nicola R. Stanley-Wall, and Maria Doitsidou. 2020. “Probiotic Bacillus Subtilis Protects against α-Synuclein Aggregation in C. Elegans.” Cell Reports 30 (2): 367–80.e7.

Gregersen, Niels, Peter Bross, Søren Vang, and Jane H. Christensen. 2006. “Protein Misfolding and Human Disease.” Annual Review of Genomics and Human Genetics 7: 103–24.

Guarner, Francisco, and Juan-R Malagelada. 2003. “Gut Flora in Health and Disease.” The Lancet 361 (9356): 512–19.

Haikal, Caroline, Qian-Qian Chen, and Jia-Yi Li. 2019. “Microbiome Changes: An Indicator of Parkinson’s Disease?” Translational Neurodegeneration 8 (December): 38.

Hamamichi, Shusei, Renee N. Rivas, Adam L. Knight, Songsong Cao, Kim A. Caldwell, and Guy A. Caldwell. 2008. “Hypothesis-Based RNAi Screening Identifies Neuroprotective Genes in a Parkinson’s Disease Model.” Proceedings of the National Academy of Sciences of the United States of America 105 (2): 728–33.

Ham, Tjakko J. van, Karen L. Thijssen, Rainer Breitling, Robert M. W. Hofstra, Ronald H. A. Plasterk, and Ellen A. A. Nollen. 2008. “C. Elegans Model Identifies Genetic Modifiers of Alpha-Synuclein Inclusion Formation during Aging.” PLoS Genetics 4 (3): e1000027.

Hawkes, C. H., K. Del Tredici, and H. Braak. 2007. “Parkinson’s Disease: A Dual-Hit Hypothesis.” Neuropathology and Applied Neurobiology 33 (6): 599–614.

Healy, Daniel G., Mario Falchi, Sean S. O’Sullivan, Vincenzo Bonifati, Alexandra Durr, Susan Bressman, Alexis Brice, et al. 2008. “Phenotype, Genotype, and Worldwide Genetic Penetrance of LRRK2-Associated Parkinson’s Disease: A Case-Control Study.” Lancet Neurology 7 (7): 583–90.

Ho, Philip Wing-Lok, Chi-Ting Leung, Huifang Liu, Shirley Yin-Yu Pang, Colin Siu-Chi Lam, Jiawen Xian, Lingfei Li, Michelle Hiu-Wai Kung, David Boyer Ramsden, and Shu-Leong Ho. 2020. “Age-Dependent Accumulation of Oligomeric SNCA/α-Synuclein from Impaired Degradation in Mutant LRRK2 Knockin Mouse Model of Parkinson Disease: Role for Therapeutic Activation of Chaperone-Mediated Autophagy (CMA).” Autophagy 16 (2): 347–70.

Hosokawa, Nao, Taichi Hara, Takeshi Kaizuka, Chieko Kishi, Akito Takamura, Yutaka Miura, Shun-Ichiro Iemura, et al. 2009. “Nutrient-Dependent mTORC1 Association with the ULK1–Atg13–FIP200 Complex Required for Autophagy.” Molecular Biology of the Cell 20 (7): 1981–91.

Human Microbiome Project Consortium. 2012. “Structure, Function and Diversity of the Healthy Human Microbiome.” Nature 486 (7402): 207–14.

Ichimura, Yoshinobu, Satoshi Waguri, Yu-Shin Sou, Shun Kageyama, Jun Hasegawa, Ryosuke Ishimura, Tetsuya Saito, et al. 2013. “Phosphorylation of p62 Activates the Keap1-Nrf2 Pathway during Selective Autophagy.” Molecular Cell 51 (5): 618–31.

Indellicato, Rossella, and Marco Trinchera. 2019. “The Link between Gaucher Disease and Parkinson’s Disease Sheds Light on Old and Novel Disorders of Sphingolipid Metabolism.” International Journal of Molecular Sciences 20 (13). https://doi.org/10.3390/ijms20133304.

Isogai, Shin, Daichi Morimoto, Kyohei Arita, Satoru Unzai, Takeshi Tenno, Jun

Hasegawa, Yu-Shin Sou, et al. 2011. “Crystal Structure of the Ubiquitin-Associated (UBA) Domain of p62 and Its Interaction with Ubiquitin.” The Journal of Biological Chemistry 286 (36): 31864–74.

Jung, Chang Hwa, Chang Bong Jun, Seung-Hyun Ro, Young-Mi Kim, Neil Michael Otto, Jing Cao, Mondira Kundu, and Do-Hyung Kim. 2009. “ULK-Atg13-FIP200 Complexes Mediate mTOR Signaling to the Autophagy Machinery.” Molecular Biology of the Cell 20 (7): 1992–2003.

Kaletta, Titus, and Michael O. Hengartner. 2006. “Finding Function in Novel Targets: C. Elegans as a Model Organism.” Nature Reviews. Drug Discovery 5 (5): 387–98.

Kalogeropulou, Alexia F., Elena Purlyte, Francesca Tonelli, Sven M. Lange, Melanie Wightman, Alan R. Prescott, Shalini Padmanabhan, Esther Sammler, and Dario R. Alessi. 2022. “Impact of 100 LRRK2 Variants Linked to Parkinson’s Disease on Kinase Activity and Microtubule Binding.” Biochemical Journal 479 (17): 1759–83.

Kaushik, Susmita, and Ana Maria Cuervo. 2016. “AMPK-Dependent Phosphorylation of Lipid Droplet Protein PLIN2 Triggers Its Degradation by CMA.” Autophagy 12 (2): 432–38.

Kazlauskaite, Agne, Chandana Kondapalli, Robert Gourlay, David G. Campbell, Maria Stella Ritorto, Kay Hofmann, Dario R. Alessi, Axel Knebel, Matthias Trost, and Miratul M. K. Muqit. 2014. “Parkin Is Activated by PINK1-Dependent Phosphorylation of Ubiquitin at Ser65.” Biochemical Journal 460 (1): 127–39.

Ke, Rong, Qicao Xu, Cong Li, Lingyu Luo, and Deqiang Huang. 2018. “Mechanisms of AMPK in the Maintenance of ATP Balance during Energy Metabolism.” Cell Biology International 42 (4): 384–92.

Keshavarzian, Ali, Stefan J. Green, Phillip A. Engen, Robin M. Voigt, Ankur Naqib, Christopher B. Forsyth, Ece Mutlu, and Kathleen M. Shannon. 2015. “Colonic Bacterial Composition in Parkinson’s Disease.” Movement Disorders: Official Journal of the Movement Disorder Society 30 (10): 1351–60.

Kim, Joungmok, Mondira Kundu, Benoit Viollet, and Kun-Liang Guan. 2011. “AMPK and mTOR Regulate Autophagy through Direct Phosphorylation of Ulk1.” Nature Cell Biology 13 (2): 132–41.

Kim, Woojin, Ryan S. Underwood, Iva Greenwald, and Daniel D. Shaye. 2018. “OrthoList 2: A New Comparative Genomic Analysis of Human and Caenorhabditis Elegans Genes.” Genetics 210 (2): 445–61.

Kitada, T., S. Asakawa, N. Hattori, H. Matsumine, Y. Yamamura, S. Minoshima, M. Yokochi, Y. Mizuno, and N. Shimizu. 1998. “Mutations in the Parkin Gene Cause Autosomal Recessive Juvenile Parkinsonism.” Nature 392 (6676): 605–8.

Klingberg, Eva, Maria K. Magnusson, Hans Strid, Anna Deminger, Arne Ståhl, Johanna Sundin, Magnus Simrén, Hans Carlsten, Lena Öhman, and Helena Forsblad-d'Elia. 2019. "A Distinct Gut Microbiota Composition in Patients with Ankylosing Spondylitis Is Associated with Increased Levels of Fecal Calprotectin." Arthritis Research & Therapy 21 (1): 248.

Koyano, Fumika, Kei Okatsu, Hidetaka Kosako, Yasushi Tamura, Etsu Go, Mayumi Kimura, Yoko Kimura, et al. 2014. "Ubiquitin Is Phosphorylated by PINK1 to Activate Parkin." Nature 510 (7503): 162–66.

Kriegenburg, Franziska, Christian Ungermann, and Fulvio Reggiori. 2018. "Coordination of Autophagosome-Lysosome Fusion by Atg8 Family Members." Current Biology: CB 28 (8): R512–18.

Kulkarni, Amrita, Kumari Preeti, Kamatham Pushpa Tryphena, Saurabh Srivastava, Shashi Bala Singh, and Dharmendra Kumar Khatri. 2023. "Proteostasis in Parkinson's Disease: Recent Development and Possible Implication in Diagnosis and Therapeutics." Ageing Research Reviews 84 (February): 101816.

Kuwahara, Tomoki, Akihiko Koyama, Keiko Gengyo-Ando, Mayumi Masuda, Hisatomo Kowa, Makoto Tsunoda, Shohei Mitani, and Takeshi Iwatsubo. 2006. "Familial Parkinson Mutant α-Synuclein Causes Dopamine Neuron Dysfunction in Transgenic Caenorhabditis Elegans." The Journal of Biological Chemistry 281 (1): 334–40.

Lakso, Merja, Suvi Vartiainen, Anu-Maarit Moilanen, Jouni Sirviö, James H. Thomas, Richard Nass, Randy D. Blakely, and Garry Wong. 2003. "Dopaminergic Neuronal Loss and Motor Deficits in Caenorhabditis Elegans Overexpressing Human Alpha-Synuclein." Journal of Neurochemistry 86 (1): 165–72.

Lesage, Suzanne, and Alexis Brice. 2009. "Parkinson's Disease: From Monogenic Forms to Genetic Susceptibility Factors." Human Molecular Genetics 18 (R1): R48–59.

Li, Hongyu, Ahrom Ham, Thong Chi Ma, Sheng-Han Kuo, Ellen Kanter, Donghoon Kim, Han Seok Ko, et al. 2019. "Mitochondrial Dysfunction and Mitophagy Defect Triggered by Heterozygous GBA Mutations." Autophagy 15 (1): 113–30.

Lin, Chin-Hsien, Chieh-Chang Chen, Han-Lin Chiang, Jyh-Ming Liou, Chih-Min Chang, Tzu-Pin Lu, Eric Y. Chuang, et al. 2019. "Altered Gut Microbiota and Inflammatory Cytokine Responses in Patients with Parkinson's Disease." Journal of Neuroinflammation 16 (1): 129.

Li, Peipei, Bryan A. Killinger, Elizabeth Ensink, Ian Beddows, Ali Yilmaz, Noah Lubben, Jared Lamp, et al. 2021. "Gut Microbiota Dysbiosis Is Associated with Elevated Bile Acids in Parkinson's Disease." Metabolites 11 (1). https://doi.org/10.3390/metabo11010029.

Li, Qing, Ling-Bing Meng, Li-Jun Chen, Xia Shi, Ling Tu, Qi Zhou, Jin-Long Yu, Xin

Liao, Yuan Zeng, and Qiao-Ying Yuan. 2023. “The Role of the Microbiota-Gut-Brain Axis and Intestinal Microbiome Dysregulation in Parkinson’s Disease.” Frontiers in Neurology 14 (May): 1185375.

Li, Zhe, Hongfeng Liang, Yingyu Hu, Lin Lu, Chunye Zheng, Yuzhen Fan, Bin Wu, et al. 2023. “Gut Bacterial Profiles in Parkinson’s Disease: A Systematic Review.” CNS Neuroscience & Therapeutics 29 (1): 140–57.

Long-Smith, Caitríona, Kenneth J. O’Riordan, Gerard Clarke, Catherine Stanton, Timothy G. Dinan, and John F. Cryan. 2020. “Microbiota-Gut-Brain Axis: New Therapeutic Opportunities.” Annual Review of Pharmacology and Toxicology 60 (January): 477–502.

Lubomski, Michal, Xiangnan Xu, Andrew J. Holmes, Samuel Muller, Jean Y. H. Yang, Ryan L. Davis, and Carolyn M. Sue. 2022. “The Gut Microbiome in Parkinson’s Disease: A Longitudinal Study of the Impacts on Disease Progression and the Use of Device-Assisted Therapies.” Frontiers in Aging Neuroscience 14 (May): 875261.

MacLeod, David A., Herve Rhinn, Tomoki Kuwahara, Ari Zolin, Gilbert Di Paolo, Brian D. McCabe, Karen S. Marder, et al. 2013. “RAB7L1 Interacts with LRRK2 to Modify Intraneuronal Protein Sorting and Parkinson’s Disease Risk.” Neuron 77 (3): 425–39.

Maeda, Shintaro, Hayashi Yamamoto, Lisa N. Kinch, Christina M. Garza, Satoru Takahashi, Chinatsu Otomo, Nick V. Grishin, Stefano Forli, Noboru Mizushima, and Takanori Otomo. 2020. “Structure, Lipid Scrambling Activity and Role in Autophagosome Formation of ATG9A.” Nature Structural & Molecular Biology 27 (12): 1194–1201.

Marasco, Giovanni, Anna Rita Di Biase, Ramona Schiumerini, Leonardo Henry Eusebi, Lorenzo Iughetti, Federico Ravaioli, Eleonora Scaioli, Antonio Colecchia, and Davide Festi. 2016. “Gut Microbiota and Celiac Disease.” Digestive Diseases and Sciences 61 (6): 1461–72.

Marzella, L., J. Ahlberg, and H. Glaumann. 1981. “Autophagy, Heterophagy, Microautophagy and Crinophagy as the Means for Intracellular Degradation.” Virchows Archiv. B, Cell Pathology Including Molecular Pathology 36 (2-3): 219–34.

Maulik, Malabika, Swarup Mitra, Abel Bult-Ito, Barbara E. Taylor, and Elena M. Vayndorf. 2017. “Behavioral Phenotyping and Pathological Indicators of Parkinson’s Disease in C. Elegans Models.” Frontiers in Genetics 8 (June): 77.

Mayer, Emeran A. 2011. “Gut Feelings: The Emerging Biology of Gut-Brain Communication.” Nature Reviews. Neuroscience 12 (8): 453–66.

Migliore, Lucia, and Fabio Coppedè. 2009. “Genetics, Environmental Factors and the

Emerging Role of Epigenetics in Neurodegenerative Diseases." Mutation Research 667 (1-2): 82–97.

Mir, Rafeeq, Francesca Tonelli, Pawel Lis, Thomas Macartney, Nicole K. Polinski, Terina N. Martinez, Meng-Yun Chou, et al. 2018. "The Parkinson's Disease VPS35[D620N] Mutation Enhances LRRK2-Mediated Rab Protein Phosphorylation in Mouse and Human." Biochemical Journal 475 (11): 1861–83.

Mizushima, Noboru, Akiko Kuma, Yoshinori Kobayashi, Akitsugu Yamamoto, Masami Matsubae, Toshifumi Takao, Tohru Natsume, Yoshinori Ohsumi, and Tamotsu Yoshimori. 2003. "Mouse Apg16L, a Novel WD-Repeat Protein, Targets to the Autophagic Isolation Membrane with the Apg12-Apg5 Conjugate." Journal of Cell Science 116 (Pt 9): 1679–88.

Mizushima, Noboru, Beth Levine, Ana Maria Cuervo, and Daniel J. Klionsky. 2008. "Autophagy Fights Disease through Cellular Self-Digestion." Nature 451 (7182): 1069–75.

Mizushima, Noboru, Akitsugu Yamamoto, Makoto Matsui, Tamotsu Yoshimori, and Yoshinori Ohsumi. 2004. "In Vivo Analysis of Autophagy in Response to Nutrient Starvation Using Transgenic Mice Expressing a Fluorescent Autophagosome Marker." Molecular Biology of the Cell 15 (3): 1101–11.

Moors, Tim E., Silvia Paciotti, Angela Ingrassia, Marialuisa Quadri, Guido Breedveld, Anna Tasegian, Davide Chiasserini, et al. 2019. "Characterization of Brain Lysosomal Activities in GBA-Related and Sporadic Parkinson's Disease and Dementia with Lewy Bodies." Molecular Neurobiology 56 (2): 1344–55.

Moors, Tim, Silvia Paciotti, Davide Chiasserini, Paolo Calabresi, Lucilla Parnetti, Tommaso Beccari, and Wilma D. J. van de Berg. 2016. "Lysosomal Dysfunction and α-Synuclein Aggregation in Parkinson's Disease: Diagnostic Links." Movement Disorders: Official Journal of the Movement Disorder Society 31 (6): 791–801.

Mueller, Noel T., Elizabeth Bakacs, Joan Combellick, Zoya Grigoryan, and Maria G. Dominguez-Bello. 2015. "The Infant Microbiome Development: Mom Matters." Trends in Molecular Medicine 21 (2): 109–17.

Mulak, Agata, Magdalena Koszewicz, Magdalena Panek-Jeziorna, Ewa Koziorowska-Gawron, and Sławomir Budrewicz. 2019. "Fecal Calprotectin as a Marker of the Gut Immune System Activation Is Elevated in Parkinson's Disease." Frontiers in Neuroscience 13 (September): 992.

Murphy, Karen E., Amanda M. Gysbers, Sarah K. Abbott, Adena S. Spiro, Akiko Furuta, Antony Cooper, Brett Garner, Tomohiro Kabuta, and Glenda M. Halliday. 2015. "Lysosomal-Associated Membrane Protein 2 Isoforms Are Differentially Affected in Early Parkinson's Disease." Movement Disorders: Official Journal of the Movement

Disorder Society 30 (12): 1639–47.

Narendra, Derek, Atsushi Tanaka, Der-Fen Suen, and Richard J. Youle. 2008. "Parkin Is Recruited Selectively to Impaired Mitochondria and Promotes Their Autophagy." The Journal of Cell Biology 183 (5): 795–803.

Nascimbeni, Anna Chiara, Patrice Codogno, and Etienne Morel. 2017. "Phosphatidylinositol-3-Phosphate in the Regulation of Autophagy Membrane Dynamics." The FEBS Journal 284 (9): 1267–78.

Nass, Richard, and Randy D. Blakely. 2003. "The Caenorhabditis Elegans Dopaminergic System: Opportunities for Insights into Dopamine Transport and Neurodegeneration." Annual Review of Pharmacology and Toxicology 43: 521–44.

Nass, Richard, David H. Hall, David M. Miller 3rd, and Randy D. Blakely. 2002. "Neurotoxin-Induced Degeneration of Dopamine Neurons in Caenorhabditis Elegans." Proceedings of the National Academy of Sciences of the United States of America 99 (5): 3264–69.

Nixon, Ralph A., Dun-Sheng Yang, and Ju-Hyun Lee. 2008. "Neurodegenerative Lysosomal Disorders: A Continuum from Development to Late Age." Autophagy 4 (5): 590–99.

Obara, Keisuke, Takayuki Sekito, Kaori Niimi, and Yoshinori Ohsumi. 2008. "The Atg18-Atg2 Complex Is Recruited to Autophagic Membranes via Phosphatidylinositol 3-Phosphate and Exerts an Essential Function." The Journal of Biological Chemistry 283 (35): 23972–80.

Ohsumi, Y. 2001. "Molecular Dissection of Autophagy: Two Ubiquitin-like Systems." Nature Reviews. Molecular Cell Biology 2 (3): 211–16.

Ordureau, Alban, Shireen A. Sarraf, David M. Duda, Jin-Mi Heo, Mark P. Jedrychowski, Vladislav O. Sviderskiy, Jennifer L. Olszewski, et al. 2014. "Quantitative Proteomics Reveal a Feedforward Mechanism for Mitochondrial PARKIN Translocation and Ubiquitin Chain Synthesis." Molecular Cell 56 (3): 360–75.

Orenstein, Samantha J., Sheng-Han Kuo, Inmaculada Tasset, Esperanza Arias, Hiroshi Koga, Irene Fernandez-Carasa, Etty Cortes, et al. 2013. "Interplay of LRRK2 with Chaperone-Mediated Autophagy." Nature Neuroscience 16 (4): 394–406.

Ortiz de Ora, Lizett, and Elizabeth N. Bess. 2021. "Emergence of Caenorhabditis Elegans as a Model Organism for Dissecting the Gut–Brain Axis." mSystems 6 (4): 10.1128/msystems.00755–21.

Osellame, Laura D., Ahad A. Rahim, Iain P. Hargreaves, Matthew E. Gegg, Angela Richard-Londt, Sebastian Brandner, Simon N. Waddington, Anthony H. V. Schapira, and Michael R. Duchen. 2013. "Mitochondria and Quality Control Defects in a

Mouse Model of Gaucher Disease--Links to Parkinson's Disease." Cell Metabolism 17 (6): 941–53.

Pankiv, Serhiy, Terje Høyvarde Clausen, Trond Lamark, Andreas Brech, Jack-Ansgar Bruun, Heidi Outzen, Aud Øvervatn, Geir Bjørkøy, and Terje Johansen. 2007. "p62/SQSTM1 Binds Directly to Atg8/LC3 to Facilitate Degradation of Ubiquitinated Protein Aggregates by Autophagy." The Journal of Biological Chemistry 282 (33): 24131–45.

Park, Caroline, Yousin Suh, and Ana Maria Cuervo. 2015. "Regulated Degradation of Chk1 by Chaperone-Mediated Autophagy in Response to DNA Damage." Nature Communications 6 (April): 6823.

Park, Jeehye, Sung Bae Lee, Sungkyu Lee, Yongsung Kim, Saera Song, Sunhong Kim, Eunkyung Bae, et al. 2006. "Mitochondrial Dysfunction in Drosophila PINK1 Mutants Is Complemented by Parkin." Nature 441 (7097): 1157–61.

Perera, Rushika M., and Roberto Zoncu. 2016. "The Lysosome as a Regulatory Hub." Annual Review of Cell and Developmental Biology 32 (October): 223–53.

Pham, Janette V., Mariamawit A. Yilma, Adriana Feliz, Murtadha T. Majid, Nicholas Maffetone, Jorge R. Walker, Eunji Kim, et al. 2019. "A Review of the Microbial Production of Bioactive Natural Products and Biologics." Frontiers in Microbiology 10 (June): 1404.

Plowey, Edward D., Salvatore J. Cherra 3rd, Yong-Jian Liu, and Charleen T. Chu. 2008. "Role of Autophagy in G2019S-LRRK2-Associated Neurite Shortening in Differentiated SH-SY5Y Cells." Journal of Neurochemistry 105 (3): 1048–56.

Polymeropoulos, M. H., C. Lavedan, E. Leroy, S. E. Ide, A. Dehejia, A. Dutra, B. Pike, et al. 1997. "Mutation in the Alpha-Synuclein Gene Identified in Families with Parkinson's Disease." Science 276 (5321): 2045–47.

Pringsheim, Tamara, Nathalie Jette, Alexandra Frolkis, and Thomas D. L. Steeves. 2014. "The Prevalence of Parkinson's Disease: A Systematic Review and Meta-Analysis." Movement Disorders: Official Journal of the Movement Disorder Society 29 (13): 1583–90.

Puschmann, Andreas, Fabienne C. Fiesel, Thomas R. Caulfield, Roman Hudec, Maya Ando, Dominika Truban, Xu Hou, et al. 2017. "Heterozygous PINK1 p.G411S Increases Risk of Parkinson's Disease via a Dominant-Negative Mechanism." Brain: A Journal of Neurology 140 (1): 98–117.

Quintavalle, Cristina, Stefania Di Costanzo, Ciro Zanca, Immaculada Tasset, Alessandro Fraldi, Mariarosaria Incoronato, Peppino Mirabelli, et al. 2014. "Phosphorylation-Regulated Degradation of the Tumor-Suppressor Form of PED by Chaperone-Mediated Autophagy in Lung Cancer Cells." Journal of Cellular Physiology 229 (10):

1359–68.

Rabinowitz, Joshua D., and Eileen White. 2010. “Autophagy and Metabolism.” Science 330 (6009): 1344–48.

Ray, A., B. A. Martinez, L. A. Berkowitz, G. A. Caldwell, and K. A. Caldwell. 2014. “Mitochondrial Dysfunction, Oxidative Stress, and Neurodegeneration Elicited by a Bacterial Metabolite in a C. Elegans Parkinson’s Model.” Cell Death & Disease 5 (1): e984.

Roager, Henrik M., Lea B. S. Hansen, Martin I. Bahl, Henrik L. Frandsen, Vera Carvalho, Rikke J. Gøbel, Marlene D. Dalgaard, et al. 2016. “Colonic Transit Time Is Related to Bacterial Metabolism and Mucosal Turnover in the Gut.” Nature Microbiology 1 (9): 16093.

Saftig, Paul, and Judith Klumperman. 2009. “Lysosome Biogenesis and Lysosomal Membrane Proteins: Trafficking Meets Function.” Nature Reviews. Molecular Cell Biology 10 (9): 623–35.

Saha, Shamol, Peter E. A. Ash, Vivek Gowda, Liqun Liu, Orian Shirihai, and Benjamin Wolozin. 2015. “Mutations in LRRK2 Potentiate Age-Related Impairment of Autophagic Flux.” Molecular Neurodegeneration 10 (July): 26.

Saha, Shamol, Maria D. Guillily, Andrew Ferree, Joel Lanceta, Diane Chan, Joy Ghosh, Cindy H. Hsu, et al. 2009. “LRRK2 Modulates Vulnerability to Mitochondrial Dysfunction in Caenorhabditis Elegans.” The Journal of Neuroscience: The Official Journal of the Society for Neuroscience 29 (29): 9210–18.

Salat-Foix, D., K. Tran, R. Ranawaya, J. Meddings, and O. Suchowersky. 2012. “Increased Intestinal Permeability and Parkinson Disease Patients: Chicken or Egg?” The Canadian Journal of Neurological Sciences. Le Journal Canadien Des Sciences Neurologiques 39 (2): 185–88.

Salvador, N., C. Aguado, M. Horst, and E. Knecht. 2000. “Import of a Cytosolic Protein into Lysosomes by Chaperone-Mediated Autophagy Depends on Its Folding State.” The Journal of Biological Chemistry 275 (35): 27447–56.

Sampson, Timothy R., and Sarkis K. Mazmanian. 2015. “Control of Brain Development, Function, and Behavior by the Microbiome.” Cell Host & Microbe 17 (5): 565–76.

Schröder, Bernd A., Christian Wrocklage, Andrej Hasilik, and Paul Saftig. 2010. “The Proteome of Lysosomes.” Proteomics 10 (22): 4053–76.

Schwiertz, Andreas, Jörg Spiegel, Ulrich Dillmann, David Grundmann, Jan Bürmann, Klaus Faßbender, Karl-Herbert Schäfer, and Marcus M. Unger. 2018. “Fecal Markers of Intestinal Inflammation and Intestinal Permeability Are Elevated in Parkinson’s Disease.” Parkinsonism & Related Disorders 50 (May): 104–7.

Seibler, Philip, John Graziotto, Hyun Jeong, Filip Simunovic, Christine Klein, and Dimitri Krainc. 2011. "Mitochondrial Parkin Recruitment Is Impaired in Neurons Derived from Mutant PINK1 Induced Pluripotent Stem Cells." The Journal of Neuroscience: The Official Journal of the Society for Neuroscience 31 (16): 5970–76.

Sender, Ron, Shai Fuchs, and Ron Milo. 2016. "Revised Estimates for the Number of Human and Bacteria Cells in the Body." PLoS Biology 14 (8): e1002533.

Sharma, Manu, John P. A. Ioannidis, Jan O. Aasly, Grazia Annesi, Alexis Brice, Lars Bertram, Maria Bozi, et al. 2012. "A Multi-Centre Clinico-Genetic Analysis of the VPS35 Gene in Parkinson Disease Indicates Reduced Penetrance for Disease-Associated Variants." Journal of Medical Genetics 49 (11): 721–26.

Shen, Ting, Yumei Yue, Tingting He, Cong Huang, Boyi Qu, Wen Lv, and Hsin-Yi Lai. 2021. "The Association Between the Gut Microbiota and Parkinson's Disease, a Meta-Analysis." Frontiers in Aging Neuroscience 13 (February): 636545.

Song, Saera, Seoyeon Jang, Jeehye Park, Sunhoe Bang, Sekyu Choi, Kyum-Yil Kwon, Xiaoxi Zhuang, Eunjoon Kim, and Jongkyeong Chung. 2013. "Characterization of PINK1 (PTEN-Induced Putative Kinase 1) Mutations Associated with Parkinson Disease in Mammalian Cells and Drosophila." The Journal of Biological Chemistry 288 (8): 5660–72.

Spillantini, M. G., R. A. Crowther, R. Jakes, M. Hasegawa, and M. Goedert. 1998. "Alpha-Synuclein in Filamentous Inclusions of Lewy Bodies from Parkinson's Disease and Dementia with Lewy Bodies." Proceedings of the National Academy of Sciences of the United States of America 95 (11): 6469–73.

Sugawara, Kenji, Nobuo N. Suzuki, Yuko Fujioka, Noboru Mizushima, Yoshinori Ohsumi, and Fuyuhiko Inagaki. 2004. "The Crystal Structure of Microtubule-Associated Protein Light Chain 3, a Mammalian Homologue of Saccharomyces Cerevisiae Atg8." Genes to Cells: Devoted to Molecular & Cellular Mechanisms 9 (7): 611–18.

Svensson, Elisabeth, Erzsébet Horváth-Puhó, Reimar W. Thomsen, Jens Christian Djurhuus, Lars Pedersen, Per Borghammer, and Henrik Toft Sørensen. 2015. "Vagotomy and Subsequent Risk of Parkinson's Disease." Annals of Neurology 78 (4): 522–29.

Tamtaji, Omid Reza, Mohsen Taghizadeh, Reza Daneshvar Kakhaki, Ebrahim Kouchaki, Fereshteh Bahmani, Shokoofeh Borzabadi, Shahrbanoo Oryan, Alireza Mafi, and Zatollah Asemi. 2019. "Clinical and Metabolic Response to Probiotic Administration in People with Parkinson's Disease: A Randomized, Double-Blind, Placebo-Controlled Trial." Clinical Nutrition 38 (3): 1031–35.

Tan, Ai Huey, Chun Wie Chong, Shen-Yang Lim, Ivan Kok Seng Yap, Cindy Shuan Ju Teh, Mun Fai Loke, Sze-Looi Song, et al. 2021. "Gut Microbial Ecosystem in Parkinson Disease: New Clinicobiological Insights from Multi-Omics." Annals of Neurology 89 (3): 546–59.

Tang, Fu-Lei, Joanna R. Erion, Yun Tian, Wei Liu, Dong-Min Yin, Jian Ye, Baisha Tang, Lin Mei, and Wen-Cheng Xiong. 2015. "VPS35 in Dopamine Neurons Is Required for Endosome-to-Golgi Retrieval of Lamp2a, a Receptor of Chaperone-Mediated Autophagy That Is Critical for α-Synuclein Degradation and Prevention of Pathogenesis of Parkinson's Disease." The Journal of Neuroscience: The Official Journal of the Society for Neuroscience 35 (29): 10613–28.

Tanji, Kunikazu, Fumiaki Mori, Akiyoshi Kakita, Hitoshi Takahashi, and Koichi Wakabayashi. 2011. "Alteration of Autophagosomal Proteins (LC3, GABARAP and GATE-16) in Lewy Body Disease." Neurobiology of Disease 43 (3): 690–97.

Taymans, Jean-Marc, Matt Fell, Tim Greenamyre, Warren D. Hirst, Adamantios Mamais, Shalini Padmanabhan, Inga Peter, Hardy Rideout, and Avner Thaler. 2023. "Perspective on the Current State of the LRRK2 Field." NPJ Parkinson's Disease 9 (1): 104.

Theije, Caroline G. M. de, Harm Wopereis, Mohamed Ramadan, Tiemen van Eijndthoven, Jolanda Lambert, Jan Knol, Johan Garssen, Aletta D. Kraneveld, and Raish Oozeer. 2014. "Altered Gut Microbiota and Activity in a Murine Model of Autism Spectrum Disorders." Brain, Behavior, and Immunity 37 (March): 197–206.

Toh, Tzi Shin, Chun Wie Chong, Shen-Yang Lim, Jeff Bowman, Mihai Cirstea, Chin-Hsien Lin, Chieh-Chang Chen, Silke Appel-Cresswell, B. Brett Finlay, and Ai Huey Tan. 2022. "Gut Microbiome in Parkinson's Disease: New Insights from Meta-Analysis." Parkinsonism & Related Disorders 94 (January): 1–9.

Tooze, Sharon A. 2013. "Current Views on the Source of the Autophagosome Membrane." Essays in Biochemistry 55: 29–38.

Turnbaugh, Peter J., Ruth E. Ley, Micah Hamady, Claire M. Fraser-Liggett, Rob Knight, and Jeffrey I. Gordon. 2007. "The Human Microbiome Project." Nature 449 (7164): 804–10.

Unger, Marcus M., Jörg Spiegel, Klaus-Ulrich Dillmann, David Grundmann, Hannah Philippeit, Jan Bürmann, Klaus Faßbender, Andreas Schwiertz, and Karl-Herbert Schäfer. 2016. "Short Chain Fatty Acids and Gut Microbiota Differ between Patients with Parkinson's Disease and Age-Matched Controls." Parkinsonism & Related Disorders 32 (November): 66–72.

Valente, Enza Maria, Patrick M. Abou-Sleiman, Viviana Caputo, Miratul M. K. Muqit, Kirsten Harvey, Suzana Gispert, Zeeshan Ali, et al. 2004. "Hereditary Early-Onset

Parkinson's Disease Caused by Mutations in PINK1." Science 304 (5674): 1158–60.

Vandeputte, Doris, Gwen Falony, Sara Vieira-Silva, Raul Y. Tito, Marie Joossens, and Jeroen Raes. 2016. "Stool Consistency Is Strongly Associated with Gut Microbiota Richness and Composition, Enterotypes and Bacterial Growth Rates." Gut 65 (1): 57–62.

Vilariño-Güell, Carles, Christian Wider, Owen A. Ross, Justus C. Dachsel, Jennifer M. Kachergus, Sarah J. Lincoln, Alexandra I. Soto-Ortolaza, et al. 2011. "VPS35 Mutations in Parkinson Disease." American Journal of Human Genetics 89 (1): 162–67.

Vogt, Nicholas M., Robert L. Kerby, Kimberly A. Dill-McFarland, Sandra J. Harding, Andrew P. Merluzzi, Sterling C. Johnson, Cynthia M. Carlsson, et al. 2017. "Gut Microbiome Alterations in Alzheimer's Disease." Scientific Reports 7 (1): 13537.

Vyas, Usha, and Natarajan Ranganathan. 2012. "Probiotics, Prebiotics, and Synbiotics: Gut and beyond." Gastroenterology Research and Practice 2012 (September): 872716.

Wakabayashi, K., H. Takahashi, S. Takeda, E. Ohama, and F. Ikuta. 1988. "Parkinson's Disease: The Presence of Lewy Bodies in Auerbach's and Meissner's Plexuses." Acta Neuropathologica 76 (3): 217–21.

Wang, Chenyin, Chun Yin Lau, Fuqiang Ma, and Chaogu Zheng. 2021. "Genome-Wide Screen Identifies Curli Amyloid Fibril as a Bacterial Component Promoting Host Neurodegeneration." Proceedings of the National Academy of Sciences of the United States of America 118 (41). https://doi.org/10.1073/pnas.2116257118.

Wang, Lei, Zijian Zhao, Lei Zhao, Yujuan Zhao, Ge Yang, Chao Wang, Lei Gao, Chunhua Niu, and Shengyu Li. 2022. "Lactobacillus Plantarum DP189 Reduces α-SYN Aggravation in MPTP-Induced Parkinson's Disease Mice via Regulating Oxidative Damage, Inflammation, and Gut Microbiota Disorder." Journal of Agricultural and Food Chemistry 70 (4): 1163–73.

Wang, Lv, Claus T. Christophersen, Michael J. Sorich, Jacobus P. Gerber, Manya T. Angley, and Michael A. Conlon. 2011. "Low Relative Abundances of the Mucolytic Bacterium Akkermansia Muciniphila and Bifidobacterium Spp. in Feces of Children with Autism." Applied and Environmental Microbiology 77 (18): 6718–21.

Wang, Tingting, Guoxiang Cai, Yunping Qiu, Na Fei, Menghui Zhang, Xiaoyan Pang, Wei Jia, Sanjun Cai, and Liping Zhao. 2012. "Structural Segregation of Gut Microbiota between Colorectal Cancer Patients and Healthy Volunteers." The ISME Journal 6 (2): 320–29.

Weidberg, Hilla, Elena Shvets, Tomer Shpilka, Frida Shimron, Vera Shinder, and Zvulun Elazar. 2010. "LC3 and GATE-16/GABARAP Subfamilies Are Both Essential yet

Act Differently in Autophagosome Biogenesis." The EMBO Journal 29 (11): 1792–1802.

White, J. G., E. Southgate, J. N. Thomson, and S. Brenner. 1986. "The Structure of the Nervous System of the Nematode Caenorhabditis Elegans." Philosophical Transactions of the Royal Society of London. Series B, Biological Sciences 314 (1165): 1–340.

Williams, Erin T., Xi Chen, P. Anthony Otero, and Darren J. Moore. 2022. "Understanding the Contributions of VPS35 and the Retromer in Neurodegenerative Disease." Neurobiology of Disease 170 (August): 105768.

Wong, Pui-Mun, Cindy Puente, Ian G. Ganley, and Xuejun Jiang. 2013. "The ULK1 Complex: Sensing Nutrient Signals for Autophagy Activation." Autophagy 9 (2): 124–37.

Wong, Yvette C., and Erika L. F. Holzbaur. 2015. "Temporal Dynamics of PARK2/parkin and OPTN/optineurin Recruitment during the Mitophagy of Damaged Mitochondria." Autophagy 11 (2): 422–24.

Yang, Zhifen, and Daniel J. Klionsky. 2009. "An Overview of the Molecular Mechanism of Autophagy." Current Topics in Microbiology and Immunology 335: 1–32.

Yao, Chen, Rabih El Khoury, Wen Wang, Tara A. Byrd, Elizabeth A. Pehek, Colin Thacker, Xiongwei Zhu, Mark A. Smith, Amy L. Wilson-Delfosse, and Shu G. Chen. 2010. "LRRK2-Mediated Neurodegeneration and Dysfunction of Dopaminergic Neurons in a Caenorhabditis Elegans Model of Parkinson's Disease." Neurobiology of Disease 40 (1): 73–81.

Yin, Zhangyuan, Hana Popelka, Yuchen Lei, Ying Yang, and Daniel J. Klionsky. 2020. "The Roles of Ubiquitin in Mediating Autophagy." Cells 9 (9). https://doi.org/10.3390/cells9092025.

Youle, Richard J., and Derek P. Narendra. 2011. "Mechanisms of Mitophagy." Nature Reviews. Molecular Cell Biology 12 (1): 9–14.

Zavodszky, Eszter, Matthew N. J. Seaman, Kevin Moreau, Maria Jimenez-Sanchez, Sophia Y. Breusegem, Michael E. Harbour, and David C. Rubinsztein. 2014. "Mutation in VPS35 Associated with Parkinson's Disease Impairs WASH Complex Association and Inhibits Autophagy." Nature Communications 5 (May): 3828.

Zhao, J., X. Yuan, Z. Li, F. Li, L. Y. Kwok, and S. Zhang. 2022. "Probiotics Synergized with Conventional Regimen in Managing Parkinson's Disease." Parkinson's Disease. https://www.nature.com/articles/s41531-022-00327-6.

Zhou, Shaoyu, Zemin Wang, and James E. Klaunig. 2013. "Caenorhabditis Elegans Neuron Degeneration and Mitochondrial Suppression Caused by Selected

Environmental Chemicals." International Journal of Biochemistry and Molecular Biology 4 (4): 191–200.

Zhu, Feng, Chuling Li, Jianfeng Gong, Weiming Zhu, Lili Gu, and Ning Li. 2019. "The Risk of Parkinson's Disease in Inflammatory Bowel Disease: A Systematic Review and Meta-Analysis." Digestive and Liver Disease: Official Journal of the Italian Society of Gastroenterology and the Italian Association for the Study of the Liver 51 (1): 38–42.

Zhu, Jian-Hui, Fengli Guo, John Shelburne, Simon Watkins, and Charleen T. Chu. 2003. "Localization of Phosphorylated ERK/MAP Kinases to Mitochondria and Autophagosomes in Lewy Body Diseases." Brain Pathology 13 (4): 473–81.

Zimprich, Alexander, Anna Benet-Pagès, Walter Struhal, Elisabeth Graf, Sebastian H. Eck, Marc N. Offman, Dietrich Haubenberger, et al. 2011. "A Mutation in VPS35, Encoding a Subunit of the Retromer Complex, Causes Late-Onset Parkinson Disease." American Journal of Human Genetics 89 (1): 168–75.

CHAPTER TWO - Assessing the impact of anaerobic gut microbiotal bacteria on dopaminergic neurodegeneration in a *C. elegans* model of Parkinson's Disease

G. Sophie Ngana[1], Michael G. Surette[1,2,3], Lesley T. MacNeil[1,2,3]

[1]Department of Biochemistry and Biomedical Sciences, McMaster University, 1280 Main St W. Hamilton, ON, Canada, [2]Farncombe Family Digestive Health Research Institute, [3]Michael G. DeGroote Institute for Infectious Disease Research

Declaration: Research presented as part of this chapter has been prepared for publication

Contributions: GSN and LTM designed the experiments and wrote the manuscript. GSN performed all experiments and prepared the figures. MGS provided bacterial isolates.

Abstract

The human gastrointestinal tract is home to a complex community of trillions of microorganisms, predominantly bacteria, collectively known as the gut microbiota. Over the last decade, the role of the gut microbiota in human health has become increasingly apparent, with evidence demonstrating its contribution to nutrient metabolism, immune system development, immune function, neurodevelopment, and maintenance of the integrity of the gut mucosal barrier. Conversely, gut microbiota dysbiosis has been linked to many intra- and extraintestinal disorders, including Parkinson's Disease (PD), a chronic neurodegenerative disorder of the central nervous system. However, despite accumulating evidence linking the gut microbiota to the development of PD, minimal work has successfully identified causal mechanisms between bacterial molecules and the neurodegenerative process. Additionally, existing research centred on identifying bacterial modifiers of PD pathogenesis has largely focused on oxygen-tolerant bacteria despite over 99% of bacterial species residing in the colon being obligate anaerobes. In order to identify and interrogate the relationship between human gut commensals and the neurodegenerative process, we employed a single-bacterium approach, using the nematode *Caenorhabditis elegans* as a gnotobiotic model. Using animals expressing disease-associated G2019S mutant human leucine-rich repeat kinase (LRRK2) protein in dopaminergic neurons as a model for neurodegeneration, we were able to design a protocol to systematically test the influence of 57 bacteria, both facultative and obligate anaerobes, representative of the human gut microbiome to identify novel effects of human gut commensals on PD pathophysiology.

Introduction

Parkinson's disease (PD) is a complex progressive neurodegenerative disease affecting millions of elderly individuals globally (Pringsheim et al., 2014). PD is characterized by the selective degeneration of dopaminergic neurons, primarily in the substantia nigra pars compacta and the accumulation of alpha-synuclein enriched protein aggregates within neurons. (Polymeropoulos et al., 1997). The pathogenesis of PD is still not completely understood, and no treatments exist that target or alter disease progression. Obvious genetic causes are detected in only a small number of PD patients (~10%), suggesting that environmental factors, including the gut microbiota, play a major role in disease development (Migliore & Coppedè, 2009).

The human gut microbiota consists of a complex community of over 30 trillion microorganisms and an estimated 500-1000 bacteria species within the gastrointestinal tract (Sender et al., 2016; Turnbaugh et al., 2007). Over the last decade, the importance of the gut microbiota in human health has become increasingly evident, with alterations of its composition being reported in both intestinal and extraintestinal diseases, including PD (Z. Li et al., 2023; Shen et al., 2021; Toh et al., 2022). Simultaneously, emerging research has begun to characterize the influence of the gut microbiota on the nervous system via the gut-brain axis (Collins et al., 2012; Mayer, 2011). Despite the well-documented presence of taxonomic changes in the gut microbiota of PD patients, there is a paucity of evidence determining the causative relationship between bacterial molecules and disease pathogenesis. Various studies have examined the effects of select oxygen-tolerant probiotic species and laboratory bacterial strains in preclinical models of PD (Castelli et

al., 2020; Chen et al., 2016; Goya et al., 2020; L. Wang et al., 2022). However, few studies specifically investigate the effects of individual human gut commensals on PD pathophysiology, leaving a sizeable gap in the literature.

Researchers have primarily used gnotobiotic mice to study host-microbe interactions; however, their complex physiology limits the ability to resolve molecular-level mechanisms (Ortiz de Ora & Bess, 2021). The nematode *Caenorhabditis elegans*, a relatively simple organism with a well-characterized physiology, is a promising alternative gnotobiotic model for elucidating the impacts of bacterial molecules in disease contexts. In terms of suitability for host-microbiota studies, *C. elegans* are easily maintained monoxenically in laboratory conditions and are bacterivorous, allowing for the selective manipulation of their microbiota. Additionally, *C. elegans* has high conservation of underlying molecular pathways implicated in human disease with several well-established PD models. However, currently, there is a paucity of research using *C. elegans* as a model organism to examine the role of the gut microbiota in PD (Chen et al., 2016; Goya et al., 2020; C. Wang et al., 2021). Additionally, despite over 99% of bacterial species residing in the colon being obligate anaerobes (Eckburg et al., 2005), the majority of studies on host-microbiota interactions in the context of *C. elegans* research have focused primarily on oxygen-tolerant aerobically grown bacteria. The barriers of culturing obligate anaerobic bacteria in a laboratory environment are omnipresent, generally requiring specialized equipment and techniques. Therefore, we sought to develop a protocol to grow and examine the effects of a broad range of anaerobic human microbiotal isolates on PD pathophysiology using the nematode as a model organism.

The age-dependent loss of dopaminergic neurons is a major pathological hallmark of PD. For the purposes of our study, we opted to use *LRRK2* transgenic animals as a model of neurodegeneration. Leucine-rich repeat kinase 2 (*LRRK2*) mutations are the most common genetic risk factor in both familial and sporadic PD, accounting for 4% of familial and 1% of sporadic PD across all populations (Healy et al., 2008). The strain SCG856, used in this work, drives expression of disease-associated G2019S mutant human LRRK2 protein in dopaminergic neurons via the *dat-1* promoter (*lin-15*(*n765ts*)*; cwrIs856* [*dat-1p::GFP, dat-1p::LRRK2*(*G2019S*)*, lin-15*(+)]) while using the same promoter to drive expression of GFP for visualization of the neurons. In addition to exhibiting age-dependent dopaminergic neurodegeneration, these animals also experience motor dysfunction and deficits in dopamine-dependent behaviours (Cooper et al., 2015; Yao et al., 2010). The BZ555 strain, carrying only the dopaminergic neuronal marker (*egIs1*[*dat-1p::GFP*]), acted as a control. Using these strains and our developed protocol, we were able to successfully screen 57 facultative and obligate microbiotal isolates to identify bacteria influencing neurodegeneration.

Materials and Methods

Media Preparation

Brain Heart Infusion 3 (BHI3) Broth + 5% Fetal Bovine Serum (FBS), 500 mL	
Brain Heart Infusion Broth	18.5 g
H_2O	470 mL
Autoclave and let cool to 50-55°C, then add:	

50 mg/mL L-cysteine in 1.0M HCl	5 mL
10 mM hemin in 0.1M NaOH	766.5 µL
5 mg/mL vitamin K_1 in ethanol	100 µL
FBS (Heat inactivate for 30 minutes at 56°C with mixing)	25 mL
Note: Add 7.5 g agar prior to autoclaving to make solid media plates	

Nematode Growth Media (NGM), 500 mL	
NaCl	1.5 g
Peptone	1.25 g
Agar	8.5 g
H_2O	487.5 mL
Autoclave and let cool to 50-55°C, then add:	
1M $MgSO_4$	500 µL
1M $CaCl_2$	500 µL
5 mg/mL cholesterol in ethanol	500 µL
12.5 mL 1M KPO_4 (pH = 6.0)	12.5 mL
Note: Add 165 µL 150 mM 5-Fluoro-2′-deoxyuridine (FUDR) and 500 µL 100 mg/mL Ampicillin (Amp) to make NGM Amp/FUDR plates	

Bleaching Solution, 10 mL	
H_2O	7 mL
5% w/v sodium hypochlorite	2 mL
5M NaOH	1 mL

M9 Buffer, 500 mL	
KH_2PO_4	1.5 g

Na_2HPO_4	3 g
NaCl	2.5 g
Autoclave and let cool to 50-55°C, then add:	
1M $MgSO_4$	500 µL

Equipment

Anaerobic environments were achieved using the Advanced Anoxomat® III jar system as an alternative to an anaerobic chamber. All bacterial culture techniques were done aerobically, as rapidly as possible to minimize oxygen exposure, in a Biosafety Level 2 biological safety cabinet.

C. elegans strains and maintenance conditions

C. elegans strains were handled according to standard procedures for nematode maintenance (Stiernagle, 2006). Animals were grown and maintained at 20°C on nematode growth medium (NGM) plates seeded with the non-pathogenic *Escherichia coli* OP50. The following strains were used to evaluate dopaminergic neurodegeneration: BZ555 (*egIs1*[*dat-1p::GFP*]) (obtained from the Caenorhabditis Genetics Center) and SGC856 (*lin-15*(*n765ts*)*; cwrIs856*[*Pdat-1::GFP, Pdat-1::LRRK2*(*G2019S*)*, lin-15*(+)]) (a gift from Dr. Shu G. Chen, University of Alabama at Birmingham).

Protocol

A. Preparation of anaerobic lawns

Three to five millilitres of BHI3 + 5% FBS broth was aliquoted into 14 mL snap cap culture tubes. BHI3 + 5% FBS broth can be made in advance and stored for up to four

months at room temperature. To equilibrate the media, the aliquoted broth was transferred to anaerobic conditions, with the lids of the culture tubes in the loose position. This was done a minimum of 24 hours prior to inoculation to ensure oxygen-free conditions in the cultivation media. Bacterial strains were inoculated from frozen glycerol stocks and incubated anaerobically for 48-72 hours at 37°C. Sixty-millimetre BHI3 + 5% FBS agar plates were equilibrated in anaerobic conditions 24 hours prior to the completion of the culture intubation period. BHI3 + 5% FBS agar plates can be made in advance and stored for up to one month at 4°C. Cultures that grew successfully had a visible bacterial pellet at the bottom of the culture tube. Excess BHI3 + 5% FBS media was slowly removed to avoid disturbing the pellet, leaving only 1 mL of liquid. The bacterial pellet was resuspended in the remaining media, and 50 µL of concentrated culture was dispensed per 60 mm equilibrated BHI3 + 5% FBS agar plate. BHI3 + 5% FBS agar plates were seeded by spreading the culture evenly using a sterile L-shaped spreader, avoiding the edges of the agar. Plates were allowed to dry and then incubated anaerobically for 24-72 h at 37°C. Anaerobic bacterial lawns were gently scraped off the BHI3 + 5% FBS agar plates and transferred to 60 mm NGM Amp/FUDR plates using a sterile L-shaped spreader, avoiding the transfer of pieces of the BHI3 + 5% FBS agar. Two to three anaerobic bacterial lawns were transferred per NGM Amp/FUDR plate, depending on the growth, to ensure sufficient bacteria for the worms over the course of the experiment. NGM Amp/FUDR plates were prepared fresh for each experiment. NGM is supplemented with ampicillin (Amp) to prevent foreign bacterial contamination. Additionally, supplementation with 5-Fluoro-2′-deoxyuridine (FUDR) is done to inhibit embryo production and development in

order to isolate aging animals. The bacteria were gently spread across the NGM Amp/FUDR plate to form a uniform lawn. If the surface of the agar was at all disturbed, the process was restarted with a fresh plate, as the worms have a tendency to burrow into broken agar. Anaerobic bacterial lawns were used immediately after preparation. *E. coli* OP30 control lawns were generated by inoculating 3-5 mL of Luria-Bertani (LB) Broth with a single colony of *E. coli* OP50. Cultures were incubated overnight in a 37°C shaking incubator. BHI3 + 5% FBS agar plates were seeded with 50 µL of culture and incubated at 37°C overnight to allow lawn growth. *E. coli* OP50 lawns were transferred to the NGM Amp/FUDR plates using a similar technique as described with the anaerobic bacteria. Half an E. *coli* OP50 lawn was transferred per NGM amp/FUDR plate. Lawns were used immediately after preparation.

B. *C. elegans* population synchronization

Plates with plenty of gravid adults and embryos from each of the required strains were identified. Animals and embryos were washed off the plate using M9 into a 15 mL conical tube. Worms and embryos were pelleted via centrifugation for 2 minutes at 300 g. The supernatant was removed and discarded, being mindful not to disturb the pellet. Two and a half millilitres of bleaching solution and 2.5 mL of M9 were added to each pellet. Tubes were gently agitated for 5-10 minutes but no longer than 10 minutes to avoid embryo damage. Tubes were checked under the microscope at the end of the bleaching process to ensure no animal carcasses remained. M9 was added to a complete volume of 15 mL, followed by gentle mixing to stop the bleaching process. Embryos were centrifuged for 2 minutes at 300 g. The supernatant was removed without disturbing the pellet. The volume

was topped up to 10 mL with M9, and the pellet was resuspended in solution to complete the wash. This process was repeated three times to wash the embryos sufficiently. The supernatant was removed, and the pellet resuspended in 7.5 mL of M9 after the third wash. Embryos were hatched and synchronized for 18-24 hours at 20°C with nutation to ensure proper aeration. Twenty microlitres of the synchronized suspension of L1s (first larval stage) was dispensed onto the lid of a Petri plate. The number of L1s present in the droplet was counted, and the volume required to obtain 100 animals was calculated. The calculated volume was dispensed onto 60 mm *E. coli* OP50 seeded NGM plates, with inversion of the suspension between plates to ensure even distribution of the animals in the solution. Three plates of the appropriate strain were prepared per condition for technical replicates. Excess liquid was dried, and plates were placed at 20°C. Forty to 48 hours post-plating, L1 animals were checked to confirm that they had reached the fourth larval stage (L4). Worms were washed off the plates into 1.5 mL Eppendorf tubes, keeping the population of one plate per Eppendorf. Animals were allowed to pellet via gravity for approximately one minute. The supernatant was removed without disturbing the pellet, and 1 mL of M9 was added. Tubes were then inverted to gently wash the worms. This process was repeated three times to sufficiently wash the animals. After the final wash, the supernatant was removed, leaving the pellet undisturbed. A glass Pasteur pipette was used to transfer the population of worms from a single Eppendorf to individual NGM amp/FUDR plates with the anaerobic bacterial lawns or the control *E. coli* OP50 lawns. Excess liquid was allowed to dry, and plates were placed at 20°C. Plates

were checked for a couple of days post-transfer to ensure that no progeny hatched or developed. Worms were incubated until they reached day 7 of adulthood.

C. Dopaminergic neurodegeneration assay

A 2% agarose solution was prepared in water and boiled to melt. A clean microscope slide was placed between two slides with tape across them. A drop of molten agarose was placed on the center slide using a glass Pasteur pipette. A fourth slide was immediately placed on top of the agarose perpendicular to and across all three slides. The slide was gently pressed down to flatten the agarose to the thickness of the tape. Once the agarose had set, the taped slides were removed. The remaining slides were separated by carefully sliding them apart. Agarose slides were prepared as needed and made fresh to avoid them drying out. Worms were washed off a plate into a 1.5 mL Eppendorf tube. Animals were allowed to pellet via gravity for approximately one minute. As much supernatant as possible was removed without disturbing the pellet. Five microliters of % 0.1 sodium azide or 12 mM levamisole was added to the pellet to anesthetize the worms. Worms were transferred to the prepared agarose pad, and a coverslip was gently lowered over the animals. The presence and health of the cephalic (CEP) neurons were assessed using a microscope that allows for the visualization of GFP. A minimum of thirty animals were scored per replicate. Neurons that exhibited blebbing, breaks or dendritic loss were counted as degenerated (Figure 1). All replicates were scored across all conditions.

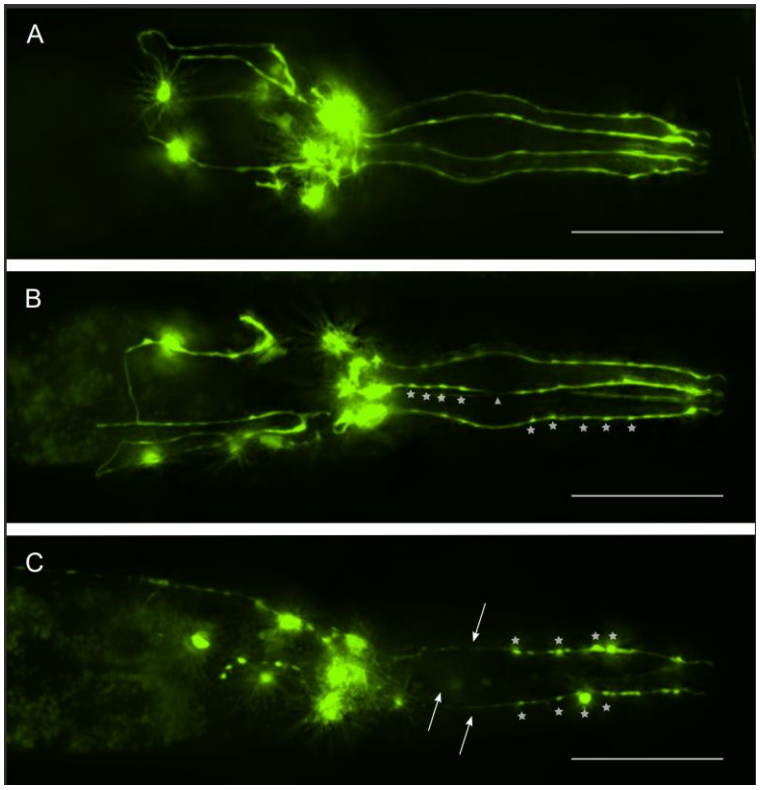

Figure 1. *LRRK2(G2019S)* expression leads to dopaminergic neurodegeneration. Representative images of the head regions of day-7 adults of strain SGC856 (*lin-15*(*n765ts*)*; cwrIs856*[*dat-1p::GFP, dat-1p::LRRK2*(*G2019S*)*, lin-15*(+)]). The images show (A) four healthy CEP neurons with cellular processes, or dendrites, extending from the pharynx to the tip of the nose, (B) mild blebbing (stars) and abrupt gaps or breaks (arrowhead) along the dendrites and (C) a more severe pattern of blebbing (stars) and dendritic loss (arrows). (Scale bars, 100 μm).

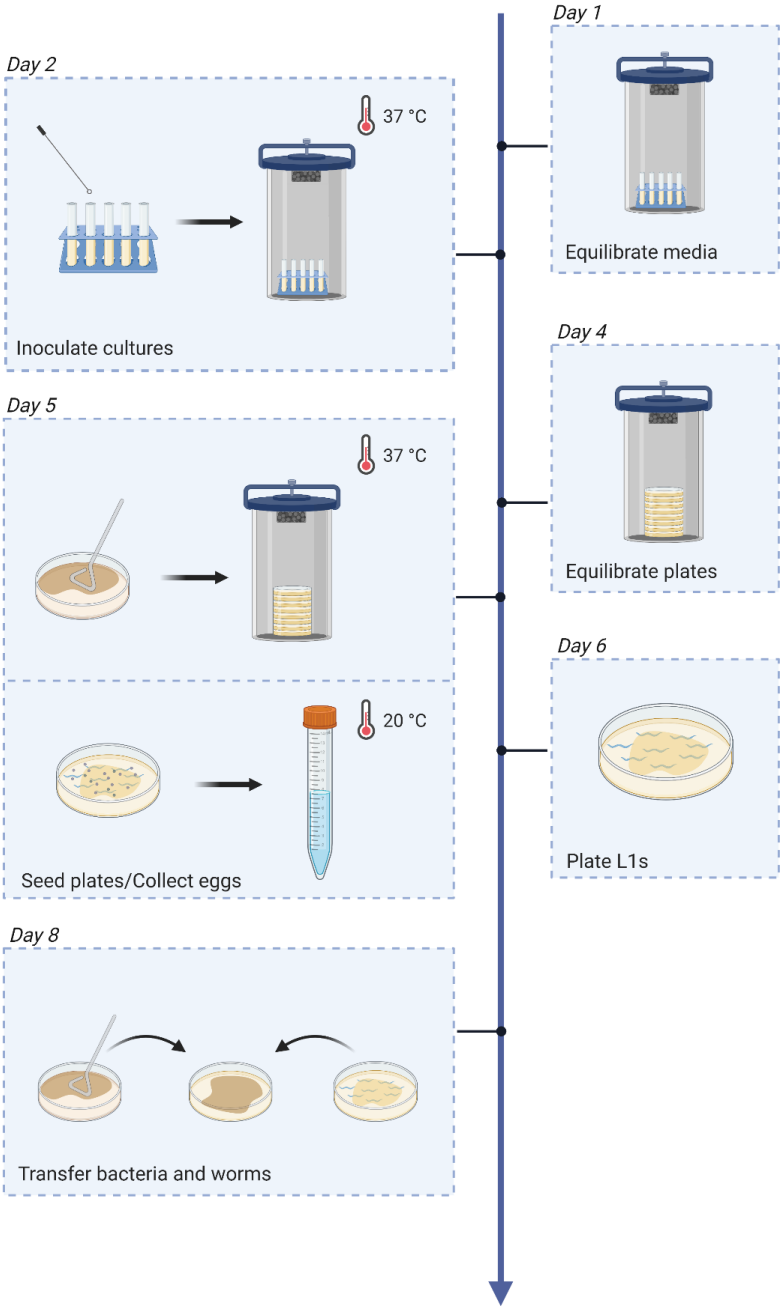

Figure 2. Microbiotal isolate screen protocol workflow. Liquid and solid media were equilibrated in anaerobic conditions for a minimum of 24 hours prior to use. Both liquid cultures and bacterial lawns were incubated for 72 hours at 37°C to maximize growth. Eggs were collected via hypochlorite treatment of gravid adults and hatch for 18-24h to obtain a synchronized population of L1s. Animals were then transferred to microbiotal isolates as L4s. *Figure created with BioRender.com*.

Results

In order to successfully screen microbiotal isolates for their influence on PD pathophysiology, we first developed a reliable protocol for the growth of sufficient bacteria to avoid nematode starvation during exposure. BHI Broth, a non-selective nutrient-rich media, was used for both liquid and solid culture media, given its ability to accommodate the growth of a wide variety of fastidious microorganisms. BHI was supplemented with hemin and vitamin K_1 to support the growth of the anaerobes, especially the *Bacteroides* and *Prevotella* species, representing approximately 30% of the library (Finegold et al., 1974; Gibbons & Macdonald, 1960; Mac Faddin, 1985). Similarly, media was supplemented with FBS for its growth-supporting properties (Shibayama et al., 2006), and L-cysteine was added as a relatively non-toxic reducing agent to support anaerobic conditions (Fukushima et al., 2003). Given that more fastidious bacteria grow poorly in liquid broth (Speers et al., 2009; Wornell et al., 2022), we opted to use solid media to facilitate the majority of bacterial growth. We were mindful of the potential for these bacteria, a novel food source, to exert developmental effects on our model organism. Therefore, we transferred animals from *E. coli* OP50 to the experimental bacteria at L4, bypassing larval development, in order to maintain a developmentally synchronous population throughout the study. This would allow us to capture changes in neurodegeneration unrelated to the developmental age of the animal. Additionally, as our study focused on aging animals, we supplemented NGM with FUDR to inhibit embryo production and development. For this reason, microbiotal bacteria were

grown separately on BHI3 + 5% FBS agar plates and transferred to experimental plates to avoid FUDR, a bacteriostatic and bactericidal compound, from inhibiting growth.

To assess the effects of the human gut microbiota on neurodegeneration, we used an established *C. elegans* model of PD, strain SCG856, expressing the pathogenic human *LRRK2(G2019S)* in dopaminergic neurons via the *dat-1* promoter while using the same promoter to drive expression of GFP for visualization of the neurons (*lin-15*(*n765ts*)*; cwrIs856* [*dat-1p::GFP, dat-1p::LRRK2*(*G2019S*)*, lin-15*(+)]) (Yao et al., 2010). The BZ555 strain was used as a control, carrying only the dopaminergic neuronal GFP marker (*egIs1*[*dat-1p::GFP*]). We sought to establish when the *LRRK2* transgenic animals exhibit significant and reproducible neurodegeneration compared to the control strain on *E. coli* OP50, the standard laboratory diet of *C. elegans*. We assayed dopaminergic neurodegeneration by scoring degenerative phenotypes in the CEP neurons of adult animals (Figure 1). We determined that *LRRK2* transgenic animals consistently exhibited significant dopaminergic neurodegeneration at day 7 of adulthood (Figure 3). All assays were scored at day 7 adulthood as a result.

Using our developed protocol, we were able to screen 57 bacterial strains (Table 1), representing the predominant phyla of the human gut microbiota, for their impacts on dopaminergic neurodegeneration in *LRRK2* transgenic (Figure 3B) and wildtype animals. Recent estimates suggest that these three phyla, Actinobacteria (predominantly *Bifidobacterium*), Firmicute (predominantly *Clostridium*) and Bacteroidetes (predominantly *Bacteroides* and *Prevotella*) constitute 20%, 40%, and 19.7% of intestinal bacterial species, respectively (Arumugam et al., 2011; King et al., 2019). In the

initial screen, nine strains were neuroprotective in *LRRK2* transgenic animals, including *Alistipes shahii* WAL 8301*, Actinomyces oris, Actinomyces naeslundii, Actinomyces viscosus, Butyricimonas paravirosa, Butyricimonas virosa, Bifidobacterium dentium, Eggerthella lenta and Odoribacter laneus* YIT 12061 (Figure 4). Similarly, six strains promoted neurodegeneration in *LRRK2* transgenic animals, including *Bifidobacterium scardovii, Parabacteroides merdae, Corynebacterium durum, Phocaeicola vulgatus* ATCC 8482, *Bacteroides intestinalis*, *Coprobacter fastidiosus* NSB1 (Figure 4). Interestingly, *Coprobacter fastidiosus* NSB1, *Parabacteroides merdae, and Bifidobacterium scardovii* also induced dopaminergic neurodegeneration in a wildtype genetic background independent of *LRRK2(G2019S)* expression.

To validate these pilot screen hits, we retested these bacteria to determine the reproducibility of the effects seen in the initial screen. During the second trial, six of the nine neuroprotective bacteria identified in the screen reproduced the effect (*Alistipes shahii* WAL 8301, *Actinomyces oris, Actinomyces naeslundii, Actinomyces viscosus, Butyricimonas paravirosa* and *Butyricimonas virosa*) and one of the six neurodegenerative bacteria identified in the screen reproduced the effect (*Parabacteroides merdae*). We then ran a final set of neurodegenerative assays and found that *Alistipes shahii* WAL 8301, *Actinomyces oris, Actinomyces naeslundii, Actinomyces viscosus* and *Butyricimonas paravirosa* were again neuroprotective (Figure 5, Table 2). Next, using NCBI taxonomy, we generated a phylogenetic tree to determine any lineage similarities between the *Actinoymces* species, *Alistipes shahii* WAL 8301 and *Butyricimonas paravirosa* as well as their similarity to other species within the library

(Figure 6). The *Actinomyces* species, *Butyricimonas paravirosa* and *Alistipes shahii* were more closely related to other species in the screen than to each other. Identification of three neuroprotective *Actinomyces* species may suggest that the mechanisms underlying the neuroprotective properties of these bacteria are similar and may potentially be intrinsic to the genus. However, more *Actinomyces* strains must be tested to determine if this is the case.

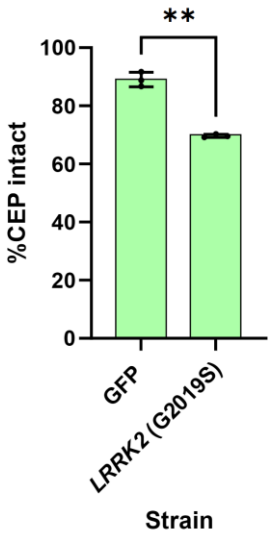

Figure 3. *LRRK2* transgenic animals exhibit neurodegeneration at day 7 adulthood
LRRK2(G2019S) expression leads to dopaminergic neurodegeneration. Dopaminergic neurodegeneration was quantified by the loss of CEP neurons in SCG856 (*LRRK2* (G2019S)) and BZ555 (GFP) animals grown to adult day 7. Each point represents an independent trial of >60 worms for a total of 3 independent trials. The total number of CEP neurons expected from all animals (4 per animal) was regarded as 100%, and the number of degenerated CEP neurons detected in each experiment was used to calculate the percent intact dopaminergic neurons. Error bars indicate SD. Statistical significance was calculated using an unpaired t-test with Welch's correction ** $p < 0.01$. SGC856; (*lin-15*(*n765ts*)*; cwrIs856* [*dat-1p::GFP, dat-1p::LRRK2*(*G2019S*)*, lin-15*(+)]), BZ555; (*egIs1*[*dat-1p::GFP*])

Table 1. List of microbiotal isolates screened. Fifty-seven bacteria representative of the human gut microbiome tested in neurodegeneration assays for neuroprotective or neurodegenerative properties categorized by phyla.

Bacteroidota	
Alistipes communis	*Bacteroides fragilis*
Alistipes finegoldii	*Bacteroides intestinalis*
Alistipes indistinctus YIT 12060	*Barnesiella intestinihominis* YIT 11860
Alistipes onderdonkii	*Butyricimonas paravirosa*
Alistipes putredinis	*Butyricimonas virosa*
Alistipes senegalensis JC50	*Coprobacter fastidiosus* NSB1
Alistipes shahii WAL 8301	*Odoribacter laneus* YIT 12061
Bacteroides caccae	*Odoribacter splanchnicus*
Bacteroides nordii WAL 11050 = JCM 12987	*Parabacteroides distasonis*
Bacteroides ovatus	*Parabacteroides merdae*
Bacteroides stercoris ATCC 43183	*Paraprevotella clara*
Bacteroides thetaiotaomicron	*Paraprevotella clara* YIT 11840
Bacteroides uniformis	*Phocaeicola dorei*
Bacteroides xylanisolvens XB1A	*Phocaeicola massiliensis*
Bacteroides caecimuris	*Phocaeicola vulgatus* ATCC 8482
Bacteroides cellulosilyticus	*Prevotella histicola*
Bacteroides clarus YIT12056	*Prevotella melaninogenica* ATCC 25845
Bacteroides eggerthii	*Prevotella salivae*
Bacteroides faecis MAJ27	*Tidjanibacter massiliensis*
Bacteroides finegoldii	
Actinomycetota	
Actinomyces naeslundii	*Bifidobacterium pseudocatenulatum*
Actinomyces oris	*Bifidobacterium scardovii*
Actinomyces viscosus	*Corynebacterium coyleae*
Bifidobacterium adolescentis ATCC 15703	*Corynebacterium durum*
Bifidobacterium breve	*Corynebacterium simulans*
Bifidobacterium dentium	*Eggerthella lenta*
Bifidobacterium faecale	*Rothia mucilaginosa*
Bifidobacterium longum subsp.	*Schaalia odontolytica*
Bifidobacterium adolescentis JCM 15918	
Bacillota	
Bacillus subtilis	

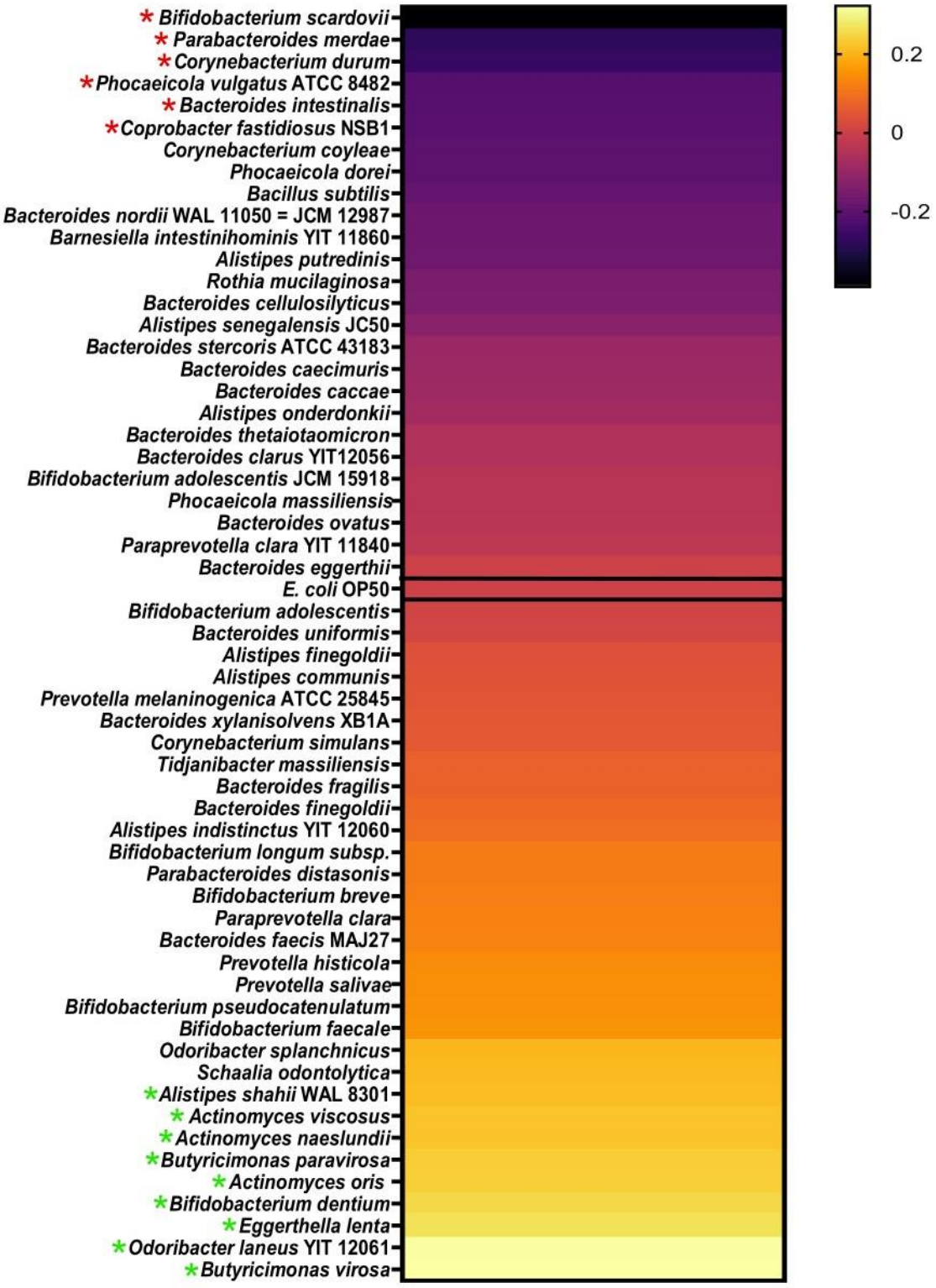
* Bifidobacterium scardovii
* Parabacteroides merdae
* Corynebacterium durum
* Phocaeicola vulgatus ATCC 8482
* Bacteroides intestinalis
* Coprobacter fastidiosus NSB1
Corynebacterium coyleae
Phocaeicola dorei
Bacillus subtilis
Bacteroides nordii WAL 11050 = JCM 12987
Barnesiella intestinihominis YIT 11860
Alistipes putredinis
Rothia mucilaginosa
Bacteroides cellulosilyticus
Alistipes senegalensis JC50
Bacteroides stercoris ATCC 43183
Bacteroides caecimuris
Bacteroides caccae
Alistipes onderdonkii
Bacteroides thetaiotaomicron
Bacteroides clarus YIT12056
Bifidobacterium adolescentis JCM 15918
Phocaeicola massiliensis
Bacteroides ovatus
Paraprevotella clara YIT 11840
Bacteroides eggerthii
E. coli OP50
Bifidobacterium adolescentis
Bacteroides uniformis
Alistipes finegoldii
Alistipes communis
Prevotella melaninogenica ATCC 25845
Bacteroides xylanisolvens XB1A
Corynebacterium simulans
Tidjanibacter massiliensis
Bacteroides fragilis
Bacteroides finegoldii
Alistipes indistinctus YIT 12060
Bifidobacterium longum subsp.
Parabacteroides distasonis
Bifidobacterium breve
Paraprevotella clara
Bacteroides faecis MAJ27
Prevotella histicola
Prevotella salivae
Bifidobacterium pseudocatenulatum
Bifidobacterium faecale
Odoribacter splanchnicus
Schaalia odontolytica
* Alistipes shahii WAL 8301
* Actinomyces viscosus
* Actinomyces naeslundii
* Butyricimonas paravirosa
* Actinomyces oris
* Bifidobacterium dentium
* Eggerthella lenta
* Odoribacter laneus YIT 12061
* Butyricimonas virosa
0.2
0
-0.2

Figure 4. Microbiota species influence neurodegeneration in *C. elegans*.
Microbiotal isolates influence neurodegeneration in *LRRK2* transgenic animals. Log2Fold change in the percentage of intact CEP neurons observed in SGC856 (*lin-15*(*n765ts*)*; cwrIs856*[*Pdat-1::GFP, Pdat-1::LRRK2*(*G2019S*)*, lin-15*(+)]) worms grown on the 57 screened bacteria normalized to those grown on *E. coli* OP50 (indicated in the black box). Per bacterial strain, >70 worms were scored across three technical replicates. Strains to the left of *E. coli* OP50 are more neurodegenerative than OP50, and those to the right are more neuroprotective than OP50. Strains denoted by a red asterisk (*) significantly increased neurodegeneration in the initial screen. Strains denoted by a green asterisk (*) significantly decreased neurodegeneration in the initial screen. Raw data was analyzed via two-way ANOVA with Tukey's multiple comparisons test * $p < 0.05$.

Table 2. Summary of bacteria identified as being neuroprotective or neurodegenerative in the initial screen and the two subsequent replication experiments.

Screen Hits	
Neuroprotective bacteria	Neurodegenerative bacteria
Alistipes shahii WAL 8301	*Corynebacterium durum*
Actinomyces oris	*Phocaeicola vulgatus* ATCC 8482
Actinomyces naeslundii	*Bacteroides intestinalis*
Actinomyces viscosus	*Coprobacter fastidiosus* NSB1
Butyricimonas paravirosa	*Parabacteroides merdae*
Butyricimonas virosa	*Bifidobacterium scardovii*
Bifidobacterium dentium	
Odoribacter laneus YIT 12061	
Eggerthella lenta	
Replication Experiment 1	
Neuroprotective bacteria	Neurodegenerative bacteria
Alistipes shahii WAL 8301	*Parabacteroides merdae*
Actinomyces oris	
Actinomyces naeslundii	
Actinomyces viscosus	
Butyricimonas paravirosa	
Butyricimonas virosa	
Replication Experiment 2	
Neuroprotective bacteria	Neurodegenerative bacteria
Alistipes shahii WAL 8301	
Actinomyces oris	
Actinomyces naeslundii	
Actinomyces viscosus	
Butyricimonas paravirosa	

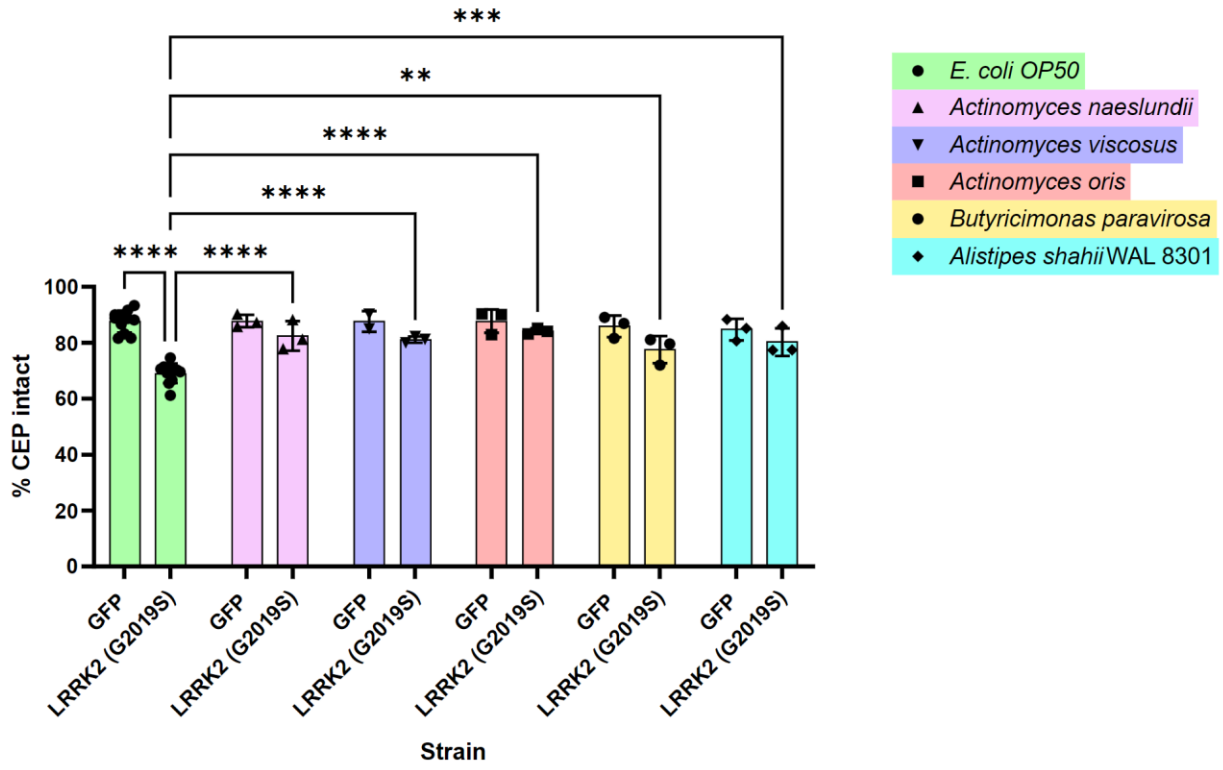

Figure 5. Microbiotal isolates are neuroprotective in *LRRK2* transgenic animals
LRRK2(G2019S) expression leads to dopaminergic neurodegeneration, rescued by exposure to *Actinomyces naeslundii, Actinomyces viscosus, Actinomyces oris, Butyricimonas paravirosa,* and *Alistipes shahii* WAL 8301. Dopaminergic neurodegeneration was quantified by the loss of CEP neurons in SCG856 (*LRRK2* (G2019S)) and BZ555 (GFP) grown to adult day 7. Each point represents an independent trial of >60 worms for a total of 3 independent trials. The total number of CEP neurons expected from all animals (4 per animal) was regarded as 100%, and the number of degenerated CEP neurons detected in each experiment was used to calculate the percent intact dopaminergic neurons. Error bars indicate SD. Statistical significance was calculated using two-way ANOVA with Sidak's multiple comparisons test ** p <0.01 *** p <0.001 **** p <0.0001. SGC856; (*lin-15*(*n765ts*)*; cwrIs856* [*dat-1p::GFP, dat-1p::LRRK2*(*G2019S*)*, lin-15*(+)]), BZ555; (*egIs1*[*dat-1p::GFP*]).

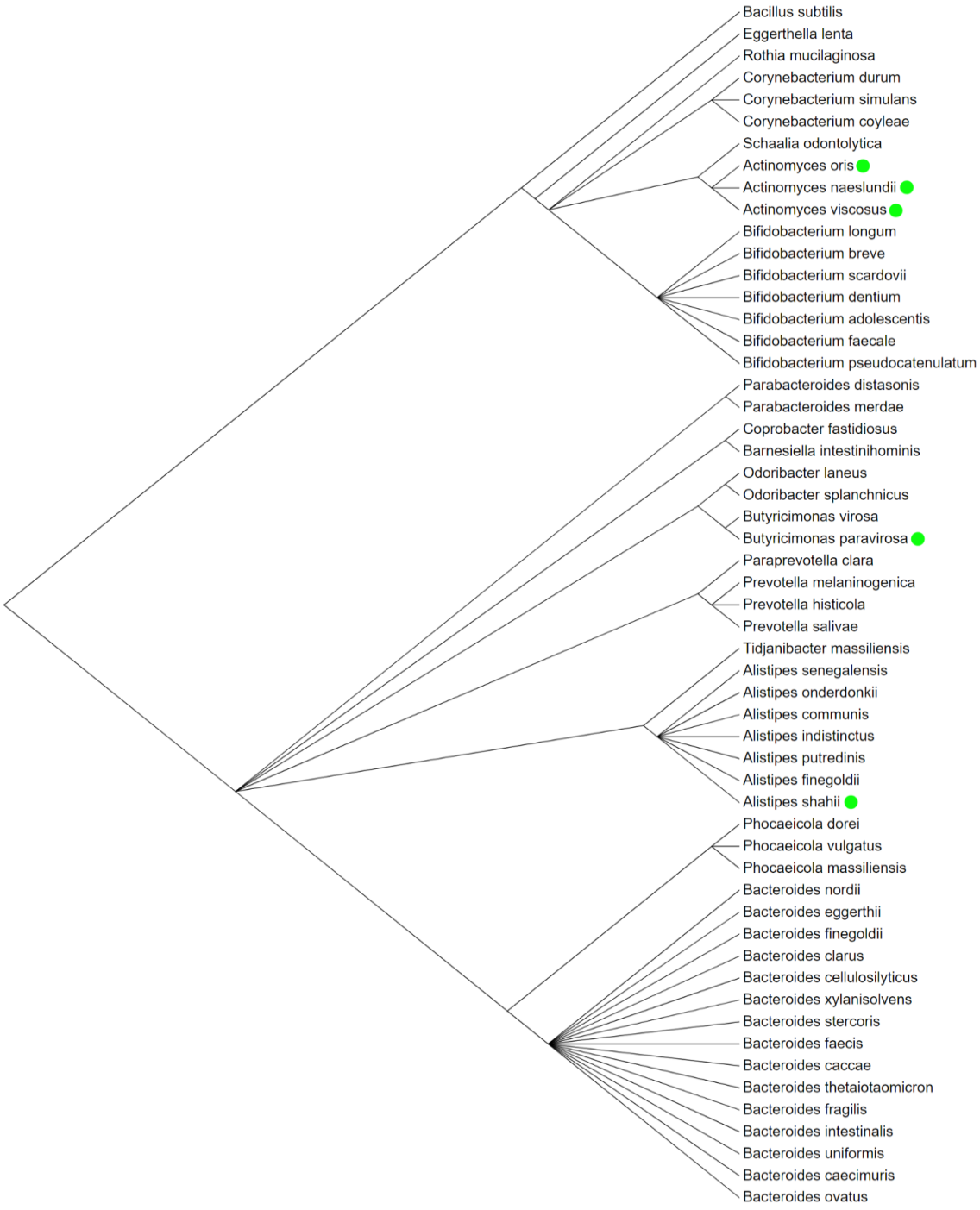

Figure 6. Phylogenetic tree of screened microbiotal isolates. A phylogenetic tree was generated based on the NCBI taxonomy. Species highlighted with a green circle were significantly neuroprotective in 3 independent trials.

Discussion

The cellular mechanisms underlying the connection between the gastrointestinal environment and the central nervous system, and more specifically, the role it plays in PD, are largely uncharacterized. Using this protocol and *C. elegans* as a model, we were able to take a single-bacterium approach to determine the effects of individual species on neurodegeneration. A research group successfully identified anaerobically grown probiotic bacteria *L. helveticus, L. plantarum, L. rhamnosus, B. infantis*, and *B. longum* were able to increase longevity in *C. elegans* (Ikeda et al., 2007), demonstrating the ability of anaerobes to tangibly impact host health. However, the effects of anaerobically grown bacteria on *C. elegans* host physiology are largely unexplored, given existing barriers surrounding the growth and maintenance of anaerobic species. Therefore, we developed and optimized a protocol applicable in various laboratory contexts. Additionally, this protocol is highly adaptable to alternative *C. elegans* disease models. This protocol was intentionally developed with the understanding that anaerobic chambers may not be easily accessible at all research institutions. The Advanced Anoxomat® III jar system and comparable systems lower the barrier of entry for researchers interested in cultivating and testing anaerobic bacteria. Using the jar system, we were able to successfully grow not only facultative but obligate anaerobes, including *Alistipes shahii* and *Bacteroides fragilis.* However, this system may not be ideal for less aerotolerant species, which may require an anaerobic chamber for cultivation. Furthermore, the use of the jar system introduces a level of variability in the growth conditions, with varying levels of bacterial oxygen exposure between independent

experiments. A study of *E. coli* identified significant changes in gene expression between anaerobic and aerobic metabolism (von Wulffen et al., 2016), suggesting activation of different bacterial pathways in response to the environment. The differential expression of bacteria genes in response to oxygen exposure may explain the varied reproducibility seen with the screen validation experiments.

C. elegans as an organism has minimal tolerance for anaerobic conditions undergoing arrest and eventual death in anoxic environments (Padilla et al., 2002; Van Voorhies & Ward, 2000). Therefore, despite the benefits of *C. elegans* as a model organism, the use of the nematode in this context necessitates the eventual exposure of the bacteria to an aerobic environment, resulting in an inability to capture the effects of live obligate anaerobe-host interactions. However, previous work has identified the benefits of dead bacteria on *C. elegans* health span (Nakagawa et al., 2016; S. Wang et al., 2020), therefore validating the utility of testing obligate anaerobes for the potential of identifying stable bioactive molecules that affect host physiology. Specifically, bioactive molecules from bacteria have yielded important therapeutics in the treatment of other diseases, and so the identification of neuroprotective factors in microbiotal bacteria, including through the screening of aero-intolerant obligate anaerobes, may lead to the development of novel therapeutics in the treatment of PD. Additionally, despite these limitations, we were able to identify a novel neuroprotective, strictly anaerobic strain, *Alistipes shahii* WAL 8301 (Song et al., 2006).

The results of the screen and subsequent replication experiments identified five reproducibly neuroprotective bacteria: *Alistipes shahii* WAL 8301, *Actinomyces oris,*

Actinomyces naeslundii, Actinomyces viscosus and *Butyricimonas paravirosa*. Interestingly, the genus *Alistipes* has been identified as having an increased abundance in PD patients in several microbiotal composition studies (C. Li et al., 2019; A. Lin et al., 2018; Li Y. et al., 2020; Qian et al., 2018, 2020) and was also found to be in an increased abundance in PD patients with mild cognitive impairment compared to PD patients with normal cognition (Ren et al., 2020). A single study identified a decreased abundance of *Actinomyces* (A. Lin et al., 2018) in PD patients compared to healthy individuals. Additionally, individual studies have identified a decreased and increased abundance of *Actinomyces* (A. Lin et al., 2018) and *Butyricimonas* (C.-H. Lin et al., 2019), respectively, in PD patients compared to healthy individuals. It is important to emphasize that these compositional studies are correlative and, by nature, are unable to elucidate the effects of a single genus on the neurodegenerative process. Therefore, the increased representation of *Alistipes* and *Butyricimonas* in the microbiome of PD patients is not sufficient to deduce a contribution to pathophysiology. Additionally, the human microbiome varies greatly from the conditions of our experiment as a complex community of microorganisms with dynamic interactions affecting overall composition (Coyte & Rakoff-Nahoum, 2019). However, we were interested to see, albeit in one study, a decreased abundance of *Actinomyces* in the microbiome of PD, as it aligned with a picture of the genus being neuroprotective.

Existing studies have demonstrated (Chen et al., 2016; Goya et al., 2020; Ray et al., 2014; C. Wang et al., 2021) the viability of *C. elegans* as a model organism in resolving specific mechanisms underlying host-microbe interactions in the context of

neurodegenerative disease. However, no studies have successfully employed the model system to test the impacts of anaerobic gut bacteria in disease contexts. Our work successfully identified human gut commensal bacteria able to protect against a major aspect of PD pathophysiology, dopaminergic neurodegeneration. Additionally, we successfully developed a protocol to systematically test the impact of individual anaerobic bacteria on host physiology and disease pathogenesis that may be expanded to alternative disease models. Future work is required to fully characterize bacterial and host mechanisms underlying the protective effects of the identified bacteria; however, we anticipate that employment of this protocol could lead to the identification of novel interventions and therapeutics.

References

Arumugam, M., Raes, J., Pelletier, E., Le Paslier, D., Yamada, T., Mende, D. R., Fernandes, G. R., Tap, J., Bruls, T., Batto, J.-M., Bertalan, M., Borruel, N., Casellas, F., Fernandez, L., Gautier, L., Hansen, T., Hattori, M., Hayashi, T., Kleerebezem, M., … Bork, P. (2011). Enterotypes of the human gut microbiome. *Nature*, *473*(7346), 174–180.

Castelli, V., d'Angelo, M., Lombardi, F., Alfonsetti, M., Antonosante, A., Catanesi, M., Benedetti, E., Palumbo, P., Cifone, M. G., Giordano, A., Desideri, G., & Cimini, A. (2020). Effects of the probiotic formulation SLAB51 in in vitro and in vivo Parkinson's disease models. *Aging*, *12*(5), 4641–4659.

Chen, S. G., Stribinskis, V., Rane, M. J., Demuth, D. R., Gozal, E., Roberts, A. M., Jagadapillai, R., Liu, R., Choe, K., Shivakumar, B., Son, F., Jin, S., Kerber, R., Adame, A., Masliah, E., & Friedland, R. P. (2016). Exposure to the Functional Bacterial Amyloid Protein Curli Enhances Alpha-Synuclein Aggregation in Aged Fischer 344 Rats and Caenorhabditis elegans. *Scientific Reports*, *6*, 34477.

Collins, S. M., Surette, M., & Bercik, P. (2012). The interplay between the intestinal microbiota and the brain. *Nature Reviews. Microbiology*, *10*(11), 735–742.

Cooper, J. F., Dues, D. J., Spielbauer, K. K., Machiela, E., Senchuk, M. M., & Van Raamsdonk, J. M. (2015). Delaying aging is neuroprotective in Parkinson's disease: a genetic analysis in C. elegans models. *NPJ Parkinson's Disease*, *1*, 15022.

Coyte, K. Z., & Rakoff-Nahoum, S. (2019). Understanding Competition and Cooperation within the Mammalian Gut Microbiome. *Current Biology: CB*, *29*(11), R538–R544.

Eckburg, P. B., Bik, E. M., Bernstein, C. N., Purdom, E., Dethlefsen, L., Sargent, M., Gill, S. R., Nelson, K. E., & Relman, D. A. (2005). Diversity of the human intestinal microbial flora. *Science*, *308*(5728), 1635–1638.

Finegold, S. M., Sutter, V. L., Attebery, H. R., & Rosenblatt, J. E. (1974). Isolation of anaerobic bacteria. *Manual of Clinical Microbiology*.

Fukushima, R. S., Weimer, P. J., & Kunz, D. A. (2003). Use of photocatalytic reduction to hasten preparation of culture media for saccharolytic Clostridium species. *Brazilian Journal of Microbiology: [publication of the Brazilian Society for Microbiology]*, *34*(1), 22–26.

Gibbons, R. J., & Macdonald, J. B. (1960). Hemin and vitamin K compounds as required factors for the cultivation of certain strains of Bacteroides melaninogenicus. *Journal of Bacteriology*, *80*(2), 164–170.

Goya, M. E., Xue, F., Sampedro-Torres-Quevedo, C., Arnaouteli, S., Riquelme-

Dominguez, L., Romanowski, A., Brydon, J., Ball, K. L., Stanley-Wall, N. R., & Doitsidou, M. (2020). Probiotic Bacillus subtilis Protects against α-Synuclein Aggregation in C. elegans. *Cell Reports*, *30*(2), 367–380.e7.

Healy, D. G., Falchi, M., O'Sullivan, S. S., Bonifati, V., Durr, A., Bressman, S., Brice, A., Aasly, J., Zabetian, C. P., Goldwurm, S., Ferreira, J. J., Tolosa, E., Kay, D. M., Klein, C., Williams, D. R., Marras, C., Lang, A. E., Wszolek, Z. K., Berciano, J., … International LRRK2 Consortium. (2008). Phenotype, genotype, and worldwide genetic penetrance of LRRK2-associated Parkinson's disease: a case-control study. *Lancet Neurology*, *7*(7), 583–590.

Ikeda, T., Yasui, C., Hoshino, K., Arikawa, K., & Nishikawa, Y. (2007). Influence of lactic acid bacteria on longevity of Caenorhabditis elegans and host defense against salmonella enterica serovar enteritidis. *Applied and Environmental Microbiology*, *73*(20), 6404–6409.

King, C. H., Desai, H., Sylvetsky, A. C., LoTempio, J., Ayanyan, S., Carrie, J., Crandall, K. A., Fochtman, B. C., Gasparyan, L., Gulzar, N., Howell, P., Issa, N., Krampis, K., Mishra, L., Morizono, H., Pisegna, J. R., Rao, S., Ren, Y., Simonyan, V., … Mazumder, R. (2019). Baseline human gut microbiota profile in healthy people and standard reporting template. *PloS One*, *14*(9), e0206484.

Li, C., Cui, L., Yang, Y., Miao, J., Zhao, X., Zhang, J., Cui, G., & Zhang, Y. (2019). Gut Microbiota Differs Between Parkinson's Disease Patients and Healthy Controls in Northeast China. *Frontiers in Molecular Neuroscience*, *12*, 171.

Lin, A., Zheng, W., He, Y., Tang, W., Wei, X., He, R., Huang, W., Su, Y., Huang, Y., Zhou, H., & Xie, H. (2018). Gut microbiota in patients with Parkinson's disease in southern China. *Parkinsonism & Related Disorders*, *53*, 82–88.

Lin, C.-H., Chen, C.-C., Chiang, H.-L., Liou, J.-M., Chang, C.-M., Lu, T.-P., Chuang, E. Y., Tai, Y.-C., Cheng, C., Lin, H.-Y., & Wu, M.-S. (2019). Altered gut microbiota and inflammatory cytokine responses in patients with Parkinson's disease. *Journal of Neuroinflammation*, *16*(1), 129.

Li Y., Li R. X., Du Y. T., Xu X. J., Xue Y., Gao D., Gao T., Sheng Z., Zhang L. Y., & Tuo H. Z. (2020). Features of gut microbiota in patients with idiopathic Parkinson's disease. *Zhonghua yi xue za zhi*, *100*(13), 1017–1022.

Li, Z., Liang, H., Hu, Y., Lu, L., Zheng, C., Fan, Y., Wu, B., Zou, T., Luo, X., Zhang, X., Zeng, Y., Liu, Z., Zhou, Z., Yue, Z., Ren, Y., Li, Z., Su, Q., & Xu, P. (2023). Gut bacterial profiles in Parkinson's disease: A systematic review. *CNS Neuroscience & Therapeutics*, *29*(1), 140–157.

Mac Faddin, J. F. (1985). Media for isolation-cultivation-identification-maintenance of medical bacteria. *(No Title)*. https://cir.nii.ac.jp/crid/1130282269777342976

Mayer, E. A. (2011). Gut feelings: the emerging biology of gut-brain communication. *Nature Reviews. Neuroscience*, *12*(8), 453–466.

Migliore, L., & Coppedè, F. (2009). Genetics, environmental factors and the emerging role of epigenetics in neurodegenerative diseases. *Mutation Research*, *667*(1-2), 82–97.

Nakagawa, H., Shiozaki, T., Kobatake, E., Hosoya, T., Moriya, T., Sakai, F., Taru, H., & Miyazaki, T. (2016). Effects and mechanisms of prolongevity induced by Lactobacillus gasseri SBT2055 in Caenorhabditis elegans. *Aging Cell*, *15*(2), 227–236.

Ortiz de Ora, L., & Bess, E. N. (2021). Emergence of Caenorhabditis elegans as a Model Organism for Dissecting the Gut–Brain Axis. *mSystems*, *6*(4), 10.1128/msystems.00755–21.

Padilla, P. A., Nystul, T. G., Zager, R. A., Johnson, A. C. M., & Roth, M. B. (2002). Dephosphorylation of Cell Cycle–regulated Proteins Correlates with Anoxia-induced Suspended Animation in Caenorhabditis elegans. *Molecular Biology of the Cell*, *13*(5), 1473–1483.

Polymeropoulos, M. H., Lavedan, C., Leroy, E., Ide, S. E., Dehejia, A., Dutra, A., Pike, B., Root, H., Rubenstein, J., Boyer, R., Stenroos, E. S., Chandrasekharappa, S., Athanassiadou, A., Papapetropoulos, T., Johnson, W. G., Lazzarini, A. M., Duvoisin, R. C., Di Iorio, G., Golbe, L. I., & Nussbaum, R. L. (1997). Mutation in the alpha-synuclein gene identified in families with Parkinson's disease. *Science*, *276*(5321), 2045–2047.

Pringsheim, T., Jette, N., Frolkis, A., & Steeves, T. D. L. (2014). The prevalence of Parkinson's disease: a systematic review and meta-analysis. *Movement Disorders: Official Journal of the Movement Disorder Society*, *29*(13), 1583–1590.

Qian, Y., Yang, X., Xu, S., Huang, P., Li, B., Du, J., He, Y., Su, B., Xu, L. M., Wang, L., Huang, R., Chen, S., & Xiao, Q. (2020). Gut metagenomics-derived genes as potential biomarkers of Parkinson's disease. *Brain: A Journal of Neurology*, *143*(12), e109.

Qian, Y., Yang, X., Xu, S., Wu, C., Song, Y., Qin, N., Chen, S.-D., & Xiao, Q. (2018). Alteration of the fecal microbiota in Chinese patients with Parkinson's disease. *Brain, Behavior, and Immunity*, *70*, 194–202.

Ray, A., Martinez, B. A., Berkowitz, L. A., Caldwell, G. A., & Caldwell, K. A. (2014). Mitochondrial dysfunction, oxidative stress, and neurodegeneration elicited by a bacterial metabolite in a C. elegans Parkinson's model. *Cell Death & Disease*, *5*(1), e984.

Ren, T., Gao, Y., Qiu, Y., Jiang, S., Zhang, Q., Zhang, J., Wang, L., Zhang, Y., Wang, L.,

& Nie, K. (2020). Gut Microbiota Altered in Mild Cognitive Impairment Compared With Normal Cognition in Sporadic Parkinson's Disease. *Frontiers in Neurology*, *11*, 137.

Sender, R., Fuchs, S., & Milo, R. (2016). Revised Estimates for the Number of Human and Bacteria Cells in the Body. *PLoS Biology*, *14*(8), e1002533.

Shen, T., Yue, Y., He, T., Huang, C., Qu, B., Lv, W., & Lai, H.-Y. (2021). The Association Between the Gut Microbiota and Parkinson's Disease, a Meta-Analysis. *Frontiers in Aging Neuroscience*, *13*, 636545.

Shibayama, K., Nagasawa, M., Ando, T., Minami, M., Wachino, J.-I., Suzuki, S., & Arakawa, Y. (2006). Usefulness of adult bovine serum for Helicobacter pylori culture media. *Journal of Clinical Microbiology*, *44*(11), 4255–4257.

Song, Y., Könönen, E., Rautio, M., Liu, C., Bryk, A., Eerola, E., & Finegold, S. M. (2006). Alistipes onderdonkii sp. nov. and Alistipes shahii sp. nov., of human origin. *International Journal of Systematic and Evolutionary Microbiology*, *56*(Pt 8), 1985–1990.

Speers, A. M., Cologgi, D. L., & Reguera, G. (2009). Anaerobic cell culture. *Current Protocols in Microbiology*, *Appendix 4*, Appendix 4F.

Stiernagle, T. (2006). Maintenance of C. elegans. WormBook. The C. elegans research community. *WormBook: The Online Review of C. Elegans Biology*.

Toh, T. S., Chong, C. W., Lim, S.-Y., Bowman, J., Cirstea, M., Lin, C.-H., Chen, C.-C., Appel-Cresswell, S., Finlay, B. B., & Tan, A. H. (2022). Gut microbiome in Parkinson's disease: New insights from meta-analysis. *Parkinsonism & Related Disorders*, *94*, 1–9.

Turnbaugh, P. J., Ley, R. E., Hamady, M., Fraser-Liggett, C. M., Knight, R., & Gordon, J. I. (2007). The human microbiome project. *Nature*, *449*(7164), 804–810.

Van Voorhies, W. A., & Ward, S. (2000). Broad oxygen tolerance in the nematode Caenorhabditis elegans. *The Journal of Experimental Biology*, *203*(16), 2467–2478.

von Wulffen, J., RecogNice-Team, Sawodny, O., & Feuer, R. (2016). Transition of an Anaerobic Escherichia coli Culture to Aerobiosis: Balancing mRNA and Protein Levels in a Demand-Directed Dynamic Flux Balance Analysis. *PloS One*, *11*(7), e0158711.

Wang, C., Lau, C. Y., Ma, F., & Zheng, C. (2021). Genome-wide screen identifies curli amyloid fibril as a bacterial component promoting host neurodegeneration. *Proceedings of the National Academy of Sciences of the United States of America*, *118*(41). https://doi.org/10.1073/pnas.2116257118

Wang, L., Zhao, Z., Zhao, L., Zhao, Y., Yang, G., Wang, C., Gao, L., Niu, C., & Li, S. (2022). Lactobacillus plantarum DP189 reduces α-SYN aggravation in MPTP-induced Parkinson's disease mice via regulating oxidative damage, inflammation, and gut Microbiota disorder. *Journal of Agricultural and Food Chemistry*, *70*(4), 1163–1173.

Wang, S., Ahmadi, S., Nagpal, R., Jain, S., Mishra, S. P., Kavanagh, K., Zhu, X., Wang, Z., McClain, D. A., Kritchevsky, S. B., Kitzman, D. W., & Yadav, H. (2020). Lipoteichoic acid from the cell wall of a heat killed Lactobacillus paracasei D3-5 ameliorates aging-related leaky gut, inflammation and improves physical and cognitive functions: from C. elegans to mice. *GeroScience*, *42*(1), 333–352.

Wornell, K., Pardesi, B., Lee, K., Boycheva, S., Roberton, A. M., & White, W. L. (2022). High-throughput method for novel medium development for culture of anaerobic gut bacteria. *Current Protocols*, *2*(7), e463.

Yao, C., El Khoury, R., Wang, W., Byrd, T. A., Pehek, E. A., Thacker, C., Zhu, X., Smith, M. A., Wilson-Delfosse, A. L., & Chen, S. G. (2010). LRRK2-mediated neurodegeneration and dysfunction of dopaminergic neurons in a Caenorhabditis elegans model of Parkinson's disease. *Neurobiology of Disease*, *40*(1), 73–81.

CHAPTER THREE: Elucidating Mechanisms of *Actinomyces* Mediated Neuroprotection in *C. elegans* Models of Parkinson's Disease

G. Sophie Ngana[1], Mercedes A. Di Bernardo[1], Michael G. Surette[1,2,3], Lesley T. MacNeil[1,2,3]

[1]Department of Biochemistry and Biomedical Sciences, McMaster University, 1280 Main St W. Hamilton, ON, Canada, [2]Farncombe Family Digestive Health Research Institute, [3]Michael G. DeGroote Institute for Infectious Disease Research

Declaration: Research presented as part of this chapter has been prepared for publication

Contributions: GSN and LTM designed the experiments and wrote the manuscript. GSN, MAD and LTM collected the RNA for sequencing experiments. GSN and MAD performed crosses. LTM performed injections. MGS provided bacterial isolates. GSN performed all other experiments and prepared the figures.

Abstract

Parkinson's disease (PD) is a common complex neurodegenerative disorder with a global prevalence of over 3% among persons 80 years of age and older. Pathologically, PD is characterized by selective degeneration of dopaminergic neurons, primarily in the substantia nigra pars compacta, as well as accumulation of alpha-synuclein enriched protein aggregates within neurons. The pathogenesis of PD is still not completely understood, and no treatments exist that alter disease progression. Obvious genetic causes are detected in only a small number of PD patients (5-10%), suggesting that environmental factors play a major role in its development. Specifically, correlative studies show that the microbiota may be one of these important environmental modifiers of neurodegeneration.

The identification of genes that cause monogenic forms of PD allowed for the generation of several *Caenorhabditis elegans* models of PD, recapitulating specific aspects of PD pathology. Here we identified a microbiotal isolate, *Actinomyces viscosus,* able to reduce neurodegeneration in animals expressing a pathological mutant form of leucine-rich repeat kinase 2 (*LRRK2*) in dopaminergic neurons. Additionally, the bacteria reduced alpha-synuclein aggregation in a synucleinopathy model. Global gene expression analysis via RNA sequencing revealed increased expression of *C. elegans* aspartic cathepsins in response to neuroprotective *A. viscosus.* Additionally, monitoring of autophagic markers confirmed that *A. viscosus* suppresses autophagic dysfunction associated with pathogenic *LRRK2* expression. RNAi-mediated and genetic knockdown of identified aspartic cathepsins induced neurodegeneration in the *LRRK2* transgenic

model confirming their implication in neuronal health. Our findings contribute to the current understanding of how the gut microbiota can influence host physiology in the context of PD, elucidating a potential mechanism of microbiota-mediated neuroprotection.

Introduction

Parkinson's disease (PD) is a common complex progressive neurodegenerative disease affecting millions of elderly individuals globally. PD is clinically characterized by cardinal motor features (bradykinesia, rigidity, tremor and postural instability) and non-motor symptoms including disorders of mood, cognitive decline and autonomic dysfunction (Poewe 2008; Langston 2006). Neuropathologically, PD is marked by the selective degeneration of dopaminergic neurons primarily in the substantia nigra pars compacta and the accumulation of abnormal alpha-synuclein enriched cytoplasmic deposits within neuronal cell bodies and neurites known as Lewy bodies and Lewy neurites, respectively (Polymeropoulos et al. 1997). In addition to abnormal protein aggregation, protein dyshomeostasis is a known early disease feature thought to contribute to PD pathogenesis.

Protein homeostasis, or proteostasis, is the mechanism by which cells regulate the proteome by controlling protein expression, folding, localization, and elimination (Gregersen et al. 2006). Maintenance of eukaryotic proteostasis requires the degradation of aberrant proteins by the evolutionary conserved autophagy lysosomal pathway (Nixon, Yang, and Lee 2008; Perera and Zoncu 2016). The autophagy lysosomal pathway consists of multiple distinct autophagic pathways that culminate in the degradation of cellular

components via the lysosome (Majeski and Dice 2004; Kunz, Schwarz, and Mayer 2004; Klionsky 2005). Within the lysosomal lumen, individual lysosomal hydrolases facilitate the degradation of specific substrates, with the most abundant family of hydrolases being the cathepsin proteases (Saftig and Klumperman 2009; Schröder et al. 2010). Various post-mortem pathological studies have identified autophagic and lysosomal dysfunction in the brain of PD patients (Alvarez-Erviti et al. 2010; Dehay et al. 2010; Tanji et al. 2011; Anglade et al. 1997; Zhu et al. 2003; Murphy et al. 2015; Moors et al. 2019) Additionally, identification of causative genetic mutations in PD further reveals a link between PD and autophagy with the corresponding gene products implicated in the functioning of the lysosomal autophagy pathway (Lynch-Day et al. 2012).

A small fraction of PD cases have identifiable causative genetic mutations but the vast majority, approximately 90%, have no clear etiological origin (Verstraeten, Theuns, and Van Broeckhoven 2015) emphasizing the importance of environmental factors in disease development. Over the last decade, a connection has been established between the gastrointestinal environment, more specifically the gut microbiota, and the pathogenesis of several neurological disorders, including PD. The human gut microbiota consists of a complex community of over 30 trillion microorganisms, including eukaryotes, archaea and predominantly bacteria, within the gastrointestinal tract (Sender, Fuchs, and Milo 2016; Turnbaugh et al. 2007). Historically, studies of neurological disorders have been restricted to the central nervous system; however, the gastrointestinal tract and the gut microbiota have been linked to the onset and/or progression of PD via the gut-brain axis (Q. Li et al. 2023) with several studies reporting significant differences in microbiotal

composition between PD patients and healthy control individuals (Bedarf et al. 2017; Hill-Burns et al. 2017; Lin et al. 2019; Scheperjans et al. 2015; Hopfner et al. 2017; Keshavarzian et al. 2015; Li Y. et al. 2020; Qian et al. 2018). Despite the well-documented presence of taxonomic changes in the gut microbiota of PD patients, there is a paucity of evidence determining the causative relationship between bacterial molecules and disease pathogenesis, with limited studies investigating the impacts of human gut commensals on PD pathophysiology (Sampson et al. 2016).

We employed the nematode *Caenorhabditis elegans* as a gnotobiotic model to determine the impacts of human microbiotal isolates on PD pathophysiology. A variety of established *C. elegans* models of PD are available to date, recapitulating specific aspects of PD pathology. Protein aggregation has been modelled in *C. elegans* via the expression of an alpha-synuclein GFP or YFP fusion protein in the body wall muscle (*unc-54* promoter), allowing researchers to monitor alpha-synuclein aggregation *in vivo* (Hamamichi et al. 2008; van Ham et al. 2008). To model neurodegeneration in *C. elegans,* a variety of strains have been developed, exhibiting age-dependent neuronal loss, including *LRRK2* transgenic animals. These worms express either wild-type or pathogenic forms of LRRK2 protein either pan-neuronally (*aex-3 or snb-1* promoter) or in dopaminergic neurons (*dat-1* promoter). Mutations in leucine-rich repeat kinase 2 (*LRRK2*) are the most common genetic risk factor in both familial and sporadic PD accounting for 4% of familial and 1% of sporadic PD cases across all populations (Healy et al. 2008). Seven PD-associated pathogenic missense mutations (N1437H, R1441G/C/H, Y1699C, G2019S, I2020T) have been identified to date, with the G2019S

mutation being the most common (Bardien et al. 2011; Alessi and Sammler 2018; Taymans et al. 2023). The expression of these human proteins in *C. elegans* provides a simple and relevant system to study the factors impacting the major pathologies of PD (Lakso et al. 2003; Cao et al. 2005; Kuwahara et al. 2006; Saha et al. 2009; Yao et al. 2010).

Through the screening of microbiotal isolates representative of the human gut microbiota, we identified *Actinomyces* species, when fed to *C. elegans*, able to inhibit *LRRK2* mediated neurodegeneration with *Actinomyces viscosus* inhibiting alpha-synuclein aggregation. We further showed that *A. viscosus* colonizes the *C. elegans* gut, increases gut granule autofluorescence and induces dietary restriction-associated phenotypes in the animals, including developmental delay, reduced fecundity and body size and lifespan extension. We also demonstrated that *A. viscosus* is able to mediate neuroprotection in a dietary restriction-independent manner. Analysis characterizing changes in host gene expression in response to the neuroprotective bacteria identified *C. elegans* aspartic cathepsins as being upregulated in response to the neuroprotective bacteria. Additionally, RNAi-mediated, and genetic knockdown of aspartic cathepsins exacerbated neurodegeneration in *LRRK2* transgenic animals. Furthermore, we showed that *A. viscosus* improved *LRRK2*-mediated autophagic dysfunction in neurons. Altogether, our findings suggest that microbiota species from the human gut can modulate host pathways, including autophagy, to influence protein aggregation and neurodegeneration in *C. elegans*.

Results

Actinomyces species are neuroprotective in *LRRK2* transgenic animals and inhibit alpha-synuclein aggregation in a *C. elegans* model of synucleinopathy

To assess the effects of the human gut microbiota on neurodegeneration, we used an established *C. elegans* model of PD, strain SCG856, expressing pathogenic G2019S mutant human *LRRK2* in dopaminergic neurons via the *dat-1* promoter while using the same promoter to drive expression of GFP for visualization of the neurons (*lin-15*(*n765ts*)*; cwrIs856* [*dat-1p::GFP, dat-1p::LRRK2*(*G2019S*)*, lin-15*(+)]) (Yao et al. 2010). These worms exhibit age-dependent dopaminergic neurodegeneration, motor dysfunction and deficits in dopamine-dependent behaviours (Cooper et al. 2015; S. Long et al. 2018; Yao et al. 2010). The BZ555 strain was used as a control, carrying only the dopaminergic neuronal GFP marker (*egIs1*[*dat-1p::GFP*]). Animals were fed *E. coli* OP50, the standard *C. elegans* lab diet (Brenner 1974), until the fourth larval stage (L4) and then shifted plates containing lawns of single gut microbiotal isolates or control lawns of *E. coli* OP50 (Figure 1A). Animals were initially grown from their first larval stage (L1) on *E. coli* OP50 to avoid the developmental impacts of the different bacterial diets. Specifically, we were mindful of the potential for these bacteria, as novel food sources, to accelerate or delay development. Therefore, we opted to transfer animals to the experimental bacteria at L4, bypassing larval development, in order to maintain a developmentally synchronous population throughout the study. Dopaminergic neurodegeneration can be reliably assayed by monitoring changes in neuronal morphology. Therefore, neurodegeneration was quantified by scoring four of the eight

dopaminergic neurons in *C. elegans,* known as the cephalic (CEP) neurons, the easiest to consistently visualize in the animal, for various neurodegeneration phenotypes at day 7 adulthood (Figures 1A and 1B) (Berkowitz et al. 2008). Among the bacterial species tested, three *Actinomyces* species (Table S1) were identified as being significantly neuroprotective in *LRRK2* transgenic animals with no impacts on neuronal health in a wild-type background (Figure 1C).

Given the centrality of alpha-synuclein aggregation in the pathophysiology of PD, we examined the impact of the neuroprotective bacteria in a *C. elegans* model of synucleinopathy. The strain used, NL5901, expresses human alpha-synuclein fused to yellow fluorescent protein (YFP) in the body wall muscle via the *unc-54* promoter (*pkIs2386* [*unc-54p::alpha-synuclein::YFP* + *unc-119*(+)]) (van Ham et al. 2008). On the standard diet of *E. coli* OP50, alpha-synuclein aggregates can be visualized via fluorescence microscopy in live animals at day 5 of adulthood (Figure 1D). Of the neuroprotective *Actinomyces*, we chose to test the effects of *A. viscosus* due to its relatively reliable and abundant bacterial growth. We followed a similar feeding protocol as the neurodegeneration assays (Figure 1A). Interestingly, animals fed *A. viscosus* had significantly fewer aggregates than *E. coli* OP50 fed animals (Figures 1D and 1E), suggesting that this dietary condition is also able to promote host proteostasis.

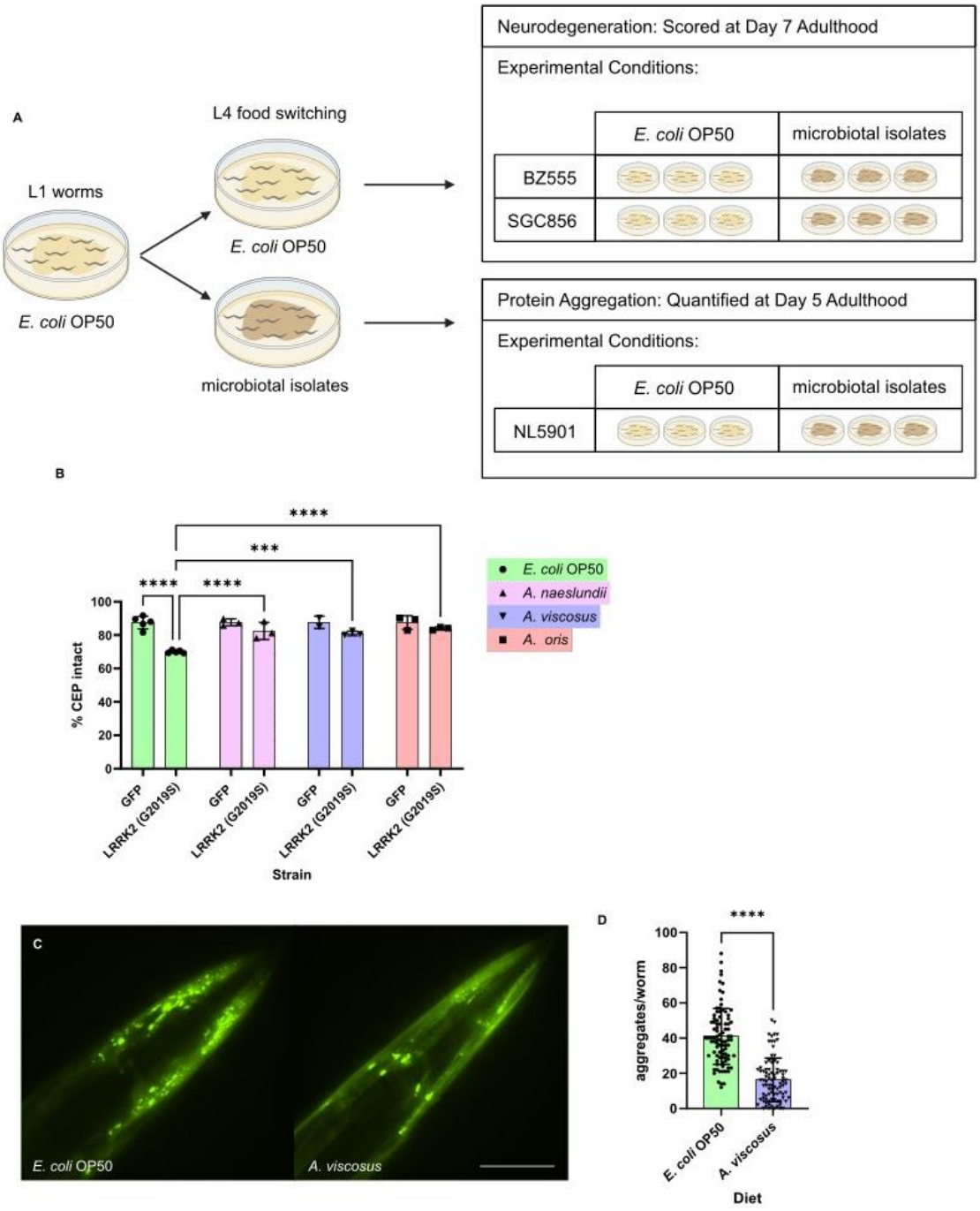

Figure 1. *Actinomyces* species induce neuroprotection and prevent alpha-synuclein aggregation in *C. elegans* models of PD.
A. Protocol overview for neurodegeneration and protein aggregation assays.
B. *LRRK2(G2019S)* expression leads to dopaminergic neurodegeneration, rescued by exposure to *Actinomyces naeslundii, Actinomyces viscosus* and *Actinomyces oris* strains.

Dopaminergic neurodegeneration was quantified by the loss of CEP neurons in SCG856 (*LRRK2* (G2019S)) and BZ555 (GFP) grown to adult day 7. Each point represents an independent trial of >60 worms for a total of three independent trials. The total number of CEP neurons expected from all animals (4 per animal) was regarded as 100%, and the number of degenerated CEP neurons detected in each experiment was used to calculate the percent intact dopaminergic neurons. Error bars indicate SD. Statistical significance was calculated using two-way ANOVA with Sidak's multiple comparisons test *** p <0.001 **** p <0.0001. SGC856; (*lin-15*(*n765ts*)*; cwrIs856* [*dat-1p::GFP, dat-1p::LRRK2*(*G2019S*)*, lin-15*(+)]), BZ555; (*egIs1*[*dat-1p::GFP*]).
C. Representative fluorescent image of alpha-synuclein aggregates in the head of day 5 adult NL5901 (*pkIs2386* [*unc-54p::alpha-synuclein::YFP* + *unc-119*(+)]) animals fed on *E. coli* OP50 or *A. viscosus*. (Scale bar, 50 μm).
D. *Actinomyces viscosus* significantly decreases the number of alpha-synuclein aggregates in a *C. elegans* model of synucleinopathy. Quantification of alpha-synuclein aggregates per animal in the head regions of day 5 adult animals. Each point represents a single animal with a total of 90 worms per condition from three independent experiments. Error bars indicate SD. Statistical significance was calculated using an unpaired t-test with Welch's correction **** p <0.0001.

Actinomyces viscosus **induces phenotypes associated with dietary restriction in** ***C. elegans***

Dietary restriction (DR) suppresses proteotoxicity in *C. elegans* models of polyglutamine, amyloid beta (Steinkraus et al. 2008) and alpha-synuclein aggregation (Goya et al. 2020). Additionally, DR is neuroprotective in alternative neurodegenerative models, including protecting against 6-hydroxydopamine-induced dopaminergic neurodegeneration in a toxin-based *C. elegans* model of PD (Jadiya et al. 2011) and preventing amyloid beta-induced glutaminergic neurodegeneration in a *C. elegans* model of Alzheimer's Disease (Griffin et al. 2019). As a novel food source for *C. elegans,* the edibility and nutritional profile of *A. viscosus* is unknown. Therefore, we wanted to determine if the suppression of alpha-synuclein aggregation and inhibition of *LRRK2*-mediated neurotoxicity may result from a diet of *A. viscosus* failing to provide or lacking critical dietary components required by *C. elegans* for adequate nutrition.

The impact of DR on life history traits has been well documented in *C. elegans,* resulting in delayed development, reduced body size, reduced fecundity, and extended lifespan (Vanfleteren and Braeckman 1999; Houthoofd et al. 2003, 2002; Seidel and Kimble 2011). Consequently, we assess the impact of this novel dietary condition on these life history traits using wild-type (N2) animals. To determine the effects of *A. viscosus* on development, we allowed animals to develop from the first larval stage (L1) on the bacteria. Interestingly, *A. viscosus* caused a strong developmental delay compared to *E. coli* OP50 when scored 48h after bacterial exposure (Figure 2A). L1s plated on *A. viscosus* eventually developed to adulthood, delayed by 5-7 days compared to *E. coli* OP50. Given the significant developmental delay observed in L1s plated on the bacteria, animals were developed on *E. coli* OP50 and transferred to *A. viscosus* lawns as L4s to determine the impacts of the bacteria on adult body size, fecundity, and lifespan. Animals transferred to *A. viscosus* were significantly smaller than animals sustained on *E. coli* OP50 24- and 48-hours post-transfer (Figures 2B and C). Animals transferred to *A. viscosus* also had a significantly smaller brood size (Figure 2D), with 10% of animals scored exhibiting the bagging phenotype (offspring hatching within the animal), a sign of severe DR or starvation (Seidel and Kimble 2011). Finally, animals transferred to *A. viscosus* experienced a significantly extended lifespan, a phenomenon which was replicated with *LRRK2* transgenic animals (Figure 2E). Taken together, these results suggest that *A. viscosus* fails to provide critical dietary components required for normal *C. elegans* development, therefore inducing a state of DR that may be driving the protective phenotypes observed in the tested PD models.

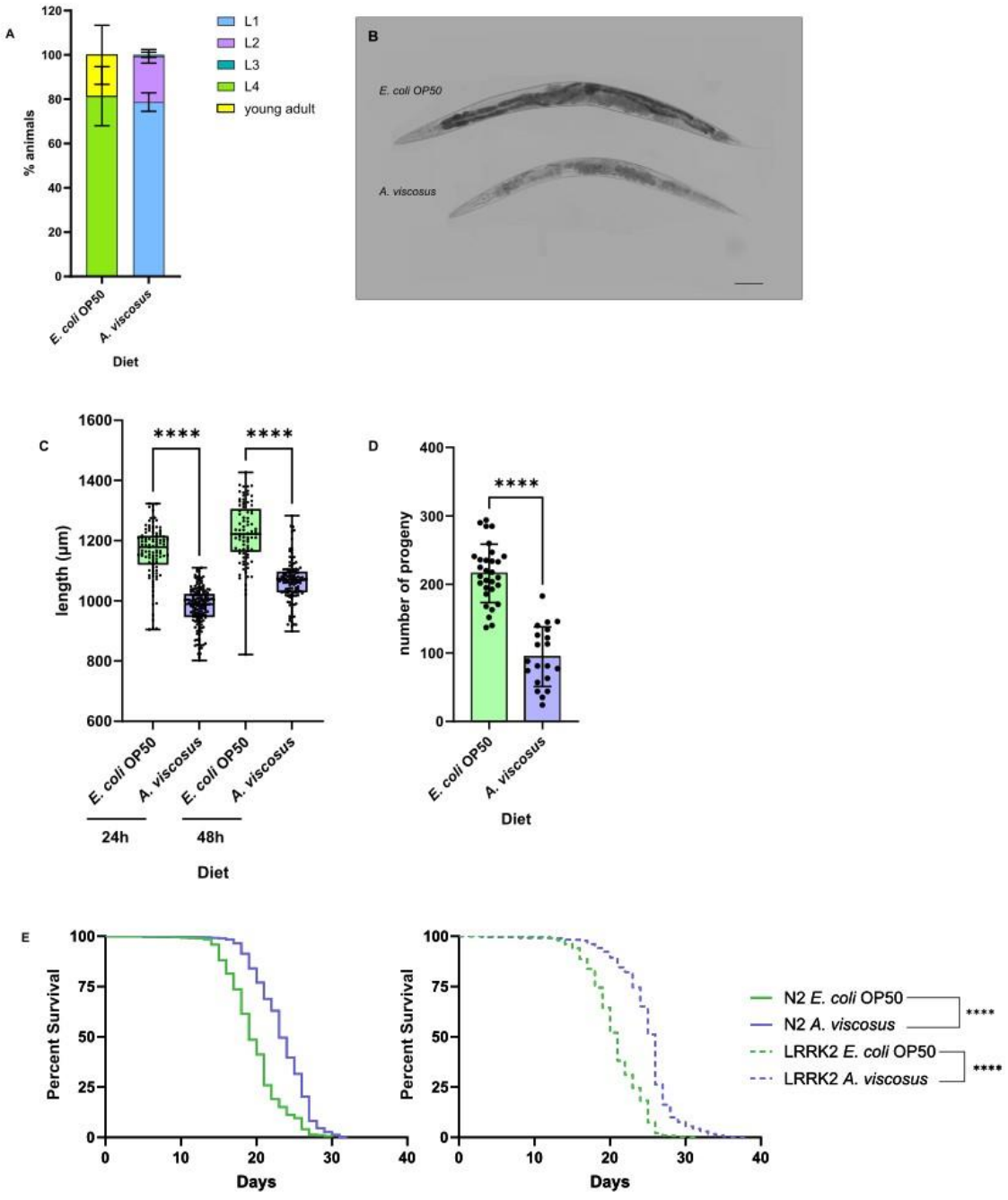

Figure 2. *A. viscosus* induces phenotypes associated with dietary restriction.
A. L1s exposed to *Actinomyces viscosus* experience a significant developmental delay. Development stage of N2 animals was scored 48 h post-initial exposure to the bacterial

diet. A total of 150 worms were scored per condition from three independent experiments. Error bars indicate SD.
B. Representative images of N2 animals transferred to *A. viscosus* lawns or sustained on *E. coli* OP50 at L4 48h post transfer. (Scale bar, 100 μm).
C. N2 L4s transferred to *A. viscosus* are significantly smaller than animals grown on *E. coli* OP50 24 and 48h post transfer. Each point represents a single animal with a total of >80 worms per condition from three independent trials. Statistical significance was calculated using one-way ANOVA with Sidak's multiple comparisons test **** p <0.0001.
D. N2 L4s transferred to *A. viscosus* produce significantly less progeny than animals grown on *E. coli* OP50. Each point represents a single animal with a total of >20 worms per condition from three independent trials. Error bars indicate SD. Statistical significance was calculated using an unpaired t-test with Welch's correction **** p <0.0001.
E. *Actinomyces viscosus* significantly extends lifespan in both N2 and SGC856 (LRRK2) animals. Each curve represented a population of >750 worms from two independent experiments. Statistical significance was calculated using Log-rank (Mantel-Cox) test **** p <0.0001. SGC856; (*lin-15*(*n765ts*)*; cwrIs856* [*dat-1p::GFP, dat-1p::LRRK2*(*G2019S*)*, lin-15*(+)]).

Actinomyces viscosus **colonizes the** ***C. elegans*** **intestine and induces rapid accumulation of autofluorescent material in intestinal lysosome-related organelles**

Specific bacteria have been characterized as inedible or indigestible by *C. elegans* including *Bacillus subtilis* spores (Laaberki and Dworkin 2008; Portal-Celhay, Bradley, and Blaser 2012) and *Staphylococcus saprophyticus (Geng et al. 2022)*. Animals fed diets of these bacteria experienced severe developmental delays and accumulation of the bacteria in the intestinal lumen (Laaberki and Dworkin 2008; Portal-Celhay, Bradley, and Blaser 2012; Goya et al. 2020; Geng et al. 2022; Qi and Han 2018; Qi, Kniazeva, and Han 2017). Given the similarities in developmental phenotypes between *A. viscosus* and these previously characterized indigestible bacteria, we determined whether *A. viscosus* is able to colonize the gut. We observed the accumulation of *A. viscosus* in N2 day one adult animals, resulting in bloating of the intestinal lumen, suggesting colonization or

indigestibility (Figure 3A). Interestingly, we also observed an increased accumulation of autofluorescent material in intestinal lysosome-related organelles or gut granules (Figure 3B). Gut granule autofluorescence increases with age in *C. elegans* (Gerstbrein et al. 2005). Additionally, exposure to host stressors, including benzaldehyde and pathological *Pseudomonas aeruginosa* PA14, rapidly induces autofluorescence; however, the mechanism underlying this induction is largely unknown (Hajdú et al. 2023).

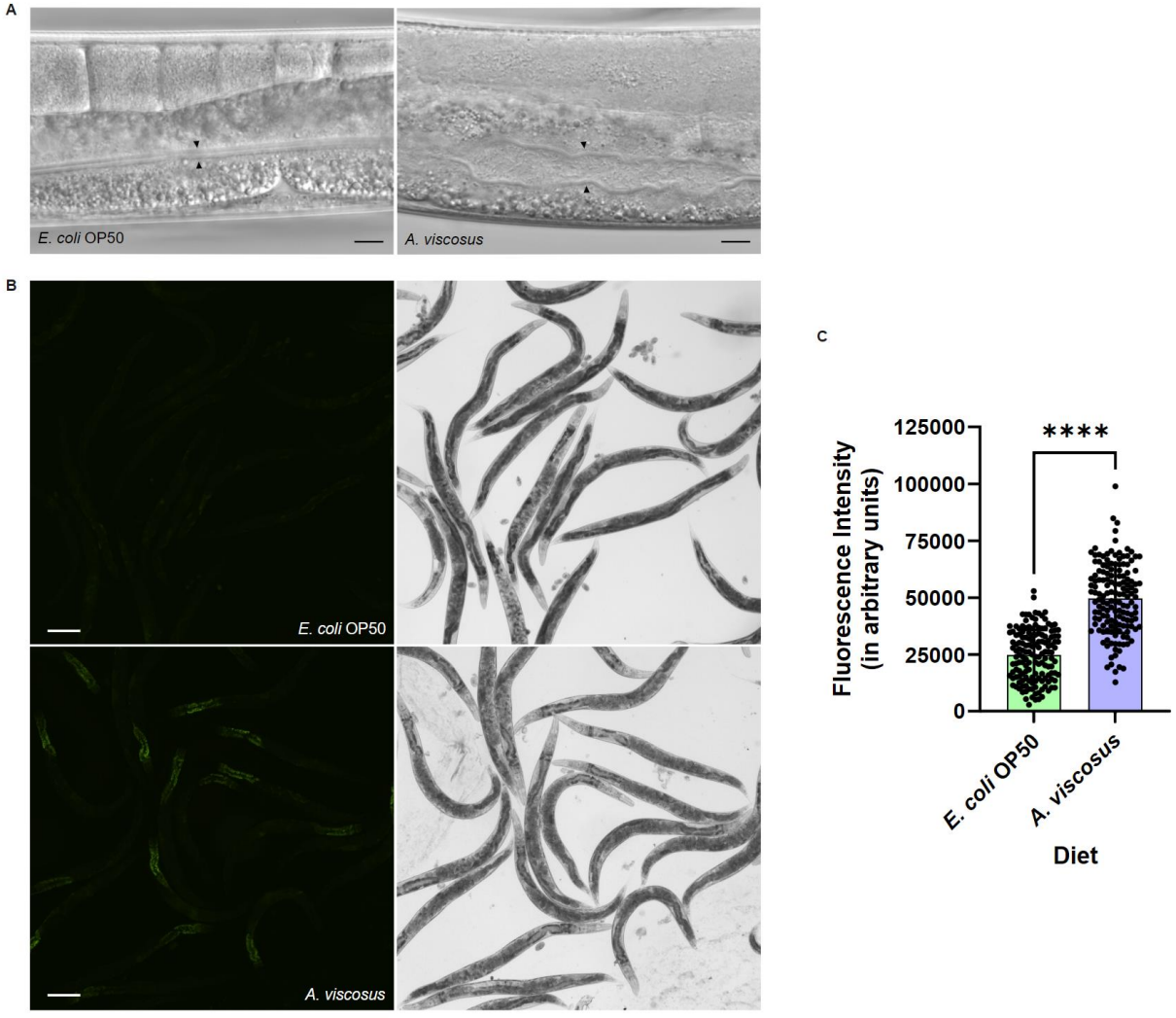

Figure 3. *A. viscosus* accumulates in the intestinal lumen and increases autofluorescence of gut granules.
A. Representative images of intestinal accumulation of *Actinomyces viscosus* day 1 adult N2 animals fed *A. viscosus* compared to *E. coli* OP50. (Scale bar, 10 μm).
B. Representative images of autofluorescence in Day 7 adult N2 animals transferred to *A. viscosus* lawns or sustained on *E. coli* OP50. (Scale bar, 100 μm).
C. *Actinomyces viscosus* significantly increases gut granule autofluorescence in Day 7 adult N2 animals. Quantification of intestinal autofluorescence per animal of day 7 adult animals. Each point represents a single animal with a total of 15 worms per condition from three independent experiments. Error bars indicate SD. Statistical significance was calculated using an unpaired t-test with Welch's correction **** $p < 0.0001$.

Actinomyces viscosus can induce neuroprotection in *LRRK2* transgenic animals through a mechanism independent of dietary restriction

Given the evidence suggesting *A. viscosus* induces DR, we examined if the bacteria's mechanisms of neuroprotection are DR-dependent. We hypothesized that if *A. viscosus* failed to provide critical nutrients required for *C. elegans* development, supplementation of *A. viscosus* lawns with *E. coli* OP50 would rescue the DR phenotypes observed on *A. viscosus* only lawns. Interestingly, we found that animals transferred to mixed *A. viscosus E. coli* OP50 lawns were significantly smaller than animals sustained on *E. coli* OP50 at 48 but not 24 hours post-transfer (Figure 2A). However, L1s plated on mixed *A. viscosus E. coli* OP50 lawns developed similarly to animals plated on *E. coli* (Figure 2B). Established methods of DR in *C. elegans* are initiated at the L4 stage or during adulthood because of the detrimental effects on development (Greer et al. 2007; Houthoofd et al. 2003; Bishop and Guarente 2007; Park, Link, and Johnson 2010; Kaeberlein et al. 2006; Lee et al. 2006; Klass 1977; Chen, Thomas, and Kapahi 2009; Mair et al. 2009). Additionally, in a study implementing a mild DR during development via bacterial dilution, worms still experienced a mild developmental delay (Palgunow,

Klapper, and Döring 2012). Therefore, we hypothesize that an alternative mechanism, independent of DR, is driving the smaller body size observed in animals 48h post L4 transfer, as no differences in development were observed between animals grown on mixed lawns and *E. coli* OP50. Given that supplementation of *A. viscosus* lawns with *E. coli* OP50 attenuated the *A. viscosus* induced DR, we measured dopaminergic neurodegeneration in *LRRK2* transgenic animals transferred to mixed *A. viscosus E. coli* OP50 lawns to determine if *A. viscosus* is able to induce neuroprotection independent of DR. Interestingly, animals transferred to mixed lawns of *A. viscosus* and *E. coli* OP50 experienced levels of neuroprotection similar to animals transferred to *A. viscosus* only lawns suggesting that *A. viscosus* is able to induce neuroprotection independent of DR (Figure 4C).

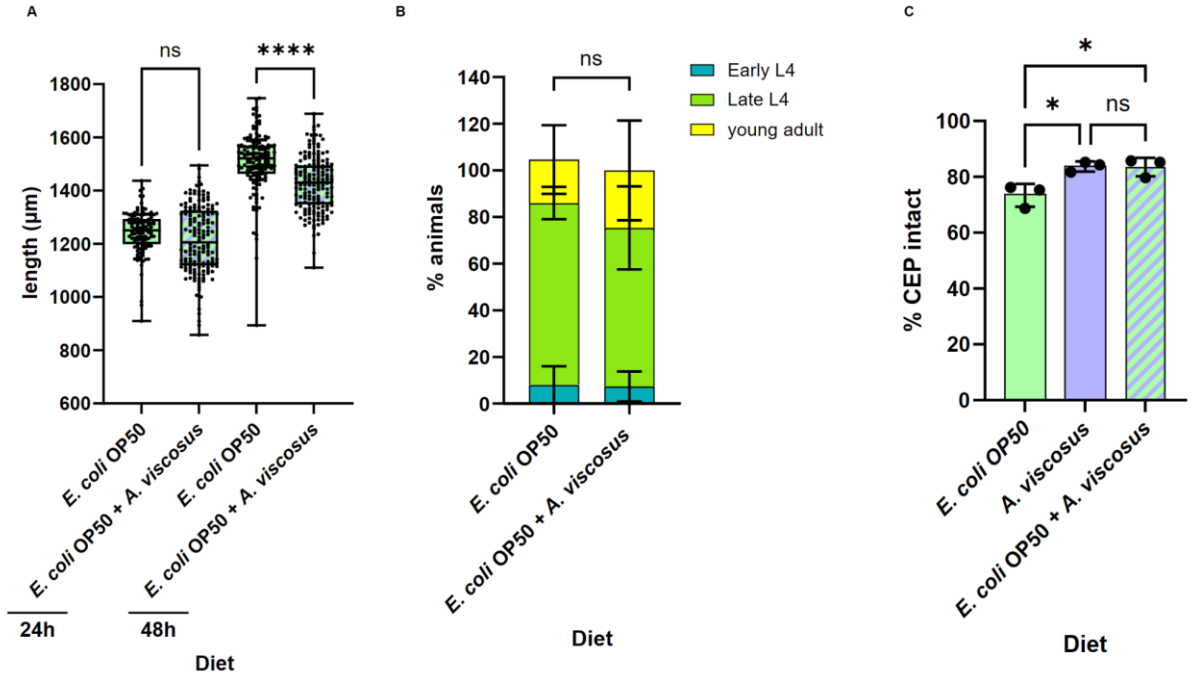

Figure 4. *A. viscosus* induces neuroprotection in a dietary restriction-independent manner.
A. N2 L4s transferred to mixed *A. viscosus E. coli* OP50 lawns are significantly smaller than animals grown on *E. coli* OP50 at 48 but not 24h post transfer. Each point represents a single animal with a total of >80 worms per condition from three independent trials. Statistical significance was calculated using one-way ANOVA with Sidak's multiple comparisons test **** $p < 0.0001$.
B. L1s exposed to mixed *A. viscosus E. coli* OP50 lawns develop similarly to animals on *E. coli* OP50. Development stage of N2 animals was scored 48h post initial exposure to the bacteria. A total of 150 worms were scored per condition from three independent experiments. Error bars indicate SD.
C. Mixed *A. viscosus E. coli* OP50 lawns induce neuroprotection at levels comparable to *A. viscosus* only lawns. Dopaminergic neurodegeneration was quantified by the loss of CEP neurons in SCG856 ((*lin-15*(*n765ts*)*; cwrIs856* [*dat-1p::GFP, dat-1p::LRRK2*(*G2019S*)*, lin-15*(+)]) animals. Each point represents an independent trial of 150 worms per condition for a total of three independent trials. The total number of CEP neurons expected from all animals (4 per animal) was regarded as 100%, and the number of degenerated CEP neurons detected in each experiment was used to calculate the percent intact dopaminergic neurons. Error bars indicate SD. Statistical significance was calculated using one-way ANOVA with Sidak's multiple comparisons test * $p < 0.05$.

Actinomyces viscosus induces changes in expression of protein coding genes in wild-type and *LRRK2* transgenic animals

To identify host genes implicated in the neuroprotective effects of *A. viscosus,* we performed global gene expression analysis via RNA sequencing (RNA-seq) in wild-type N2 and *LRRK2* transgenic animals exposed to *E. coli* OP50 and *A. viscosus*. RNA samples were collected from day 7 adult worms, and gene expression changes were quantified between animals grown on the control and neuroprotective diets in both genetic backgrounds. By including both genetic backgrounds in our experiment and subsequent analysis, we were able to identify environmentally responsive protein-coding genes and pathways that were modulated in response to the neuroprotective bacteria while additionally identifying *A. viscosus* induced gene expression changes unique to the neurodegenerative model. One hundred fifteen genes were downregulated and 407

upregulated on *A. viscosus* in a wild-type background, while 190 genes were downregulated and 330 upregulated on *A. viscosus* in the *LRRK2* transgenic background. Additionally, 198 genes were upregulated, and 53 genes were downregulated by *A. viscosus* in both genetic backgrounds (Figure 5A, Supplementary Table 3-6).

Differentially regulated genes were categorized by function via WormCat, a web-based gene set enrichment analysis tool, to determine enriched biological processes. Gene annotations in WormCat are done as a list of nested categories with broader categorization done based on physiological function and more specific categorization based on molecular function or cellular location (Holdorf et al. 2020). We sought to identify categories enriched across both genetic backgrounds to determine biological processes modulated by our neuroprotective bacteria. Interestingly, among the genes downregulated by *A. viscosus,* we saw enrichment of various transcription-related genes categorized as "Transcription factor: T-box", "Transcription: chromatin modification", and "Transcription dosage compensation" (Figure 5B, Supplementary Table 2). However, upon further examination of genes in these categories, we found that the vast majority are embryonically expressed. In *C. elegans,* the dosage compensation complex contains a sub-complex, Condensin I^{DC}, composed of DPY-27, MIX-1, DPY-26, DPY-28, and CAPG-1 and associated proteins SDC-1, SDC-2, SDC-3, DPY-30, and DPY-21 (Chuang, Albertson, and Meyer 1994; Csankovszki et al. 2009; Lieb et al. 1998, 1996; Hsu and Meyer 1994; Yonker and Meyer 2003). Five of these genes were present in our data set *mix-1, dpy-26, dpy-27, dpy-28,* and *sdc-1.* Genes of the dosage compensation complex assemble and function during a 4-5 hour critical window of embryogenesis (Dawes et al.

1999; Plenefisch, DeLong, and Meyer 1989) serving a limited role post-embryonically (Dumas et al. 2013). One of the major categories of chromatin remodelling genes downregulated in our dataset were SWI/SNF complex-associated genes including, C52B9.8, *swsn-7,* and *swsn-4* which have an important function in early development (Large and Mathies 2014). Similarly, T-box transcription factors downregulated in our dataset, including *tbx-43, tbx-8, tbx-11, tbx-37* and *tbx-38,* have been implicated in embryonic morphogenesis and cell fate determination (Good et al. 2004; Levin et al. 2012). Therefore, we hypothesized that the presence of these embryonically active genes among genes downregulated on the *A. viscous* may be an artifact of the RNA collection protocol. L4 animals were transferred to 5-Fluoro-2′-deoxyuridine (FUDR) supplemented plates, a drug that inhibits embryonic development; however, it does not fully inhibit egg laying. As previously characterized, animals produce significantly more progeny on *E. coli* OP50, therefore allowing for greater embryo contamination during RNA collection, in turn resulting in an overrepresentation of embryonically expressed genes in the control. However, we were able to identify some links between T-box transcription factors and neurodegeneration. One study found downregulation of *tbx-37* and *tbx-11,* both present in our dataset, in *dnj-14* mutants, a model for the neurodegenerative disorder neuronal ceroid lipofuscinosis (McCue et al. 2015). Another found decreased expression of *tbx-11, tbx-38* and *tbx-43* following *anc-1* knockdown, a gene protective against amyloid beta and polyQ35 aggregation (Levine, Grushko, and Cohen 2019). Additionally, they predicted that these T-box transcription factors positively regulate the expression of components of the E3 ubiquitin ligase SCF (Skp-1-Cul1-F-box protein) complex thereby

regulating proteasome-mediated protein degradation (Levine, Grushko, and Cohen 2019). Interestingly, of the three SCF complex components found to be downregulated during *anc-1* knockdown, two were present in our dataset as being downregulated in response to *Actinomyces, skr-7* and *skr-10.* However, together, these studies suggest that loss of T-box transcription factor activity perturbs proteostasis and promotes neurodegeneration, which in turn suggests that the downregulation of these same T-box transcription factors is not driving the protective phenotypes of *A. viscosus.*

Stress response-associated categories were enriched for among the genes upregulated in response to *Actinomyces*, in both genetic backgrounds, including “Stress response: C-type Lectin", “Stress response: pathogen: saposin”, and “Unassigned: regulated by multiple stresses” (Figure 5B, Supplementary Table 2). Upregulation of these stress response genes, specifically antimicrobial effectors like C-type Lectins and saponins, may result from bloating of the intestinal lumen secondary to *A. viscosus* gut colonization (Singh and Aballay 2019) or may indicate the bacteria are pathogenic. Additionally, among the upregulated genes in both genetic backgrounds, there was significant enrichment for ribosomal subunits (Figure 5B, Supplementary Table 2). We initially hypothesized that the increased expression of ribosomal subunits may have been an indication of increased TOR/LET-363 (Target of Rapamycin) signalling. TOR/LET-363 is a highly conserved serine threonine kinase that modulates protein biosynthetic capacity by positively regulating ribosomal biogenesis (X. Long et al. 2002; Mayer and Grummt 2006). TOR/LET-363 has two mutually exclusive binding proteins, regulatory association protein of TOR (Raptor) (DAF-15 in *C. elegans*) (Hara et al. 2002) and

rapamycin-insensitive companion of TOR (Rictor) (RICT-1 in *C. elegans*) (Soukas et al. 2009; Jones et al. 2009), which when bound with TOR form the core of the TOR Complex 1 (TORC1) and TOR Complex 2 (TORC2) respectively. Other proteins are found in these complexes and are required for TOR signalling. Additionally, TOR signalling has been implicated in PD; however, its specific role remains controversial, with activation of TOR being neuroprotective and neurodegenerative in different disease models (Lan et al. 2017). However, the DR-associated phenotypes and increased gut granule fluorescence observed in animals fed *A. viscosus* are not in line with a picture of increased TOR/LET-363 activation as inhibition of TOR/LET-363 causes developmental arrest and increased autofluorescent gut granules (X. Long et al. 2002).

The final biological category enriched among the upregulated genes in both genetic backgrounds was “Proteolysis general: aspartate” with *C. elegans* aspartic cathepsins being specifically enriched in the *LRRK2* genetic background (Figure 5B, Supplementary Table 2). Six aspartic endopeptidases (*asp-1, asp-2, asp-6, asp-8, asp-12, hrg-7*) were upregulated in the wild-type background with three (*asp-1, asp-8, asp-12*) of these proteins categorized as cathepsins. Similarly, eight aspartic endopeptidases (*asp-1, asp-2, asp-3, asp-5, asp-6, asp-8, asp-12, asp-13*) were upregulated in the *LRRK2* transgenic background with five (*asp-1, asp-3, asp-5, asp-8, asp-12, asp-13*) of these proteases categorized as cathepsins. *C. elegans* has linked aspartic cathepsins to aspects of PD pathology. Specifically, alpha-synuclein aggregation increased in animals expressing the protein in the body wall muscle with knockdown of asp-*4*, another aspartic cathepsin in *C. elegans* (Qiao et al. 2008). Furthermore, the introduction of cathepsin D, a

human aspartic cathepsin, in dopaminergic neurons mitigated alpha-synuclein induced neurodegeneration (Qiao et al. 2008). Therefore, we hypothesized that the upregulation of these cathepsins in response to the diet of *A. viscosus* may be driving the protective effects of the bacteria in the PD models.

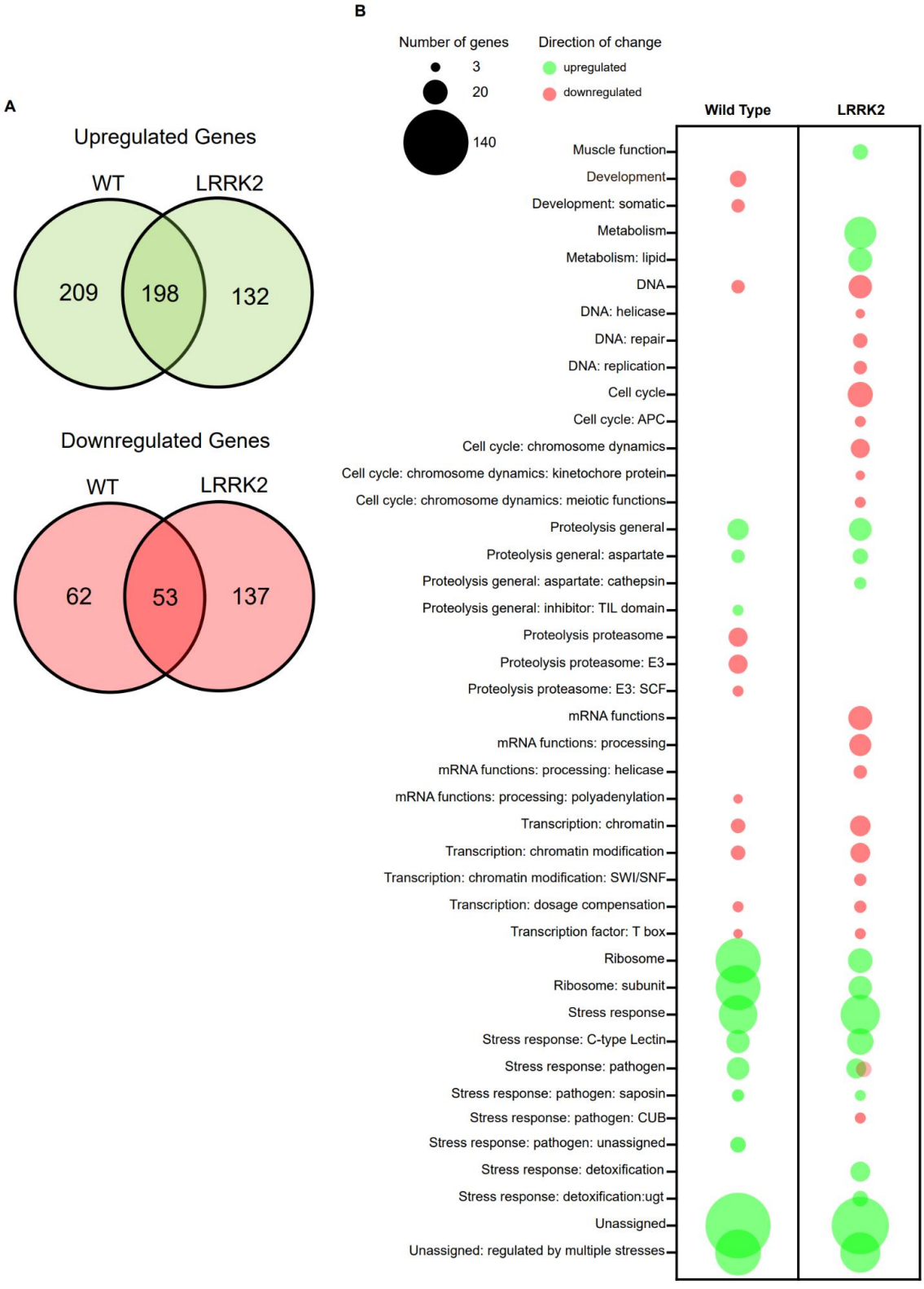
A
Upregulated Genes
WT
LRRK2
209
198
132
Downregulated Genes
WT
LRRK2
62
53
137
B
Number of genes
3
20
140
Direction of change
upregulated
downregulated
Wild Type
LRRK2
Muscle function
Development
Development: somatic
Metabolism
Metabolism: lipid
DNA
DNA: helicase
DNA: repair
DNA: replication
Cell cycle
Cell cycle: APC
Cell cycle: chromosome dynamics
Cell cycle: chromosome dynamics: kinetochore protein
Cell cycle: chromosome dynamics: meiotic functions
Proteolysis general
Proteolysis general: aspartate
Proteolysis general: aspartate: cathepsin
Proteolysis general: inhibitor: TIL domain
Proteolysis proteasome
Proteolysis proteasome: E3
Proteolysis proteasome: E3: SCF
mRNA functions
mRNA functions: processing
mRNA functions: processing: helicase
mRNA functions: processing: polyadenylation
Transcription: chromatin
Transcription: chromatin modification
Transcription: chromatin modification: SWI/SNF
Transcription: dosage compensation
Transcription factor: T box
Ribosome
Ribosome: subunit
Stress response
Stress response: C-type Lectin
Stress response: pathogen
Stress response: pathogen: saposin
Stress response: pathogen: CUB
Stress response: pathogen: unassigned
Stress response: detoxification
Stress response: detoxification:ugt
Unassigned
Unassigned: regulated by multiple stresses

Figure 5. *A. viscosus* induces changes in expression of protein-coding genes.
A. Summary of the number of protein coding genes identified to be up- and downregulated on *Actinomyces* in the wild-type (WT) and *LRRK2* transgenic (LRRK2) background.
B. Genes differentially regulated in response to *A. viscosus* enrich for different biological processes. Bubble chart summarizing WormCat generated enrichment categories for the differentially regulated mRNA on *E. coli* OP50 versus *A. viscosus* in the wild-type (WT) and *LRRK2* transgenic (LRRK2) background.

Actinomyces viscosus induces changes in expression of select microRNAs in wild-type and *LRRK2* transgenic animals

In addition to sequencing the mRNA, to capture gene expression changes in coding genes, we also sequenced small RNAs, mainly microRNAs (miRNAs), to understand if and how post-transcriptional regulation contributes to our phenotype. We observed no significant difference in miRNA expression between wild-type and *LRRK2* transgenic animals grown on *E. coli* OP50 nor between wild-type and *LRRK2* transgenic animals grown on *A. viscosus.* This lack of difference may suggest that miRNAs are not implicated in pathogenesis in our model. Alternatively, given that RNA was collected from day 7 adult animals, we may have failed to capture pathogenic miRNA dysregulation earlier on in the animals' lifespan prior to the onset of the neurodegenerative phenotype. When comparing miRNA expression changes in wild-type animals grown on *E. coli* OP50 to wild-type animals grown on *A. viscosus,* gene products of *mir-1832a*, which were downregulated on the neuroprotective diet, were the only significant changes observed (Figure 6A). However, when comparing miRNA expression changes in *LRRK2* transgenic animals grown on *E. coli* OP50 versus *LRRK2* transgenic animals grown on *A. viscosus* 7 miRNAs were significantly downregulated (including one of the *mir-1832a* gene products) and 12 miRNAs were significantly upregulated (Figure

6A). The miRNAs observed to be differentially regulated between the control and neuroprotective diet in the *LRRK2* transgenic background may be implicated in the neuroprotective phenotype or could be differentially regulated in response to the differing environmental conditions independent of the neuroprotective phenotype.

We identified any known targets of the differentially regulated miRNAs via miRTarBase, a database containing experimentally validated miRNA target interactions, to see which genes may be affected by the differential expression of identified miRNAs (Huang et al. 2021). Ninety-five gene targets were identified for the seven downregulated miRNAs, suggesting these genes were upregulated in LRRK2 transgenic animals grown on *A. viscosus*, and 57 targets were identified for the 12 upregulated miRNAs, suggesting these genes were downregulated in LRRK2 transgenic animals grown on *A. viscosus* (Figure 6B and Supplementary Tables 7 & 8). Additionally, 45 gene targets were identified as being targets for both up and downregulated miRNAs (Figure 6B). It is important to note that the majority of the gene targets for the miRNAs of interest, with the exception of targets of *lin-4,* a well-characterized miRNA in *C. elegans*, were determined via CLIP-seq (Zisoulis et al. 2010). In this protocol, whole organisms are subject to UV-irradiation to covalently cross-link proteins with interacting nucleotides. Argonaute, an essential component of the RNA-induced silencing complex, is then immunoprecipitated to isolate miRNAs and their mRNA targets. After immunoprecipitation, samples are treated with an RNA ligase to ligate the miRNA and its target, forming a miRNA-target chimera, and then treated with proteinase to isolate the RNA. This miRNA-target chimera is then extracted and sequenced to determine miRNA targets. Limitations of the protocol

result from the low efficiency UV RNA- protein crosslinking and a low fraction of reproducible miRNA-target chimera (Broughton and Pasquinelli 2016). Therefore, without additional validation for these target sites, it is possible that some of the identified sites are false positives and that other target sites were missed. Additionally, CLIP-seq only identifies binding activity and does not confirm that these miRNAs regulate a specific target's expression. However, despite these limitations, it does present a reasonable starting point.

To potentially link the miRNA and mRNA sequencing data, we compared up and down-regulated protein-coding genes to the identified targets of the differentially regulated miRNAs. The only gene shared between these datasets was F29B9.8, which was upregulated in response to *Actinomyces* in the mRNA sequencing data and was identified as a target of downregulated miRNAs *mir-38* and *mir-1829b*. According to the AlphaFold sequence-based similarity search, F29B9.8 shares similarities to various rodents and human trace amine-associated receptors (TAAR), including TAAR6 and TAAR8 (Steinegger and Söding 2018; Jumper et al. 2021; Varadi et al. 2022). Trace amines, amino acid-derived biogenic amines, have previously been linked to PD pathogenesis, with PD patients having lower levels of circulating octopamine compared to healthy controls (D'Andrea et al. 2010). Interestingly, a TAAR1 agonist results in increased dopaminergic neurodegeneration in a 6-hydroxydopamine mouse model of PD; however, knockout of TAAR1 in mice results in reduced dopaminergic neurodegeneration (Alvarsson et al. 2015). Generally, the role of trace amines in the nervous system is still largely uncharacterized, and the role of the other five TAAR functional isoforms is largely

unknown. However, the link between TAAR proteins and PD pathophysiology suggests that F29B9.8 may be implicated in neuronal health in *LRRK2* transgenic animals and may be implicated in the mechanism of *Actinomyces* mediated neuroprotection. In addition to sharing similarity to TAAR proteins, a previous study identified that knockdown of F29B9.8 results in a receptor-mediated endocytosis defect, suppressing yolk uptake by oocytes (Balklava et al. 2007). The LRRK2 protein and the *C. elegans* ortholog have previously been implicated in vesicular trafficking, including endocytosis (Connor-Robson et al. 2019; Abeliovich and Gitler 2016; Xiong, Dawson, and Dawson 2017; Xiong and Yu 2018; Sakaguchi-Nakashima et al. 2007). Expression of *G2019S* mutant *LRRK2* in the dopaminergic neurons of mice induced a significant reduction in the number of synaptic vesicles and an accumulation of clathrin-coated vesicles at synapses, suggesting a defect in receptor-mediated endocytosis (Xiong et al. 2018). Knockdown of F29B9.8 resulted in defective receptor-mediated endocytosis, suggesting that the gene product is required for proper vesicular trafficking. Therefore, increased expression of F29B9.8, as seen in response to *Actinomyces*, may be neuroprotective, rectifying potential trafficking defects resulting from *LRRK2(G2019S)* expression. MiRNAs exert gene regulation by binding to mRNA targets with exact complementarity, inducing the RNAi pathway and degrading the transcript or by binding to targets with imperfect complementarity and blocking translation without transcript degradation (Ambros, 2003). The latter pathway would not reflect changes in mRNA sequencing data and may be an explanation for the lack of significant overlap between the gene lists. Additionally, the

limitations in methods used to identify the miRNA targets may also contribute to the lack of concordance between the data sets.

The known miRNA target genes were categorized by function via WormCat (Figure 6C). No biological processes were significantly enriched for among the gene targets of the upregulated miRNA. However, targets of downregulated miRNAs enriched for genes categorized broadly under "metabolism" as well as genes categorized more specifically under "trafficking: ER/Golgi" (Figure 6C). Despite enrichment of these categories, the target genes assigned to these categories have divergent molecular functions, giving no clearer indication of the specific cellular impacts of the differentially regulated miRNA.

We compared sequencing findings to published miRNA gene expression data for *C. elegans* models of PD (Asikainen et al. 2010; Shen et al. 2021) (Table 1). Asikanien et al. (2010) looked at changes in miRNA gene expression via microarray in a variety of PD models, including *cat-1* (dopamine/serotonin symporter) and *pdr-1* (*parkin* ortholog in *C. elegans*) mutants as well as a transgenic strain expressing A53T mutant alpha-synuclein. When comparing the datasets, *mir-51* was identified as being downregulated in *cat-1* mutants but upregulated in response to *A. viscosus.* Additionally, both *mir-241* and *mir-230* were upregulated in *pdr-1* mutants as well as in response to *Actinomyces.* Shen et al. (2021) examined changes in miRNA gene expression via RNA sequencing in transgenic worms overexpressing wild-type alpha-synuclein as well as worms expressing A53T mutant alpha-synuclein. In this comparison, *mir-38* was upregulated in transgenic animals expressing A53T mutant alpha-synuclein but downregulated in response to *Actinomyces.*

Conversely, *mir-56* was upregulated in animals expressing A53T mutant alpha-synuclein and in response to *Actinomyces.* Additionally, *mir-230* and *mir-788* were upregulated in animals expressing wild-type alpha-synuclein as well as in response to *Actinomyces*. Assuming the differentially regulated miRNAs are implicated in the neuroprotective phenotype, I would expect to see changes in the opposite direction in miRNA expression of overlapping miRNA when comparing expression changes seen on *Actinomyces* to expression changes seen in the PD models. Given that both *mir-38* and *mir-51* show the opposite expression changes on *Actinomyces* compared to expression changes seen in the PD models, these miRNAs offer an obvious candidate for further investigation of the implications of the miRNAs in the neuroprotective phenotype of *A. viscosus.*

A

***E. coli* OP50 vs *Actinomyces viscosus* (Wild-type genetic background)**			
MirGeneDB ID	**MiRBase ID**	**log2 Fold Change**	**adjusted P-value**
Downregulated			
Cel-Mir-1832-P1_5p*	*cel-mir-1832a*	**-2.3881**	2.08E-06
Cel-Mir-1832-P1_3p	*cel-mir-1832a*	**-2.3912**	1.23E-05
***E. coli* OP50 vs *Actinomyces viscosus* (*LRRK2* genetic background)**			
MirGeneDB ID	**MiRBase ID**	**log2 Fold Change**	**adjusted P-value**
Downregulated			
Cel-Mir-36-P4_5p*	*cel-mir-38*	**-1.7683**	0.023453
Cel-Mir-1829-P2_5p	*cel-mir-1829b*	**-1.6118**	0.02889
Cel-Mir-1832-P1_5p*	*cel-mir-1832a*	**-1.4751**	0.023453
Cel-Mir-9-P14_3p	*cel-mir-75*	**-1.2836**	0.023453
Cel-Mir-2-P11_3p	*cel-mir-250*	**-1.0634**	0.049588
Cel-Mir-52-P2_5p	*cel-mir-53*	**-1.0628**	0.049588
Cel-Mir-70_3p	*cel-mir-70*	**-1.0283**	0.034701
Upregulated			
Cel-Let-7-P7_3p*	*cel-mir-241*	**1.12935**	0.034701
Cel-Let-7-P7_5p	*cel-mir-241*	**1.19523**	0.033603
Cel-Mir-788-v1_5p*	*cel-mir-788*	**1.20584**	0.049588
Cel-Mir-788-v2_5p*	*cel-mir-788*	**1.20584**	0.049588
Cel-Mir-54-P3_3p	*cel-mir-56*	**1.25794**	0.040959
Cel-Mir-54-P1_5p*	*cel-mir-54*	**1.26991**	0.023453
Cel-Mir-2208-P1_5p	*cel-mir-2208a*	**1.27388**	0.033603
Cel-Mir-230_5p	*cel-mir-230*	**1.28087**	0.023453
Cel-Bantam-P5a_3p	*cel-mir-2209a*	**1.4593**	0.023453
Cel-Mir-10-P2_5p	*cel-mir-51*	**1.54113**	0.023453
Cel-Mir-246_5p*	*cel-mir-246*	**1.58858**	0.023453
Cel-Mir-10-P3m_3p*	*cel-lin-4*	**1.68869**	0.02889

B

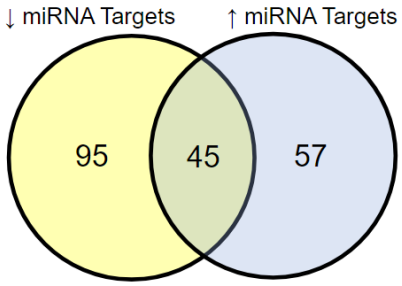

C

Category	RGS	AC	P Value	Bonferroni
Metabolism	20	1601	7.543122951336897e-07	1.357762131240064e-05
Trafficking: ER/Golgi	4	87	0.000197147606169852	0.008871642277643340

Figure 6. *A. viscosus* induces changes in expression of miRNA genes.
A. Differentially regulated miRNAs between *E. coli* OP50 and *Actinomyces viscosus* in a wild-type and *LRRK2* genetic background. The MiRBase ID indicates the miRNA gene in the *C. elegans* genome while the MirGeneDB ID indicates the mature products of the miRNA gene. The 5p/3p annotation in the MiRGeneDB ID indicates the position of the product in the pre-miRNA hairpin and the (*) indicates the "passenger strand" or "star strand" which is less expressed and thought to be the inactive product of the miRNA gene. Comparisons were done via DESeq2 in which p-values attained by the Wald test are corrected for multiple testing using the Benjamini and Hochberg method (adjusted P-values).
B. Venn diagram showing the number of mRNA targets identified for miRNAs up- and downregulated on *Actinomyces* in *LRRK2* transgenic animals.
C. WormCat output for gene targets of downregulated miRNA. RGS denotes the number of genes in the input gene set belonging to the indicated category. AC denotes the total number of *C. elegans* genes belonging to the category. *P* values are obtained from Fisher's exact test with a Bonferroni multiple hypothesis testing correction.

Table 1. Comparison of miRNAs differentially regulated in worms fed *A. viscosus* to existing miRNA gene expression data in PD models.

PD model	Differentially regulated miRNA identified in study	Direction of change identified in study	Differentially regulated on *A. viscosus*?	Log2 Fold change on *A. viscosus*
(Asikainen et al. 2010)				
A53T alpha-synuclein	*cel-miR-50*	Upregulated	N	-
	cel-miR-83	Upregulated	N	-
	cel-miR-58a	Upregulated	N	-
	cel-miR-77	Upregulated	N	-
	cel-miR-238	Upregulated	N	-
	cel-miR-1	downregulated	N	-
	cel-miR-48	downregulated	N	-
	cel-miR-65	downregulated	N	-
	cel-miR-64	downregulated	N	-
	cel-miR-80	downregulated	N	-
	cel-miR-84	downregulated	N	-
	cel-let-7	downregulated	N	-
cat-1	*cel-miR-58*	upregulated	N	-
	cel-miR-236	upregulated	N	-
	cel-miR-51	downregulated	Y	1.541128537
	cel-miR-64	downregulated	N	-
	cel-miR-65	downregulated	N	-
pdr-1	*cel-miR-241*	upregulated	Y	1.129353332
	cel-miR-230	upregulated	Y	1.280868007
	cel-miR-48	downregulated	N	-
(Shen et al. 2021)				
A53T alpha-synuclein	*cel-miR-239b*	downregulated	N	-
	cel-miR-239a	downregulated	N	-
	cel-miR-35	downregulated	N	-
	cel-miR-41	downregulated	N	-
	cel-miR-40	downregulated	N	-
	cel-miR-39	downregulated	N	-
	cel-miR-36	downregulated	N	-
	cel-miR-38	downregulated	Y	-1.768251152
	cel-miR-37	downregulated	N	-
	cel-miR-355	downregulated	N	-
	cel-miR-4807	downregulated	N	-
	cel-miR-44	downregulated	N	-
	cel-miR-2217b	downregulated	N	-
	cel-miR-56	downregulated	Y	1.257937975
	cel-miR-74	downregulated	N	-
	cel-miR-45	downregulated	N	-
	cel-miR-1018	downregulated	N	-
	cel-miR-5553	upregulated	N	-
	cel-miR-799	upregulated	N	-
	cel-miR-8196b	upregulated	N	-
	cel-miR-58c	upregulated	N	-
	cel-miR-789	upregulated	N	-
	cel-miR-1829a	upregulated	N	-
WT alpha-synuclein	*cel-miR-2217b*	downregulated	N	-
	cel-miR-797	downregulated	N	-
	cel-miR-44	downregulated	N	-
	cel-miR-230	downregulated	Y	1.280868007
	cel-miR-788	downregulated	Y	1.205844803
	cel-miR-85	upregulated	N	-
	cel-miR-4937	upregulated	N	-
	cel-miR-124	upregulated	N	-

Actinomyces viscosus induces changes in gene expression overlapping with changes seen in a model dietary restriction

In order to isolate gene expression changes linked to DR, we sought to compare our gene expression data to existing DR gene expression analysis. Multiple methods of DR have been developed in *C. elegans,* including various food dilution strategies and genetic models (Greer and Brunet 2009). Similarly, various studies have looked at transcriptional changes in response to established DR paradigms (Rollins et al. 2019; Jordan et al. 2019; Honjoh et al. 2017; Gao et al. 2018; Kogure et al. 2017; Hou et al. 2016; Wu et al. 2021; Pandit et al. 2014). We opted to compare our data set to the Wu et al. (2021) study, which used a food dilution paradigm of DR (growth-arrested bacteria). This study was selected given the similar DR induction time at L4, and the RNA collection occurring in older animals (day 6 adulthood) (Wu et al. 2021). We compared the differentially regulated genes from the Wu et al. dataset to gene expression data from wild-type animals grown on *A. viscosus.* We then used WormCat to identify categories enriched for among the overlapping genes (Table 2). Interestingly, we saw a major overlap in genes associated with stress response upregulated in both datasets. Punitive antimicrobial effectors and detoxification mechanisms, including C-type lectins, LYS-class genes, glutathione-S-transferases (GST) and UDP-glucuronosyl transferases (ugt), have been upregulated in other long-lived scenarios, suggesting that activation of these genes may contribute to increased lifespan across mechanisms of longevity extension (Shore and Ruvkun 2013) and can function independent of pathogenesis as we previously hypothesized. We also saw enrichment of aspartic endopeptidases among the genes

overlapping between the datasets. Wu *et al* (2021) saw upregulation of four aspartic endopeptidases *asp-1, asp-3, asp-6,* and *asp-12* two of which were categorized as cathepsins (*asp-1, asp-12*). In *LRRK2* transgenic animals we saw upregulation of four additional aspartic endopeptidases of the 33 identified in the *C. elegans* genome. This suggests that DR may be driving the upregulation of some of the aspartic cathepsins seen in our dataset but may not be the sole cause of the increased aspartyl protease expression observed in *LRRK2* transgenic animals.

Table 2. Wormcat categories and relevant genes enriched for in a comparison between DR gene expression data and differentially regulated genes in wild-type worms fed *A. viscosus.*

Dietary Restriction vs *Actinomyces viscosus*				
Downregulated Genes				
Category 3	**RGS**	**AC**	**P Value**	**Bonferroni**
Proteolysis proteasome: E3: SCF	3	30	3.03E-06	4.54E-05
Transcription factor: T box	2	21	0.000164646	0.002469692
Upregulated Genes				
Category 1	**RGS**	**AC**	**P Value**	**Bonferroni**
Stress response	19	833	8.28E-12	9.94E-11
Category 2	**RGS**	**AC**	**P Value**	**Bonferroni**
Proteolysis general: aspartate	3	33	0.000109973	0.002639361
Stress response: C-type Lectin	7	256	7.06E-06	0.000169463
Stress response: pathogen	5	192	0.000173586	0.004166062

Sequence ID	Gene Name	WormCat Category
Downregulated Genes		
Y47D7A.1	*skr-7*	Proteolysis proteasome: E3: SCF
C52D10.7	*skr-9*	
Y105C5B.13	*skr-10*	
F40H6.4	*tbx-11*	Transcription factor: T box
Y46E12A.4	*tbx-43*	
Upregulated Genes		
Y39B6A.20	*asp-1*	Proteolysis general: aspartate: cathepsin
F21F8.4	*asp-12*	
F21F8.7	*asp-6*	Proteolysis general: aspartate: unassigned
Y43C5A.3	Y43C5A.3	Stress response: pathogen: unassigned
F08G2.5	F08G2.5	
F58B3.2	*lys-5*	Stress response: pathogen: lysozyme
C28C12.5	*spp-8*	Stress response: pathogen: saposin
F27C8.4	*spp-18*	
B0218.6	*clec-51*	Stress response: C-type Lectin
B0218.8	*clec-52*	
ZK666.6	*clec-60*	
F35C5.5	*clec-62*	
Y46C8AL.3	*clec-70*	
Y54G2A.39	*clec-80*	
Y54G2A.8	*clec-82*	
Y51B9A.8	Y51B9A.8	Stress response: heavy metal
F15E11.12	*pud-4*	
ZC443.5	*ugt-18*	Stress response: detoxification: ugt
Y49C4A.8	*ugt-29*	
C18C4.3	*ugt-48*	
F37B1.1	*gst-24*	Stress response: detoxification: GST
C29E4.7	*gsto-1*	Stress response: unassigned

Actinomyces viscosus increases autophagic flux in LRRK2 transgenic animals

In humans, microtubule-associated protein 1A/1B-light chain 3 (LC3), orthologous to *C. elegans lgg-1*, is a central component of autophagy forming the autophagic membrane. The resulting autophagosomes then fuse with the lysosomes, leading to degradation of the sequestered cellular components along with degradation of LC3 (Rubinsztein, Shpilka, and Elazar 2012; Saha et al. 2015). In *C. elegans,* optical reporters for autophagic activity have been constructed by expressing *lgg-1* fused to a fluorescent protein to monitor the formation of autophagosomes, observed as fluorescent puncta.

Given that cathepsins function in the lysosome autophagy pathway as the main drivers of the lysosomal degradative capacity (Saftig and Klumperman 2009; Schröder et al. 2010), we wanted to determine the impacts, if any, of *A. viscous* on autophagic flux in *LRRK2* transgenic animals by monitoring autophagosome accumulation. AMH5 (*unc-119(ed3), sosIs5* [*rab-3p::Cerulean-Venus::lgg-1* + *unc-119*(+)]) is a strain expressing fluorescently labeled LGG-1 specifically in neurons using the *rab-3* promoter. We performed crosses with these worms and the WLZ3 (*wlzIs3* [*snb-1p::Hsa-LRRK2(G2019S)* + *lin15*(+)] strain, which pan-neuronally expresses G2019S mutant *LRRK2* using the *snb-1* promoter to obtain animals homozygous for both the *sosIs5* and *wlzIs3* transgenes. These progeny, carrying both transgenes, allowed us to monitor the impacts of *A. viscosus* on autophagosome accumulation in *LRRK2* transgenic animals. Similar to previous reports (Saha et al. 2015), we saw an increase in fluorescent puncta in *LRRK2* transgenic animals (Figures 7A and B), an increase which was rescued in animals

fed *A. viscosus* (Figures 7A and B). A decline in fluorescent puncta was also observed in animals transferred to mixed lawns of *A. viscosus* and *E. coli* OP50; however, the difference was not as large as *A. viscosus* only fed animals (Figure 7C).

LGG-1::GFP accumulation may result from impairment in or induction of autophagic activity. For example, during starvation, LGG-1::GFP puncta increases in the hypodermis, seam cells and intestinal cells as a result of overall increased autophagic activity; however, an accumulation of LGG-1::GFP can also be seen when the formation of autophagosomes or autolysosomes is impaired (Zhang et al. 2015). Therefore, we wanted to monitor an additional substrate of autophagy to obtain a fuller picture of the impacts of *A. viscosus* on autophagic flux. The *SQSTM1* gene*,* orthologous to *C. elegans sqst-1,* encodes p62 a scaffold protein that functions to anchor ubiquitinated proteins to the autophagic membrane, promoting degradation of unwanted cellular components (Vadlamudi and Shin 1998). Similar to mammalian p62, SQST-1 is degraded during the autophagic process with autophagic impairment resulting in the accumulation of SQST-1 (Tian et al. 2010). MAH349 (*sqIs35* [*sqst-1p::sqst-1::GFP + unc-122p::RFP*]) is a strain expressing fluorescently labelled SQST-1 from the endogenous *sqst-1* promoter. We crossed these worms with the WLZ3 (*wlzIs3* [*snb-1p::Hsa-LRRK2(G2019S) + lin15(+)*] to produce progeny carrying both transgenes, allowing us to monitor the impacts of *A. viscosus* on SQST-1 accumulation. Similar to LGG-1, *LRRK2(G2019S)* animals accumulated SQST-1 (Figures 7D and E). As expected, animals transferred to *A. viscosus* only and mixed *A. viscosus E. coli* OP50 lawns saw a significant reduction in SQST-1::GFP, with the former observing a more dramatic decline (Figure 7E and F). The

difference between animals on the *A. viscosus* only and mixed *A. viscosus E. coli* OP50 lawn suggests that DR may contribute to a portion of the increased autophagic flux of *A. viscosus;* however, it is not the sole mechanism of improved autophagic clearance. Altogether, these results suggest that *A. viscosus* improves autophagic flux in *LRRK2* transgenic animals in a DR-dependent and independent manner.

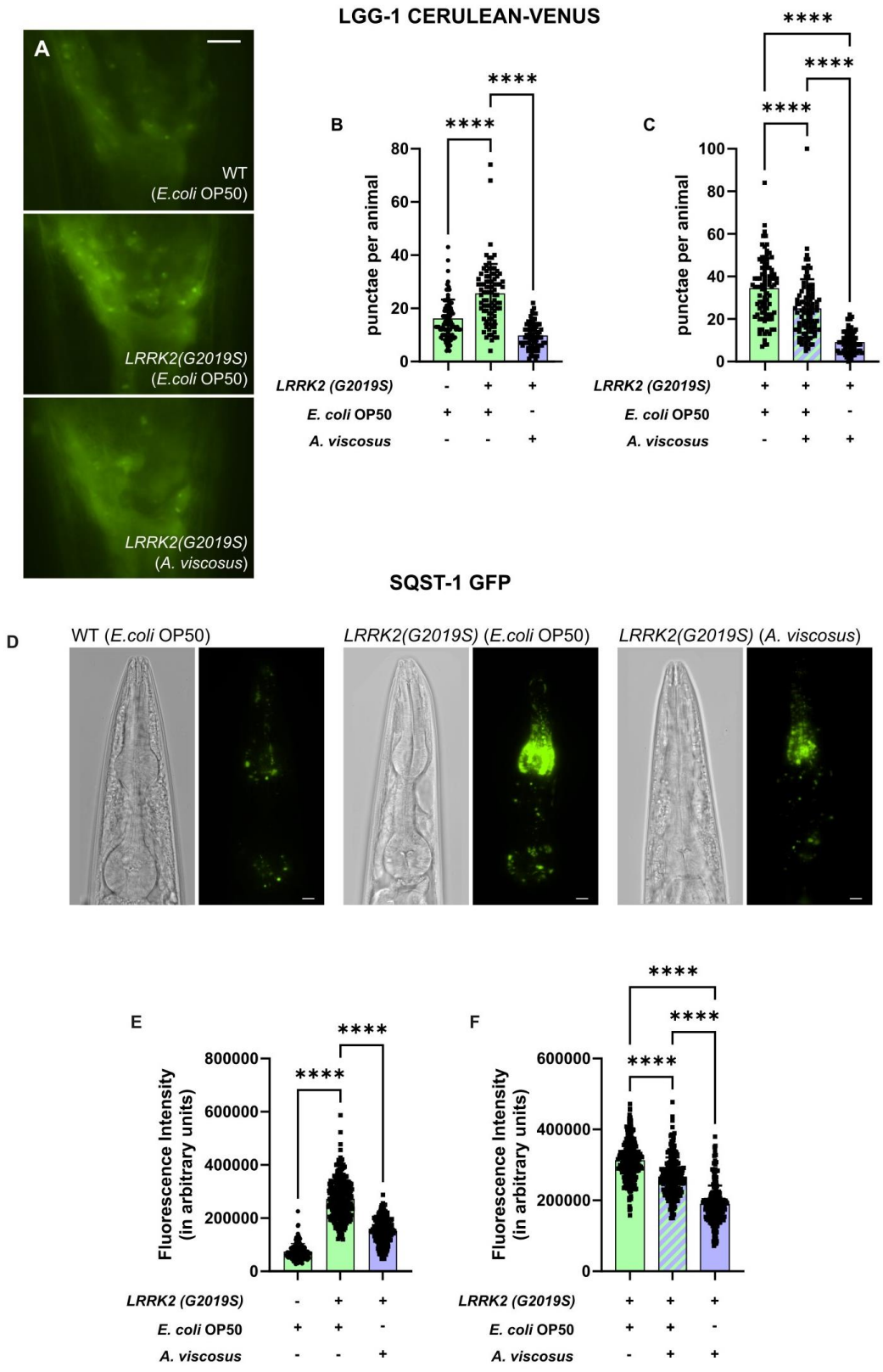
LGG-1 CERULEAN-VENUS
A
WT
(E.coli OP50)
LRRK2(G2019S)
(E.coli OP50)
LRRK2(G2019S)
(A. viscosus)
B
punctae per animal
****
****
LRRK2 (G2019S)
E. coli OP50
A. viscosus
C
punctae per animal
****
****
****
LRRK2 (G2019S)
E. coli OP50
A. viscosus
SQST-1 GFP
D
WT (E.coli OP50)
LRRK2(G2019S) (E.coli OP50)
LRRK2(G2019S) (A. viscosus)
E
Fluorescence Intensity
(in arbitrary units)
****
****
LRRK2 (G2019S)
E. coli OP50
A. viscosus
F
Fluorescence Intensity
(in arbitrary units)
****
****
****
LRRK2 (G2019S)
E. coli OP50
A. viscosus

Figure 7. *A. viscous* increases autophagic flux in *LRRK2* transgenic animals.
A. Representative images of CERULEAN-VENUS::LGG-1 in the head neurons of day 7 adult AMH5 (WT) (*unc-199(ed3)*; *sosIs5*[*rab-3p::Cerulean-Venus::lgg-1 + unc-119*(+)]) on *E. coli* OP50 and LMN059 (*LRRK2*(*G2019S*)) (*wlzIs3*[*snb-1p::Hsa-LRRK2(G2019S) + lin15*(+)]; *sosIs5*[*rab-3p::Cerulean-Venus::lgg-1 + unc-119*(+)]) on both *E. coli* OP50 and *A. viscosus.*
B. *Actinomyces viscosus* significantly decreases *LRRK2(G2019S)* mediated accumulation of CERULEAN-VENUS::LGG-1 punctae in head neurons. Quantification of CERULEAN-VENUS::LGG-1 in head neurons of day 7 adult animals in a wild-type and *LRRK2* transgenic background transferred to *E. coli* OP50 and *A. viscosus*. Each point represents a single animal with a total of 90 worms per condition from three independent experiments. Error bars indicate SD. Statistical significance was calculated using one-way ANOVA with Tukey's multiple comparisons test **** $p < 0.0001$.
C. *Actinomyces viscosus* significantly decreases *LRRK2(G2019S)* mediated accumulation of CERULEAN-VENUS:: LGG-1 punctae in neurons independent of dietary restriction. Quantification of CERULEAN-VENUS::LGG-1 in head neurons of day 7 adult animals in a *LRRK2* transgenic background transferred to *E. coli* OP50, *A. viscosus,* and *E. coli* OP50 *A. viscosus* mixed lawns. Each point represents a single animal with a total of 90 worms per condition from three independent experiments. Error bars indicate SD. Statistical significance was calculated using one-way ANOVA with Tukey's multiple comparisons test **** $p < 0.0001$.
D. Representative images of SQST-1::GFP in the head region of day 7 adult MAH349 (WT) (*sqIs35*[*sqst-1p::sqst-1::GFP + unc-122p::RFP*]) on *E. coli* OP50 and LMN060 (*LRRK2*(*G2019S*)) (*wlzIs3*[*snb-1p::Hsa-LRRK2(G2019S) + lin15*(+)]; *sqIs35*[*sqst-1p::sqst-1::GFP + unc-122p::RFP*]) on both *E. coli* OP50 and *A. viscosus.*
E. *Actinomyces viscosus* significantly decreases the *LRRK2(G2019S)* mediated accumulation of SQST-1::GFP in the head region of animals. Quantification of SQST-1::GFP fluorescence in the head of day 7 adult animals in a wild-type and *LRRK2* transgenic background transferred to *E. coli* OP50 and *A. viscosus*. Each point represents a single animal with a total of >150 worms per condition from three independent experiments. Error bars indicate SD. Statistical significance was calculated using one-way ANOVA with Tukey's multiple comparisons test **** $p < 0.0001$.
F. *Actinomyces viscosus* significantly decreases the *LRRK2(G2019S)* mediated accumulation of SQST-1::GFP in the head region independent of dietary restriction. Quantification of SQST-1::GFP fluorescence in the head of day 7 adult animals in a *LRRK2* transgenic background transferred to *E. coli* OP50, *A. viscosus,* and *E. coli* OP50 *A. viscosus* mixed lawns. Each point represents a single animal with a total of >150 worms per condition from three independent experiments. Error bars indicate SD. Statistical significance was calculated using one-way ANOVA with Tukey's multiple comparisons test **** $p < 0.0001$.

Aspartic cathepsins are integral to neuronal health in *LRRK2* transgenic animals

To determine if aspartic cathepsins are integral to neuronal health in *LRRK2* transgenic animals, we conducted RNAi mediated knockdown of the five aspartic cathepsins upregulated by *A. viscosus* in the *LRRK2* transgenic background and observed the impacts on neurodegeneration. Knockdown of all five aspartic cathepsins (*asp-1, asp-5, asp-8, asp-12* and *asp-13*) significantly induced neurodegeneration in comparison to the control (Figure 8A). However, knockdown of these same cathepsins had no impact on dopaminergic neurodegeneration in wild-type animals (Figure 8B). We aligned the sequence of the RNAi clones to the *C. elegans* genomes using BlastN to determine the probability of off-target effects. Generally, with RNAi 80% identity over 200 bp is predictive of gene silencing (Kamath and Ahringer 2003). Given this rule, *asp-5* and *asp-12* are predicted to have cross-interference with *asp-1* and *asp 5,* respectively (Figure 8C). Taken together, this suggests that aspartic cathepsins are implicated in neuronal health in a *LRRK2* sensitized genetic background.

In order to confirm the results of the RNAi experiment and determine if increased expression of aspartyl proteases is required for the neuroprotective effects of *A. viscosus* we sought to test a genetic model of cathepsin knockdown. In order to do this, we crossed a *cad-1* mutant strain PJ2 (*cad-1(j1)*), with the SGC856 (*lin-15(n765ts); cwrIs856 [dat-1p::GFP, dat-1p::LRRK2(G2019S), lin-15(+)]*) strain. Animals carrying the *cad-1(j1)* mutation have approximately 10% of the aspartic cathepsin activity when compared to wild-type animals (Jacobson et al. 1988). Further characterization of the mutant concluded that the *cad-1* gene product may be involved in the processing of aspartic

proteases (Tcherepanova et al. 2000); however, the gene product is still unknown. By genetically reducing aspartic cathepsin activity globally in the *LRRK2* transgenic background, we were able to better characterize the role that aspartic cathepsins play in neuronal health and *A. viscosus* mediated neuroprotection. *LRRK2* transgenic animals carrying the *cad-1(j1)* mutation had significantly greater neurodegeneration compared to *LRRK2* transgenic animals. Additionally, *A. viscosus* was able to induce neuroprotection in *cad-1(j1) LRRK2* transgenic animals. This may suggest that increased cathepsin expression is not required for *A. viscosus* mediated neuroprotection or that pathways independent of cathepsin activity are activated in response to *A. viscosus,* resulting in neuroprotection. Alternatively, given the uncharacterized nature of the *cad-1* gene and the *cad-1(j1)* mutation, *A. viscosus* may still be able to induce a significant enough increase in aspartic cathepsin activity to induce neuroprotection.

With genetic confirmation of the role of aspartic cathepsins in neuronal health in *LRRK2* transgenic animals, we were interested in better understanding the mechanism underlying their involvement by determining their gene expression patterns. Specifically, determining whether these cathepsins are expressed in dopaminergic neurons will allow us to determine if the effects of cathepsin on neuronal health are cell-autonomous or cell non-autonomous. Previous characterization of *asp-1* expression using a β-galactosidase transcriptional reporter demonstrated exclusively intestinal expression with the highest level of expression in the posterior intestine (Tcherepanova et al. 2000); however, no reporter strains have been developed for *asp-8* or *asp-12*. Therefore, we generated GFP reporter vectors for three aspartic cathepsins, *asp-1, asp-8,* and *asp-12*, upregulated on *A.*

viscosus in both the wild-type and *LRRK2* transgenic background (Figure 9A) to confirm and determine expression patterns of these genes. Transcriptional reporter lines can be developed by microinjecting reporter gene vectors with a co-injection marker to identify animals containing reporter gene extrachromosomal arrays (Boulin and Hobert 2012). *Asp-1* and *asp-8* transcriptional reporter lines, with a *rol-6*(*su1006*) co-injection marker, were successfully developed, demonstrating intestinal expression suggesting that these proteins affect neuronal health through a cell non-autonomous mechanism (Figure 9B). Intestinal activation of the p38 MAPK (PMK-1)/ATF-7 pathway was previously found to be neuroprotective against rotenone mediated dopaminergic neurodegeneration with induction of intestinal autophagy being required for the effect (Chikka et al. 2016). Therefore, we assessed the differential expression of previously reported PMK-1 target genes (Troemel et al. 2006) in our datasets to determine if p38 MAPK (PMK-1)/ATF-7 pathway activation may be driving the neuroprotective effects of *A. viscosus*. Of the 127 genes reported to be differentially expressed in *daf-2(e1368)* versus *daf-2 (e1368); pmk-1(km25),* only 12 and 13 PMK-1 targets were differently regulated on *A. viscosus* in a wild-type and *LRRK2* transgenic background respectively (Table 3). Additionally, four of the targets differentially expressed in the wild-type background and six of the targets differentially expressed in the *LRRK2* transgenic background exhibited expression changes suggestive of decreased PMK-1 activity. Given the limited overlap between our datasets and previously identified PMK-1 targets, we were inclined to believe that activation of p38MAPK (PMK-1)/ATF-7 is not the primary mechanism of *A. viscosus*

mediate neuroprotection; however further characterization is needed to definitively determine the role of the pathway in our phenotype.

Finally, we wanted to confirm that overexpression of these cathepsins is neuroprotective in the *LRRK2* transgenic animals. To this end, we cloned the coding sequences of three aspartic cathepsins (*asp-1, asp-8, asp-12*) into an expression vector downstream of the *rab-3* promoter (Schade et al. 2005) to drive expression of these genes pan-neuronally (Figure 9A). Injection of these plasmids into *LRRK2* transgenic animals will allow for the overexpression of individual cathepsins, mimicking the expression patterns of these genes on *A. viscosus (Boulin and Hobert 2012)* therefore determining if increased cathepsin expression can recapitulate the neuroprotective effect in the absence of the experimental bacteria.

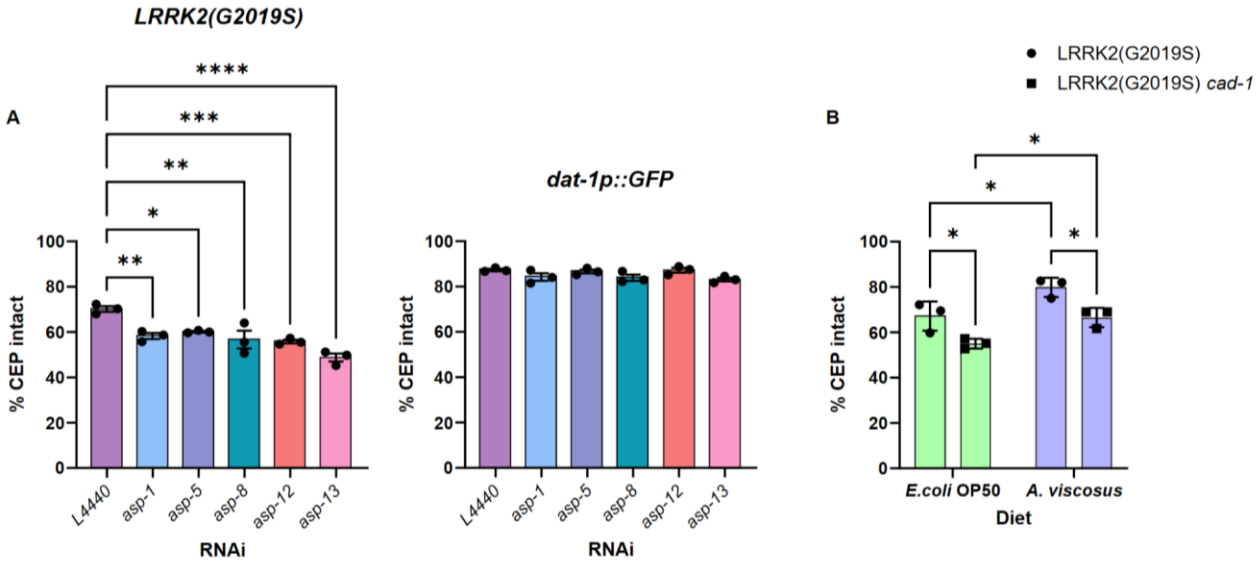

C

Gene name	Log2 Fold Change	Clone has >80% Sequence Identity to ONLY target gene
asp-1	2.378283081	Y
asp-5	2.634767596	N (91.92% *asp-1*)
asp-8	3.991782019	Y
asp-12	2.48346351	N (80.60% *asp 5*)
asp-13	1.852112717	Y

Figure 8. Aspartic cathepsins are required for neuronal health in *LRRK2* transgenic animals

A. Knockdown of aspartic cathepsins (*asp-1, asp-5, asp-8, asp-12,* and *asp-13*) significantly induces neurodegeneration in *LRRK2* transgenic animals but has no impact in a wildtype genetic background. Dopaminergic neurodegeneration was quantified by the loss of CEP neurons in SCG856 (*LRRK2(G2019S))* and BZ555 (*egIs1*[*dat-1p::GFP*]) animals grown to adult day 7. Each point represents an independent trial of 150 worms per condition for a total of three independent trials. The total number of CEP neurons expected from all animals (4 per animal) was regarded as 100%, and the number of degenerated CEP neurons detected in each experiment was used to calculate the percent intact dopaminergic neurons remaining. Error bars indicate SD. Statistical significance was calculated using one-way ANOVA with Tukey's multiple comparisons test * $p < 0.05$.
B. *Actinomyces viscosus* induces neuroprotection in *cad-1(j1) LRRK2* transgenic animals. Dopaminergic neurodegeneration was quantified by the loss of CEP neurons in SCG856 (*LRRK2(G2019S)*) and LMN061((*LRRK2(G2019S) cad-1*) (*cwrIs856* [*dat-1p::GFP, dat-1p::LRRK2(G2019S), lin-15(+)*]; *cad-1(j1)*) animals grown to adult day 7. Each point represents an independent trial of 150 worms per condition for a total of three independent trials. The total number of CEP neurons expected from all animals (4 per animal) was regarded as 100%, and the number of degenerated CEP neurons detected in each experiment was used to calculate the percent intact dopaminergic neurons. Error bars

indicate SD. Statistical significance was calculated using two-way ANOVA with Holm-Sidak's multiple comparisons test * p <0.05.

C. Sequence overlap of Ahringer RNAi clones for tested aspartic cathepsins.

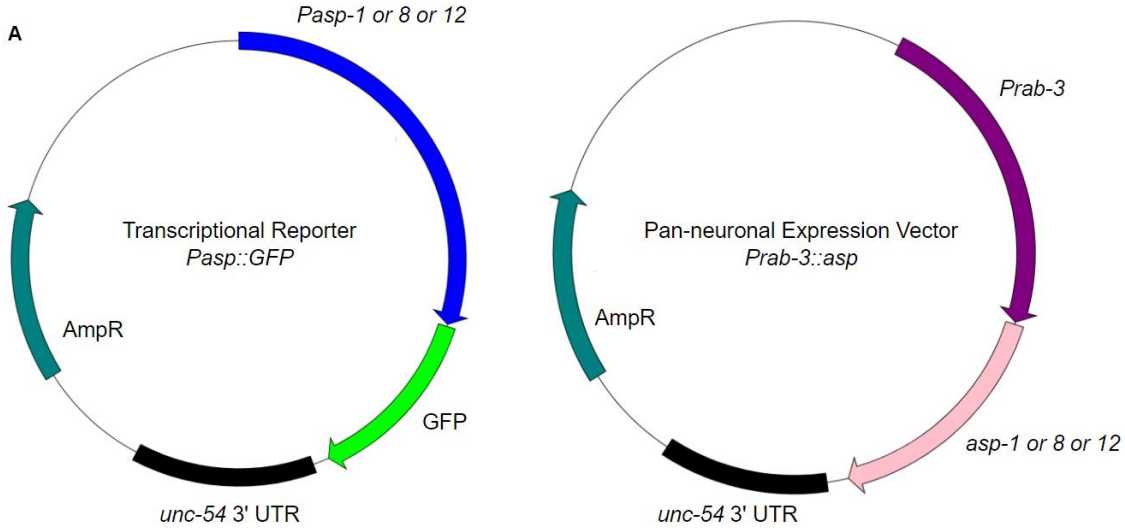

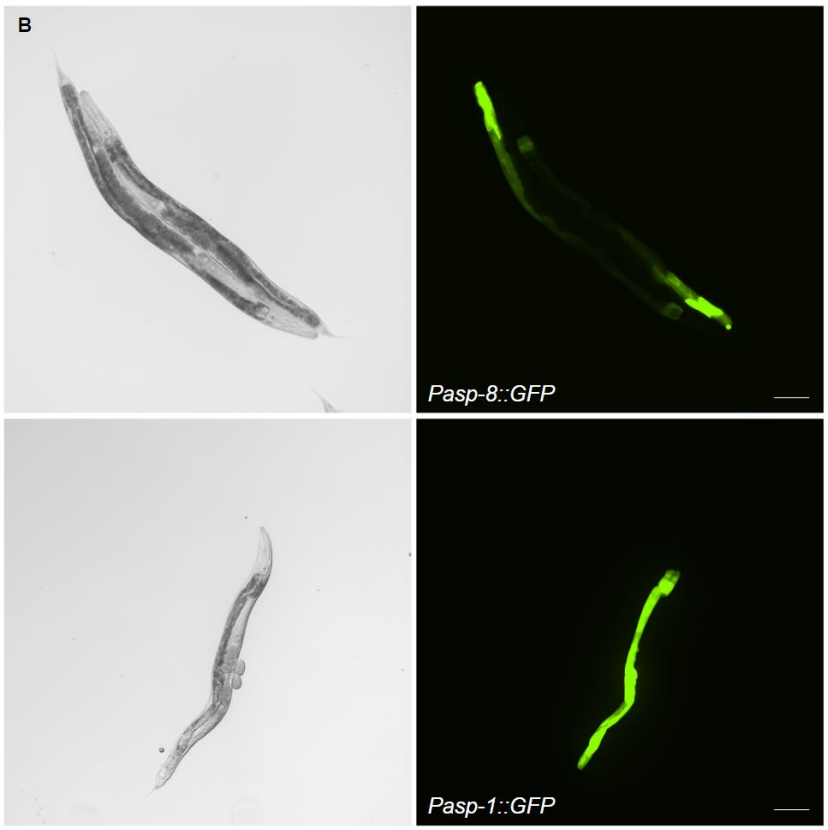

Figure 9. Expression of ASP-1 and ASP–8 is localized to the intestine
A. Plasmid maps for GFP aspartic cathepsin transcriptional reporter and pan-neuronal aspartic cathepsin overexpression vector.
B. Representative images of *Pasp-1::GFP* and *Pasp-8::GFP* in day 1 adult animals. (Scale bar, 100 μm)

Table 3. Summary of PMK-1 target genes differentially regulated in wild-type and *LRRK2* transgenic worms fed *A. viscosus*

PMK-1 *target gene*	*Fold change* by WT PMK-1 in *daf-2(e1368) background*	*Fold change E. coli* OP50 vs. *A. viscosus* (WT background)	*Fold change E. coli* OP50 vs. *A. viscosus* (*LRRK2* background)
T24B8.5	6.7	N/A	-6.06849963
F55G11.8	6.8	-3.169598826	-2.673129949
K02F3.4	2.6	1.948590579	2.149245566
Y45F10D.6	2.6	2.271035488	N/A
M02F4.7	2.7	2.435970141	N/A
C24B9.9	2.2	2.580219152	3.125450339
F56D6.2	5.0	3.053548993	2.438575632
Y39G10AR.6	2.4	3.184863441	3.487544905
K07A1.6	2.3	3.365830593	2.714650163
C03H5.1	-2.0	3.376461163	3.441986297
Y58A7A.5	2.2	4.321061208	3.928731899
B0218.8	-3.2	6.019116824	7.582342786
ZK666.6	-3.3	6.521987578	8.436066973
F08G5.6	28.9	N/A	2.728634852
Y38E10A.14	-2.4	N/A	3.169664008

Discussion

The human microbiota is a complex community of microorganisms essential for the maintenance of host homeostasis and health. At present, a large number of studies have suggested a link between intestinal bacteria and PD pathogenesis; however, minimal work has been done to identify the impact of individual species on host physiology in the disease context. We used a simple metazoan model, *Caenorhabditis elegans*, to study the effects of human microbiotal isolates on neurodegeneration and organismal proteostasis. Using a single-bacterium approach, we were able to isolate bacteria impacting disease pathogenesis in the context of our PD models. Specifically, we were able to identify that

exposure to Actinomyces *viscosus* promoted neuroprotection in *LRRK2* transgenic animals and inhibited alpha-synuclein aggregation in a synucleinopathy model.

As a novel food source for *C. elegans,* we attempted to disentangle the effects of *A. viscosus* as a host environmental interactor from its capacity as a viable nutrient source. Specifically, we assayed the impacts of *A. viscosus* on life history traits including lifespan, development, fecundity, and body size. We identified that *A. viscosus* exposure resulted in delayed development, reduced body size, reduced fecundity, and extended lifespan, well-documented phenotypes of DR in *C. elegans* (Vanfleteren and Braeckman 1999; Houthoofd et al. 2003, 2002; Seidel and Kimble 2011). Evidence of the protective effects of DR in the context of PD has been well documented across model organisms (Zhou et al. 2019; Jadiya et al. 2011; Goya et al. 2020; Maswood et al. 2004). However, we determined that *A. viscosus* is able to induce neuroprotection via a DR-independent mechanism.

Via transcriptomic analysis, we were able to identify *A. viscosus* induced changes in gene expression of coding and non-coding genes both outside of and within the context of our disease model. Interestingly, we observed no significant difference in miRNA expression between wild-type and *LRRK2* transgenic animals grown on *E. coli* OP50 nor between wild-type and *LRRK2* transgenic animals grown on *A. viscosus* suggesting that the expression changes of miRNA identified in response to the neuroprotective diet are specifically resulting from *A. viscosus* exposure. Many studies have reported dysregulation of miRNA expression in PD patients versus control individuals, with other studies implicating some miRNAs in the pathogenesis of the disease (Briggs et al. 2015;

Gui et al. 2015; Kern et al. 2021). However, generally, the role of miRNAs in PD is not well understood and therefore, specifically sequencing small RNAs in our model and in response to a neuroprotective diet allowed us to identify environmentally responsive miRNA potentially implicated in neuronal health (Goh et al. 2019; Kuo et al. 2021). Additionally, by comparing our dataset to existing miRNA gene expression data (Asikainen et al. 2010; Shen et al. 2021) we identified *mir-38* and *mir-51* as potential targets for further characterization in the context of *A. viscosus* mediated neuroprotection.

Sequencing of protein coding RNAs notably identified a significant upregulation of aspartic cathepsins in response to *A. viscosus.* The role of aspartic cathepsins in PD pathophysiology has been previously investigated. The *CTSD* gene encoding human aspartic cathepsin, cathepsin D, has been identified as a susceptibility gene for PD (Robak et al. 2017). Additionally, nigral cathepsin D activity and levels are reduced in post-mortem PD patient samples (Moors et al. 2019). Existing evidence in *C. elegans* has also linked aspartic cathepsins to aspects of PD pathology. Specifically, knockdown of *asp-4* increased alpha-synuclein aggregation in animals expressing the protein in the body wall muscle. Additionally, alpha-synuclein induced neurodegeneration was attenuated by the expression of human cathepsin D in dopaminergic neurons (Qiao et al. 2008). Given that cathepsins act as a main driver of lysosomal degradation activity (Saftig and Klumperman 2009; Schröder et al. 2010), we assayed the impacts of *A. viscosus* on autophagic flux. We demonstrated that *A. viscosus* was able to rescue *LRRK2*-mediated autophagic dysfunction by monitoring autophagosome turnover and degradation of autophagic substrates. More importantly, we were able to demonstrate that *A. viscosus* improved

LRRK2-induced autophagic dysfunction, albeit less significantly, in the absence of DR, a potent positive regulator of autophagy (Mizushima et al. 2008), suggesting that *A. viscosus* protects against *LRRK2* autophagic impairment in a DR dependent and independent manner.

Through the comparison of miRNA targets and mRNA sequencing data, we identified F29B9.8 as the only gene shared between these datasets. Specifically, F29B9.8 was upregulated in response to *Actinomyces* and was identified as a target of downregulated miRNAs *mir-38* and *mir-1829b*. According to the AlphaFold sequence-based similarity search, F29B9.8 was found to share significant similarity to various TAARs in both rodents and humans (Steinegger and Söding 2018; Jumper et al. 2021; Varadi et al. 2022). Additionally, knockdown of F29B9.8 results in a receptor-mediated endocytosis defect (Balklava et al. 2007). These two pathways, the TAAR signalling pathway and receptor-mediated endocytosis (Connor-Robson et al. 2019; Abeliovich and Gitler 2016; Xiong, Dawson, and Dawson 2017; Xiong and Yu 2018; Sakaguchi-Nakashima et al. 2007), have previously been linked to PD pathophysiology, with trace amine octopamine being significantly lower in PD patients versus health controls (D'Andrea et al. 2010), and activation of TAAR1 promoting neurodegeneration in a 6-hydroxydopamine model of PD (Alvarsson et al. 2015). Additionally, receptor-mediated endocytosis was perturbed with a reduction in the number of synaptic vesicles and an accumulation of clathrin-coated vesicles at synapses in mice expressing pathogenic *LRRK2* in dopaminergic neurons (Xiong et al. 2018). However, the F29B9.8 gene product remains largely uncharacterized; therefore, more work needs to be done to determine the

role, if any, the protein plays in neuronal health in *LRRK2* transgenic animals as well as its implications in *A. viscosus* mediated neuroprotection.

We confirmed the importance of aspartic cathepsins in neuronal health in the context of *LRRK2* transgenic animals by demonstrating that RNAi and genetic knockdown (*cad-1(j1)*) of aspartic cathepsins induced neurodegeneration in the model. We also determined that *A. viscosus* was still able to induce neuroprotection in the context of genetic knockdown of aspartic cathepsins. These results may suggest that *A. viscosus* is able to induce neurodegeneration in a pathway independent of cathepsin activity. However, without further characterization of the function of *cad-1* and the nature of the allele, it is difficult to definitively determine the significance of aspartic cathepsins in *A. viscosus* mediated neuroprotection.

Development of a transcriptional reporter for *asp-1* and *asp-8,* as well as previous characterization of *asp-1* (Tcherepanova et al. 2000) allowed us to determine that both *asp-1* and *asp-8,* expressed in the intestine, function in maintaining neuronal health via a cell non-autonomous mechanism. Intestinal activation of the p38 MAPK (PMK-1)/ATF-7 pathway is neuroprotective against rotenone-mediated dopaminergic neurodegeneration with induction of intestinal autophagy required for the effect (Chikka et al. 2016). Increased expression of intestinally localized *asp-1* and *asp-8* may suggest increased intestinal autophagy similar to what is observed in p38 MAPK (PMK-1) overexpression mutants exposed to rotenone. However, without directly monitoring intestinal autophagy in our model we are unable to conclude its role in *A. viscosus* mediated neuroprotection. The same study also found that overexpression of p38/MAPK (PMK-1) in intestinal cells

did not affect neuronal autophagy in the context of rotenone exposure but decreased the number of LGG-1::GFP punctae in wild-type animals (Chikka et al. 2016), however, no additional autophagy marker was assayed making it difficult to determine what this means biologically and how intestinal p38/MAPK (PMK-1) activation influences neuronal autophagy. A preliminary analysis of differential expression of PMK-1 targets yielded minimal significant changes in gene expression in line with a state of PMK-1 activation. This suggests that activation of the (PMK-1)/ATF-7 pathway is not the primary mechanism of *A. viscosus* mediate neuroprotection, however, further characterization is needed to completely rule out its implication in our phenotype.

Our work successfully identified a human gut commensal able to protect against major aspects of PD pathophysiology, dopaminergic neurodegeneration and alpha-synuclein aggregation. Additionally, we were able to characterize aspects of the host's genetic response to the bacteria. Future work is required to fully characterize bacterial and host mechanisms underlying the protective effects; however, we anticipate that this analysis could lead to intervention that would improve health through modification of the microbiome. Bioactive molecules from bacteria have yielded important therapeutics in the treatment of other diseases, and so the identification of neuroprotective factors in microbiotal bacteria may lead to the development of novel therapeutics.

Methods

C. elegans strains and maintenance conditions

C. elegans strains were handled according to standard procedures for nematode maintenance (Stiernagle 2006). Animals were grown and maintained at 20°C on nematode growth medium (NGM) plates seeded with the non-pathogenic *Escherichia coli* OP50. N2, obtained from the Caenorhabditis Genetics Centre (CGC), was used as wild type. The following strains were used to evaluate dopaminergic neurodegeneration: BZ555 (*egIs1*[*dat-1p::GFP*]) (obtained from the CGC), SGC856 (*lin-15*(*n765ts*)*; cwrIs856*[*Pdat-1::GFP, Pdat-1::LRRK2*(*G2019S*)*, lin-15*(+)]) (a gift from Dr. Shu G. Chen, University of Alabama at Birmingham) and LMN061 (*cwrIs856* [*dat-1p::GFP, dat-1p::LRRK2(G2019S), lin-15*(+)]; *cad-1(j1)*). LMN061 was created by crossing SGC856 with PJ2 (*cad-1(j1)*) (obtained from the CGC). NL5901 (*pkIs2386*[*Punc-54::α-synuclein::YFP + unc-119*(+)]) (obtained from the CGC) was used to monitor alpha-synuclein aggregation. The following strains were used to monitor autophagy: AMH5 (*unc-119(ed3), sosIs5* [*rab-3p::Cerulean-Venus::lgg-1 + unc-119(+)*]) (obtained from the CGC), LMN059 (*wlzIs3*[*snb-1p::Hsa-LRRK2(G2019S) + lin15*(+)]; *sosIs5*[*rab-3p::Cerulean-Venus::lgg-1 + unc-119*(+)]), MAH349 (*sqIs35*[*sqst-1p::sqst-1::GFP + unc-122p::RFP*]) and LMN060 (*wlzIs3*[*snb-1p::Hsa-LRRK2(G2019S) + lin15*(+)]; *sqIs35*[*sqst-1p::sqst-1::GFP + unc-122p::RFP*]). LMN059 was created by crossing AMH5 with WLZ3 (*wlzIs3* [*snb-1p::Hsa-LRRK2(G2019S) + lin15*(+)]) (obtained from the CGC). LMN060 was created by crossing MAH349 with WLZ3.

Bacterial strains

Actinomyces species were obtained from fecal samples collected from healthy individuals by Dr. Michael Surette's lab at McMaster University. Anaerobic environments were achieved using the Advanced Anoxomat® III jar system, the BD GasPak™ EZ container system or an anaerobic chamber. *Actinomyces* species were inoculated from frozen and grown anaerobically for 48h in liquid Brain Heart Infusion (BHI) 3 (0.5 g/L L-cysteine hydrochloride hydrate, 10 mg/L hemin and 1 mg/L Vitamin K) + 5% heat inactivated FBS. Lawns of *Actinomyces* species were grown anaerobically for 24 h on BHI3 (15g/L agar, 0.5 g/L L-cysteine hydrochloride hydrate, 10 mg/L hemin and 1 mg/L Vitamin K) + 5% heat-inactivated FBS agar plates and transferred to NGM or 5-Fluoro-2'-deoxyuridine (FUDR) (50mM) and Ampicillin (Amp) (100 μg/mL) treated NGM plates for experiments. All media was equilibrated anaerobically for a minimum of 24 h prior to use. *E. coli* OP50 was obtained from the CGC. To generate *E. coli* OP50 experimental control plates single colonies of *E. coli* OP50 were inoculated and grown in Luria-Bertani Broth overnight and seeded on BHI3 + 5% FBS agar plates. Plates were incubated at 37°C overnight and transferred to NGM or FUDR (50mM) and Amp (100 μg/mL) treated NGM plates. Mixed lawns were generated by mixing equal parts of BHI3 + 5% FBS agar grown *E. coli* OP50 and *Actinomyces viscosus* prior to transferring to NGM or FUDR (50mM) and Amp (100 μg/mL) treated NGM plates.

Neurodegeneration assay

Age-synchronized worms were obtained by treating gravid adults with 2% sodium hypochlorite and 0.5M NaOH to isolate eggs. These eggs were hatched overnight for 18-24h at 20°C with gentle shaking. L1 worms were then transferred onto NGM plates seeded with *E. coli* OP50 and incubated at 20°C. L4 worms were then washed and transferred to FUDR (50mM) and Amp (100 μg/mL) treated NGM plates with lawns of *E. coli* OP50 or an *Actinomyces* species. Animals were anesthetized using 12 mM levamisole and mounted on 2% agarose pads. Degeneration of dopaminergic neurons in Day 7 adults was monitored via visualization for GFP fluorescence of the four CEP neurons in the head of the animals.

Quantification of alpha-synuclein aggregates

Age-synchronized worms were obtained by treating gravid adults with 2% sodium hypochlorite and 0.5M NaOH to isolate eggs. These eggs were hatched overnight for 18-24h at 20°C with gentle shaking. L1 worms were then plated onto NGM plates seeded with *E. coli* OP50 and incubated at 20°C. L4 worms were then washed and transferred to FUDR (50mM) and Amp (100 μg/mL) treated NGM plates with lawns of *E. coli* OP50 or *A. viscosus*. Day 5 adult worms were anesthetized using 10% sodium azide and mounted on 2% agarose pads. 60x objective Z stack images of the head were obtained using a Nikon Eclipse Ni-U. Fluorescent spots present in the region between the tip of head and the end of the pharyngeal bulb were quantified using the ImageJ analyze particle function. Thresholds were applied to images prior to the analysis of the number of particles.

Developmental staging

Age-synchronized worms were obtained by treating gravid adults with 2% sodium hypochlorite and 0.5M NaOH to isolate eggs. These eggs were hatched overnight for 18-24h at 20°C with gentle shaking. L1 worms were then plated onto NGM plates with lawns of *E. coli* OP50, *A. viscosus* or mixed *E. coli* OP50 *A. viscosus*. Exactly 48h post L1 plating, animals were anesthetized using 12 mM levamisole, mounted on 2% agarose pads, and observed at 60x objective. Individual worms were staged as L1, L2, L3, L4 and young adult using gonadal development (Altun and Hall 2009) or as early L4 (L4.1 to L4.4), late L4 (L4.5 to L4.9) or young adult using the 9 stages of vulval development (Mok, Sternberg, and Inoue 2015).

Size Measurement

Age-synchronized worms were obtained by treating gravid adults with 2% sodium hypochlorite and 0.5M NaOH to isolate eggs. These eggs were hatched overnight for 18-24h at 20°C with gentle shaking. L1 worms were then plated onto NGM plates seeded with *E. coli* OP50 and incubated at 20°C. L4s were transferred onto FUDR (50mM) supplemented NGM plates with lawns of *E. coli* OP50, *A. viscosus* or mixed *E. coli* OP50 *A. viscosus.* Size was measured 24 and 48 h post transfer. Worms were anesthetized using 12 mM levamisole and mounted on 2% agarose pads, then imaged at 10x objective using a Nikon Eclipse Ni-U. A segmented line was drawn along the center of each worm and quantified using the measure function in ImageJ calibrated to the scale bar.

Brood size

Age-synchronized worms were obtained by treating gravid adults with 2% sodium hypochlorite and 0.5M NaOH to isolate eggs. These eggs were hatched overnight for 18-24h at 20°C with gentle shaking. L1 worms were then plated onto NGM plates seeded with *E. coli* OP50 and incubated at 20°C. Single L4s were transferred to 10 separate NGM plates per condition. Animals were transferred to fresh plates every 24 h until day 5 adulthood and resulting progeny from each day of egg-laying were counted after 48h. Animals that died before day 5 adulthood were omitted.

Lifespan assays

Age-synchronized worms were obtained by treating gravid adults with 2% sodium hypochlorite and 0.5M NaOH to isolate eggs. These eggs were hatched overnight for 18-24h at 20°C with gentle shaking. L1 worms were then plated onto NGM plates seeded with *E. coli* OP50 and incubated at 20°C. L4 worms were then washed and transferred to FUDR (50mM) and Amp (100 μg/mL) treated NGM plates with lawns of *E. coli* OP50 or *A. viscosus*. 24h post transfer (day 1 adult) animals were scored daily. Worms that failed to respond to external stimuli were considered dead and picked off the plate.

Gut Colonization

Age-synchronized worms were obtained by treating gravid adults with 2% sodium hypochlorite and 0.5M NaOH to isolate eggs. These eggs were hatched overnight for 18-24h at 20°C with gentle shaking. L1 worms were then plated onto NGM plates seeded with *E. coli* OP50 and incubated at 20°C. L4s were transferred onto FUDR (50mM)

supplemented NGM plates with lawns of *E. coli* OP50 or *A. viscosus.* 24 h post transferred 30 animals were picked into a 1.5 mL microfuge tube containing 1 mL of M9 buffer. Animals were washed a minimum of 3 times and incubated for a minimum of 1h at 20°C with gentle shaking. Worms were anesthetized using 12 mM levamisole and mounted on 2% agarose pads then imaged at 60x objective using a Nikon Eclipse Ni-U to observe bacterial presence in the intestine.

Gut granule quantification

Age-synchronized worms were obtained by treating gravid adults with 2% sodium hypochlorite and 0.5M NaOH to isolate eggs. These eggs were hatched overnight for 18-24h at 20°C with gentle shaking. L1 worms were then plated onto NGM plates seeded with *E. coli* OP50 and incubated at 20°C. L4s were transferred onto FUDR (50mM) supplemented NGM plates with lawns of *E. coli* OP50 or *A. viscosus.* Day 7 adult animals were anesthetized using 2 mM levamisole and mounted on 2% agarose pads, then imaged at 4x objective using a Nikon Eclipse Ni-U. Whole animals were outlined in imageJ, and fluorescent intensity was calculated as Integrated Density – (Measurement Area x Mean Fluorescence of Background).

RNA extraction and purification

Age-synchronized worms were obtained by treating gravid adults with 2% sodium hypochlorite and 0.5M NaOH to isolate eggs. These eggs were hatched overnight for 18-24h at 20°C with gentle shaking. A minimum of 25, 000 L1 worms per condition were then plated onto NGM plates seeded with *E. coli* OP50 and incubated at 20°C. L4 worms

were then washed and transferred to FUDR (50mM) and Amp (100 μg/mL) treated NGM plates with lawns of *E. coli* OP50 or a microbiotal isolate. Day 4 adult animals were washed and transferred to fresh FUDR (50mM) and Amp (100 μg/mL) treated NGM plates with lawns of *E. coli* OP50 or a microbiotal isolate to avoid starvation. Day 7 animals were washed and collected, and RNA was extracted using a Trizol-based extraction protocol. Samples were purified using the Monarch Total RNA Miniprep Kit (NEB #T2010) and associated protocol.

Identification of differentially expressed microRNAs

The quality of reads was measured by FastQC, and the raw reads were trimmed using Cutadapt and Trimmomatic to remove contaminating adaptor sequences (Bolger et al., 2014; Martin, 2011). Samples were run through FastQC once again to ensure quality and successful trimming. For the miRNA analysis, trimmed reads were mapped to the genome using bowtie2, and the WS280 *C. elegans* genome sequence. Reads were assigned to miRNAs using HTseq-count (Putri et al. 2022). The htseq analysis was performed using a gff file obtained from mirGeneDB (Fromm et al. 2020). DeSeq2 was used to identify differentially expressed miRNAs between groups with the following comparisons: N2 *E. coli* vs. SGC856 *E. coli,* N2 *A. viscosus* vs SGC856 *A. viscosus,* N2 *E. coli* vs. N2 *A. viscosus,* SGC856 *E. coli* vs. SGC856 *A. viscosus.* All tools described were accessed through the Galaxy platform (Galaxy Community 2022).

Identification of differentially expressed mRNAs

The quality of reads was measured by FastQC, and the raw reads were trimmed using Trimmomatic to remove contaminating adaptor sequences (Bolger, Lohse, and Usadel 2014). Samples were run through FasTQC once again to ensure quality and successful trimming. For the mRNA analysis, trimmed reads were mapped to the genome using HISAT2, and the WS280 *C. elegans* genome sequence, with known splice sites provided (Kim et al. 2019). Reads were assigned to mRNAs using HTseq-count (Putri et al. 2022). DeSeq2 was used to identify differentially expressed mRNAs between groups with the following comparisons: N2 *E. coli* vs. SGC856 *E. coli,* N2 *A. viscosus* vs SGC856 *A. viscosus,* N2 *E. coli* vs. N2 *A. viscosus,* SGC856 *E. coli* vs. SGC856 *A. viscosus (Love, Huber, and Anders 2014)*. All tools described were accessed through the Galaxy platform (Galaxy Community 2022).

Enrichment analysis of the differentially expressed mRNA & target genes of differentially expressed microRNAs

The miRNA target information was downloaded from miRTarBase (Huang et al. 2021). WormCat, a web-based gene set enrichment analysis tool, was used to determine enrichment of biological processes among identified miRNA target genes. Similarly, WormCat was used to determine the enrichment of biological processes among the identified differentially expressed mRNAs.

RNAi mediated gene knockdown

RNAi bacteria from the Ahringer library (Kamath & Ahringer, 2003) were inoculated from frozen and grown at 37°C overnight in LB supplemented with ampicillin (50 μg/mL). Overnight cultures were subcultured by ratio of 1/100 in fresh LB ampicillin and grown for 6 hours at 37°C. Medium (6 cm) NGM plates supplemented with carbenicillin (100 μg/mL) and 1 mM isopropyl β-D-1-thiogalactopyranoside (IPTG) were seeded with 200 μL of subculture and grown overnight at 37°C. Age-synchronized worms were obtained by treating gravid adults with 2% sodium hypochlorite and 0.5M NaOH to isolate eggs. These eggs were hatched overnight for 18-24h at 20°C with gentle shaking. L1 worms were plated onto NGM plates seeded with the RNAi bacteria and incubated at 20°C. L4 worms where then washed and transferred to the same RNAi bacterial lawns on large (10 cm) NGM plates supplemented with carbenicillin (100 μg/mL), 1 mM IPTG and 5-Fluoro-2'-deoxyuridine (50mM). RNAi bacteria were cultured similarly as initially described however, large plates were seeded by concentrating subcultures 5x and seeding 333 μL per plate.

LGG-1::CERULEAN VENUS punctae quantification

Age-synchronized worms were obtained by treating gravid adults with 2% sodium hypochlorite and 0.5M NaOH to isolate eggs. These eggs were hatched overnight for 18-24h at 20°C with gentle shaking. L1 worms were then plated onto NGM plates seeded with *E. coli* OP50 and incubated at 20°C. L4s were transferred onto FUDR (50mM) and Amp (100 μg/mL) supplemented NGM plates with lawns of *E. coli* OP50, *A. viscosus* or

mixed *E. coli* OP50 *A. viscosus.* Day 7 adult worms were anesthetized using 10% sodium azide and mounted on 2% agarose pads. 60x objective Z stack images of the head were obtained using a Nikon Eclipse Ni-U. Fluorescent punctae were manually counted in the region between the pharyngeal bulbs.

SQST-1::GFP fluorescence quantification

Age-synchronized worms were obtained by treating gravid adults with 2% sodium hypochlorite and 0.5M NaOH to isolate eggs. These eggs were hatched overnight for 18-24h at 20°C with gentle shaking. L1 worms were then plated onto NGM plates seeded with *E. coli* OP50 and incubated at 20°C. L4s were transferred onto FUDR (50mM) and Amp (100 µg/mL) supplemented NGM plates with lawns of *E. coli* OP50, *A. viscosus* or mixed *E. coli* OP50 *A. viscosus.* Day 7 adult worms were anesthetized using 10% sodium azide and mounted on 2% agarose pads. 10x objective images were obtained using a Nikon Eclipse Ni-U. The head (tip of the head to the end of the pharyngeal bulb) of individual animals was traced in ImageJ, and fluorescent intensity was calculated as Integrated Density – (Measurement Area x Mean Fluorescence of Background).

Transcription reporter vector assembly

Promoter sequence was defined as the sequence upstream from ATG start codon of the open reading frame (ORF) to the extremity of the ORF of the next adjacent gene or 2 kb upstream if the next adjacent gene is farther than 2 kb away. Promoter sequence was amplified from genomic DNA via PCR with primers designed to add complementarity to pPD95.75 and inserted into the pPD95.75 backbone by Gibson assembly (NEB #E2611)

between the HincII and BamHI restriction sites in the pPD95.75 multiple cloning site. pPD95_75 was a gift from Andrew Fire (Addgene plasmid # 1494; http://n2t.net/addgene:1494 ; RRID:Addgene_1494)

Pan-neuronal expression vector assembly

Age-synchronized worms were obtained by treating gravid adults with 2% sodium hypochlorite and 0.5M NaOH to isolate eggs. These eggs were hatched overnight for 18-24h at 20°C with gentle shaking. Approximately 5000 L1 worms per condition were then plated onto NGM plates seeded with *E. coli* OP50 and incubated at 20°C. Day 1 adult worms were washed and collected, and RNA was extracted using a Trizol-based extraction protocol. Samples were purified using the Monarch Total RNA Miniprep Kit (NEB #T2010) and associated protocol. cDNA (NEB #M0253) was synthesized using extracted RNA. Coding sequences were amplified from cDNA via PCR with primers designed to add complementarity to KG#470 and inserted into the KG#470 backbone by Gibson assembly (NEB #E2611) in between the SmaI and BamHI restriction sites in the KG#470 multiple cloning site. KG#470 was a gift from Kenneth Miller (Addgene plasmid # 110930; http://n2t.net/addgene:110930 ; RRID:Addgene_110930) (Schade et al. 2005)

Generation of transcriptional reporter via microinjection

Injection mix was prepared with the 20 ng/µL of the GFP reporter construct, 50 ng/µL of rol-*6*(*su1006*) co-injection marker. The final concentration of the injection mix was

brought to 100 ng/µL using unlabeled 1 kb ladder (NEB #N3232). Worms were injected following a protocol previously described (Evans 2006)

Supplementary Material

Supplementary Table 1. 16s rRNA sequences of the *Actinomyces* species

Bacterium	16s rRNA Sequence
A. naeslundii	TTANNNNTGCAGTCGAACGGTGAAGGGGCCTGCTTTTGTGGGTCCTGGATGAGTGGCGAACGGGTGAGTAACACGT GAGTAACCTGCCCCCTTCTTCTGGATAACCGCATGAAAGTGTGGCTAATACGGGATATTCTGGGTCTGTCGCATGGTG GGCCTGGGAAAGATTGCGCTTTTTTGGTGTTTTTGGTGGGGGATGGGCTCGCGGCCTATCAGCTTGTTGGTGGGGTG ATGGCCTACCAAGGCGGTGACGGGTAGCCGGCCTGAGAGGGTGGACGGTCACACTGGGACTGAGACACGGCCCAG ACTCCTACGGGAGGCAGCAGTGGGGAATATTGCACAATGGGCGCAAGCCTGATGCAGCGACGCCGCGTGAGGGATG GAGGCCTTCGGGTTGTGAACCTCTTTCGCCAGTGAAGCAGGCCTGCCTCGTTTGTGGGTGGGTTGACGGTAGCTGG ATAAGAAGCGCCGGCTAACTACGTGCCAGCAGCCGCGGTAATACGTAGGGCGCGAGCGTTGTCCGGAATTATTGGGC GTAAAGAGCTCGTAGGCGGCTGGTCGCGTCTGTCGTGAAATCCTCTGGCTTAACTGGGGGCTTGCGGTGGGTACGG GCCGGCTTGAGTGCGGTAGGGGAGACTGGAACTCCTGGTGTAGCGGTGGAATGCGCAGATATCAGGAAGAACACCG GTGGCGAAGGCGGGTCTCTGGGCCGTTACTGACGCTGAGGAGCGAAAGCGTGGGGAGCGAACAGGATTAGATACC CTGGTAGTCCACGCCGTAAACGTTGGGCACTANGTGTGGGGGGCCTTTTCCGGGTCTTCCGCGCCGTANCTAACGCA TTAAGTGCCCCGCCTGGGGAGTACGGCCGCNNNGCTAAAACTCNAAGGAATTGACG
A. oris	CCTTCGACCGCTCCCGTAGGGCCACGGGCTTCGGGTGTTGCCGACTTTCATGACGTGACGGGCGGTGTGTACAAGG CCCGAGAACGTATTCACCGCAGCGTTGCTGATCTGCGATTACTAGCGACTCCAACTTCACGGTGTCGAGTTGCAGAC ACCGATCCGAACTGAGACCGGCTTTAAGGGATTCGCTCCACCTCACGGTATCGCAGCCCTCTGTACCGGCCATTGTA GCATGCGTGAAGCCCAAGACATAAGGGGCATGATGATTTGACGTCATCCCCACCTTCCTCCGAGTTGACCCCGGCAG TCTCCCGCGAGTCCCCACCACAACGTGCTGGCAACACGGGACAAGGGTTGCGCTCGTTGCGGGACTTAACCCAACA TCTCACGACACGAGCTGACGACAACCATGCACCACCTGTGAACCGGCCCCACAAGGAGGAAACCCCGTCTCCGGA GCCGACCGGCACATGTCAAGCCTTGGTAAGGTTCTTCGCGTTGCATCGAATTAATCCGCATGCTCCGCCGCTTGTGCG GGCCCCCGTCAATTCCTTTGAGTTTTAGCCTTGCGGCCGTACTCCCCAGGCGGGGCACTTAATGCGTTAGCTACGGC GCGGAAGACCCGGAAAAGGCCCCCCACACCTAGTGCCCAACGTTTACGGCGTGGACTACCAGGGTATCTAATCCTG TTCGCTCCCCACGCTTTCGCTCCTCAGCGTCAGTAACGGCCCAGAGACCCGCCTTCGCCACCGGTGTTCTTCCTGAT ATCTGCGCATTCCACCGCTACACCAGGAGTTCCAGTCTCCCCTACCGCACTCAAGCCGGCCCGTACCCACCGCAAGC CCCCAGTTAAGCCAGAGGATTTCACGACAGACGCGACCAGCCGCCTACGAGCTCTTTACGCCCAATAATTCCG
A. viscosus	CNNCCTTCGACCGCTCCCCGTAGGGCCACGGGCTTCGGGTGTTGCCGACTTTCATGACGTGACGGGCGGTGTGTAC AAGGCCCGAGAACGTATTCACCGCAGCGTTGCTGATCTGCGATTACTAGCGACTCCAACTTCACGGTGTCGAGTTGC AGACACCGATCCGAACTGAGACCGGCTTTAAGGGATTCGCTCCACCTCACGGTATCGCAGCCCTCTGTACCGGCCAT TGTAGCATGCGTGAAGCCCAAGACATAAGGGGCATGATGATTTGACGTCATCCCCACCTTCCTCCGAGTTGACCCCG GCAGTCTCCCGCGAGTCCCCACCACAACGTGCTGGCAACACGGGACAAGGGTTGCGCTCGTTGCGGGACTTAACCC AACATCTCACGACACGAGCTGACGACAACCATGCACCACCTGTGAACCGGCCCCACAAGGAGGAAGCCCCGTCTC CGGAGCCGACCGGCACATGTCAAGCCTTGGTAAGGTTCTTCGCGTTGCATCGAATTAATCCGCATGCTCCGCCGCTT GTGCGGGCCCCCGTCAATTCCTTTGAGTTTTAGCCTTGCGGCCGTACTCCCCAGGCGGGGCACTTAATGCGTTAGCTA CGGCGCGGAAGACCCGGAAAAGGTCCCCCACACCTAGTGCCCAACGTTTACGGCGTGGACTACCAGGGTATCTAAT CCTGTTCGCTCCCCACGCTTTCGCTCCTCAGCGTCAGTAACGGCCCAGAGACCCGCCTTCGCCACCGGTGTTCTTCC TGATATCTGCGCATTCCACCGCTACACCAGGAGTTCCAGTCTCCCCTACCGCACTCAAGCCGGCCCGTACCCACCGC AAGCCCCCAGTTAAGCCAGAGGATTTCACGACAGACGCGACCAGCCGCCTACGAGCTCTTTACGCCCAATAN

Supplementary Table 2. WormCat output for differentially regulated mRNA in wild-type and *LRRK2* transgenic animals fed *E. coli* OP50 versus those fed *A. viscosus*. RGS, number of genes in the input gene set belonging to the indicated category; AC, total number of *C. elegans* genes belonging to the category.

***E. coli* OP50 vs *Actinomyces viscosus* (Wild-type genetic background)**				
Downregulated Genes				
Category 1	**RGS**	**AC**	**P Value**	**Bonferroni**
Development	9	295	3.21E-06	7.38E-05
DNA	6	176	7.36E-05	0.00169178
Proteolysis proteasome	12	733	4.04E-05	0.000928124
Transcription: chromatin	7	222	3.08E-05	0.000708951
Transcription: dosage compensation	4	10	1.88E-07	4.32E-06
Category 2	**RGS**	**AC**	**P Value**	**Bonferroni**
Development: somatic	6	122	1.03E-05	0.000440798
Proteolysis proteasome: E3	12	590	5.14E-06	0.000220974
Transcription factor: T box	3	21	9.77E-05	0.004199622
Transcription: chromatin modification	7	117	5.53E-07	2.38E-05
Transcription: dosage compensation	4	10	1.88E-07	8.07E-06
Category 3	**RGS**	**AC**	**P Value**	**Bonferroni**
Development: somatic	6	122	1.03E-05	0.00055356
mRNA functions: processing: polyadenylation	3	23	0.000124753	0.00673668
Proteolysis proteasome: E3: SCF	4	30	8.19E-06	0.000442071
Transcription factor: T box	3	21	9.77E-05	0.005273944
Upregulated Genes				
Category 1	**RGS**	**AC**	**P Value**	**Bonferroni**
Proteolysis general	15	394	0.000371835	0.007808543
Ribosome	67	244	1.04E-57	2.18E-56
Stress response	49	833	2.53E-16	5.31E-15
Unassigned	140	6343	1.69E-07	3.55E-06
Category 2	**RGS**	**AC**	**P Value**	**Bonferroni**
Proteolysis general: aspartate	6	33	1.04E-05	0.000647401
Ribosome: subunit	66	92	1.37E-78	8.46E-77
Stress response: C-type Lectin	18	256	3.36E-08	2.08E-06
Stress response: pathogen	17	192	3.40E-09	2.11E-07
Unassigned	140	6343	1.69E-07	1.05E-05
Category 3	**RGS**	**AC**	**P Value**	**Bonferroni**
Proteolysis general: inhibitor: TIL domain	4	14	7.28E-05	0.00633097
Ribosome: subunit	66	92	1.37E-78	1.19E-76
Stress response: C-type Lectin	18	256	3.36E-08	2.92E-06
Stress response: pathogen: saposin	5	14	3.56E-06	0.000309637
Stress response: pathogen: unassigned	8	96	6.65E-05	0.005788429
Unassigned: regulated by multiple stresses	69	1707	3.17E-14	2.76E-12
***E. coli* OP50 vs *Actinomyces oris* (*LRRK2* genetic background)**				
Downregulated Genes				
Category 1	**RGS**	**AC**	**P Value**	**Bonferroni**
Cell cycle	21	172	1.56E-19	3.89E-18
DNA	18	176	8.85E-16	2.21E-14
mRNA functions	19	407	6.50E-11	1.63E-09
Transcription: chromatin modification	14	222	4.69E-10	1.17E-08
Transcription: dosage compensation	5	10	2.43E-08	6.07E-07
Category 2	**RGS**	**AC**	**P Value**	**Bonferroni**
Cell cycle: APC	4	16	6.18E-06	0.000315124
Cell cycle: chromosome dynamics	12	65	8.38E-14	4.27E-12
DNA: helicase	3	9	4.74E-05	0.002418705
DNA: repair	7	68	4.51E-07	2.30E-05
DNA: replication	6	69	7.37E-06	0.000375834

mRNA functions: processing	16	296	2.49E-10	1.27E-08
Stress response: pathogen	8	192	3.92E-05	0.001997446
Transcription factor: T box	4	21	1.57E-05	0.000802733
Transcription: chromatin modification	13	117	2.80E-12	1.43E-10
Transcription: dosage compensation	5	10	2.43E-08	1.24E-06
Category 3	**RGS**	**AC**	**P Value**	**Bonferroni**
Cell cycle: APC	4	16	6.18E-06	0.000475775
Cell cycle: chromosome dynamics: kinetochore protein	3	10	6.14E-05	0.004725497
Cell cycle: chromosome dynamics: meiotic functions	4	23	2.16E-05	0.001664943
DNA: helicase	3	9	4.74E-05	0.003651771
DNA: repair	7	68	4.51E-07	3.47E-05
DNA: replication	6	69	7.37E-06	0.000567435
mRNA functions: processing: helicase	6	47	9.44E-07	7.27E-05
Stress response: pathogen: CUB	4	25	2.90E-05	0.002231143
Transcription factor: T box	4	21	1.57E-05	0.00121197
Transcription: chromatin modification: SWI/SNF	5	14	9.22E-08	7.10E-06
Transcription: dosage compensation	5	10	2.43E-08	1.87E-06
Upregulated Genes				
Category 1	**RGS**	**AC**	**P Value**	**Bonferroni**
Metabolism	34	1601	0.000267734	0.005086951
Muscle Function	8	62	8.00E-07	1.52E-05
Proteolysis general	17	394	2.94E-06	5.59E-05
Ribosome	20	244	1.67E-11	3.17E-10
Stress Response	51	833	5.38E-21	1.02E-19
Unassigned	108	6343	2.13E-05	0.00040408
Category 2	**RGS**	**AC**	**P Value**	**Bonferroni**
Extracellular material: matrix	6	67	0.00012509	0.008130848
Metabolism: lipid	19	526	9.34E-06	0.000607211
Muscle function	8	62	8.00E-07	5.20E-05
Proteolysis general: aspartate	8	33	1.07E-08	6.93E-07
Ribosome: subunit	18	92	2.57E-16	1.67E-14
Stress response: C-type Lectin	23	256	9.80E-14	6.37E-12
Stress response: detoxification	13	206	8.26E-07	5.37E-05
Stress response: pathogen	13	192	3.92E-07	2.55E-05
Unassigned	108	6343	2.13E-05	0.001382381
Category 3	**RGS**	**AC**	**P Value**	**Bonferroni**
Muscle function	8	62	8.00E-07	7.28E-05
Proteolysis general: aspartate: cathepsin	5	22	8.47E-06	0.000770954
Ribosome: subunit	18	92	2.57E-16	2.34E-14
Stress response: C-type Lectin	23	256	9.80E-14	8.92E-12
Stress response: detoxification: ugt	8	69	1.67E-06	0.000151946
Stress response: pathogen: saposin	4	14	3.28E-05	0.002985738
Unassigned: regulated by multiple stresses	53	1707	1.37E-10	1.24E-08

Supplementary Table 3. Genes downregulated in wild-type worms fed *A. viscosus*.

GeneID	Sequence ID	log2(FC)	P-value	P-adj
WBGene00009706	F44G3.2	-6.58989913	4.61E-55	1.93E-51
WBGene00007873	C32H11.10	-5.6947239	1.65E-16	1.97E-14
WBGene00010928	M162.2	-5.14921195	7.26E-21	2.21E-18
WBGene00219888	F09G2.14	-4.68365812	4.10E-12	1.85E-10
WBGene00009047	F22B8.4	-3.97645538	1.73E-10	5.92E-09
WBGene00006775	F56A12.1	-3.96360574	2.40E-13	1.41E-11
WBGene00011844	T19C9.8	-3.75643814	1.94E-18	3.38E-16
WBGene00011672	T10B9.2	-3.68518118	1.37E-20	3.83E-18
WBGene00022559	ZC204.9	-3.57340241	1.33E-12	6.62E-11

WBGene00000453	W05E10.3	-3.45160204	2.14E-19	4.59E-17
WBGene00003377	C39E6.4	-3.36556163	9.27E-16	9.46E-14
WBGene00018442	F45C12.11	-3.29322687	1.84E-10	6.21E-09
WBGene00008958	F19H6.3	-3.26154568	2.14E-10	7.07E-09
WBGene00010128	F55G11.8	-3.16959883	1.51E-13	9.30E-12
WBGene00044798	Y46E12A.4	-3.0873675	3.36E-15	2.99E-13
WBGene00020081	R52.10	-3.07253218	1.89E-10	6.29E-09
WBGene00006545	T07C4.2	-3.06112917	9.45E-14	6.13E-12
WBGene00000620	ZC513.8	-3.03863642	2.59E-14	1.99E-12
WBGene00012186	W01F3.3	-3.03437884	3.78E-11	1.47E-09
WBGene00012176	W01C9.2	-2.9677547	1.20E-12	6.06E-11
WBGene00009048	F22B8.6	-2.9457665	5.05E-18	8.04E-16
WBGene00013652	Y105C5B.12	-2.93092985	3.40E-14	2.50E-12
WBGene00022265	Y73C8C.8	-2.92344456	2.32E-12	1.11E-10
WBGene00018647	F49F1.7	-2.9122388	3.14E-14	2.35E-12
WBGene00206414	F31D5.7	-2.87449956	8.07E-11	2.95E-09
WBGene00019418	K05F6.7	-2.82333338	1.03E-11	4.34E-10
WBGene00017253	F08D12.10	-2.79728289	3.70E-13	2.09E-11
WBGene00019415	K05F6.4	-2.79525465	1.05E-13	6.78E-12
WBGene00007182	B0462.3	-2.71773394	6.36E-12	2.76E-10
WBGene00044694	F12E12.10	-2.71392029	3.33E-14	2.46E-12
WBGene00006547	F40H6.4	-2.71083368	1.35E-15	1.31E-13
WBGene00010808	M01E5.6	-2.70645555	3.51E-17	4.66E-15
WBGene00044200	H37A05.4	-2.67856119	1.35E-11	5.64E-10
WBGene00045265	K10C2.8	-2.67185577	9.43E-13	4.92E-11
WBGene00022418	Y102A11A.8	-2.63679136	1.43E-12	7.06E-11
WBGene00004106	C24A8.3	-2.63337969	1.13E-16	1.39E-14
WBGene00000227	Y48G1BL.2	-2.62482293	1.12E-17	1.65E-15
WBGene00000478	F27E11.3	-2.58227386	7.67E-12	3.31E-10
WBGene00006331	R10E4.2	-2.57407506	7.43E-19	1.48E-16
WBGene00018746	F53C3.2	-2.52984092	5.02E-14	3.57E-12
WBGene00009939	F52F12.6	-2.5272143	1.25E-15	1.22E-13
WBGene00006382	W04A8.7	-2.50789474	4.62E-19	9.42E-17
WBGene00003983	Y46G5A.27	-2.46009299	9.45E-11	3.39E-09
WBGene00010519	K03A11.1	-2.44781258	5.72E-13	3.11E-11
WBGene00007053	T04D1.4	-2.44394119	1.04E-12	5.33E-11
WBGene00020073	R52.1	-2.36094981	5.73E-14	3.99E-12
WBGene00001833	Y110A7A.1	-2.35176982	4.94E-14	3.53E-12
WBGene00004166	Y43H11AL.3	-2.35061751	4.50E-16	4.99E-14
WBGene00012581	Y38E10A.3	-2.3504013	4.00E-11	1.55E-09
WBGene00014006	ZK596.1	-2.34769362	6.23E-12	2.71E-10
WBGene00016868	C52B9.8	-2.34461802	2.33E-13	1.38E-11
WBGene00000396	F25F2.2	-2.32913682	2.24E-16	2.62E-14
WBGene00014115	ZK858.1	-2.32206536	4.01E-15	3.50E-13
WBGene00007028	C47D12.1	-2.30759146	9.26E-13	4.84E-11
WBGene00016457	C35E7.5	-2.29914672	3.21E-18	5.31E-16
WBGene00017423	F13C5.2	-2.28379821	8.40E-11	3.06E-09
WBGene00019922	R07C3.6	-2.27765617	2.82E-13	1.63E-11
WBGene00001086	R13G10.1	-2.25358338	8.38E-14	5.48E-12
WBGene00019792	M116.5	-2.21128808	8.02E-11	2.94E-09
WBGene00004818	C52D10.6	-2.210677	4.48E-16	4.99E-14
WBGene00004751	K10G6.3	-2.15567788	2.26E-10	7.43E-09
WBGene00021468	Y39G10AR.10	-2.14647843	1.94E-13	1.16E-11
WBGene00220246	ZK858.10	-2.14251051	4.99E-11	1.90E-09
WBGene00010013	F54B3.1	-2.13853018	1.89E-13	1.13E-11
WBGene00017140	EEED8.12	-2.12764583	2.20E-10	7.24E-09
WBGene00020911	W01A11.5	-2.12759381	1.31E-12	6.52E-11
WBGene00003133	W10C6.1	-2.11704205	1.70E-14	1.36E-12

WBGene00018898	F55F10.1	-2.11118125	1.03E-10	3.68E-09
WBGene00003367	M106.1	-2.10070975	3.45E-14	2.52E-12
WBGene00001186	F55A8.1	-2.09153001	1.28E-12	6.42E-11
WBGene00000783	T10H4.12	-2.07397724	9.85E-12	4.17E-10
WBGene00001562	B0513.1	-2.0658263	2.58E-12	1.22E-10
WBGene00021458	Y39G10AL.1	-2.0636818	1.38E-10	4.84E-09
WBGene00001080	Y59A8B.1	-2.06045146	3.01E-10	9.68E-09
WBGene00021316	Y32H12A.8	-2.05294077	1.37E-11	5.70E-10
WBGene00004815	C52D10.7	-2.05177282	1.76E-13	1.07E-11
WBGene00007501	C09H10.7	-2.04357373	3.02E-11	1.20E-09
WBGene00001087	Y39A1B.3	-2.03990655	4.33E-12	1.95E-10
WBGene00011562	T07C4.10	-2.0361013	2.23E-11	8.98E-10
WBGene00008145	C47E8.8	-2.02488711	1.72E-10	5.89E-09
WBGene00012100	T27F2.2	-2.0143787	1.60E-10	5.52E-09
WBGene00017135	EEED8.4	-2.01263643	1.80E-10	6.11E-09
WBGene00010044	F54C9.9	-2.00518757	5.31E-14	3.77E-12
WBGene00019871	R04E5.8	-1.99897731	2.79E-10	9.03E-09
WBGene00004782	C26E6.9	-1.98309644	3.72E-12	1.70E-10
WBGene00006384	C11G6.1	-1.97609637	1.72E-10	5.89E-09
WBGene00016603	C43E11.3	-1.97068896	4.36E-12	1.96E-10
WBGene00000461	F17A2.5	-1.95920871	2.91E-10	9.39E-09
WBGene00002637	F26F12.7	-1.94598287	1.05E-10	3.73E-09
WBGene00004816	Y105C5B.13	-1.93679877	5.45E-13	2.99E-11
WBGene00014199	ZK1053.4	-1.9058056	3.22E-11	1.27E-09
WBGene00019313	K02E7.9	-1.89902893	2.79E-11	1.11E-09
WBGene00009368	F33H2.5	-1.88723327	9.30E-11	3.35E-09
WBGene00000482	T14G8.1	-1.88510542	1.82E-10	6.17E-09
WBGene00000884	D1009.2	-1.87092102	3.15E-14	2.35E-12
WBGene00012436	Y11D7A.13	-1.85973888	6.15E-12	2.70E-10
WBGene00004874	F35G12.8	-1.85661123	7.42E-12	3.21E-10
WBGene00018520	F46H5.4	-1.8519865	6.18E-11	2.31E-09
WBGene00000939	K12H4.8	-1.84913666	4.59E-12	2.05E-10
WBGene00017607	F19F10.11	-1.84649602	4.59E-12	2.05E-10
WBGene00007761	C27B7.4	-1.84603368	3.73E-13	2.10E-11
WBGene00018778	F53H1.4	-1.84334421	7.54E-12	3.26E-10
WBGene00011820	T18D3.1	-1.84107435	1.53E-10	5.30E-09
WBGene00004873	Y47D3A.26	-1.83829707	2.51E-12	1.19E-10
WBGene00004371	Y42H9B.2	-1.82773535	1.14E-10	4.04E-09
WBGene00010369	H06O01.2	-1.82250979	7.01E-11	2.59E-09
WBGene00001596	ZC308.1	-1.82068836	9.21E-11	3.33E-09
WBGene00017800	F25G6.9	-1.80296849	3.05E-10	9.77E-09
WBGene00017313	F09G2.4	-1.79771107	9.22E-12	3.93E-10
WBGene00007975	C36B1.8	-1.78857411	5.55E-11	2.09E-09
WBGene00019862	R04A9.2	-1.78000843	1.43E-10	4.99E-09
WBGene00004813	Y47D7A.1	-1.77003682	8.01E-11	2.94E-09
WBGene00006773	W02D3.9	-1.72366615	6.17E-12	2.70E-10
WBGene00004510	F10B5.7	-1.70882749	6.11E-11	2.29E-09
WBGene00000995	C18D1.1	-1.70313731	2.19E-11	8.85E-10

Supplementary Table 4. Genes upregulated in wild-type worms fed *A. viscosus.*

GeneID	Sequence ID	log2(FC)	P-value	P-adj
WBGene00010085	F55B11.3	1.534411962	2.76E-10	8.96E-09
WBGene00004439	F52B5.6	1.612942906	5.25E-11	1.99E-09
WBGene00002023	C09B8.6	1.647608157	5.17E-11	1.96E-09
WBGene00023451	K08E3.10	1.666419976	5.40E-11	2.04E-09
WBGene00001909	C50F4.13	1.677393401	9.09E-13	4.77E-11

WBGene00014253	ZK1320.3	1.692017104	4.92E-11	1.88E-09
WBGene00012213	W02D9.7	1.704960487	3.80E-12	1.73E-10
WBGene00003773	ZK892.2	1.719954875	1.04E-10	3.68E-09
WBGene00004478	F40F8.10	1.736394526	6.22E-11	2.32E-09
WBGene00008393	D1086.6	1.737312595	4.77E-11	1.83E-09
WBGene00194641	F47G3.4	1.746455801	8.98E-11	3.26E-09
WBGene00019780	M60.4	1.76006332	2.20E-10	7.24E-09
WBGene00017923	F29B9.8	1.768428716	5.25E-12	2.32E-10
WBGene00010084	F55B11.2	1.791043745	1.76E-10	5.98E-09
WBGene00022820	ZK813.1	1.809376547	2.41E-14	1.86E-12
WBGene00014108	ZK856.7	1.811522861	1.40E-10	4.90E-09
WBGene00001385	F02A9.2	1.812316711	1.41E-13	8.73E-12
WBGene00008378	D1054.11	1.812814011	1.51E-12	7.41E-11
WBGene00003371	F09F7.2	1.830803879	1.52E-14	1.22E-12
WBGene00000081	Y50D7A.7	1.834592181	8.78E-12	3.76E-10
WBGene00023489	F42A10.9	1.835069491	1.54E-10	5.34E-09
WBGene00018951	F56C9.7	1.835786059	1.43E-11	5.91E-10
WBGene00014000	ZK550.6	1.864265132	1.33E-13	8.36E-12
WBGene00000221	T04C10.4	1.867899971	2.95E-10	9.51E-09
WBGene00020155	T02B11.3	1.870373524	9.73E-11	3.49E-09
WBGene00000175	M02F4.8	1.871370861	3.89E-11	1.51E-09
WBGene00044686	W07E11.4	1.874328862	4.09E-13	2.29E-11
WBGene00004995	C28C12.7	1.875635249	2.13E-13	1.26E-11
WBGene00004096	F40F8.7	1.878904478	1.29E-12	6.47E-11
WBGene00013266	Y57A10A.26	1.880282501	3.82E-12	1.74E-10
WBGene00015671	C10B5.3	1.891998485	6.12E-14	4.18E-12
WBGene00009091	F23D12.7	1.893223338	2.79E-11	1.11E-09
WBGene00004484	F36A2.6	1.896006628	7.34E-13	3.92E-11
WBGene00011330	T01D3.6	1.900123765	2.58E-10	8.40E-09
WBGene00022410	Y97E10C.1	1.908375527	8.35E-11	3.05E-09
WBGene00016918	C54E4.2	1.911269586	5.13E-12	2.28E-10
WBGene00021350	Y37E3.8	1.915368918	9.73E-13	5.06E-11
WBGene00012148	VF13D12L.1	1.918048804	5.61E-13	3.05E-11
WBGene00006863	F56B6.4	1.93569954	1.85E-11	7.55E-10
WBGene00003375	T04C9.4	1.937245699	3.38E-11	1.33E-09
WBGene00004486	T08B2.10	1.938648873	1.57E-13	9.65E-12
WBGene00003097	C17G10.5	1.939864819	2.65E-11	1.06E-09
WBGene00004488	T05F1.3	1.941488403	2.69E-12	1.27E-10
WBGene00006725	H06I04.4	1.94667312	5.26E-13	2.90E-11
WBGene00012216	W02D9.10	1.946716442	2.04E-10	6.79E-09
WBGene00019327	K02F3.4	1.948590579	3.08E-13	1.76E-11
WBGene00004493	T07A9.11	1.95270573	4.97E-11	1.89E-09
WBGene00002100	F56F3.6	1.95804562	2.87E-11	1.14E-09
WBGene00013181	Y53H1B.2	1.958308117	2.82E-12	1.33E-10
WBGene00000277	C23H4.1	1.959910142	5.50E-14	3.87E-12
WBGene00022748	ZK484.1	1.960692318	7.16E-15	6.01E-13
WBGene00012909	Y46G5A.19	1.979826951	8.57E-13	4.54E-11
WBGene00004451	C54C6.1	1.981276555	8.20E-13	4.35E-11
WBGene00013579	Y79H2A.2	1.983431654	1.85E-10	6.23E-09
WBGene00007652	C17G1.5	1.984996303	2.37E-10	7.74E-09
WBGene00004453	C26F1.9	1.987687525	1.86E-10	6.23E-09

WBGene00019779	M60.2	1.988171149	1.12E-12	5.71E-11
WBGene00009995	F53F4.13	1.991174155	1.23E-13	7.76E-12
WBGene00021709	Y49C4A.8	1.993477823	1.16E-11	4.84E-10
WBGene00017909	F28H1.4	1.998309589	9.07E-11	3.28E-09
WBGene00004421	F10B5.1	2.000436195	1.29E-13	8.12E-12
WBGene00014505	T05E11.9	2.001994736	1.88E-11	7.65E-10
WBGene00004475	Y71A12B.1	2.002436227	3.32E-12	1.54E-10
WBGene00018532	F47B7.1	2.008882538	4.81E-13	2.67E-11
WBGene00012585	Y38E10A.7	2.009370657	6.24E-14	4.24E-12
WBGene00019361	K03E5.2	2.01302576	1.01E-12	5.21E-11
WBGene00003765	B0213.2	2.019200893	2.68E-14	2.05E-12
WBGene00012179	W01D2.1	2.02279935	1.39E-12	6.88E-11
WBGene00002065	F54C9.1	2.025686583	3.17E-15	2.83E-13
WBGene00004427	K11H12.2	2.033917907	3.46E-12	1.60E-10
WBGene00014137	ZK896.6	2.035105804	6.84E-14	4.63E-12
WBGene00002054	F10C1.7	2.037503839	1.17E-12	5.91E-11
WBGene00020340	T08B1.1	2.046001358	1.78E-11	7.28E-10
WBGene00006530	F44F4.11	2.051842716	1.82E-16	2.16E-14
WBGene00004410	Y62E10A.1	2.057215118	2.90E-14	2.19E-12
WBGene00004499	C26F1.4	2.061366437	1.94E-14	1.53E-12
WBGene00013702	Y106G6D.6	2.068281671	1.11E-12	5.69E-11
WBGene00004444	Y106G6H.3	2.071605059	3.96E-16	4.51E-14
WBGene00017780	F25E2.2	2.072598353	6.94E-16	7.40E-14
WBGene00015598	C08E3.6	2.074072438	2.15E-14	1.69E-12
WBGene00004417	R151.3	2.074764522	8.84E-13	4.65E-11
WBGene00000219	F21F8.7	2.077485196	6.81E-15	5.77E-13
WBGene00022822	ZK813.3	2.081031572	2.47E-18	4.13E-16
WBGene00020339	T08A9.11	2.084569473	4.05E-11	1.56E-09
WBGene00044178	C30G7.4	2.085119494	1.61E-10	5.56E-09
WBGene00020886	T28B4.3	2.088005036	8.87E-12	3.79E-10
WBGene00018729	F53A9.6	2.088277412	2.52E-13	1.47E-11
WBGene00013118	Y51H4A.24	2.093333981	1.62E-11	6.67E-10
WBGene00044082	D1086.12	2.09760781	5.55E-11	2.09E-09
WBGene00009130	F25H5.8	2.101629211	1.45E-10	5.05E-09
WBGene00004442	R11D1.8	2.104787394	6.83E-15	5.77E-13
WBGene00004432	E04A4.8	2.105632392	9.76E-13	5.06E-11
WBGene00045394	ZK813.7	2.106708826	6.58E-18	1.01E-15
WBGene00045245	F09A5.9	2.113480461	2.76E-14	2.10E-12
WBGene00017069	D2096.1	2.114314322	3.25E-13	1.84E-11
WBGene00004473	Y43B11AR.4	2.114415862	4.94E-16	5.44E-14
WBGene00008356	D1025.4	2.116659992	1.32E-14	1.07E-12
WBGene00012487	Y18D10A.23	2.116935999	5.96E-14	4.10E-12
WBGene00004431	C09D4.5	2.125686097	2.86E-12	1.34E-10
WBGene00004497	Y41D4B.5	2.130024425	3.90E-12	1.77E-10
WBGene00004472	C23G10.3	2.131485412	5.71E-16	6.21E-14
WBGene00021050	W05H9.3	2.133302542	5.89E-14	4.07E-12
WBGene00009637	F42F12.6	2.133313835	1.81E-15	1.69E-13
WBGene00006728	ZK1010.1	2.138278762	1.94E-15	1.80E-13
WBGene00016599	C42D8.1	2.138372617	9.89E-13	5.11E-11
WBGene00021544	Y43B11AR.3	2.141152286	9.27E-16	9.46E-14
WBGene00004415	B0041.4	2.142248934	3.00E-12	1.39E-10

WBGene00194985	Y25C1A.14	2.149073512	3.11E-13	1.78E-11
WBGene00004479	D1007.6	2.149955806	1.28E-15	1.24E-13
WBGene00017258	F08F1.4	2.151512082	4.66E-13	2.59E-11
WBGene00019204	H14N18.4	2.151755992	9.30E-11	3.35E-09
WBGene00000608	ZK1193.1	2.163021873	2.41E-13	1.41E-11
WBGene00010007	F53H4.2	2.166533929	2.01E-11	8.16E-10
WBGene00004416	F54C9.5	2.16887746	7.57E-14	5.07E-12
WBGene00002268	ZK1248.16	2.169495509	1.26E-14	1.02E-12
WBGene00020811	T25G12.3	2.170080217	7.98E-13	4.25E-11
WBGene00015619	C08G9.1	2.171515686	2.97E-13	1.71E-11
WBGene00044553	T23B12.11	2.173366902	3.74E-11	1.46E-09
WBGene00004477	F42C5.8	2.175071255	2.82E-16	3.27E-14
WBGene00004452	C06B8.8	2.178961955	2.44E-15	2.22E-13
WBGene00011923	T22C8.2	2.180368006	1.88E-10	6.28E-09
WBGene00004445	W09C5.6	2.184382909	6.09E-20	1.43E-17
WBGene00005180	Y25C1A.11	2.184431554	1.17E-10	4.11E-09
WBGene00005003	F27C8.4	2.18806856	3.45E-11	1.35E-09
WBGene00004249	Y39A3CL.6	2.188118961	2.11E-10	7.00E-09
WBGene00004491	F53A3.3	2.191906023	1.13E-17	1.65E-15
WBGene00008577	F08G2.5	2.197111455	1.78E-10	6.05E-09
WBGene00012101	T27F2.4	2.197372604	9.79E-11	3.50E-09
WBGene00015756	C14C6.2	2.20470998	7.84E-12	3.37E-10
WBGene00002255	F40F4.4	2.206467011	7.18E-17	9.17E-15
WBGene00004482	C16A3.9	2.206563744	1.70E-15	1.62E-13
WBGene00004429	Y48G8AL.8	2.207847054	4.32E-15	3.72E-13
WBGene00005000	C48E7.10	2.209819468	6.49E-11	2.42E-09
WBGene00000728	F55C10.3	2.211545224	4.67E-12	2.08E-10
WBGene00010049	F54D5.3	2.211723893	3.49E-12	1.60E-10
WBGene00015495	C05E11.6	2.214094287	6.23E-12	2.71E-10
WBGene00008572	F08B12.4	2.214997282	5.63E-14	3.94E-12
WBGene00004446	T24B8.1	2.218238944	6.45E-13	3.47E-11
WBGene00004418	F53G12.10	2.219324923	3.24E-14	2.41E-12
WBGene00004487	Y57G11C.16	2.219991712	1.17E-14	9.59E-13
WBGene00006634	F33C8.3	2.222812423	2.02E-11	8.17E-10
WBGene00004480	F40F11.1	2.226461597	4.76E-18	7.74E-16
WBGene00004454	C09H10.2	2.22891832	1.45E-12	7.11E-11
WBGene00013901	ZC443.6	2.22960386	2.98E-10	9.60E-09
WBGene00010086	F55B11.4	2.230765311	1.43E-12	7.06E-11
WBGene00004470	F56F3.5	2.234587789	1.62E-18	2.92E-16
WBGene00004426	C04F12.4	2.234946811	1.77E-14	1.41E-12
WBGene00004441	C53H9.1	2.238818458	9.28E-19	1.83E-16
WBGene00045392	F26D11.12	2.239704955	3.25E-11	1.28E-09
WBGene00008865	F15G9.1	2.242971204	2.91E-12	1.36E-10
WBGene00000779	F28H1.2	2.24611457	2.05E-17	2.88E-15
WBGene00019101	F59B1.10	2.254156049	4.60E-11	1.77E-09
WBGene00018376	F43C9.2	2.256319594	8.79E-11	3.20E-09
WBGene00015936	C17H12.11	2.264706753	1.72E-15	1.62E-13
WBGene00012886	Y45F10D.6	2.271035488	2.60E-11	1.05E-09
WBGene00002052	NA	2.278829304	1.23E-12	6.18E-11
WBGene00013392	Y62H9A.4	2.283978719	2.85E-16	3.29E-14
WBGene00007295	C04C11.1	2.288734389	1.80E-13	1.08E-11

WBGene00014252	ZK1320.2	2.291306069	2.49E-15	2.26E-13
WBGene00236786	C17H12.37	2.291716243	1.19E-15	1.17E-13
WBGene00004492	F28D1.7	2.291870974	2.00E-15	1.84E-13
WBGene00016099	C25E10.10	2.292578965	2.81E-10	9.09E-09
WBGene00004435	B0336.10	2.297309538	1.02E-19	2.31E-17
WBGene00011829	T19A6.4	2.298135328	3.95E-13	2.22E-11
WBGene00004440	F28C6.7	2.298740531	7.12E-22	2.43E-19
WBGene00004495	F39B2.6	2.301379836	7.25E-14	4.87E-12
WBGene00017678	F21F8.4	2.302223915	1.77E-13	1.07E-11
WBGene00021556	Y45G5AM.3	2.303039365	6.68E-18	1.02E-15
WBGene00004430	Y45F10D.12	2.305323056	2.21E-17	3.09E-15
WBGene00004433	C14B9.7	2.309886634	1.02E-20	2.89E-18
WBGene00016493	C37A2.7	2.315255188	6.60E-20	1.53E-17
WBGene00002254	F40F4.2	2.324652197	4.76E-14	3.41E-12
WBGene00013391	Y62H9A.3	2.326236874	1.20E-17	1.75E-15
WBGene00004447	F10E7.7	2.326450519	2.13E-18	3.59E-16
WBGene00004436	D1007.12	2.330681351	9.27E-17	1.16E-14
WBGene00004420	R13A5.8	2.338857582	3.43E-17	4.59E-15
WBGene00004476	ZC434.2	2.33926217	9.25E-17	1.16E-14
WBGene00269383	ZK384.7	2.341630182	1.84E-10	6.20E-09
WBGene00013964	ZK287.3	2.34436628	5.75E-14	3.99E-12
WBGene00021602	Y46H3B.1	2.345961566	1.30E-11	5.44E-10
WBGene00018760	F53E10.4	2.346271854	3.11E-15	2.80E-13
WBGene00016204	C29E4.7	2.347306013	9.99E-15	8.23E-13
WBGene00020335	T08A9.2	2.348895897	1.16E-10	4.11E-09
WBGene00004483	F37C12.9	2.351921755	1.35E-17	1.95E-15
WBGene00009638	F42F12.7	2.356437543	1.37E-17	1.96E-15
WBGene00000716	T15B7.3	2.361365472	1.32E-13	8.33E-12
WBGene00014826	R13H4.2	2.361519539	1.40E-11	5.81E-10
WBGene00020662	T21H3.1	2.361902409	2.02E-15	1.85E-13
WBGene00015954	C18B2.3	2.367519745	2.39E-10	7.82E-09
WBGene00004485	T01C3.6	2.369141909	4.36E-23	1.87E-20
WBGene00009393	F35C5.5	2.371081739	3.36E-14	2.48E-12
WBGene00044757	Y55F3BR.11	2.379204597	4.78E-11	1.83E-09
WBGene00016362	C33G8.4	2.382533901	2.94E-12	1.36E-10
WBGene00009237	F28H7.3	2.387227549	1.38E-13	8.58E-12
WBGene00004449	ZK652.4	2.387549971	3.99E-17	5.21E-15
WBGene00014052	ZK669.2	2.391015023	6.78E-11	2.51E-09
WBGene00001391	K01A2.2	2.391303756	2.45E-13	1.43E-11
WBGene00014002	ZK593.2	2.393160962	5.31E-12	2.34E-10
WBGene00044296	F10C1.9	2.396351835	2.11E-12	1.01E-10
WBGene00015472	C05D9.3	2.398122818	2.25E-14	1.75E-12
WBGene00004425	C32E8.2	2.403410375	1.24E-19	2.76E-17
WBGene00015965	C18C4.3	2.405540878	2.39E-14	1.85E-12
WBGene00000713	F26F12.1	2.408334389	7.78E-14	5.14E-12
WBGene00009157	F26E4.2	2.411319368	4.61E-12	2.06E-10
WBGene00011774	T14G10.4	2.426670056	8.01E-14	5.28E-12
WBGene00017813	F26A10.1	2.435684476	1.59E-14	1.27E-12
WBGene00019738	M02F4.7	2.435970141	4.38E-13	2.44E-11
WBGene00004413	B0250.1	2.436425421	2.83E-17	3.85E-15
WBGene00004469	B0393.1	2.438339879	4.86E-18	7.82E-16

WBGene00017541	F17E9.4	2.450214028	2.12E-10	7.02E-09
WBGene00016722	C46G7.2	2.451871549	1.45E-20	3.99E-18
WBGene00012383	Y5F2A.2	2.452355015	3.47E-15	3.07E-13
WBGene00003893	C44B12.2	2.456335967	8.15E-22	2.73E-19
WBGene00019479	K07C11.7	2.466461469	2.81E-17	3.85E-15
WBGene00004448	C42C1.14	2.466743568	9.23E-22	3.03E-19
WBGene00004474	T05E11.1	2.473226496	7.72E-21	2.31E-18
WBGene00004450	F37C12.4	2.479926602	4.85E-22	1.80E-19
WBGene00012783	Y43C5A.3	2.485618012	9.08E-15	7.56E-13
WBGene00004498	B0412.4	2.486076878	7.33E-25	3.83E-22
WBGene00021520	Y41D4B.18	2.488483167	1.75E-10	5.96E-09
WBGene00012382	Y5F2A.1	2.488740988	1.71E-20	4.54E-18
WBGene00014150	ZK909.6	2.490854208	5.99E-14	4.11E-12
WBGene00004428	M01F1.2	2.492574929	3.29E-20	8.44E-18
WBGene00007605	C15C8.3	2.492753937	7.80E-16	8.15E-14
WBGene00003956	ZK112.1	2.493029208	7.19E-15	6.01E-13
WBGene00004496	F56E10.4	2.496249977	9.75E-25	4.80E-22
WBGene00009621	F41E7.5	2.499342991	1.59E-15	1.52E-13
WBGene00003991	K03E6.6	2.500125071	1.01E-18	1.97E-16
WBGene00004456	Y48B6A.2	2.508455023	1.51E-20	4.08E-18
WBGene00019645	K11D12.5	2.512088113	5.46E-14	3.85E-12
WBGene00000560	Y46E12A.1	2.515453769	1.58E-10	5.45E-09
WBGene00016424	C34H4.1	2.516580022	1.20E-13	7.69E-12
WBGene00044921	F53C11.9	2.520116548	1.78E-11	7.28E-10
WBGene00015949	C18A11.3	2.524427746	1.77E-15	1.66E-13
WBGene00045268	H01M10.3	2.529795554	4.36E-17	5.66E-15
WBGene00009640	F42F12.9	2.53226333	5.94E-22	2.14E-19
WBGene00004438	F55D10.2	2.540160815	1.52E-19	3.30E-17
WBGene00017659	F21C10.10	2.547740774	3.72E-12	1.70E-10
WBGene00010982	R03A10.2	2.551294118	2.87E-12	1.34E-10
WBGene00009394	F35C5.6	2.555174022	3.81E-20	9.52E-18
WBGene00013081	Y51A2D.14	2.557476933	1.98E-18	3.42E-16
WBGene00219709	K02F3.14	2.567676029	1.93E-16	2.28E-14
WBGene00044901	Y41G9A.10	2.578431568	1.85E-13	1.11E-11
WBGene00015828	C16C4.4	2.579385681	1.94E-12	9.36E-11
WBGene00016052	C24B9.9	2.580219152	1.59E-13	9.72E-12
WBGene00008369	D1053.4	2.587760187	9.41E-12	4.00E-10
WBGene00009818	F47B10.7	2.588120794	4.42E-16	4.96E-14
WBGene00020229	T05A8.3	2.589392587	8.18E-21	2.40E-18
WBGene00001500	C54F6.14	2.596858274	8.03E-16	8.35E-14
WBGene00004490	F37C12.11	2.599148679	6.02E-22	2.14E-19
WBGene00016893	C53B7.2	2.604538498	1.10E-25	6.82E-23
WBGene00019478	K07C11.5	2.605339569	2.21E-14	1.73E-12
WBGene00009620	F41E7.4	2.611726465	1.06E-10	3.77E-09
WBGene00007366	C06B3.7	2.62219176	3.37E-11	1.33E-09
WBGene00021492	Y40B10A.7	2.628918941	2.28E-10	7.49E-09
WBGene00000214	Y39B6A.20	2.653720652	3.33E-20	8.44E-18
WBGene00194713	F19B10.13	2.654059818	9.55E-16	9.56E-14
WBGene00000169	F32A5.5	2.654965985	3.62E-21	1.16E-18
WBGene00004875	F47G4.7	2.65917909	1.02E-15	1.01E-13
WBGene00004000	T21E8.1	2.66320572	2.10E-18	3.59E-16

WBGene00011821	T18D3.3	2.677515387	3.53E-15	3.10E-13
WBGene00020878	T28A11.16	2.680949523	8.69E-13	4.58E-11
WBGene00020954	W02G9.4	2.684591265	3.12E-13	1.78E-11
WBGene00219609	T22E6.2	2.69195209	1.10E-11	4.63E-10
WBGene00004409	Y37E3.7	2.70706258	6.92E-22	2.41E-19
WBGene00021978	Y58A7A.4	2.713014195	2.64E-12	1.25E-10
WBGene00044238	C30H6.12	2.715973004	1.88E-12	9.10E-11
WBGene00002090	ZK1251.2	2.716665674	6.83E-16	7.33E-14
WBGene00008621	F09C8.1	2.720423251	1.09E-16	1.36E-14
WBGene00013334	Y57G11C.45	2.724436882	1.19E-24	5.70E-22
WBGene00020617	T20D4.11	2.744994023	2.01E-12	9.65E-11
WBGene00020747	T24A6.7	2.752042686	1.73E-11	7.09E-10
WBGene00000671	Y41C4A.19	2.755664487	2.37E-19	4.96E-17
WBGene00000373	F08F3.7	2.776238245	5.97E-13	3.23E-11
WBGene00015055	B0222.3	2.804615411	1.04E-18	2.00E-16
WBGene00004408	F25H2.10	2.820787282	1.33E-26	8.90E-24
WBGene00007142	B0334.1	2.827883079	3.73E-14	2.70E-12
WBGene00044607	K02A11.4	2.833478003	5.46E-15	4.66E-13
WBGene00235094	K08D9.9	2.83594099	4.99E-15	4.28E-13
WBGene00007120	B0250.3	2.83656891	1.85E-18	3.26E-16
WBGene00012582	Y38E10A.4	2.838539521	7.72E-14	5.14E-12
WBGene00020047	R13A5.3	2.841555138	7.75E-14	5.14E-12
WBGene00009158	F26E4.3	2.8422488	1.29E-16	1.57E-14
WBGene00003648	R11G11.2	2.851715654	1.54E-11	6.35E-10
WBGene00011801	T16G1.7	2.852381251	3.53E-14	2.57E-12
WBGene00001890	ZK131.10	2.857871559	5.03E-13	2.77E-11
WBGene00010225	F58A3.5	2.871212106	3.41E-11	1.33E-09
WBGene00043062	Y54G2A.39	2.886165021	1.72E-13	1.05E-11
WBGene00004993	C28C12.5	2.888781739	1.49E-18	2.82E-16
WBGene00010019	F54B8.4	2.904213907	1.23E-23	5.57E-21
WBGene00020049	R13A5.6	2.905192391	6.02E-18	9.41E-16
WBGene00021768	Y51F10.7	2.913659965	1.93E-12	9.33E-11
WBGene00017250	F08D12.7	2.916366976	1.86E-15	1.73E-13
WBGene00011708	T11B7.5	2.92058964	5.57E-13	3.05E-11
WBGene00271636	W05G11.8	2.931671339	1.76E-10	5.98E-09
WBGene00001886	ZK131.6	2.947703676	2.43E-12	1.16E-10
WBGene00013090	Y51B9A.8	2.955463231	9.02E-21	2.60E-18
WBGene00004423	F07D10.1	2.988914284	7.70E-25	3.90E-22
WBGene00044783	T26H5.10	2.992198151	1.27E-10	4.46E-09
WBGene00008891	F16H6.1	3.026168408	2.70E-10	8.78E-09
WBGene00044206	T26H5.9	3.046791222	2.39E-17	3.31E-15
WBGene00018971	F56D6.2	3.053548993	3.75E-22	1.46E-19
WBGene00015046	B0213.17	3.064387638	6.80E-13	3.65E-11
WBGene00018221	F40A3.6	3.093957574	7.64E-17	9.68E-15
WBGene00009969	F53B7.7	3.094044097	1.63E-12	7.97E-11
WBGene00009466	F36D1.7	3.099733781	6.64E-11	2.47E-09
WBGene00009778	F46C5.1	3.108618786	1.01E-13	6.50E-12
WBGene00008566	F08A8.3	3.124025768	6.13E-12	2.70E-10
WBGene00003093	F58B3.1	3.124864191	1.00E-15	1.00E-13
WBGene00011707	T11B7.2	3.138411614	6.09E-18	9.43E-16
WBGene00008634	F10A3.4	3.149544314	1.52E-10	5.28E-09

WBGene00022653	ZK105.1	3.170296007	1.58E-18	2.90E-16
WBGene00206361	K02G10.15	3.181722508	8.68E-14	5.65E-12
WBGene00000051	R01E6.4	3.182497764	8.35E-14	5.48E-12
WBGene00021464	Y39G10AR.6	3.184863441	1.36E-25	7.84E-23
WBGene00000215	T18H9.2	3.189452219	3.26E-25	1.82E-22
WBGene00013459	Y67A10A.10	3.196609758	1.12E-12	5.69E-11
WBGene00044811	F12E12.11	3.199500431	3.01E-13	1.73E-11
WBGene00219959	F52D2.14	3.200344305	1.34E-16	1.61E-14
WBGene00219700	F52D2.13	3.209543966	6.25E-17	8.05E-15
WBGene00220180	Y54G2A.74	3.222694339	1.45E-19	3.20E-17
WBGene00001884	ZK131.4	3.241234995	4.16E-15	3.61E-13
WBGene00001888	ZK131.8	3.24461832	3.96E-15	3.46E-13
WBGene00004989	T08A9.8	3.250379706	3.57E-16	4.09E-14
WBGene00043702	NA	3.250730698	2.19E-20	5.73E-18
WBGene00015602	C08E3.10	3.264054682	9.50E-16	9.56E-14
WBGene00020616	T20D4.10	3.274387896	1.62E-18	2.92E-16
WBGene00045411	C25F9.11	3.276843771	4.35E-35	4.85E-32
WBGene00011494	T05F1.9	3.279656916	6.36E-13	3.43E-11
WBGene00018314	F41H10.1	3.28255966	4.19E-20	1.03E-17
WBGene00015695	C10H11.6	3.300187002	4.29E-22	1.63E-19
WBGene00220003	K02G10.16	3.343223394	1.15E-13	7.36E-12
WBGene00007565	C14A6.1	3.353468737	7.48E-16	7.92E-14
WBGene00045412	C25F9.12	3.364648448	1.10E-11	4.63E-10
WBGene00015182	B0416.7	3.364701672	5.84E-16	6.30E-14
WBGene00010613	K07A1.6	3.365830593	1.84E-17	2.61E-15
WBGene00015403	C03H5.1	3.376461163	5.29E-16	5.79E-14
WBGene00013900	ZC443.5	3.39775498	2.34E-19	4.95E-17
WBGene00009854	F49A5.2	3.4333734	3.34E-17	4.50E-15
WBGene00010790	K12G11.3	3.43554927	5.24E-32	4.61E-29
WBGene00012821	Y43F8B.11	3.442145378	1.32E-22	5.51E-20
WBGene00003740	T24D8.5	3.456380587	1.18E-25	7.06E-23
WBGene00017197	F07C3.9	3.456626295	7.69E-16	8.10E-14
WBGene00001781	C02A12.1	3.459299032	2.12E-13	1.26E-11
WBGene00018342	F42A10.6	3.485245574	2.36E-28	1.98E-25
WBGene00016920	C54E4.5	3.493652508	2.05E-32	2.02E-29
WBGene00015600	C08E3.8	3.497138617	1.87E-10	6.25E-09
WBGene00019717	M01H9.1	3.501719059	4.80E-11	1.84E-09
WBGene00018696	F52E1.8	3.510943724	2.65E-13	1.54E-11
WBGene00019021	F57H12.6	3.514661828	8.48E-12	3.64E-10
WBGene00008553	F07C6.2	3.526467677	1.21E-14	9.91E-13
WBGene00000212	ZK455.4	3.53496492	8.28E-34	8.66E-31
WBGene00000611	F36A4.10	3.570163392	6.03E-24	2.80E-21
WBGene00020613	T20D4.7	3.571975304	3.54E-27	2.82E-24
WBGene00005833	C25F9.7	3.57617869	3.92E-17	5.16E-15
WBGene00007937	C34E11.4	3.5798832	1.54E-18	2.90E-16
WBGene00045261	H29C22.1	3.580851761	3.90E-25	2.11E-22
WBGene00019146	H02F09.3	3.650699525	6.60E-21	2.05E-18
WBGene00023425	B0286.6	3.696170391	1.72E-12	8.37E-11
WBGene00194803	C25F9.16	3.71565729	8.64E-18	1.30E-15
WBGene00011799	T16G1.5	3.724469429	1.31E-26	8.90E-24
WBGene00012591	Y38E10A.13	3.725080114	4.06E-14	2.93E-12

WBGene00015050	B0218.6	3.725628658	2.07E-42	4.95E-39
WBGene00003734	F58E1.6	3.725854441	4.29E-16	4.85E-14
WBGene00044488	Y54G2A.45	3.731518909	5.23E-20	1.25E-17
WBGene00012604	Y38E10A.26	3.737159452	2.81E-14	2.13E-12
WBGene00005552	Y27F2A.3	3.805085251	9.27E-15	7.67E-13
WBGene00016450	C35D10.14	3.833808986	7.64E-20	1.75E-17
WBGene00195084	C43C3.4	3.865619897	1.69E-12	8.25E-11
WBGene00007521	C11E4.7	3.879591577	1.58E-18	2.90E-16
WBGene00007203	B0564.3	3.944152413	5.69E-18	8.98E-16
WBGene00015342	C02E7.10	3.94646091	1.34E-13	8.39E-12
WBGene00015839	C16C4.15	3.950945845	7.11E-14	4.79E-12
WBGene00000968	T05F1.10	3.953561423	4.27E-18	7.01E-16
WBGene00017498	F15E11.12	3.953625793	6.46E-21	2.04E-18
WBGene00021873	Y54G2A.8	3.963694176	4.08E-19	8.43E-17
WBGene00016017	C23G10.11	3.9762873	8.98E-27	6.83E-24
WBGene00017378	F11C7.6	3.979595265	3.22E-11	1.27E-09
WBGene00009221	F28F8.2	4.022987337	2.19E-44	6.12E-41
WBGene00044379	F40H7.12	4.057042988	8.82E-16	9.11E-14
WBGene00010769	K11D2.2	4.057933938	1.65E-22	6.74E-20
WBGene00019105	F59D6.3	4.096772063	1.56E-35	1.86E-32
WBGene00002094	C17C3.4	4.102886433	6.77E-11	2.51E-09
WBGene00010062	F54F3.3	4.112249842	1.39E-35	1.78E-32
WBGene00019652	K11G9.1	4.113636926	2.11E-23	9.29E-21
WBGene00010515	K02E11.6	4.126815249	1.22E-13	7.76E-12
WBGene00016336	C33C12.4	4.143629162	1.79E-18	3.18E-16
WBGene00018568	F47E1.4	4.153433629	3.08E-22	1.23E-19
WBGene00001772	F37B1.1	4.161733028	2.56E-39	4.75E-36
WBGene00010514	K02E11.5	4.183689944	9.40E-16	9.53E-14
WBGene00020881	T28A11.19	4.281759514	9.95E-37	1.39E-33
WBGene00007726	C25F9.6	4.302077944	7.06E-19	1.42E-16
WBGene00021979	Y58A7A.5	4.321061208	8.25E-37	1.26E-33
WBGene00045272	F59C12.4	4.383410643	1.22E-26	8.87E-24
WBGene00021335	Y34D9A.11	4.548153285	2.35E-26	1.51E-23
WBGene00015890	C17C3.5	4.883883571	9.00E-18	1.34E-15
WBGene00044046	ZK666.13	4.932531337	7.60E-11	2.80E-09
WBGene00008220	C50B6.7	5.220609328	1.42E-54	4.76E-51
WBGene00020700	T22F3.11	5.372414753	2.54E-42	5.32E-39
WBGene00044284	T25C12.4	5.615714222	5.43E-80	4.54E-76
WBGene00018343	F42A10.7	5.650873652	1.47E-15	1.41E-13
WBGene00003094	F58B3.2	5.866982614	4.77E-32	4.43E-29
WBGene00008647	F10C2.7	5.917075428	1.24E-16	1.51E-14
WBGene00015052	B0218.8	6.019116824	1.63E-61	9.12E-58
WBGene00014046	ZK666.6	6.521987578	5.25E-20	1.25E-17
WBGene00011103	R07E3.2	7.398931589	2.02E-80	3.38E-76
WBGene00021581	Y46C8AL.3	7.936385535	1.38E-38	2.31E-35
WBGene00017250	F08D12.7	2.916366976	1.86E-15	1.73E-13
WBGene00011708	T11B7.5	2.92058964	5.57E-13	3.05E-11
WBGene00271636	W05G11.8	2.931671339	1.76E-10	5.98E-09
WBGene00001886	ZK131.6	2.947703676	2.43E-12	1.16E-10
WBGene00013090	Y51B9A.8	2.955463231	9.02E-21	2.60E-18
WBGene00004423	F07D10.1	2.988914284	7.70E-25	3.90E-22

WBGene00044783	T26H5.10	2.992198151	1.27E-10	4.46E-09
WBGene00008891	F16H6.1	3.026168408	2.70E-10	8.78E-09
WBGene00044206	T26H5.9	3.046791222	2.39E-17	3.31E-15
WBGene00018971	F56D6.2	3.053548993	3.75E-22	1.46E-19
WBGene00015046	B0213.17	3.064387638	6.80E-13	3.65E-11
WBGene00018221	F40A3.6	3.093957574	7.64E-17	9.68E-15
WBGene00009969	F53B7.7	3.094044097	1.63E-12	7.97E-11
WBGene00009466	F36D1.7	3.099733781	6.64E-11	2.47E-09
WBGene00009778	F46C5.1	3.108618786	1.01E-13	6.50E-12
WBGene00008566	F08A8.3	3.124025768	6.13E-12	2.70E-10
WBGene00003093	F58B3.1	3.124864191	1.00E-15	1.00E-13
WBGene00011707	T11B7.2	3.138411614	6.09E-18	9.43E-16
WBGene00008634	F10A3.4	3.149544314	1.52E-10	5.28E-09
WBGene00022653	ZK105.1	3.170296007	1.58E-18	2.90E-16
WBGene00206361	K02G10.15	3.181722508	8.68E-14	5.65E-12
WBGene00000051	R01E6.4	3.182497764	8.35E-14	5.48E-12
WBGene00021464	Y39G10AR.6	3.184863441	1.36E-25	7.84E-23
WBGene00000215	T18H9.2	3.189452219	3.26E-25	1.82E-22
WBGene00013459	Y67A10A.10	3.196609758	1.12E-12	5.69E-11
WBGene00044811	F12E12.11	3.199500431	3.01E-13	1.73E-11
WBGene00219959	F52D2.14	3.200344305	1.34E-16	1.61E-14
WBGene00219700	F52D2.13	3.209543966	6.25E-17	8.05E-15
WBGene00220180	Y54G2A.74	3.222694339	1.45E-19	3.20E-17
WBGene00001884	ZK131.4	3.241234995	4.16E-15	3.61E-13
WBGene00001888	ZK131.8	3.24461832	3.96E-15	3.46E-13
WBGene00004989	T08A9.8	3.250379706	3.57E-16	4.09E-14
WBGene00043702	NA	3.250730698	2.19E-20	5.73E-18
WBGene00015602	C08E3.10	3.264054682	9.50E-16	9.56E-14
WBGene00020616	T20D4.10	3.274387896	1.62E-18	2.92E-16
WBGene00045411	C25F9.11	3.276843771	4.35E-35	4.85E-32
WBGene00011494	T05F1.9	3.279656916	6.36E-13	3.43E-11
WBGene00018314	F41H10.1	3.28255966	4.19E-20	1.03E-17
WBGene00015695	C10H11.6	3.300187002	4.29E-22	1.63E-19
WBGene00220003	K02G10.16	3.343223394	1.15E-13	7.36E-12
WBGene00007565	C14A6.1	3.353468737	7.48E-16	7.92E-14
WBGene00045412	C25F9.12	3.364648448	1.10E-11	4.63E-10
WBGene00015182	B0416.7	3.364701672	5.84E-16	6.30E-14
WBGene00010613	K07A1.6	3.365830593	1.84E-17	2.61E-15
WBGene00015403	C03H5.1	3.376461163	5.29E-16	5.79E-14
WBGene00013900	ZC443.5	3.39775498	2.34E-19	4.95E-17
WBGene00009854	F49A5.2	3.4333734	3.34E-17	4.50E-15
WBGene00010790	K12G11.3	3.43554927	5.24E-32	4.61E-29
WBGene00012821	Y43F8B.11	3.442145378	1.32E-22	5.51E-20
WBGene00003740	T24D8.5	3.456380587	1.18E-25	7.06E-23
WBGene00017197	F07C3.9	3.456626295	7.69E-16	8.10E-14
WBGene00001781	C02A12.1	3.459299032	2.12E-13	1.26E-11
WBGene00018342	F42A10.6	3.485245574	2.36E-28	1.98E-25
WBGene00016920	C54E4.5	3.493652508	2.05E-32	2.02E-29
WBGene00015600	C08E3.8	3.497138617	1.87E-10	6.25E-09
WBGene00019717	M01H9.1	3.501719059	4.80E-11	1.84E-09
WBGene00018696	F52E1.8	3.510943724	2.65E-13	1.54E-11

WBGene00019021	F57H12.6	3.514661828	8.48E-12	3.64E-10
WBGene00008553	F07C6.2	3.526467677	1.21E-14	9.91E-13
WBGene00000212	ZK455.4	3.53496492	8.28E-34	8.66E-31
WBGene00000611	F36A4.10	3.570163392	6.03E-24	2.80E-21
WBGene00020613	T20D4.7	3.571975304	3.54E-27	2.82E-24
WBGene00005833	C25F9.7	3.57617869	3.92E-17	5.16E-15
WBGene00007937	C34E11.4	3.5798832	1.54E-18	2.90E-16
WBGene00045261	H29C22.1	3.580851761	3.90E-25	2.11E-22
WBGene00019146	H02F09.3	3.650699525	6.60E-21	2.05E-18
WBGene00023425	B0286.6	3.696170391	1.72E-12	8.37E-11
WBGene00194803	C25F9.16	3.71565729	8.64E-18	1.30E-15
WBGene00011799	T16G1.5	3.724469429	1.31E-26	8.90E-24
WBGene00012591	Y38E10A.13	3.725080114	4.06E-14	2.93E-12
WBGene00015050	B0218.6	3.725628658	2.07E-42	4.95E-39
WBGene00003734	F58E1.6	3.725854441	4.29E-16	4.85E-14
WBGene00044488	Y54G2A.45	3.731518909	5.23E-20	1.25E-17
WBGene00012604	Y38E10A.26	3.737159452	2.81E-14	2.13E-12
WBGene00005552	Y27F2A.3	3.805085251	9.27E-15	7.67E-13
WBGene00016450	C35D10.14	3.833808986	7.64E-20	1.75E-17
WBGene00195084	C43C3.4	3.865619897	1.69E-12	8.25E-11
WBGene00007521	C11E4.7	3.879591577	1.58E-18	2.90E-16
WBGene00007203	B0564.3	3.944152413	5.69E-18	8.98E-16
WBGene00015342	C02E7.10	3.94646091	1.34E-13	8.39E-12
WBGene00015839	C16C4.15	3.950945845	7.11E-14	4.79E-12
WBGene00000968	T05F1.10	3.953561423	4.27E-18	7.01E-16
WBGene00017498	F15E11.12	3.953625793	6.46E-21	2.04E-18
WBGene00021873	Y54G2A.8	3.963694176	4.08E-19	8.43E-17
WBGene00016017	C23G10.11	3.9762873	8.98E-27	6.83E-24
WBGene00017378	F11C7.6	3.979595265	3.22E-11	1.27E-09
WBGene00009221	F28F8.2	4.022987337	2.19E-44	6.12E-41
WBGene00044379	F40H7.12	4.057042988	8.82E-16	9.11E-14
WBGene00010769	K11D2.2	4.057933938	1.65E-22	6.74E-20
WBGene00019105	F59D6.3	4.096772063	1.56E-35	1.86E-32
WBGene00002094	C17C3.4	4.102886433	6.77E-11	2.51E-09
WBGene00010062	F54F3.3	4.112249842	1.39E-35	1.78E-32
WBGene00019652	K11G9.1	4.113636926	2.11E-23	9.29E-21
WBGene00010515	K02E11.6	4.126815249	1.22E-13	7.76E-12
WBGene00016336	C33C12.4	4.143629162	1.79E-18	3.18E-16
WBGene00018568	F47E1.4	4.153433629	3.08E-22	1.23E-19
WBGene00001772	F37B1.1	4.161733028	2.56E-39	4.75E-36
WBGene00010514	K02E11.5	4.183689944	9.40E-16	9.53E-14
WBGene00020881	T28A11.19	4.281759514	9.95E-37	1.39E-33
WBGene00007726	C25F9.6	4.302077944	7.06E-19	1.42E-16
WBGene00021979	Y58A7A.5	4.321061208	8.25E-37	1.26E-33
WBGene00045272	F59C12.4	4.383410643	1.22E-26	8.87E-24
WBGene00021335	Y34D9A.11	4.548153285	2.35E-26	1.51E-23
WBGene00015890	C17C3.5	4.883883571	9.00E-18	1.34E-15
WBGene00044046	ZK666.13	4.932531337	7.60E-11	2.80E-09
WBGene00008220	C50B6.7	5.220609328	1.42E-54	4.76E-51
WBGene00020700	T22F3.11	5.372414753	2.54E-42	5.32E-39
WBGene00044284	T25C12.4	5.615714222	5.43E-80	4.54E-76

WBGene00018343	F42A10.7	5.650873652	1.47E-15	1.41E-13
WBGene00003094	F58B3.2	5.866982614	4.77E-32	4.43E-29
WBGene00008647	F10C2.7	5.917075428	1.24E-16	1.51E-14
WBGene00015052	B0218.8	6.019116824	1.63E-61	9.12E-58
WBGene00014046	ZK666.6	6.521987578	5.25E-20	1.25E-17
WBGene00011103	R07E3.2	7.398931589	2.02E-80	3.38E-76
WBGene00021581	Y46C8AL.3	7.936385535	1.38E-38	2.31E-35

Supplementary Table 5. Genes downregulated in *LRRK2* transgenic worms fed *A. viscosus*.

GeneID	Sequence ID	log2(FC)	P-value	P-adj
WBGene00009706	F44G3.2	-6.62524252	8.67E-54	1.63E-50
WBGene00011979	T24B8.5	-6.06849963	1.08E-43	1.23E-40
WBGene00010928	M162.2	-5.61483308	2.73E-26	1.13E-23
WBGene00007872	C32H11.9	-5.50965355	2.13E-18	3.61E-16
WBGene00009047	F22B8.4	-5.09661429	3.93E-15	3.98E-13
WBGene00006075	F22B8.5	-4.90014006	1.26E-21	3.25E-19
WBGene00015932	C17H12.6	-4.3782915	4.97E-23	1.46E-20
WBGene00019214	H20E11.2	-4.27356714	1.50E-12	8.99E-11
WBGene00006557	C24H11.3	-4.05910863	4.90E-16	5.90E-14
WBGene00007873	C32H11.10	-4.04922364	8.04E-14	6.17E-12
WBGene00009048	F22B8.6	-3.73459202	2.14E-24	7.27E-22
WBGene00045265	K10C2.8	-3.57009014	2.95E-13	2.06E-11
WBGene00013652	Y105C5B.12	-3.45865992	1.24E-18	2.17E-16
WBGene00019418	K05F6.7	-3.40632222	7.77E-15	7.44E-13
WBGene00011844	T19C9.8	-3.36937076	6.02E-19	1.09E-16
WBGene00012176	W01C9.2	-3.24498079	6.13E-17	8.74E-15
WBGene00000453	W05E10.3	-3.20714887	1.26E-22	3.51E-20
WBGene00010745	K10D11.1	-3.13763693	7.21E-11	2.90E-09
WBGene00007097	B0024.4	-3.12682325	8.59E-11	3.37E-09
WBGene00011672	T10B9.2	-3.11142962	6.83E-13	4.41E-11
WBGene00021186	Y9D1A.1	-3.08637191	2.27E-11	1.03E-09
WBGene00018647	F49F1.7	-3.00049526	5.07E-16	6.06E-14
WBGene00010747	K10D11.3	-2.98779679	1.75E-13	1.28E-11
WBGene00044798	Y46E12A.4	-2.9557403	5.71E-14	4.53E-12
WBGene00015449	C04F5.7	-2.90995435	3.76E-10	1.23E-08
WBGene00020665	T22B2.1	-2.90414557	1.11E-19	2.27E-17
WBGene00006545	T07C4.2	-2.87643124	3.11E-11	1.37E-09
WBGene00021779	Y51H7C.1	-2.77081202	6.51E-17	9.21E-15
WBGene00044200	H37A05.4	-2.7246649	4.66E-13	3.08E-11
WBGene00010128	F55G11.8	-2.67312995	5.63E-13	3.66E-11
WBGene00003377	C39E6.4	-2.63060041	1.34E-10	4.96E-09
WBGene00006382	W04A8.7	-2.57527048	4.07E-19	7.50E-17
WBGene00010808	M01E5.6	-2.57231504	5.17E-14	4.16E-12
WBGene00001833	Y110A7A.1	-2.55371965	2.53E-25	9.77E-23
WBGene00006556	Y47D3A.12	-2.54549278	4.58E-12	2.48E-10
WBGene00010367	H05L14.2	-2.45911972	2.66E-17	3.96E-15
WBGene00007501	C09H10.7	-2.43759775	2.69E-14	2.26E-12
WBGene00017471	F14H12.3	-2.4047498	2.90E-10	9.74E-09
WBGene00017800	F25G6.9	-2.38853101	2.60E-16	3.26E-14
WBGene00017948	F31D5.5	-2.38553434	1.12E-10	4.27E-09
WBGene00004166	Y43H11AL.3	-2.35305602	1.83E-15	1.97E-13
WBGene00003367	M106.1	-2.35165068	2.26E-19	4.30E-17
WBGene00000227	Y48G1BL.2	-2.32957448	1.78E-14	1.55E-12
WBGene00000939	K12H4.8	-2.32584612	5.39E-14	4.31E-12
WBGene00007028	C47D12.1	-2.32182312	9.83E-18	1.60E-15

WBGene00003133	W10C6.1	-2.31473945	1.01E-16	1.36E-14
WBGene00008958	F19H6.3	-2.30906364	7.51E-11	2.98E-09
WBGene00019712	M01E11.3	-2.29836482	4.43E-12	2.41E-10
WBGene00009086	F23D12.2	-2.2882919	7.06E-15	6.89E-13
WBGene00013569	Y75B12B.4	-2.27853497	4.49E-12	2.44E-10
WBGene00019792	M116.5	-2.25317718	5.88E-16	6.98E-14
WBGene00010013	F54B3.1	-2.22785059	4.37E-12	2.40E-10
WBGene00000783	T10H4.12	-2.2271551	7.83E-11	3.10E-09
WBGene00004510	F10B5.7	-2.22698437	2.01E-11	9.24E-10
WBGene00004874	F35G12.8	-2.22447953	7.81E-15	7.44E-13
WBGene00011109	R07E5.1	-2.20888285	1.75E-11	8.12E-10
WBGene00012767	Y41E3.9	-2.19765748	3.41E-13	2.31E-11
WBGene00001571	K01C8.5	-2.18461344	1.69E-13	1.24E-11
WBGene00016695	C45H4.14	-2.18134357	1.86E-10	6.64E-09
WBGene00020935	W02D3.10	-2.17892064	7.22E-11	2.90E-09
WBGene00010369	H06O01.2	-2.16500505	5.08E-11	2.15E-09
WBGene00001352	H38K22.1	-2.15719531	8.03E-13	5.01E-11
WBGene00008145	C47E8.8	-2.14682614	3.36E-13	2.29E-11
WBGene00017313	F09G2.4	-2.13646943	1.28E-12	7.80E-11
WBGene00009939	F52F12.6	-2.12669586	7.58E-12	3.82E-10
WBGene00001214	F26A3.3	-2.12035991	1.33E-10	4.95E-09
WBGene00021832	Y54E10A.12	-2.09560085	1.77E-12	1.04E-10
WBGene00007789	C28A5.2	-2.09099026	4.33E-16	5.28E-14
WBGene00011980	T24B8.7	-2.08982171	6.15E-16	7.25E-14
WBGene00010498	K02B12.5	-2.08405409	3.26E-11	1.42E-09
WBGene00004187	C50C3.6	-2.05912203	5.20E-20	1.10E-17
WBGene00017758	F23H11.2	-2.05591403	5.92E-15	5.87E-13
WBGene00011240	R11A8.7	-2.05572545	1.69E-14	1.49E-12
WBGene00011152	R09A8.1	-2.04468502	1.71E-11	7.97E-10
WBGene00018778	F53H1.4	-2.0443458	7.44E-16	8.53E-14
WBGene00004117	F02E9.4	-2.03505894	1.24E-10	4.64E-09
WBGene00014006	ZK596.1	-1.99548277	1.36E-12	8.26E-11
WBGene00004064	H12C20.2	-1.99102964	2.24E-17	3.49E-15
WBGene00014011	ZK632.2	-1.98379926	4.39E-14	3.56E-12
WBGene00019940	R07G3.3	-1.97980199	7.69E-18	1.27E-15
WBGene00008400	D2005.5	-1.97968672	1.31E-15	1.46E-13
WBGene00004873	Y47D3A.26	-1.96922782	7.82E-17	1.08E-14
WBGene00007975	C36B1.8	-1.96342623	9.74E-13	5.99E-11
WBGene00001865	T04A11.6	-1.96206462	4.25E-11	1.83E-09
WBGene00007258	C01H6.9	-1.96186904	8.17E-11	3.23E-09
WBGene00086566	C08H9.16	-1.96095946	7.17E-15	6.95E-13
WBGene00007042	C26C6.1	-1.94961157	2.50E-17	3.83E-15
WBGene00007761	C27B7.4	-1.94885422	2.01E-12	1.17E-10
WBGene00000396	F25F2.2	-1.9417965	1.08E-14	1.00E-12
WBGene00009163	F26E4.10	-1.9289946	7.10E-11	2.86E-09
WBGene00002845	F57B9.2	-1.9272373	1.74E-16	2.28E-14
WBGene00000143	K06H7.6	-1.91379047	1.34E-10	4.96E-09
WBGene00022301	Y76B12C.7	-1.89240716	1.56E-12	9.26E-11
WBGene00015813	C16A3.8	-1.89086233	1.55E-12	9.26E-11
WBGene00009287	F31C3.5	-1.88985349	7.61E-12	3.82E-10
WBGene00008119	C46F11.4	-1.8896747	7.36E-12	3.72E-10
WBGene00016868	C52B9.8	-1.88943328	1.48E-10	5.41E-09
WBGene00002637	F26F12.7	-1.88942011	2.82E-17	4.16E-15
WBGene00018900	F55G1.4	-1.88086403	7.10E-11	2.86E-09
WBGene00018864	F55A12.5	-1.87629024	8.84E-12	4.40E-10
WBGene00009460	F36A2.13	-1.87606662	1.99E-13	1.44E-11
WBGene00010845	M03C11.8	-1.86895672	1.13E-12	6.90E-11
WBGene00016603	C43E11.3	-1.8689468	1.27E-11	6.05E-10
WBGene00009127	F25H5.5	-1.86747095	5.58E-13	3.65E-11

WBGene00014218	ZK1098.1	-1.86661867	6.08E-12	3.14E-10
WBGene00006997	ZK546.1	-1.86311389	2.59E-15	2.72E-13
WBGene00004728	F21H11.2	-1.8503267	4.90E-13	3.22E-11
WBGene00007053	T04D1.4	-1.8392243	4.17E-13	2.77E-11
WBGene00001087	Y39A1B.3	-1.83920621	1.25E-14	1.15E-12
WBGene00019245	H27M09.1	-1.83833966	1.43E-12	8.60E-11
WBGene00020496	T13H2.5	-1.83656712	7.34E-15	7.08E-13
WBGene00015743	C13F10.4	-1.83391431	2.37E-12	1.36E-10
WBGene00019002	F57B10.4	-1.83302376	1.76E-14	1.54E-12
WBGene00007913	C34B7.3	-1.82749277	1.26E-11	6.05E-10
WBGene00009173	F26H9.1	-1.82070012	2.90E-11	1.29E-09
WBGene00001086	R13G10.1	-1.81491665	4.60E-12	2.48E-10
WBGene00006571	Y75B8A.22	-1.81353286	7.30E-12	3.70E-10
WBGene00019124	F59E12.9	-1.80705377	2.21E-12	1.28E-10
WBGene00000265	K04C2.4	-1.80531507	2.81E-11	1.25E-09
WBGene00003499	K04F10.6	-1.80506942	6.82E-12	3.48E-10
WBGene00008399	D2005.4	-1.79794973	1.50E-11	7.07E-10
WBGene00006976	K02B12.8	-1.79569311	1.03E-12	6.28E-11
WBGene00011720	T11G6.5	-1.79337783	5.67E-12	2.97E-10
WBGene00019129	F59G1.8	-1.78342146	1.99E-10	7.01E-09
WBGene00009922	F52B5.3	-1.77784392	3.54E-10	1.18E-08
WBGene00006941	C46C2.1	-1.77730331	1.68E-12	9.92E-11
WBGene00019692	M01A10.1	-1.75790086	2.97E-14	2.48E-12
WBGene00006737	Y38A8.3	-1.74540051	6.29E-11	2.59E-09
WBGene00003422	Y47G6A.11	-1.73483355	7.43E-13	4.74E-11
WBGene00003210	C38D4.3	-1.73171949	1.83E-12	1.08E-10
WBGene00020463	T12E12.2	-1.73041835	4.75E-12	2.55E-10
WBGene00000537	C07H6.6	-1.72921008	7.35E-11	2.92E-09
WBGene00001973	C32F10.5	-1.72780175	2.90E-10	9.74E-09
WBGene00001085	C25G4.5	-1.72054443	3.61E-13	2.42E-11
WBGene00015017	B0205.1	-1.71241246	1.47E-14	1.32E-12
WBGene00004355	T07D4.3	-1.71090147	1.20E-11	5.77E-10
WBGene00007433	C08B11.3	-1.70555327	1.98E-12	1.16E-10
WBGene00012936	Y47D3A.29	-1.6847965	1.62E-11	7.62E-10
WBGene00015557	C06G4.1	-1.67776296	4.50E-11	1.92E-09
WBGene00001281	F10B5.6	-1.66765317	1.05E-11	5.16E-10
WBGene00016453	C35E7.1	-1.66637075	2.73E-12	1.54E-10
WBGene00077732	C30B5.1	-1.66506633	1.05E-10	4.02E-09
WBGene00007027	Y111B2A.22	-1.66448501	1.91E-10	6.79E-09
WBGene00006375	F26D2.2	-1.66200441	1.07E-10	4.11E-09
WBGene00001835	C08B11.2	-1.65011305	1.67E-10	6.00E-09
WBGene00003792	F56A3.3	-1.64900239	2.03E-12	1.18E-10
WBGene00003002	C03B8.4	-1.64606529	1.53E-12	9.13E-11
WBGene00004337	C54G10.2	-1.64514794	5.65E-12	2.97E-10
WBGene00008535	F02H6.2	-1.64338504	1.35E-10	4.98E-09
WBGene00006394	K10D3.3	-1.63793905	7.30E-11	2.91E-09
WBGene00002169	F37A4.8	-1.63461372	5.46E-11	2.29E-09
WBGene00016409	C34E10.8	-1.63447021	2.25E-10	7.84E-09
WBGene00006773	W02D3.9	-1.63253506	1.88E-11	8.71E-10
WBGene00019629	K10D2.3	-1.63199762	1.19E-10	4.45E-09
WBGene00016113	C25H3.4	-1.62482893	9.86E-11	3.80E-09
WBGene00012245	W04D2.6	-1.62357572	1.14E-11	5.53E-10
WBGene00009770	F46B6.5	-1.61161355	1.69E-10	6.07E-09
WBGene00017738	F23C8.9	-1.60939692	1.53E-10	5.54E-09
WBGene00002231	C02F5.1	-1.60488363	2.69E-12	1.52E-10
WBGene00008921	F17C11.10	-1.60297485	2.02E-10	7.08E-09
WBGene00001830	T06E4.1	-1.60121609	7.70E-12	3.86E-10
WBGene00013461	Y67H2A.2	-1.59258743	3.74E-11	1.62E-09
WBGene00022800	ZK688.5	-1.59211778	1.14E-10	4.31E-09

WBGene00001860	F28B3.7	-1.58904911	1.31E-10	4.88E-09
WBGene00001689	C38C10.4	-1.5850738	3.81E-10	1.25E-08
WBGene00002889	F20H11.2	-1.58156291	2.32E-10	8.05E-09
WBGene00001568	F32H2.1	-1.57426031	4.84E-11	2.06E-09
WBGene00000884	D1009.2	-1.56767207	1.47E-10	5.39E-09
WBGene00003785	Y53C12B.3	-1.5674263	5.68E-11	2.38E-09
WBGene00000275	R06C7.8	-1.5667739	1.66E-11	7.77E-10
WBGene00015357	C02F12.8	-1.56295875	2.50E-10	8.62E-09
WBGene00016015	C23G10.8	-1.55525522	1.93E-10	6.86E-09
WBGene00008385	D1081.7	-1.54537836	1.08E-11	5.25E-10
WBGene00001029	F38A5.13	-1.54214648	6.69E-12	3.42E-10
WBGene00003504	ZK1098.8	-1.51819466	1.95E-10	6.92E-09
WBGene00004148	T13H2.4	-1.51312013	3.08E-10	1.03E-08
WBGene00012389	Y6B3B.4	-1.50560868	2.60E-10	8.86E-09
WBGene00000079	H15N14.1	-1.50538263	3.67E-10	1.21E-08
WBGene00004738	F18E2.3	-1.50272313	1.50E-11	7.08E-10
WBGene00001258	Y80D3A.2	-1.49609056	1.97E-10	6.98E-09
WBGene00001061	T23G7.1	-1.48272055	1.18E-10	4.45E-09
WBGene00017951	F31E3.4	-1.45232295	9.70E-11	3.76E-09
WBGene00004745	F52E10.1	-1.45130282	2.53E-10	8.70E-09
WBGene00008720	F12F6.1	-1.45119366	1.80E-10	6.45E-09
WBGene00006974	M03D4.1	-1.44889567	5.91E-11	2.46E-09
WBGene00003222	Y2H9A.1	-1.44444442	1.20E-10	4.51E-09
WBGene00004204	F01G4.1	-1.43236106	1.00E-10	3.85E-09
WBGene00001869	R12B2.4	-1.42243354	3.77E-10	1.23E-08
WBGene00017643	F20D12.4	-1.39439753	2.99E-10	1.00E-08
WBGene00001829	ZK1055.1	-1.39015237	2.95E-10	9.91E-09

Supplementary Table 6. Genes upregulated in *LRRK2* transgenic worms fed *A. viscosus*.

GeneID	Sequence ID	log2(FC)	P-value	P-adj
WBGene00000081	Y50D7A.7	1.536233368	5.12E-12	2.73E-10
WBGene00016048	C24B9.3	1.571541741	8.94E-11	3.50E-09
WBGene00001000	C18A11.7	1.572556606	5.87E-11	2.45E-09
WBGene00004440	F28C6.7	1.599454551	1.46E-10	5.37E-09
WBGene00000066	M03F4.2	1.623350734	4.34E-11	1.86E-09
WBGene00004477	F42C5.8	1.628329541	1.63E-10	5.89E-09
WBGene00003495	T22E5.5	1.629089587	2.57E-13	1.82E-11
WBGene00009334	F32D8.12	1.629677118	9.67E-13	5.97E-11
WBGene00004470	F56F3.5	1.654871556	2.59E-10	8.86E-09
WBGene00013874	ZC376.2	1.659384132	1.48E-11	7.00E-10
WBGene00043302	F32D8.11	1.659586363	3.58E-11	1.56E-09
WBGene00010935	M163.1	1.663614941	3.23E-11	1.42E-09
WBGene00004473	Y43B11AR.4	1.668606544	5.86E-11	2.45E-09
WBGene00003097	C17G10.5	1.671035058	8.67E-11	3.40E-09
WBGene00004485	T01C3.6	1.672283597	2.07E-10	7.27E-09
WBGene00022047	Y66H1A.5	1.680031673	2.50E-12	1.43E-10
WBGene00021544	Y43B11AR.3	1.682363331	6.30E-11	2.59E-09
WBGene00006530	F44F4.11	1.690140459	2.50E-11	1.13E-09
WBGene00000788	F32B5.8	1.69251646	3.58E-11	1.56E-09
WBGene00001572	M03A8.4	1.701837913	2.25E-11	1.03E-09
WBGene00006861	C24H10.5	1.707575129	2.63E-10	8.94E-09
WBGene00007336	C05C12.4	1.710951285	6.95E-11	2.82E-09
WBGene00001397	W06D12.3	1.729749373	1.15E-10	4.36E-09
WBGene00016594	C42D4.1	1.738543662	4.36E-12	2.40E-10
WBGene00017329	F10D2.2	1.740219731	9.85E-11	3.80E-09
WBGene00004435	B0336.10	1.754656919	2.26E-10	7.85E-09
WBGene00006819	F08B6.4	1.769508055	3.08E-11	1.36E-09
WBGene00021977	Y58A7A.3	1.772035924	8.28E-11	3.26E-09

WBGene00004499	C26F1.4	1.772419708	3.56E-10	1.18E-08
WBGene00004420	R13A5.8	1.780677267	6.08E-11	2.52E-09
WBGene00012812	Y43F8B.1	1.785113228	1.13E-13	8.59E-12
WBGene00019547	K09C4.1	1.786271935	4.84E-12	2.59E-10
WBGene00019361	K03E5.2	1.809999349	1.15E-10	4.35E-09
WBGene00004425	C32E8.2	1.811954692	2.37E-10	8.23E-09
WBGene00012274	W05B5.1	1.815836287	7.24E-14	5.61E-12
WBGene00045394	ZK813.7	1.826270927	3.63E-10	1.20E-08
WBGene00018532	F47B7.1	1.836688413	4.78E-14	3.87E-12
WBGene00019727	M02D8.1	1.838442547	2.53E-12	1.44E-10
WBGene00011936	T22H2.6	1.844313001	1.29E-13	9.62E-12
WBGene00020808	T25F10.6	1.850010718	4.24E-14	3.46E-12
WBGene00003369	C36E6.3	1.850708614	2.25E-13	1.63E-11
WBGene00017881	F28A12.4	1.852112717	8.88E-13	5.50E-11
WBGene00004448	C42C1.14	1.8637284	1.99E-10	7.01E-09
WBGene00018966	F56D2.5	1.865681553	3.88E-11	1.68E-09
WBGene00012909	Y46G5A.19	1.874582534	1.17E-10	4.42E-09
WBGene00007748	C26E1.2	1.875130098	7.01E-11	2.84E-09
WBGene00001385	F02A9.2	1.88052522	1.44E-10	5.30E-09
WBGene00004490	F37C12.11	1.882033997	2.74E-10	9.27E-09
WBGene00013579	Y79H2A.2	1.883264621	3.61E-10	1.20E-08
WBGene00012134	T28F3.8	1.885576914	5.64E-12	2.97E-10
WBGene00010133	F55H12.2	1.890681866	4.27E-11	1.84E-09
WBGene00002054	F10C1.7	1.895889346	1.27E-11	6.08E-10
WBGene00017923	F29B9.8	1.900232131	2.52E-13	1.79E-11
WBGene00008447	E01G4.5	1.902764683	1.64E-11	7.69E-10
WBGene00004413	B0250.1	1.906209045	3.70E-10	1.21E-08
WBGene00019493	K07E3.7	1.912638214	3.49E-10	1.16E-08
WBGene00000277	C23H4.1	1.917766526	1.37E-13	1.02E-11
WBGene00004476	ZC434.2	1.919738458	6.73E-11	2.75E-09
WBGene00004428	M01F1.2	1.92498736	2.28E-11	1.03E-09
WBGene00001564	C05E4.9	1.925588888	7.14E-13	4.58E-11
WBGene00045268	H01M10.3	1.92980914	1.09E-10	4.17E-09
WBGene00010742	K10D6.2	1.941044771	2.01E-11	9.24E-10
WBGene00006408	T14G12.3	1.941230406	1.07E-14	9.99E-13
WBGene00013266	Y57A10A.26	1.946490116	1.02E-15	1.15E-13
WBGene00016210	C29F5.1	1.947491922	6.51E-12	3.34E-10
WBGene00004469	B0393.1	1.953808093	2.38E-12	1.37E-10
WBGene00004409	Y37E3.7	1.955145264	9.18E-11	3.58E-09
WBGene00022562	ZC204.12	1.956763708	2.62E-10	8.91E-09
WBGene00008865	F15G9.1	1.968305392	2.90E-15	2.98E-13
WBGene00019204	H14N18.4	1.989166013	3.81E-11	1.65E-09
WBGene00020393	T10B5.7	1.990298449	7.11E-16	8.21E-14
WBGene00000216	H22K11.1	1.990886484	4.14E-12	2.28E-10
WBGene00015619	C08G9.1	1.992173054	2.61E-11	1.17E-09
WBGene00008356	D1025.4	2.001995859	5.65E-12	2.97E-10
WBGene00021709	Y49C4A.8	2.002274178	1.97E-15	2.10E-13
WBGene00011486	T05E12.3	2.005188597	1.08E-11	5.25E-10
WBGene00044296	F10C1.9	2.005463514	3.49E-10	1.16E-08
WBGene00022130	Y71F9B.9	2.007165642	2.83E-11	1.26E-09
WBGene00012457	Y17G7B.1	2.016003828	2.41E-10	8.34E-09
WBGene00010822	M01G12.9	2.023509048	2.60E-14	2.19E-12
WBGene00016918	C54E4.2	2.023516379	1.14E-13	8.62E-12
WBGene00016728	C46H11.2	2.029191188	2.34E-12	1.35E-10
WBGene00006754	F07A5.7	2.037087565	6.94E-16	8.07E-14
WBGene00022615	ZC449.5	2.041995243	4.57E-11	1.94E-09
WBGene00010049	F54D5.3	2.045458257	7.58E-13	4.78E-11
WBGene00006634	F33C8.3	2.070705965	4.41E-12	2.41E-10
WBGene00002065	F54C9.1	2.078074856	1.09E-17	1.76E-15
WBGene00021556	Y45G5AM.3	2.095267086	4.47E-17	6.42E-15
WBGene00004096	F40F8.7	2.096787494	1.37E-15	1.51E-13
WBGene00003710	C25B8.6	2.096946896	2.55E-10	8.74E-09

WBGene00002268	ZK1248.16	2.097504689	6.16E-11	2.55E-09
WBGene00020200	T04A6.1	2.111540431	1.50E-10	5.44E-09
WBGene00014052	ZK669.2	2.123959329	7.81E-12	3.90E-10
WBGene00019779	M60.2	2.132207552	1.83E-11	8.50E-10
WBGene00000219	F21F8.7	2.13598257	1.35E-19	2.72E-17
WBGene00010593	K06A4.3	2.137458036	6.52E-14	5.08E-12
WBGene00016657	C44E12.1	2.138720468	3.15E-13	2.18E-11
WBGene00006863	F56B6.4	2.14587859	1.37E-16	1.81E-14
WBGene00002988	K03E6.1	2.148890218	3.79E-13	2.54E-11
WBGene00019327	K02F3.4	2.149245566	1.48E-14	1.32E-12
WBGene00008341	C56A3.2	2.151391499	8.08E-17	1.11E-14
WBGene00010795	M01A8.1	2.160815315	1.20E-11	5.77E-10
WBGene00007295	C04C11.1	2.166000289	1.03E-13	7.81E-12
WBGene00004987	T08A9.12	2.174372078	3.02E-13	2.09E-11
WBGene00020229	T05A8.3	2.17794055	2.95E-16	3.66E-14
WBGene00018579	F47G6.2	2.191845949	2.20E-10	7.67E-09
WBGene00020811	T25G12.3	2.195208422	4.37E-17	6.34E-15
WBGene00007650	C17G1.3	2.205672619	1.88E-16	2.44E-14
WBGene00015828	C16C4.4	2.217812635	2.28E-11	1.03E-09
WBGene00018384	F43C11.7	2.218445999	5.40E-14	4.31E-12
WBGene00015756	C14C6.2	2.233748367	2.12E-19	4.14E-17
WBGene00014826	R13H4.2	2.237042611	3.99E-12	2.21E-10
WBGene00000608	ZK1193.1	2.238874098	1.36E-14	1.23E-12
WBGene00002255	F40F4.4	2.239702877	1.32E-14	1.20E-12
WBGene00004408	F25H2.10	2.240730977	2.31E-18	3.88E-16
WBGene00010336	F59F4.1	2.241320132	1.91E-18	3.28E-16
WBGene00008621	F09C8.1	2.242961369	5.25E-12	2.79E-10
WBGene00012875	Y45F10B.13	2.250843099	3.54E-13	2.38E-11
WBGene00000857	K10B4.6	2.251956262	4.46E-11	1.91E-09
WBGene00022039	Y65B4BL.7	2.265154874	6.03E-15	5.95E-13
WBGene00013181	Y53H1B.2	2.279381701	2.11E-10	7.37E-09
WBGene00018376	F43C9.2	2.286257354	5.06E-13	3.32E-11
WBGene00220180	Y54G2A.74	2.289237129	2.22E-14	1.90E-12
WBGene00044082	D1086.12	2.299581609	9.95E-12	4.93E-10
WBGene00043702	Y54G2A.7	2.300308445	6.34E-16	7.42E-14
WBGene00015965	C18C4.3	2.311228126	1.76E-15	1.91E-13
WBGene00020886	T28B4.3	2.313046814	1.48E-10	5.41E-09
WBGene00012216	W02D9.10	2.314773268	1.29E-10	4.82E-09
WBGene00009396	F35C5.8	2.328470214	1.19E-20	2.70E-18
WBGene00020662	T21H3.1	2.331200147	2.61E-17	3.93E-15
WBGene00001395	W08D2.4	2.334290142	2.27E-13	1.63E-11
WBGene00016920	C54E4.5	2.337400297	1.82E-10	6.51E-09
WBGene00021050	W05H9.3	2.338989978	2.54E-16	3.24E-14
WBGene00009393	F35C5.5	2.34299238	4.00E-23	1.19E-20
WBGene00003991	K03E6.6	2.343573187	1.58E-14	1.40E-12
WBGene00014252	ZK1320.2	2.349446987	2.40E-14	2.04E-12
WBGene00010488	K02A11.3	2.351988214	2.70E-10	9.13E-09
WBGene00086569	F38A6.5	2.356641046	3.78E-12	2.10E-10
WBGene00017065	D2092.4	2.360791676	1.26E-14	1.15E-12
WBGene00015954	C18B2.3	2.374514554	3.48E-14	2.88E-12
WBGene00009394	F35C5.6	2.378060528	7.81E-13	4.91E-11
WBGene00000214	Y39B6A.20	2.378283081	1.41E-12	8.51E-11
WBGene00000713	F26F12.1	2.392020708	3.91E-14	3.21E-12
WBGene00013334	Y57G11C.45	2.394124168	5.38E-15	5.41E-13
WBGene00009638	F42F12.7	2.397338891	2.68E-15	2.79E-13
WBGene00015392	C03G5.2	2.409273085	3.22E-13	2.22E-11
WBGene00012383	Y5F2A.2	2.419897721	2.85E-11	1.27E-09
WBGene00008246	C50H2.13	2.421140348	6.00E-11	2.49E-09
WBGene00000716	T15B7.3	2.424182556	1.57E-13	1.16E-11
WBGene00044901	Y41G9A.10	2.42673377	2.63E-10	8.94E-09
WBGene00021978	Y58A7A.4	2.42714245	1.48E-18	2.56E-16
WBGene00001981	C44C10.8	2.431400693	9.63E-14	7.36E-12

WBGene00015949	C18A11.3	2.43318825	9.80E-15	9.25E-13
WBGene00011026	R05D7.1	2.433367043	1.41E-11	6.71E-10
WBGene00018971	F56D6.2	2.438575632	2.17E-15	2.31E-13
WBGene00019645	K11D12.5	2.43859267	2.56E-16	3.24E-14
WBGene00012382	Y5F2A.1	2.439483274	2.66E-12	1.51E-10
WBGene00194985	Y25C1A.14	2.440311824	9.60E-15	9.11E-13
WBGene00005180	Y25C1A.11	2.444210972	5.71E-13	3.70E-11
WBGene00003893	C44B12.2	2.444787722	9.36E-22	2.51E-19
WBGene00004423	F07D10.1	2.471923107	2.56E-11	1.15E-09
WBGene00000779	F28H1.2	2.473780706	1.57E-21	3.97E-19
WBGene00015055	B0222.3	2.475618317	5.79E-14	4.57E-12
WBGene00008577	F08G2.5	2.475763611	7.44E-14	5.74E-12
WBGene00017678	F21F8.4	2.48346351	1.79E-19	3.54E-17
WBGene00001752	K08F4.7	2.484855778	1.07E-11	5.22E-10
WBGene00086568	Y2H9A.6	2.490979602	2.55E-10	8.74E-09
WBGene00013964	ZK287.3	2.494540111	6.91E-18	1.15E-15
WBGene00009640	F42F12.9	2.496517825	3.85E-20	8.28E-18
WBGene00017936	F30B5.7	2.509545418	6.48E-12	3.33E-10
WBGene00011880	T21B6.3	2.520991228	1.43E-13	1.06E-11
WBGene00017303	F09F7.6	2.522513021	2.31E-21	5.69E-19
WBGene00015472	C05D9.3	2.526937699	1.45E-19	2.89E-17
WBGene00021602	Y46H3B.1	2.534439342	1.61E-10	5.81E-09
WBGene00009773	F46B6.8	2.545042205	1.81E-15	1.95E-13
WBGene00007366	C06B3.7	2.565571393	2.06E-23	6.36E-21
WBGene00008770	F13G3.12	2.565942724	4.92E-11	2.08E-09
WBGene00016722	C46G7.2	2.567401442	3.99E-21	9.54E-19
WBGene00021118	W09G10.6	2.578607054	6.64E-11	2.72E-09
WBGene00019478	K07C11.5	2.581773808	9.94E-11	3.83E-09
WBGene00023401	ZK380.t2	2.587032963	2.87E-10	9.68E-09
WBGene00044238	C30H6.12	2.600167531	1.75E-10	6.27E-09
WBGene00206361	K02G10.15	2.606761958	2.92E-13	2.05E-11
WBGene00007139	B0285.7	2.608111871	1.02E-11	5.03E-10
WBGene00000218	F21F8.3	2.634767596	7.92E-16	9.02E-14
WBGene00220003	K02G10.16	2.636062209	6.49E-11	2.66E-09
WBGene00018744	F53B3.6	2.640058244	2.23E-11	1.02E-09
WBGene00009982	F53F1.4	2.640119787	2.60E-11	1.17E-09
WBGene00004006	F22E10.1	2.646249641	6.26E-14	4.92E-12
WBGene00000671	Y41C4A.19	2.647861697	4.06E-17	5.94E-15
WBGene00004986	T07C4.4	2.65084814	9.20E-16	1.04E-13
WBGene00013118	Y51H4A.24	2.656887871	9.47E-22	2.51E-19
WBGene00003740	T24D8.5	2.661116988	1.02E-11	5.03E-10
WBGene00006789	F11C3.3	2.688174113	3.32E-19	6.26E-17
WBGene00003242	C37C3.6	2.697589826	1.13E-17	1.82E-15
WBGene00013090	Y51B9A.8	2.702170016	7.57E-13	4.78E-11
WBGene00010613	K07A1.6	2.714650163	2.74E-16	3.42E-14
WBGene00008584	F08G5.6	2.728634852	7.56E-13	4.78E-11
WBGene00011708	T11B7.5	2.730858902	7.28E-11	2.91E-09
WBGene00020191	T03F1.10	2.733982978	7.85E-13	4.92E-11
WBGene00008566	F08A8.3	2.735809005	9.14E-12	4.54E-10
WBGene00009895	F49E11.10	2.749871874	4.75E-16	5.76E-14
WBGene00000215	T18H9.2	2.7503723	9.99E-25	3.69E-22
WBGene00017054	D2024.7	2.753246188	3.19E-12	1.79E-10
WBGene00003956	ZK112.1	2.798809438	1.03E-24	3.71E-22
WBGene00009466	F36D1.7	2.804780863	5.91E-12	3.08E-10
WBGene00011362	T02B5.1	2.805937944	9.69E-11	3.76E-09
WBGene00018221	F40A3.6	2.808524346	2.57E-17	3.89E-15
WBGene00018311	F41G4.8	2.816668017	3.66E-16	4.50E-14
WBGene00009096	F23H12.8	2.82431085	3.64E-10	1.20E-08
WBGene00015598	C08E3.6	2.827201516	1.54E-16	2.03E-14
WBGene00194713	F19B10.13	2.845460288	3.56E-20	7.74E-18
WBGene00000373	F08F3.7	2.866626412	2.19E-19	4.23E-17

WBGene00017197	F07C3.9	2.866858212	3.92E-13	2.61E-11
WBGene00004875	F47G4.7	2.879097274	1.76E-24	6.10E-22
WBGene00006016	F32H5.6	2.880139897	7.24E-11	2.90E-09
WBGene00010019	F54B8.4	2.883561876	1.62E-14	1.43E-12
WBGene00017250	F08D12.7	2.883829716	1.16E-13	8.72E-12
WBGene00000169	F32A5.5	2.890675099	1.30E-37	1.10E-34
WBGene00004002	T21E8.3	2.910062795	3.53E-15	3.58E-13
WBGene00016893	C53B7.2	2.94145388	6.22E-27	2.64E-24
WBGene00045412	C25F9.12	2.968716486	3.39E-12	1.89E-10
WBGene00000611	F36A4.10	2.968766518	1.32E-16	1.77E-14
WBGene00007726	C25F9.6	2.973116775	1.19E-11	5.75E-10
WBGene00219216	K08D10.14	2.973501868	4.87E-21	1.13E-18
WBGene00015182	B0416.7	2.983651851	6.07E-12	3.14E-10
WBGene00022653	ZK105.1	2.988111404	1.85E-14	1.60E-12
WBGene00043062	Y54G2A.39	3.001177791	9.37E-24	2.94E-21
WBGene00009518	F38A1.5	3.011437106	3.31E-13	2.27E-11
WBGene00011707	T11B7.2	3.030062457	3.00E-15	3.07E-13
WBGene00009158	F26E4.3	3.044951158	2.55E-20	5.62E-18
WBGene00045411	C25F9.11	3.048184728	5.68E-23	1.63E-20
WBGene00077684	Y26D4A.21	3.056593191	1.38E-10	5.08E-09
WBGene00003380	C10A4.8	3.069517311	3.73E-19	6.96E-17
WBGene00021768	Y51F10.7	3.071897512	2.27E-14	1.93E-12
WBGene00021335	Y34D9A.11	3.094958689	7.93E-36	6.41E-33
WBGene00044811	F12E12.11	3.110250184	2.69E-15	2.79E-13
WBGene00016052	C24B9.9	3.125450339	1.12E-22	3.16E-20
WBGene00010719	K09E4.1	3.141707363	1.90E-11	8.79E-10
WBGene00009854	F49A5.2	3.14845034	5.66E-12	2.97E-10
WBGene00012821	Y43F8B.11	3.148797092	3.22E-21	7.82E-19
WBGene00012591	Y38E10A.13	3.155436794	3.82E-14	3.15E-12
WBGene00044206	T26H5.9	3.15744845	1.50E-22	4.12E-20
WBGene00012582	Y38E10A.4	3.159126267	7.66E-25	2.89E-22
WBGene00012592	Y38E10A.14	3.169664008	9.20E-11	3.58E-09
WBGene00015602	C08E3.10	3.178854927	5.55E-15	5.54E-13
WBGene00020747	T24A6.7	3.188241095	1.32E-17	2.09E-15
WBGene00004993	C28C12.5	3.231367177	1.68E-28	8.38E-26
WBGene00020700	T22F3.11	3.239081421	5.35E-11	2.25E-09
WBGene00015695	C10H11.6	3.241449394	2.92E-30	1.71E-27
WBGene00001781	C02A12.1	3.282109383	2.84E-13	2.00E-11
WBGene00270319	F26A1.19	3.282305317	3.37E-12	1.88E-10
WBGene00017659	F21C10.10	3.286433606	7.00E-19	1.25E-16
WBGene00012604	Y38E10A.26	3.331556251	2.99E-12	1.68E-10
WBGene00008593	F08H9.5	3.336514335	8.34E-13	5.18E-11
WBGene00004989	T08A9.8	3.340276427	1.01E-20	2.31E-18
WBGene00003648	R11G11.2	3.342161984	1.52E-17	2.39E-15
WBGene00018568	F47E1.4	3.355049506	1.28E-15	1.43E-13
WBGene00006636	T14B4.4	3.360202064	6.75E-11	2.75E-09
WBGene00013101	Y51H4A.5	3.368318738	1.53E-15	1.67E-13
WBGene00013900	ZC443.5	3.391783481	4.85E-40	4.84E-37
WBGene00001476	K08C7.2	3.398663972	3.39E-13	2.30E-11
WBGene00045261	H29C22.1	3.409688182	1.01E-21	2.65E-19
WBGene00045272	F59C12.4	3.420218449	2.03E-25	7.99E-23
WBGene00019699	M01D1.2	3.42822418	6.97E-15	6.84E-13
WBGene00020613	T20D4.7	3.429545517	7.33E-17	1.03E-14
WBGene00001500	C54F6.14	3.430661412	9.72E-28	4.46E-25
WBGene00015403	C03H5.1	3.441986297	1.27E-20	2.83E-18
WBGene00021464	Y39G10AR.6	3.487544905	1.21E-35	9.37E-33
WBGene00011821	T18D3.3	3.49034586	2.45E-27	1.09E-24
WBGene00194803	C25F9.16	3.517488256	1.89E-14	1.63E-12
WBGene00044783	T26H5.10	3.526402472	1.32E-24	4.66E-22
WBGene00016450	C35D10.14	3.544720837	1.52E-29	8.30E-27
WBGene00044719	K03H6.7	3.571707491	7.29E-12	3.70E-10

WBGene00018314	F41H10.1	3.5728195	1.82E-33	1.19E-30
WBGene00015839	C16C4.15	3.611156841	2.30E-17	3.54E-15
WBGene00007521	C11E4.7	3.702295278	3.27E-24	1.07E-21
WBGene00018342	F42A10.6	3.727838198	1.68E-54	4.07E-51
WBGene00000968	T05F1.10	3.735380325	1.07E-14	9.99E-13
WBGene00016786	C49G7.8	3.756450961	1.31E-14	1.20E-12
WBGene00003093	F58B3.1	3.757018833	3.43E-29	1.82E-26
WBGene00011801	T16G1.7	3.814813235	4.58E-34	3.11E-31
WBGene00271643	W07G1.25	3.81896676	7.60E-17	1.06E-14
WBGene00044379	F40H7.12	3.826696734	2.36E-13	1.69E-11
WBGene00019146	H02F09.3	3.862327389	6.32E-20	1.33E-17
WBGene00007565	C14A6.1	3.87280494	2.69E-24	8.95E-22
WBGene00015050	B0218.6	3.875138037	5.50E-42	5.83E-39
WBGene00005833	C25F9.7	3.928253697	2.41E-30	1.46E-27
WBGene00021979	Y58A7A.5	3.928731899	9.45E-40	8.92E-37
WBGene00000213	W03G1.7	3.991045871	7.06E-33	4.44E-30
WBGene00019105	F59D6.3	3.991782019	4.04E-28	1.96E-25
WBGene00015129	B0303.8	4.118505651	1.72E-13	1.26E-11
WBGene00007358	C06A12.5	4.152882463	3.14E-11	1.38E-09
WBGene00009221	F28F8.2	4.188626085	2.96E-23	8.96E-21
WBGene00010790	K12G11.3	4.211023821	4.61E-60	1.30E-56
WBGene00000212	ZK455.4	4.242024702	5.24E-27	2.28E-24
WBGene00001772	F37B1.1	4.327792018	8.72E-28	4.11E-25
WBGene00021873	Y54G2A.8	4.336275473	2.13E-16	2.74E-14
WBGene00020157	T02B11.6	4.338283105	6.32E-14	4.95E-12
WBGene00017490	F15E11.1	4.345059139	3.29E-14	2.74E-12
WBGene00044212	Y68A4A.13	4.345076302	7.27E-30	4.11E-27
WBGene00010769	K11D2.2	4.353530276	2.13E-34	1.51E-31
WBGene00044687	B0563.9	4.39848496	9.76E-17	1.32E-14
WBGene00235133	T26H5.14	4.559675572	8.88E-26	3.59E-23
WBGene00015600	C08E3.8	4.575293795	2.19E-15	2.31E-13
WBGene00044015	K06A4.8	4.642292878	3.00E-13	2.09E-11
WBGene00012631	Y38H6C.19	4.708614173	9.15E-20	1.90E-17
WBGene00008097	C44H9.1	4.785056812	6.08E-12	3.14E-10
WBGene00010062	F54F3.3	4.821049028	4.79E-54	1.02E-50
WBGene00000781	C52E4.1	4.822053963	3.11E-46	4.40E-43
WBGene00005188	T07H8.5	4.877211013	1.01E-18	1.78E-16
WBGene00044046	ZK666.13	4.943664989	5.79E-12	3.02E-10
WBGene00011799	T16G1.5	5.005420011	4.32E-52	6.67E-49
WBGene00015342	C02E7.10	5.042499105	2.01E-21	5.01E-19
WBGene00019652	K11G9.1	5.159200309	6.47E-44	7.84E-41
WBGene00006175	T22H6.3	5.166433576	5.66E-19	1.03E-16
WBGene00008477	E03H4.10	5.187217472	4.87E-21	1.13E-18
WBGene00020016	R11G11.14	5.21181665	9.94E-35	7.34E-32
WBGene00003094	F58B3.2	5.293735874	6.20E-24	1.99E-21
WBGene00021581	Y46C8AL.3	5.356130328	7.12E-13	4.58E-11
WBGene00016670	C45G7.3	5.405273093	2.49E-13	1.78E-11
WBGene00008220	C50B6.7	5.669613477	3.73E-117	6.34E-113
WBGene00016669	C45G7.2	5.717227706	7.32E-29	3.77E-26
WBGene00020326	T07H3.3	6.139160804	1.80E-38	1.61E-35
WBGene00050906	F20E11.17	6.535140921	5.18E-62	1.76E-58
WBGene00023484	Y54G2A.37	6.766734482	4.19E-52	6.67E-49
WBGene00018343	F42A10.7	6.784167731	2.78E-44	3.63E-41
WBGene00015052	B0218.8	7.582342786	2.17E-93	1.23E-89
WBGene00011103	R07E3.2	7.707657541	1.44E-97	1.22E-93
WBGene00014046	ZK666.6	8.436066973	5.79E-83	2.46E-79

Supplementary Table 7. MirTarBase identified gene targets for downregulated miRNAs in *LRRK2* transgenic worms fed *A. viscosus.*

Downregulated miRNA	Gene Target
cel-miR-1832a-3p	F13H6.1
cel-miR-1832a-3p	K10D6.4
cel-miR-1832a-3p	F26B1.2
cel-miR-38-3p	AH9.6
cel-miR-38-3p	R12E2.2
cel-miR-38-3p	T05C1.4
cel-miR-38-3p	T10B10.3
cel-miR-38-3p	C33A11.2
cel-miR-38-3p	F42H10.5
cel-miR-38-3p	C06E7.1
cel-miR-38-3p	T22B11.4
cel-miR-38-3p	F29B9.8
cel-miR-38-3p	F13H6.1
cel-miR-38-3p	W06H8.5
cel-miR-1829b-5p	T27D12.1
cel-miR-1829b-5p	F42A10.3
cel-miR-1829b-5p	drap-1
cel-miR-1829b-5p	C15H9.9
cel-miR-1829b-5p	F40E10.6
cel-miR-1829b-5p	W03C9.5
cel-miR-1829b-5p	F29B9.8
cel-miR-1829b-5p	F37B12.3
cel-miR-1829b-5p	R12E2.2
cel-miR-1829b-5p	T10B10.3
cel-miR-1829b-5p	F59B10.5
cel-miR-1829b-5p	nkb-1
cel-miR-1829b-5p	F13D12.9
cel-miR-1829b-5p	C56G2.1
cel-miR-1829b-5p	R148.3
cel-miR-1829b-5p	dlat-1
cel-miR-1829b-5p	got-2.2
cel-miR-1829b-5p	T24H10.4
cel-miR-1829b-5p	K05F1.6
cel-miR-1829b-5p	lpin-1
cel-miR-1829b-5p	eif-1
cel-miR-1829b-5p	C35C5.6
cel-miR-1829b-5p	asns-2
cel-miR-1829b-5p	ain-2
cel-miR-1829b-5p	EEED8.16
cel-miR-1829b-5p	mdh-1
cel-miR-75-3p	F42A10.3
cel-miR-75-3p	F55A11.1
cel-miR-75-3p	aldo-1
cel-miR-75-3p	W03C9.5
cel-miR-75-3p	T24B8.4
cel-miR-75-3p	B0336.3
cel-miR-75-3p	M01H9.3
cel-miR-75-3p	B0041.5
cel-miR-75-3p	pkg-2
cel-miR-75-3p	ZC395.10
cel-miR-75-3p	aagr-4
cel-miR-75-3p	R07G3.7

cel-miR-75-3p	T21G5.6
cel-miR-75-3p	dlat-1
cel-miR-75-3p	C14A4.11
cel-miR-75-3p	F26B1.2
cel-miR-75-3p	tos-1
cel-miR-75-3p	F22F7.7
cel-miR-75-3p	C34D10.2
cel-miR-75-3p	F26A3.4
cel-miR-75-3p	got-2.2
cel-miR-75-3p	K07E3.1
cel-miR-75-3p	idhb-1
cel-miR-75-3p	asns-2
cel-miR-75-3p	guk-1
cel-miR-75-3p	C52E4.5
cel-miR-75-3p	fln-1
cel-miR-75-3p	T26A5.5
cel-miR-75-3p	F37B12.3
cel-miR-75-3p	T24H10.4
cel-miR-75-3p	T12G3.7
cel-miR-75-3p	R05D3.2
cel-miR-250-3p	Y77E11A.12
cel-miR-250-3p	F59F4.2
cel-miR-250-3p	F33G12.5
cel-miR-250-3p	F13H6.1
cel-miR-250-3p	B0252.3
cel-miR-250-3p	R12E2.2
cel-miR-250-3p	R02F2.1
cel-miR-250-3p	B0303.3
cel-miR-250-3p	dmsr-7
cel-miR-250-3p	hpo-34
cel-miR-250-3p	F21F3.6
cel-miR-250-3p	lpr-5
cel-miR-250-3p	D1081.7
cel-miR-250-3p	B0336.3
cel-miR-250-3p	F22H10.3
cel-miR-250-3p	mvk-1
cel-miR-250-3p	T24B8.4
cel-miR-250-3p	C48E7.6
cel-miR-250-3p	C28H8.4
cel-miR-250-3p	ZK470.2
cel-miR-250-3p	nkb-3
cel-miR-250-3p	R06C1.4
cel-miR-250-3p	kcnl-2
cel-miR-250-3p	F01G4.6
cel-miR-250-3p	C18E9.2
cel-miR-250-3p	F36D4.5
cel-miR-250-3p	F37B12.3
cel-miR-250-3p	ZC449.3
cel-miR-250-3p	Y71F9AL.9
cel-miR-250-3p	F56D2.6
cel-miR-250-3p	mig-38
cel-miR-250-3p	sec-16
cel-miR-250-3p	C08G9.1
cel-miR-250-3p	F21D5.7
cel-miR-250-3p	cutl-20
cel-miR-250-3p	C45E1.8
cel-miR-250-3p	CELE_R52.12

cel-miR-250-3p	K08A2.12
cel-miR-250-3p	F40H3.11
cel-miR-53-5p	K03E6.7
cel-miR-53-5p	C05D11.7
cel-miR-53-5p	C49H3.9
cel-miR-53-5p	F21F3.6
cel-miR-53-5p	F16A11.1
cel-miR-53-5p	F52F10.2
cel-miR-53-5p	F21A3.3
cel-miR-53-5p	F46G10.2
cel-miR-53-5p	C35C5.6
cel-miR-53-5p	W03C9.5
cel-miR-53-5p	egg-6
cel-miR-53-5p	lpr-5
cel-miR-53-5p	F45D3.3
cel-miR-53-5p	B0410.3
cel-miR-53-5p	C03C10.4
cel-miR-53-5p	ZK131.11
cel-miR-53-5p	T27E4.7
cel-miR-53-5p	R13H4.5
cel-miR-53-5p	CC8.2
cel-miR-53-5p	M88.5
cel-miR-53-5p	F58H1.5
cel-miR-53-5p	F26A3.4
cel-miR-53-5p	Y119D3B.26
cel-miR-53-5p	K10C9.11
cel-miR-53-5p	D1005.8
cel-miR-70-3p	CC8.2
cel-miR-70-3p	T12G3.2
cel-miR-70-3p	nrde-2
cel-miR-70-3p	lec-12
cel-miR-70-3p	F44E5.5
cel-miR-70-3p	swsn-7
cel-miR-70-3p	T12G3.7
cel-miR-70-3p	C16A3.10
cel-miR-70-3p	Y53C12B.2
cel-miR-70-3p	C46C11.1
cel-miR-70-3p	C10E2.6
cel-miR-70-3p	cec-6
cel-miR-70-3p	F59B10.5
cel-miR-70-3p	F01G4.6
cel-miR-70-3p	F34D10.4
cel-miR-70-3p	C18E9.10
cel-miR-70-3p	R186.7
cel-miR-70-3p	F16A11.1
cel-miR-70-3p	R151.2
cel-miR-70-3p	B0303.3
cel-miR-70-3p	T27E9.2
cel-miR-70-3p	F13D12.9
cel-miR-70-3p	T17H7.1
cel-miR-70-3p	Y37E3.17
cel-miR-70-3p	Y74C9A.4
cel-miR-70-3p	T26A5.5
cel-miR-70-3p	erfa-3
cel-miR-70-3p	ZC190.4
cel-miR-70-3p	K10D3.4
cel-miR-70-3p	F02A9.4

cel-miR-70-3p	F35G2.1
cel-miR-70-3p	F46G10.2
cel-miR-70-3p	R53.4
cel-miR-70-3p	ogdh-1
cel-miR-70-3p	C06E1.3
cel-miR-70-3p	C44C1.5
All identified targets were determined via Chip-Seq	

Supplementary Table 8. MirTarBase identified gene targets for upregulated miRNAs in *LRRK2* transgenic worms fed *A. viscosus*

Upregulated miRNA	Gene Target
cel-miR-241-5p	prmt-1
cel-miR-241-5p	K02E10.7
cel-miR-241-5p	nkb-3
cel-miR-241-5p	C15H9.9
cel-miR-241-5p	F01G4.6
cel-miR-241-5p	Y54G2A.26
cel-miR-241-5p	lsy-22
cel-miR-241-5p	K04F10.3
cel-miR-241-5p	tos-1
cel-miR-241-5p	saeg-2
cel-miR-241-5p	R04F11.2
cel-miR-241-5p	F21C10.3
cel-miR-241-5p	lpr-5
cel-miR-241-5p	got-2.2
cel-miR-241-5p	ZK470.2
cel-miR-241-5p	ZC190.4
cel-miR-241-5p	C10E2.6
cel-miR-241-5p	B0336.3
cel-miR-241-5p	mab-31
cel-miR-241-5p	F57G12.1
cel-miR-788-5p	DH11.2
cel-miR-56-3p	C05D11.7
cel-miR-56-3p	F59B10.5
cel-miR-56-3p	F46G10.2
cel-miR-56-3p	C49H3.9
cel-miR-56-3p	T10B10.3
cel-miR-56-3p	F16A11.1
cel-miR-56-3p	F52F10.2
cel-miR-56-3p	F21A3.3
cel-miR-56-3p	mig-38
cel-miR-56-3p	T27E4.7
cel-miR-56-3p	W03C9.5
cel-miR-56-3p	R13H4.5
cel-miR-56-3p	C35C5.6
cel-miR-56-3p	F45D3.3
cel-miR-56-3p	M88.5
cel-miR-56-3p	ZK131.11
cel-miR-56-3p	C03C10.4
cel-miR-56-3p	egg-6
cel-miR-56-3p	F26A3.4
cel-miR-56-3p	CC8.2
cel-miR-56-3p	B0410.3
cel-miR-56-3p	F58H1.5
cel-miR-56-5p	Y71G12B.11

cel-miR-56-5p	K10D6.4
cel-miR-56-5p	C34D10.2
cel-miR-56-5p	idhg-1
cel-miR-56-5p	C10G11.7
cel-miR-56-5p	Y42G9A.3
cel-miR-56-5p	Y48G1A.2
cel-miR-56-3p	Y119D3B.26
cel-miR-56-3p	K10C9.11
cel-miR-56-3p	D1005.8
cel-miR-54-3p	Y119D3B.26
cel-miR-54-3p	K10C9.11
cel-miR-54-3p	D1005.8
cel-miR-230-3p	T27D12.1
cel-miR-230-3p	F59F4.2
cel-miR-230-3p	F44E5.5
cel-miR-230-3p	C05C8.7
cel-miR-230-3p	T10B10.3
cel-miR-230-3p	F46G10.2
cel-miR-230-3p	C06A8.3
cel-miR-230-3p	F21F3.6
cel-miR-230-3p	F39B2.8
cel-miR-230-3p	C05C10.3
cel-miR-230-3p	F26B1.2
cel-miR-230-3p	tos-1
cel-miR-230-3p	K07H8.2
cel-miR-230-3p	C50B8.1
cel-miR-230-3p	lsy-22
cel-miR-230-3p	noca-1
cel-miR-230-3p	K08D12.6
cel-miR-230-3p	K06A9.1
cel-miR-230-3p	lpr-5
cel-miR-230-3p	R05D3.2
cel-miR-230-3p	K08E3.5
cel-miR-2209a-3p	cfz-2
cel-miR-2209a-3p	Y51F10.12
cel-miR-2209a-3p	D2030.14
cel-miR-51-5p	F59B10.5
cel-miR-51-5p	F52F10.2
cel-miR-51-5p	F46G10.2
cel-miR-51-5p	T10B10.3
cel-miR-51-5p	F16A11.1
cel-miR-51-5p	C05D11.7
cel-miR-51-5p	C49H3.9
cel-miR-51-5p	F21A3.3
cel-miR-51-5p	T25F10.3
cel-miR-51-5p	T27E4.7
cel-miR-51-5p	mig-38
cel-miR-51-5p	R13H4.5
cel-miR-51-5p	egg-6
cel-miR-51-5p	C35C5.6
cel-miR-51-5p	M88.5
cel-miR-51-5p	C03C10.4
cel-miR-51-5p	F45D3.3
cel-miR-51-5p	ZK131.11
cel-miR-51-5p	CC8.2
cel-miR-51-5p	F58H1.5
cel-miR-51-5p	W03C9.5
cel-miR-51-5p	F26A3.4

cel-miR-51-5p	B0410.3
cel-miR-51-5p	Y119D3B.26
cel-miR-51-5p	K10C9.11
cel-miR-51-5p	D1005.8
cel-miR-246-3p	panl-3
cel-miR-246-3p	F52A8.1
cel-miR-246-3p	F44E5.1
cel-miR-246-3p	F46G10.2
cel-miR-246-3p	idhb-1
cel-miR-246-3p	R05D3.2
cel-miR-246-3p	Y47D9A.1
cel-miR-246-3p	T14B1.1
cel-miR-246-3p	R107.5
cel-miR-246-3p	ZK484.1
cel-miR-246-3p	AH9.6
cel-miR-246-3p	F45D3.2
cel-miR-246-3p	F57F4.4
cel-miR-246-3p	F44E2.4
cel-miR-246-3p	B0361.9
cel-miR-246-3p	C48E7.1
cel-miR-246-3p	C09D4.4
cel-miR-246-3p	F47D12.9
cel-miR-246-3p	W03C9.5
cel-miR-246-3p	T13C2.6
cel-miR-246-3p	F45D3.3
cel-miR-246-3p	F26A3.4
cel-miR-246-3p	R09A8.5
cel-miR-246-3p	M60.4
cel-miR-246-3p	Y71G12B.11
cel-miR-246-3p	scav-2
cel-miR-246-3p	C38H2.2
cel-miR-246-3p	D2030.14
cel-lin-4-5p	lin-14
cel-lin-4-5p	lin-28
cel-lin-4-5p	hbl-1
cel-lin-4-5p	F12B6.2
cel-lin-4-5p	C08G9.1
cel-lin-4-5p	C37H5.6
cel-lin-4-5p	CELE_C27C7.12
cel-lin-4-5p	Y50D7A.18
All identified targets were determined via Chip-Seq with the exception of cel-lin-4-5p targets lin-14 (Reporter assay, Western, qPCR), lin-28 (Reporter assay, Western), hbl-1 (Reporter assay)	

References

Abeliovich, Asa, and Aaron D. Gitler. 2016. "Defects in Trafficking Bridge Parkinson's Disease Pathology and Genetics." *Nature* 539 (7628): 207–16.

Alessi, Dario R., and Esther Sammler. 2018. "LRRK2 Kinase in Parkinson's Disease." *Science* 360 (6384): 36–37.

Altun, Z. F., and D. H. Hall. 2009. "Introduction in Worm Atlas." Cold Spring Harbor Laboratory Press): Long Island, NY, USA.

Alvarez-Erviti, Lydia, Maria C. Rodriguez-Oroz, J. Mark Cooper, Cristina Caballero, Isidro Ferrer, Jose A. Obeso, and Anthony H. V. Schapira. 2010. "Chaperone-Mediated Autophagy Markers in Parkinson Disease Brains." *Archives of Neurology* 67 (12): 1464–72.

Alvarsson, Alexandra, Xiaoqun Zhang, Tiberiu L. Stan, Nicoletta Schintu, Banafsheh Kadkhodaei, Mark J. Millan, Thomas Perlmann, and Per Svenningsson. 2015. "Modulation by Trace Amine-Associated Receptor 1 of Experimental Parkinsonism, L-DOPA Responsivity, and Glutamatergic Neurotransmission." *The Journal of Neuroscience: The Official Journal of the Society for Neuroscience* 35 (41): 14057–69.

Anglade, P., S. Vyas, F. Javoy-Agid, M. T. Herrero, P. P. Michel, J. Marquez, A. Mouatt-Prigent, M. Ruberg, E. C. Hirsch, and Y. Agid. 1997. "Apoptosis and Autophagy in Nigral Neurons of Patients with Parkinson's Disease." *Histology and Histopathology* 12 (1): 25–31.

Asikainen, Suvi, Martina Rudgalvyte, Liisa Heikkinen, Kristiina Louhiranta, Merja Lakso, Garry Wong, and Richard Nass. 2010. "Global microRNA Expression Profiling of Caenorhabditis Elegans Parkinson's Disease Models." *Journal of Molecular Neuroscience: MN* 41 (1): 210–18.

Balklava, Zita, Saumya Pant, Hanna Fares, and Barth D. Grant. 2007. "Genome-Wide Analysis Identifies a General Requirement for Polarity Proteins in Endocytic Traffic." *Nature Cell Biology* 9 (9): 1066–73.

Bardien, Soraya, Suzanne Lesage, Alexis Brice, and Jonathan Carr. 2011. "Genetic Characteristics of Leucine-Rich Repeat Kinase 2 (LRRK2) Associated Parkinson's Disease." *Parkinsonism & Related Disorders* 17 (7): 501–8.

Bedarf, J. R., F. Hildebrand, L. P. Coelho, S. Sunagawa, M. Bahram, F. Goeser, P. Bork, and U. Wüllner. 2017. "Erratum to: Functional Implications of Microbial and Viral Gut Metagenome Changes in Early Stage L-DOPA-Naïve Parkinson's Disease Patients." *Genome Medicine* 9 (1): 61.

Berkowitz, Laura A., Shusei Hamamichi, Adam L. Knight, Adam J. Harrington, Guy A. Caldwell, and Kim A. Caldwell. 2008. "Application of a C. Elegans Dopamine Neuron Degeneration Assay for the Validation of Potential Parkinson's Disease Genes." *Journal of Visualized Experiments: JoVE*, no. 17 (July). https://doi.org/10.3791/835.

Bishop, Nicholas A., and Leonard Guarente. 2007. "Two Neurons Mediate Diet-Restriction-Induced Longevity in C. Elegans." *Nature* 447 (7144): 545–49.

Bolger, Anthony M., Marc Lohse, and Bjoern Usadel. 2014. "Trimmomatic: A Flexible Trimmer for Illumina Sequence Data." *Bioinformatics* 30 (15): 2114–20.

Boulin, Thomas, and Oliver Hobert. 2012. "From Genes to Function: The C. Elegans Genetic Toolbox." *Wiley Interdisciplinary Reviews. Developmental Biology* 1 (1): 114–37.

Brenner, S. 1974. "The Genetics of Caenorhabditis Elegans." *Genetics* 77 (1): 71–94.

Briggs, Christine E., Yulei Wang, Benjamin Kong, Tsung-Ung W. Woo, Lakshmanan K. Iyer, and Kai C. Sonntag. 2015. "Midbrain Dopamine Neurons in Parkinson′ S Disease Exhibit a Dysregulated miRNA and Target-Gene Network." *Brain Research* 1618: 111–21.

Broughton, James P., and Amy E. Pasquinelli. 2016. "A Tale of Two Sequences: microRNA-Target Chimeric Reads." *Genetics, Selection, Evolution: GSE* 48 (April): 31.

Cao, Songsong, Christopher C. Gelwix, Kim A. Caldwell, and Guy A. Caldwell. 2005. "Torsin-Mediated Protection from Cellular Stress in the Dopaminergic Neurons of Caenorhabditis Elegans." *The Journal of Neuroscience: The Official Journal of the Society for Neuroscience* 25 (15): 3801–12.

Chen, Di, Emma Lynn Thomas, and Pankaj Kapahi. 2009. "HIF-1 Modulates Dietary Restriction-Mediated Lifespan Extension via IRE-1 in Caenorhabditis Elegans." *PLoS Genetics* 5 (5): e1000486.

Chikka, Madhusudana Rao, Charumathi Anbalagan, Katherine Dvorak, Kyle Dombeck, and Veena Prahlad. 2016. "The Mitochondria-Regulated Immune Pathway Activated in the C. Elegans Intestine Is Neuroprotective." *Cell Reports* 16 (9): 2399–2414.

Chuang, P. T., D. G. Albertson, and B. J. Meyer. 1994. "DPY-27:a Chromosome Condensation Protein Homolog That Regulates C. Elegans Dosage Compensation through Association with the X Chromosome." *Cell* 79 (3): 459–74.

Connor-Robson, Natalie, Heather Booth, Jeffrey G. Martin, Benbo Gao, Kejie Li, Natalie Doig, Jane Vowles, et al. 2019. "An Integrated Transcriptomics and Proteomics Analysis Reveals Functional Endocytic Dysregulation Caused by Mutations in

LRRK2." *Neurobiology of Disease* 127 (July): 512–26.

Cooper, Jason F., Dylan J. Dues, Katie K. Spielbauer, Emily Machiela, Megan M. Senchuk, and Jeremy M. Van Raamsdonk. 2015. "Delaying Aging Is Neuroprotective in Parkinson's Disease: A Genetic Analysis in C. Elegans Models." *NPJ Parkinson's Disease* 1 (November): 15022.

Csankovszki, Gyorgyi, Karishma Collette, Karin Spahl, James Carey, Martha Snyder, Emily Petty, Uchita Patel, et al. 2009. "Three Distinct Condensin Complexes Control C. Elegans Chromosome Dynamics." *Current Biology: CB* 19 (1): 9–19.

D'Andrea, Giovanni, Gianpietro Nordera, Gilberto Pizzolato, Andrea Bolner, Davide Colavito, Raffaella Flaibani, and Alberta Leon. 2010. "Trace Amine Metabolism in Parkinson's Disease: Low Circulating Levels of Octopamine in Early Disease Stages." *Neuroscience Letters* 469 (3): 348–51.

Dawes, H. E., D. S. Berlin, D. M. Lapidus, C. Nusbaum, T. L. Davis, and B. J. Meyer. 1999. "Dosage Compensation Proteins Targeted to X Chromosomes by a Determinant of Hermaphrodite Fate." *Science*.

Dehay, Benjamin, Jordi Bové, Natalia Rodríguez-Muela, Celine Perier, Ariadna Recasens, Patricia Boya, and Miquel Vila. 2010. "Pathogenic Lysosomal Depletion in Parkinson's Disease." *The Journal of Neuroscience: The Official Journal of the Society for Neuroscience* 30 (37): 12535–44.

Dumas, Kathleen J., Colin E. Delaney, Stephane Flibotte, Donald G. Moerman, Gyorgyi Csankovszki, and Patrick J. Hu. 2013. "Unexpected Role for Dosage Compensation in the Control of Dauer Arrest, Insulin-like Signaling, and FoxO Transcription Factor Activity in Caenorhabditis Elegans." *Genetics* 194 (3): 619–29.

Evans, Thomas. 2006. "Transformation and Microinjection." *WormBook: The Online Review of C. Elegans Biology*. https://doi.org/10.1895/wormbook.1.108.1.

Fromm, Bastian, Diana Domanska, Eirik Høye, Vladimir Ovchinnikov, Wenjing Kang, Ernesto Aparicio-Puerta, Morten Johansen, et al. 2020. "MirGeneDB 2.0: The Metazoan microRNA Complement." *Nucleic Acids Research* 48 (D1): D1172.

Galaxy Community. 2022. "The Galaxy Platform for Accessible, Reproducible and Collaborative Biomedical Analyses: 2022 Update." *Nucleic Acids Research* 50 (W1): W345–51.

Gao, Arwen W., Reuben L. Smith, Michel van Weeghel, Rashmi Kamble, Georges E. Janssens, and Riekelt H. Houtkooper. 2018. "Identification of Key Pathways and Metabolic Fingerprints of Longevity in C. Elegans." *Experimental Gerontology* 113 (November): 128–40.

Geng, Shengya, Qian Li, Xue Zhou, Junkang Zheng, Huimin Liu, Jie Zeng, Ruizhi Yang,

et al. 2022. “Gut Commensal E. Coli Outer Membrane Proteins Activate the Host Food Digestive System through Neural-Immune Communication.” *Cell Host & Microbe* 30 (10): 1401–16.e8.

Gerstbrein, Beate, Georgios Stamatas, Nikiforos Kollias, and Monica Driscoll. 2005. “In Vivo Spectrofluorimetry Reveals Endogenous Biomarkers That Report Healthspan and Dietary Restriction in Caenorhabditis Elegans.” *Aging Cell* 4 (3): 127–37.

Goh, Suh Yee, Yin Xia Chao, Shaikali Thameem Dheen, Eng-King Tan, and Samuel Sam-Wah Tay. 2019. “Role of MicroRNAs in Parkinson’s Disease.” *International Journal of Molecular Sciences* 20 (22). https://doi.org/10.3390/ijms20225649.

Good, Kathryn, Rafal Ciosk, Jeremy Nance, Alexandre Neves, Russell J. Hill, and James R. Priess. 2004. “The T-Box Transcription Factors TBX-37 and TBX-38 Link GLP-1/Notch Signaling to Mesoderm Induction in C. Elegans Embryos.” *Development* 131 (9): 1967–78.

Goya, María Eugenia, Feng Xue, Cristina Sampedro-Torres-Quevedo, Sofia Arnaouteli, Lourdes Riquelme-Dominguez, Andrés Romanowski, Jack Brydon, Kathryn L. Ball, Nicola R. Stanley-Wall, and Maria Doitsidou. 2020. “Probiotic Bacillus Subtilis Protects against α-Synuclein Aggregation in C. Elegans.” *Cell Reports* 30 (2): 367–80.e7.

Greer, Eric L., and Anne Brunet. 2009. “Different Dietary Restriction Regimens Extend Lifespan by Both Independent and Overlapping Genetic Pathways in C. Elegans.” *Aging Cell* 8 (2): 113–27.

Greer, Eric L., Dara Dowlatshahi, Max R. Banko, Judit Villen, Kimmi Hoang, Daniel Blanchard, Steven P. Gygi, and Anne Brunet. 2007. “An AMPK-FOXO Pathway Mediates Longevity Induced by a Novel Method of Dietary Restriction in C. Elegans.” *Current Biology: CB* 17 (19): 1646–56.

Gregersen, Niels, Peter Bross, Søren Vang, and Jane H. Christensen. 2006. “Protein Misfolding and Human Disease.” *Annual Review of Genomics and Human Genetics* 7: 103–24.

Griffin, Edward F., Samuel E. Scopel, Cayman A. Stephen, Adam C. Holzhauer, Madeline A. Vaji, Ryan A. Tuckey, Laura A. Berkowitz, Kim A. Caldwell, and Guy A. Caldwell. 2019. “ApoE-Associated Modulation of Neuroprotection from Aβ-Mediated Neurodegeneration in Transgenic Caenorhabditis Elegans.” *Disease Models & Mechanisms* 12 (2). https://doi.org/10.1242/dmm.037218.

Gui, Yaxing, Hai Liu, Lishan Zhang, Wen Lv, and Xingyue Hu. 2015. “Altered microRNA Profiles in Cerebrospinal Fluid Exosome in Parkinson Disease and Alzheimer Disease.” *Oncotarget* 6 (35): 37043–53.

Hajdú, Gábor, Milán Somogyvári, Péter Csermely, and Csaba Sőti. 2023. “Lysosome-

Related Organelles Promote Stress and Immune Responses in C. Elegans." *Communications Biology* 6 (1): 936.

Hamamichi, Shusei, Renee N. Rivas, Adam L. Knight, Songsong Cao, Kim A. Caldwell, and Guy A. Caldwell. 2008. "Hypothesis-Based RNAi Screening Identifies Neuroprotective Genes in a Parkinson's Disease Model." *Proceedings of the National Academy of Sciences of the United States of America* 105 (2): 728–33.

Ham, Tjakko J. van, Karen L. Thijssen, Rainer Breitling, Robert M. W. Hofstra, Ronald H. A. Plasterk, and Ellen A. A. Nollen. 2008. "C. Elegans Model Identifies Genetic Modifiers of Alpha-Synuclein Inclusion Formation during Aging." *PLoS Genetics* 4 (3): e1000027.

Hara, Kenta, Yoshiko Maruki, Xiaomeng Long, Ken-Ichi Yoshino, Noriko Oshiro, Sujuti Hidayat, Chiharu Tokunaga, Joseph Avruch, and Kazuyoshi Yonezawa. 2002. "Raptor, a Binding Partner of Target of Rapamycin (TOR), Mediates TOR Action." *Cell* 110 (2): 177–89.

Healy, Daniel G., Mario Falchi, Sean S. O'Sullivan, Vincenzo Bonifati, Alexandra Durr, Susan Bressman, Alexis Brice, et al. 2008. "Phenotype, Genotype, and Worldwide Genetic Penetrance of LRRK2-Associated Parkinson's Disease: A Case-Control Study." *Lancet Neurology* 7 (7): 583–90.

Hill-Burns, Erin M., Justine W. Debelius, James T. Morton, William T. Wissemann, Matthew R. Lewis, Zachary D. Wallen, Shyamal D. Peddada, et al. 2017. "Parkinson's Disease and Parkinson's Disease Medications Have Distinct Signatures of the Gut Microbiome." *Movement Disorders: Official Journal of the Movement Disorder Society* 32 (5): 739–49.

Holdorf, Amy D., Daniel P. Higgins, Anne C. Hart, Peter R. Boag, Gregory J. Pazour, Albertha J. M. Walhout, and Amy K. Walker. 2020. "WormCat: An Online Tool for Annotation and Visualization of Caenorhabditis Elegans Genome-Scale Data." *Genetics* 214 (2): 279–94.

Honjoh, Sakiko, Akiko Ihara, Yukiko Kajiwara, Takuya Yamamoto, and Eisuke Nishida. 2017. "The Sexual Dimorphism of Dietary Restriction Responsiveness in Caenorhabditis Elegans." *Cell Reports* 21 (13): 3646–52.

Hopfner, Franziska, Axel Künstner, Stefanie H. Müller, Sven Künzel, Kirsten E. Zeuner, Nils G. Margraf, Günther Deuschl, John F. Baines, and Gregor Kuhlenbäumer. 2017. "Gut Microbiota in Parkinson Disease in a Northern German Cohort." *Brain Research* 1667 (July): 41–45.

Hou, Lei, Dan Wang, Di Chen, Yi Liu, Yue Zhang, Hao Cheng, Chi Xu, et al. 2016. "A Systems Approach to Reverse Engineer Lifespan Extension by Dietary Restriction." *Cell Metabolism* 23 (3): 529–40.

Houthoofd, Koen, Bart P. Braeckman, Thomas E. Johnson, and Jacques R. Vanfleteren. 2003. “Life Extension via Dietary Restriction Is Independent of the Ins/IGF-1 Signalling Pathway in Caenorhabditis Elegans.” *Experimental Gerontology* 38 (9): 947–54.

Houthoofd, Koen, Bart P. Braeckman, Isabelle Lenaerts, Kristel Brys, Annemie De Vreese, Sylvie Van Eygen, and Jacques R. Vanfleteren. 2002. “No Reduction of Metabolic Rate in Food Restricted Caenorhabditis Elegans.” *Experimental Gerontology* 37 (12): 1359–69.

Hsu, D. R., and B. J. Meyer. 1994. “The Dpy-30 Gene Encodes an Essential Component of the Caenorhabditis Elegans Dosage Compensation Machinery.” *Genetics* 137 (4): 999–1018.

Huang, Hsi-Yuan, Yang-Chi-Dung Lin, Shidong Cui, Yixian Huang, Yun Tang, Jiatong Xu, Jiayang Bao, et al. 2021. “miRTarBase Update 2022: An Informative Resource for Experimentally Validated miRNA–target Interactions.” *Nucleic Acids Research* 50 (D1): D222–30.

Jacobson, L. A., L. Jen-Jacobson, J. M. Hawdon, G. P. Owens, M. A. Bolanowski, S. W. Emmons, M. V. Shah, R. A. Pollock, and D. S. Conklin. 1988. “Identification of a Putative Structural Gene for Cathepsin D in Caenorhabditis Elegans.” *Genetics* 119 (2): 355–63.

Jadiya, Pooja, Manavi Chatterjee, Shreesh Raj Sammi, Supinder Kaur, Gautam Palit, and Aamir Nazir. 2011. “Sir-2.1 Modulates ‘calorie-Restriction-Mediated’prevention of Neurodegeneration in Caenorhabditis Elegans: Implications for Parkinson’s Disease.” *Biochemical and Biophysical Research Communications* 413 (2): 306–10.

Jones, Kevin T., Elisabeth R. Greer, David Pearce, and Kaveh Ashrafi. 2009. “Rictor/TORC2 Regulates Caenorhabditis Elegans Fat Storage, Body Size, and Development through Sgk-1.” *PLoS Biology* 7 (3): e60.

Jordan, James M., Jonathan D. Hibshman, Amy K. Webster, Rebecca E. W. Kaplan, Abigail Leinroth, Ryan Guzman, Colin S. Maxwell, et al. 2019. “Insulin/IGF Signaling and Vitellogenin Provisioning Mediate Intergenerational Adaptation to Nutrient Stress.” *Current Biology: CB* 29 (14): 2380–88.e5.

Jumper, John, Richard Evans, Alexander Pritzel, Tim Green, Michael Figurnov, Olaf Ronneberger, Kathryn Tunyasuvunakool, et al. 2021. “Highly Accurate Protein Structure Prediction with AlphaFold.” *Nature* 596 (7873): 583–89.

Kaeberlein, Tammi L., Erica D. Smith, Mitsuhiro Tsuchiya, K. Linnea Welton, James H. Thomas, Stanley Fields, Brian K. Kennedy, and Matt Kaeberlein. 2006. “Lifespan Extension in Caenorhabditis Elegans by Complete Removal of Food.” *Aging Cell* 5 (6): 487–94.

Kamath, Ravi S., and Julie Ahringer. 2003. “Genome-Wide RNAi Screening in Caenorhabditis Elegans.” *Methods* 30 (4): 313–21.

Kern, Fabian, Tobias Fehlmann, Ivo Violich, Eric Alsop, Elizabeth Hutchins, Mustafa Kahraman, Nadja L. Grammes, et al. 2021. “Deep Sequencing of sncRNAs Reveals Hallmarks and Regulatory Modules of the Transcriptome during Parkinson’s Disease Progression.” *Nature Aging* 1 (3): 309–22.

Keshavarzian, Ali, Stefan J. Green, Phillip A. Engen, Robin M. Voigt, Ankur Naqib, Christopher B. Forsyth, Ece Mutlu, and Kathleen M. Shannon. 2015. “Colonic Bacterial Composition in Parkinson’s Disease.” *Movement Disorders: Official Journal of the Movement Disorder Society* 30 (10): 1351–60.

Kim, Daehwan, Joseph M. Paggi, Chanhee Park, Christopher Bennett, and Steven L. Salzberg. 2019. “Graph-Based Genome Alignment and Genotyping with HISAT2 and HISAT-Genotype.” *Nature Biotechnology* 37 (8): 907–15.

Klass, M. R. 1977. “Aging in the Nematode Caenorhabditis Elegans: Major Biological and Environmental Factors Influencing Life Span.” *Mechanisms of Ageing and Development* 6 (6): 413–29.

Klionsky, Daniel J. 2005. “The Molecular Machinery of Autophagy: Unanswered Questions.” *Journal of Cell Science* 118 (Pt 1): 7–18.

Kogure, Akiko, Masaharu Uno, Takako Ikeda, and Eisuke Nishida. 2017. “The microRNA Machinery Regulates Fasting-Induced Changes in Gene Expression and Longevity in Caenorhabditis Elegans.” *The Journal of Biological Chemistry* 292 (27): 11300–309.

Kunz, Joachim B., Heinz Schwarz, and Andreas Mayer. 2004. “Determination of Four Sequential Stages during Microautophagy in Vitro.” *The Journal of Biological Chemistry* 279 (11): 9987–96.

Kuo, Ming-Che, Sam Chi-Hao Liu, Ya-Fang Hsu, and Ruey-Meei Wu. 2021. “The Role of Noncoding RNAs in Parkinson’s Disease: Biomarkers and Associations with Pathogenic Pathways.” *Journal of Biomedical Science* 28 (1): 78.

Kuwahara, Tomoki, Akihiko Koyama, Keiko Gengyo-Ando, Mayumi Masuda, Hisatomo Kowa, Makoto Tsunoda, Shohei Mitani, and Takeshi Iwatsubo. 2006. “Familial Parkinson Mutant α-Synuclein Causes Dopamine Neuron Dysfunction in Transgenic Caenorhabditis Elegans.” *The Journal of Biological Chemistry* 281 (1): 334–40.

Laaberki, Maria-Halima, and Jonathan Dworkin. 2008. “Role of Spore Coat Proteins in the Resistance of Bacillus Subtilis Spores to Caenorhabditis Elegans Predation.” *Journal of Bacteriology* 190 (18): 6197–6203.

Lakso, Merja, Suvi Vartiainen, Anu-Maarit Moilanen, Jouni Sirviö, James H. Thomas,

Richard Nass, Randy D. Blakely, and Garry Wong. 2003. "Dopaminergic Neuronal Loss and Motor Deficits in Caenorhabditis Elegans Overexpressing Human Alpha-Synuclein." *Journal of Neurochemistry* 86 (1): 165–72.

Lan, Ai-Ping, Jun Chen, Yuliang Zhao, Zhifang Chai, and Yi Hu. 2017. "mTOR Signaling in Parkinson's Disease." *Neuromolecular Medicine* 19 (1): 1–10.

Langston, J. William. 2006. "The Parkinson's Complex: Parkinsonism Is Just the Tip of the Iceberg." *Annals of Neurology* 59 (4): 591–96.

Large, Edward E., and Laura D. Mathies. 2014. "Caenorhabditis Elegans SWI/SNF Subunits Control Sequential Developmental Stages in the Somatic Gonad." *G3* 4 (3): 471–83.

Lee, Garrick D., Mark A. Wilson, Min Zhu, Catherine A. Wolkow, Rafael de Cabo, Donald K. Ingram, and Sige Zou. 2006. "Dietary Deprivation Extends Lifespan in Caenorhabditis Elegans." *Aging Cell* 5 (6): 515–24.

Levine, Amir, Danielle Grushko, and Ehud Cohen. 2019. "Gene Expression Modulation by the Linker of Nucleoskeleton and Cytoskeleton Complex Contributes to Proteostasis." *Aging Cell* 18 (6): e13047.

Levin, Michal, Tamar Hashimshony, Florian Wagner, and Itai Yanai. 2012. "Developmental Milestones Punctuate Gene Expression in the Caenorhabditis Embryo." *Developmental Cell* 22 (5): 1101–8.

Lieb, J. D., M. R. Albrecht, P. T. Chuang, and B. J. Meyer. 1998. "MIX-1: An Essential Component of the C. Elegans Mitotic Machinery Executes X Chromosome Dosage Compensation." *Cell* 92 (2): 265–77.

Lieb, J. D., E. E. Capowski, P. Meneely, and B. J. Meyer. 1996. "DPY-26, a Link between Dosage Compensation and Meiotic Chromosome Segregation in the Nematode." *Science* 274 (5293): 1732–36.

Lin, Chin-Hsien, Chieh-Chang Chen, Han-Lin Chiang, Jyh-Ming Liou, Chih-Min Chang, Tzu-Pin Lu, Eric Y. Chuang, et al. 2019. "Altered Gut Microbiota and Inflammatory Cytokine Responses in Patients with Parkinson's Disease." *Journal of Neuroinflammation* 16 (1): 129.

Li, Qing, Ling-Bing Meng, Li-Jun Chen, Xia Shi, Ling Tu, Qi Zhou, Jin-Long Yu, Xin Liao, Yuan Zeng, and Qiao-Ying Yuan. 2023. "The Role of the Microbiota-Gut-Brain Axis and Intestinal Microbiome Dysregulation in Parkinson's Disease." *Frontiers in Neurology* 14 (May): 1185375.

Li Y., Li R. X., Du Y. T., Xu X. J., Xue Y., Gao D., Gao T., Sheng Z., Zhang L. Y., and Tuo H. Z. 2020. "Features of gut microbiota in patients with idiopathic Parkinson's disease." *Zhonghua yi xue za zhi* 100 (13): 1017–22.

Long, Simei, Wenyuan Guo, Sophie Hu, Fengjuan Su, Yixuan Zeng, Jinsheng Zeng, Eng-King Tan, Christopher A. Ross, and Zhong Pei. 2018. "G2019S LRRK2 Increases Stress Susceptibility Through Inhibition of DAF-16 Nuclear Translocation in a 14-3-3 Associated-Manner in Caenorhabditis Elegans." *Frontiers in Neuroscience* 12 (November): 782.

Long, Xiaomeng, Carmen Spycher, Z. Stanley Han, Ann M. Rose, Fritz Müller, and Joseph Avruch. 2002. "TOR Deficiency in C. Elegans Causes Developmental Arrest and Intestinal Atrophy by Inhibition of mRNA Translation." *Current Biology: CB* 12 (17): 1448–61.

Love, Michael I., Wolfgang Huber, and Simon Anders. 2014. "Moderated Estimation of Fold Change and Dispersion for RNA-Seq Data with DESeq2." *Genome Biology* 15 (12): 550.

Lynch-Day, Melinda A., Kai Mao, Ke Wang, Mantong Zhao, and Daniel J. Klionsky. 2012. "The Role of Autophagy in Parkinson's Disease." *Cold Spring Harbor Perspectives in Medicine* 2 (4): a009357.

Mair, William, Siler H. Panowski, Reuben J. Shaw, and Andrew Dillin. 2009. "Optimizing Dietary Restriction for Genetic Epistasis Analysis and Gene Discovery in C. Elegans." *PloS One* 4 (2): e4535.

Majeski, Amy E., and J. Fred Dice. 2004. "Mechanisms of Chaperone-Mediated Autophagy." *The International Journal of Biochemistry & Cell Biology* 36 (12): 2435–44.

Maswood, Navin, Jennifer Young, Edward Tilmont, Zhiming Zhang, Don M. Gash, Greg A. Gerhardt, Richard Grondin, et al. 2004. "Caloric Restriction Increases Neurotrophic Factor Levels and Attenuates Neurochemical and Behavioral Deficits in a Primate Model of Parkinson's Disease." *Proceedings of the National Academy of Sciences of the United States of America* 101 (52): 18171–76.

Mayer, C., and I. Grummt. 2006. "Ribosome Biogenesis and Cell Growth: mTOR Coordinates Transcription by All Three Classes of Nuclear RNA Polymerases." *Oncogene* 25 (48): 6384–91.

McCue, Hannah V., Xi Chen, Jeff W. Barclay, Alan Morgan, and Robert D. Burgoyne. 2015. "Expression Profile of a Caenorhabditis Elegans Model of Adult Neuronal Ceroid Lipofuscinosis Reveals down Regulation of Ubiquitin E3 Ligase Components." *Scientific Reports* 5 (September): 14392.

Mizushima, Noboru, Beth Levine, Ana Maria Cuervo, and Daniel J. Klionsky. 2008. "Autophagy Fights Disease through Cellular Self-Digestion." *Nature* 451 (7182): 1069–75.

Mok, Darren Z. L., Paul W. Sternberg, and Takao Inoue. 2015. "Morphologically Defined

Sub-Stages of C. Elegans Vulval Development in the Fourth Larval Stage." *BMC Developmental Biology* 15 (June): 26.

Moors, Tim E., Silvia Paciotti, Angela Ingrassia, Marialuisa Quadri, Guido Breedveld, Anna Tasegian, Davide Chiasserini, et al. 2019. "Characterization of Brain Lysosomal Activities in GBA-Related and Sporadic Parkinson's Disease and Dementia with Lewy Bodies." *Molecular Neurobiology* 56 (2): 1344–55.

Murphy, Karen E., Amanda M. Gysbers, Sarah K. Abbott, Adena S. Spiro, Akiko Furuta, Antony Cooper, Brett Garner, Tomohiro Kabuta, and Glenda M. Halliday. 2015. "Lysosomal-Associated Membrane Protein 2 Isoforms Are Differentially Affected in Early Parkinson's Disease." *Movement Disorders: Official Journal of the Movement Disorder Society* 30 (12): 1639–47.

Nixon, Ralph A., Dun-Sheng Yang, and Ju-Hyun Lee. 2008. "Neurodegenerative Lysosomal Disorders: A Continuum from Development to Late Age." *Autophagy* 4 (5): 590–99.

Palgunow, Daniela, Maja Klapper, and Frank Döring. 2012. "Dietary Restriction during Development Enlarges Intestinal and Hypodermal Lipid Droplets in Caenorhabditis Elegans." *PloS One* 7 (11): e46198.

Pandit, Awadhesh, Vaibhav Jain, Neeraj Kumar, and Arnab Mukhopadhyay. 2014. "PHA-4/FOXA-Regulated microRNA Feed Forward Loops during Caenorhabditis Elegans Dietary Restriction." *Aging* 6 (10): 835–55.

Park, Sang-Kyu, Christopher D. Link, and Thomas E. Johnson. 2010. "Life-Span Extension by Dietary Restriction Is Mediated by NLP-7 Signaling and Coelomocyte Endocytosis in C. Elegans." *FASEB Journal: Official Publication of the Federation of American Societies for Experimental Biology* 24 (2): 383–92.

Perera, Rushika M., and Roberto Zoncu. 2016. "The Lysosome as a Regulatory Hub." *Annual Review of Cell and Developmental Biology* 32 (October): 223–53.

Plenefisch, J. D., L. DeLong, and B. J. Meyer. 1989. "Genes That Implement the Hermaphrodite Mode of Dosage Compensation in Caenorhabditis Elegans." *Genetics* 121 (1): 57–76.

Poewe, W. 2008. "Non-Motor Symptoms in Parkinson's Disease." *European Journal of Neurology: The Official Journal of the European Federation of Neurological Societies* 15 Suppl 1 (s1): 14–20.

Polymeropoulos, M. H., C. Lavedan, E. Leroy, S. E. Ide, A. Dehejia, A. Dutra, B. Pike, et al. 1997. "Mutation in the Alpha-Synuclein Gene Identified in Families with Parkinson's Disease." *Science* 276 (5321): 2045–47.

Portal-Celhay, Cynthia, Ellen R. Bradley, and Martin J. Blaser. 2012. "Control of

Intestinal Bacterial Proliferation in Regulation of Lifespan in Caenorhabditis Elegans." *BMC Microbiology* 12 (1): 49.

Putri, Givanna H., Simon Anders, Paul Theodor Pyl, John E. Pimanda, and Fabio Zanini. 2022. "Analysing High-Throughput Sequencing Data in Python with HTSeq 2.0." *Bioinformatics* 38 (10): 2943–45.

Qian, Yiwei, Xiaodong Yang, Shaoqing Xu, Chunyan Wu, Yanyan Song, Nan Qin, Sheng-Di Chen, and Qin Xiao. 2018. "Alteration of the Fecal Microbiota in Chinese Patients with Parkinson's Disease." *Brain, Behavior, and Immunity* 70 (May): 194–202.

Qiao, Liyan, Shusei Hamamichi, Kim A. Caldwell, Guy A. Caldwell, Talene A. Yacoubian, Scott Wilson, Zuo-Lei Xie, et al. 2008. "Lysosomal Enzyme Cathepsin D Protects against Alpha-Synuclein Aggregation and Toxicity." *Molecular Brain* 1 (November): 17.

Qi, Bin, and Min Han. 2018. "Microbial Siderophore Enterobactin Promotes Mitochondrial Iron Uptake and Development of the Host via Interaction with ATP Synthase." *Cell* 175 (2): 571–82.e11.

Qi, Bin, Marina Kniazeva, and Min Han. 2017. "A Vitamin-B2-Sensing Mechanism That Regulates Gut Protease Activity to Impact Animal's Food Behavior and Growth." *eLife* 6 (June). https://doi.org/10.7554/eLife.26243.

Robak, Laurie A., Iris E. Jansen, Jeroen van Rooij, André G. Uitterlinden, Robert Kraaij, Joseph Jankovic, International Parkinson's Disease Genomics Consortium (IPDGC), Peter Heutink, and Joshua M. Shulman. 2017. "Excessive Burden of Lysosomal Storage Disorder Gene Variants in Parkinson's Disease." *Brain: A Journal of Neurology* 140 (12): 3191–3203.

Rollins, Jarod A., Dan Shaffer, Santina S. Snow, Pankaj Kapahi, and Aric N. Rogers. 2019. "Dietary Restriction Induces Posttranscriptional Regulation of Longevity Genes." *Life Science Alliance* 2 (4). https://doi.org/10.26508/lsa.201800281.

Rubinsztein, David C., Tomer Shpilka, and Zvulun Elazar. 2012. "Mechanisms of Autophagosome Biogenesis." *Current Biology: CB* 22 (1): R29–34.

Saftig, Paul, and Judith Klumperman. 2009. "Lysosome Biogenesis and Lysosomal Membrane Proteins: Trafficking Meets Function." *Nature Reviews. Molecular Cell Biology* 10 (9): 623–35.

Saha, Shamol, Peter E. A. Ash, Vivek Gowda, Liqun Liu, Orian Shirihai, and Benjamin Wolozin. 2015. "Mutations in LRRK2 Potentiate Age-Related Impairment of Autophagic Flux." *Molecular Neurodegeneration* 10 (July): 26.

Saha, Shamol, Maria D. Guillily, Andrew Ferree, Joel Lanceta, Diane Chan, Joy Ghosh, Cindy H. Hsu, et al. 2009. "LRRK2 Modulates Vulnerability to Mitochondrial

Dysfunction in Caenorhabditis Elegans." *The Journal of Neuroscience: The Official Journal of the Society for Neuroscience* 29 (29): 9210–18.

Sakaguchi-Nakashima, Aisa, James Y. Meir, Yishi Jin, Kunihiro Matsumoto, and Naoki Hisamoto. 2007. "LRK-1, a C. Elegans PARK8-Related Kinase, Regulates Axonal-Dendritic Polarity of SV Proteins." *Current Biology: CB* 17 (7): 592–98.

Sampson, Timothy R., Justine W. Debelius, Taren Thron, Stefan Janssen, Gauri G. Shastri, Zehra Esra Ilhan, Collin Challis, et al. 2016. "Gut Microbiota Regulate Motor Deficits and Neuroinflammation in a Model of Parkinson's Disease." *Cell* 167 (6): 1469–80.e12.

Schade, Michael A., Nicole K. Reynolds, Claudia M. Dollins, and Kenneth G. Miller. 2005. "Mutations That Rescue the Paralysis of Caenorhabditis Elegans Ric-8 (Synembryn) Mutants Activate the Gαs Pathway and Define a Third Major Branch of the Synaptic Signaling Network." *Genetics* 169 (2): 631–49.

Scheperjans, Filip, Velma Aho, Pedro A. B. Pereira, Kaisa Koskinen, Lars Paulin, Eero Pekkonen, Elena Haapaniemi, et al. 2015. "Gut Microbiota Are Related to Parkinson's Disease and Clinical Phenotype." *Movement Disorders: Official Journal of the Movement Disorder Society* 30 (3): 350–58.

Schröder, Bernd A., Christian Wrocklage, Andrej Hasilik, and Paul Saftig. 2010. "The Proteome of Lysosomes." *Proteomics* 10 (22): 4053–76.

Seidel, Hannah S., and Judith Kimble. 2011. "The Oogenic Germline Starvation Response in C. Elegans." *PloS One* 6 (12): e28074.

Sender, Ron, Shai Fuchs, and Ron Milo. 2016. "Revised Estimates for the Number of Human and Bacteria Cells in the Body." *PLoS Biology* 14 (8): e1002533.

Shen, Linjing, Changliang Wang, Liang Chen, and Garry Wong. 2021. "Dysregulation of MicroRNAs and PIWI-Interacting RNAs in a Caenorhabditis Elegans Parkinson's Disease Model Overexpressing Human α-Synuclein and Influence of Tdp-1." *Frontiers in Neuroscience* 15 (March): 600462.

Shore, David E., and Gary Ruvkun. 2013. "A Cytoprotective Perspective on Longevity Regulation." *Trends in Cell Biology* 23 (9): 409–20.

Singh, Jogender, and Alejandro Aballay. 2019. "Microbial Colonization Activates an Immune Fight-and-Flight Response via Neuroendocrine Signaling." *Developmental Cell* 49 (1): 89–99.e4.

Soukas, Alexander A., Elizabeth A. Kane, Christopher E. Carr, Justine A. Melo, and Gary Ruvkun. 2009. "Rictor/TORC2 Regulates Fat Metabolism, Feeding, Growth, and Life Span in Caenorhabditis Elegans." *Genes & Development* 23 (4): 496–511.

Steinegger, Martin, and Johannes Söding. 2018. “Clustering Huge Protein Sequence Sets in Linear Time.” *Nature Communications* 9 (1): 2542.

Steinkraus, Katherine A., Erica D. Smith, Christina Davis, Daniel Carr, William R. Pendergrass, George L. Sutphin, Brian K. Kennedy, and Matt Kaeberlein. 2008. “Dietary Restriction Suppresses Proteotoxicity and Enhances Longevity by an Hsf-1-Dependent Mechanism in Caenorhabditis Elegans.” *Aging Cell* 7 (3): 394–404.

Stiernagle, T. 2006. “Maintenance of C. Elegans. WormBook. The C. Elegans Research Community.” *WormBook: The Online Review of C. Elegans Biology*.

Tanji, Kunikazu, Fumiaki Mori, Akiyoshi Kakita, Hitoshi Takahashi, and Koichi Wakabayashi. 2011. “Alteration of Autophagosomal Proteins (LC3, GABARAP and GATE-16) in Lewy Body Disease.” *Neurobiology of Disease* 43 (3): 690–97.

Taymans, Jean-Marc, Matt Fell, Tim Greenamyre, Warren D. Hirst, Adamantios Mamais, Shalini Padmanabhan, Inga Peter, Hardy Rideout, and Avner Thaler. 2023. “Perspective on the Current State of the LRRK2 Field.” *NPJ Parkinson’s Disease* 9 (1): 104.

Tcherepanova, I., L. Bhattacharyya, C. S. Rubin, and J. H. Freedman. 2000. “Aspartic Proteases from the Nematode Caenorhabditis Elegans. Structural Organization and Developmental and Cell-Specific Expression of Asp-1.” *The Journal of Biological Chemistry* 275 (34): 26359–69.

Tian, Ye, Zhipeng Li, Wanqiu Hu, Haiyan Ren, E. Tian, Yu Zhao, Qun Lu, et al. 2010. “C. Elegans Screen Identifies Autophagy Genes Specific to Multicellular Organisms.” *Cell* 141 (6): 1042–55.

Troemel, Emily R., Stephanie W. Chu, Valerie Reinke, Siu Sylvia Lee, Frederick M. Ausubel, and Dennis H. Kim. 2006. “p38 MAPK Regulates Expression of Immune Response Genes and Contributes to Longevity in C. Elegans.” *PLoS Genetics* 2 (11): e183.

Turnbaugh, Peter J., Ruth E. Ley, Micah Hamady, Claire M. Fraser-Liggett, Rob Knight, and Jeffrey I. Gordon. 2007. “The Human Microbiome Project.” *Nature* 449 (7164): 804–10.

Vadlamudi, R. K., and J. Shin. 1998. “Genomic Structure and Promoter Analysis of the p62 Gene Encoding a Non-Proteasomal Multiubiquitin Chain Binding Protein.” *FEBS Letters* 435 (2-3): 138–42.

Vanfleteren, Jacques R., and Bart P. Braeckman. 1999. “Mechanisms of Life Span Determination in Caenorhabditis Elegans☆.” *Neurobiology of Aging* 20 (5): 487–502.

Varadi, Mihaly, Stephen Anyango, Mandar Deshpande, Sreenath Nair, Cindy Natassia,

Galabina Yordanova, David Yuan, et al. 2022. “AlphaFold Protein Structure Database: Massively Expanding the Structural Coverage of Protein-Sequence Space with High-Accuracy Models.” *Nucleic Acids Research* 50 (D1): D439–44.

Verstraeten, Aline, Jessie Theuns, and Christine Van Broeckhoven. 2015. “Progress in Unraveling the Genetic Etiology of Parkinson Disease in a Genomic Era.” *Trends in Genetics: TIG* 31 (3): 140–49.

Wu, Ziyun, Meltem Isik, Natalie Moroz, Michael J. Steinbaugh, Peng Zhang, and T. Keith Blackwell. 2021. “Dietary Restriction Extends Lifespan through Metabolic Regulation of Innate Immunity.” *Cell Metabolism* 33 (10): 2090.

Xiong, Yulan, Ted M. Dawson, and Valina L. Dawson. 2017. “Models of LRRK2-Associated Parkinson’s Disease.” *Advances in Neurobiology* 14: 163–91.

Xiong, Yulan, Stewart Neifert, Senthilkumar S. Karuppagounder, Qinfang Liu, Jeannette N. Stankowski, Byoung Dae Lee, Han Seok Ko, et al. 2018. “Robust Kinase- and Age-Dependent Dopaminergic and Norepinephrine Neurodegeneration in LRRK2 G2019S Transgenic Mice.” *Proceedings of the National Academy of Sciences of the United States of America* 115 (7): 1635–40.

Xiong, Yulan, and Jianzhong Yu. 2018. “Modeling Parkinson’s Disease in Drosophila: What Have We Learned for Dominant Traits?” *Frontiers in Neurology* 9 (April): 228.

Yao, Chen, Rabih El Khoury, Wen Wang, Tara A. Byrd, Elizabeth A. Pehek, Colin Thacker, Xiongwei Zhu, Mark A. Smith, Amy L. Wilson-Delfosse, and Shu G. Chen. 2010. “LRRK2-Mediated Neurodegeneration and Dysfunction of Dopaminergic Neurons in a Caenorhabditis Elegans Model of Parkinson’s Disease.” *Neurobiology of Disease* 40 (1): 73–81.

Yonker, Stephanie A., and Barbara J. Meyer. 2003. “Recruitment of C. Elegans Dosage Compensation Proteins for Gene-Specific versus Chromosome-Wide Repression.” *Development* 130 (26): 6519–32.

Zhang, Hong, Jessica T. Chang, Bin Guo, Malene Hansen, Kailiang Jia, Attila L. Kovács, Caroline Kumsta, et al. 2015. “Guidelines for Monitoring Autophagy in Caenorhabditis Elegans.” *Autophagy* 11 (1): 9–27.

Zhou, Zhi-Lan, Xue-Bing Jia, Meng-Fei Sun, Ying-Li Zhu, Chen-Meng Qiao, Bo-Ping Zhang, Li-Ping Zhao, et al. 2019. “Neuroprotection of Fasting Mimicking Diet on MPTP-Induced Parkinson’s Disease Mice via Gut Microbiota and Metabolites.” *Neurotherapeutics: The Journal of the American Society for Experimental NeuroTherapeutics* 16 (3): 741–60.

Zhu, Jian-Hui, Fengli Guo, John Shelburne, Simon Watkins, and Charleen T. Chu. 2003. “Localization of Phosphorylated ERK/MAP Kinases to Mitochondria and Autophagosomes in Lewy Body Diseases.” *Brain Pathology* 13 (4): 473–81.

Zisoulis, Dimitrios G., Michael T. Lovci, Melissa L. Wilbert, Kasey R. Hutt, Tiffany Y. Liang, Amy E. Pasquinelli, and Gene W. Yeo. 2010. “Comprehensive Discovery of Endogenous Argonaute Binding Sites in Caenorhabditis Elegans.” *Nature Structural & Molecular Biology* 17 (2): 173–79.

CHAPTER FOUR - Discussion

Summary of findings

In the work presented here, we were able to develop a protocol to determine the impacts of anaerobically grown bacteria on neurodegeneration in *Caenorhabditis elegans* models of Parkinson's Disease (PD). Additionally, we were able to screen through a library of microbiotal isolates representative of the human gut microbiome to identify novel bacteria able to modulate neurodegeneration. Through this screen, we identified a microbiotal isolate able to suppress alpha-synuclein aggregation and induce neuroprotection in animals expressing pathogenic G2019S mutant LRRK2. We then began to characterize changes in host gene expression of both coding and non-coding genes to determine mechanisms underlying the bacterial-induced neuroprotection.

As outlined in Chapter 2, the current research landscape investigating host-microbiota interactions using *C. elegans* as a model has primarily focused on oxygen-tolerant aerobically grown bacteria. With the development of our protocol, not only did we test and identify both obligate and facultative anaerobes able to reproducibly modulate dopaminergic neurodegeneration in *LRRK2* transgenic animals, but we were also able to develop a protocol adaptable to various disease models and laboratory contexts. Screening through 57 microbiotal isolates representing the predominant phyla of the human gut microbiota (Actinobacteria, Firmicutes and Bacteroidetes) (King et al. 2019; Arumugam et al. 2011), we identified five neuroprotective species, *Alistipes shahii* WAL 8301, *Actinomyces oris, Actinomyces naeslundii, Actinomyces viscosus* and *Butyricimonas paravirosa*. Additionally, over the course of this study, we were able to

modify and adapt the protocol to monitor alpha-synuclein aggregation in a protein aggregation model of PD. Recognizing the barriers of culturing obligate anaerobic bacteria, we optimized our protocol using the Advanced Anoxomat® III jar system and comparable systems. This lowers the barrier of entry for using the protocol by eliminating the need for an anaerobic chamber, a relatively expensive and specialized piece of equipment. Furthermore, despite not being able to capture live obligate anaerobe host interactions, by nature of the model, we were still able to identify a novel neuroprotective strictly anaerobic strain, *Alistipes shahii* WAL 8301, therefore validating the utility of testing obligate anaerobes for the potential of identifying stable bioactive molecules that affect host physiology. This work validates the utility of employing a single-bacterium approach to identify novel modulators of disease physiology while expanding the ability to test more fastidious bacteria using *C. elegans* as a gnotobiotic model.

In Chapter 3, we aimed to characterize host mechanisms underlying the neuroprotective phenotype of *Actinomyces viscosus*, one of the bacteria identified in our initial screen. We tested the impacts of the bacteria on a *C. elegans* model of synucleinopathy, another major pathological process in PD, and identified that exposure to *A. viscosus* decreased the number of alpha-synuclein aggregates compared to the control diet, *E. coli* OP50. As a novel food source with an unknown nutritional profile, we characterized the impacts of *A. viscosus* on life history traits, including lifespan, development, fecundity, and body size. We found that *A. viscosus* resulted in delayed development, reduced body size, reduced fecundity, and extended lifespan, phenotypes associated with dietary restriction (DR) in *C. elegans (Vanfleteren and Braeckman 1999;*

Houthoofd et al. 2003, 2002; Seidel and Kimble 2011). Given the well-documented protective effects of DR in the context of both neurodegeneration (Jadiya et al. 2011) and synucleinopathy (Goya et al. 2020) models of PD, we sought to determine if DR is required for *A. viscosus* induced neuroprotection by testing mixed lawns of *E. coli* OP50 and *A. viscosus.* With these experiments, we confirmed the ability of *A. viscosus* to induce neuroprotection in a DR-independent mechanism.

To identify environmentally responsive genes and host mechanisms underlying the neuroprotective phenotype, we conducted transcriptomic analysis via RNA sequencing to identify *A.viscosus* induced changes in gene expression of coding and non-coding genes in a wild-type and *LRRK2* transgenic background. The sequencing of protein coding RNAs revealed a notable increase in the expression of aspartic cathepsins when exposed to *A. viscosus*. Research in *C. elegans* has previously characterized the effects of aspartic cathepsin activity in the context of PD (Qiao et al. 2008); however, our work is the first to identify bacterial-induced changes in cathepsin expression in the context of the disease. We established the significance of aspartic cathepsins in neuronal health in the context of *LRRK2* transgenic animals by demonstrating that RNAi and genetic knockdown of aspartic cathepsins induced neurodegeneration in the model. All previous characterizations of the role of aspartic cathepsins in neuronal health in the context of *C. elegans* models of PD have focused on alpha-synuclein pathology (Qiao et al. 2008), making ours the first study to implicate cathepsin activity in the maintenance of neuronal integrity in the context of *LRRK2* pathogenesis. Additionally, we examined the effects of *A. viscosus* on neuronal autophagy, given the integral role aspartic cathepsins

play in lysosomal degradation activity (Saftig and Klumperman 2009; Schröder et al. 2010). By monitoring autophagosome turnover and degradation of autophagic substrate, we demonstrated that *A. viscosus* is able to rescue *LRRK2* mediated autophagic dysfunction in a DR-dependent and independent manner. The development of transcriptional reporters for both *asp-1* and *asp-8,* coupled with previous characterization of *asp-1* expression (Tcherepanova et al. 2000) enabled us to determine that both genes are primarily expressed in the intestine. Localization of *asp-1* and *asp-8* expression to the intestine suggests that both genes function in maintaining neuronal health via a cell non-autonomous mechanism. Previous work established that intestinal activation of the p38 MAPK (PMK-1)/ATF-7 pathway has a neuroprotective effect against rotenone-induced dopaminergic neurodegeneration (Chikka et al. 2016); therefore, using our transcriptomic data, we monitored the expression of known PMK-1 targets (Troemel et al. 2006) to determine if p38 MAPK (PMK-1)/ATF-7 pathway activation may contribute to our phenotype. However, we identified minimal changes in gene expression in line with a state of PMK-1 activation, suggesting that activation of the (PMK-1)/ATF-7 pathway is not the primary mechanism of *A. viscosus* mediate neuroprotection. In our analysis of miRNA expression, we identified miRNAs specifically differentially regulated in *LRRK2* transgenic animals in response to the neuroprotective diet, therefore identifying environmentally responsive miRNAs that may contribute to our phenotype. Additional comparison of our data to existing miRNA gene expression data (Asikainen et al. 2010; L. Shen et al. 2021) allowed us to pinpoint *mir-38* and *mir-51* as potential candidates for further characterization in the context of *A. viscosus* mediated neuroprotection.

Overall, our work in this chapter successfully identified a human gut commensal bacteria, *A. viscosus,* able to protect against major aspects of PD pathophysiology, dopaminergic neurodegeneration and alpha-synuclein aggregation. Furthermore, we began to characterize specific elements of the host's genetic response to this bacteria, providing some insight into how microbiota species may influence neurodegeneration. Further research is required to gain a comprehensive understanding of the mechanisms, both bacterial and host, responsible for these protective effects; however, we anticipate that our analysis may lead to the identification of novel neuroprotective factors in the context of PD pathogenesis.

Study limitations and future directions

PD is a clinically, pathologically, and genetically heterogeneous disorder involving several environmental and genetic factors (Migliore and Coppedè 2009). Therefore, developing a model encompassing the broad range of pathophysiological and clinical features of the disease is infeasible. Many of the existing models of PD, using various model organisms, recapitulate specific aspects of disease pathophysiology. In this study, we focused on identifying factors modulating neurodegeneration in a *LRRK2* transgenic background with limited exploration of alpha-synuclein pathology, a key component of PD pathophysiology. We briefly investigated the impact of *A, viscosus* on alpha-synuclein aggregation in a synucleinopathy model of *C. elegans*; however, further investigation is required to determine the mechanisms underlying the protective effect and how similar these mechanisms are to those underlying neuroprotection in *LRRK2* transgenic animals. Previous work identified the importance of aspartic cathepsins in *C.*

elegans neuronal health in the context of alpha-synuclein based models of PD (Qiao et al. 2008) suggesting overlap in neuroprotective pathways between models. However, we have yet to investigate the impact of *A. viscosus* on alpha-synuclein mediated neurodegeneration. We were kindly gifted the ERAS1 strain (*eraIs1*[*dat-1p:human SNCA:Venus; dat-1p:mCherry*] by Andrew Hicks (Eurac Institute for Biomedicine), which will allow us to explore the effects of our neuroprotective bacteria in alternative models of neurodegeneration (Vozdek, Pramstaller, and Hicks 2022).

The simplicity of *C. elegans* facilitates its use as a conduit for identifying novel host and bacterial neuroprotective factors; however, it is essential to acknowledge aspects of human physiology not reflected in the model organism. *C. elegans* lacks an ortholog of alpha-synuclein, a protein integral to PD pathophysiology, requiring the use of transgenics. *C. elegans* also lacks key components of human immunity, including migratory immune cells, the inflammasome, and an adaptive immune system. Mounting evidence has established a strong role of both innate and adaptive immune mechanisms in early PD progression (Tan et al. 2020). Additionally, crosstalk of the innate and adaptive immune system in both the central nervous system and peripheral tissues, including the intestine, has proven to be integral to disease pathogenesis (Schwiertz et al. 2018; Mulak et al. 2019; Chen et al. 2018; Lin et al. 2019). Therefore, in using *C. elegans* as a model of PD we fail to capture otherwise recognized components of PD pathophysiology, necessitating the use of more physiologically complex organisms, like murine models, to validate findings made in *C. elegans.* However, it is important to note that *C. elegans* models of PD broadly and alpha-synuclein transgenic animals specifically, have yielded

results predictive of and translatable to mammalian systems (Gaeta, Caldwell, and Caldwell 2019; Ma et al. 2022). Similarly, in the context of using *C. elegans* as a gnotobiotic model to study the effects of anaerobic human gut commensals, the characterization of live obligate anaerobe-host interaction extends beyond the scope of what is feasible, necessitating the use of alternative model organisms.

Human LRRK2 and the *C. elegans* ortholog LRK-1 share substantial conservation of domain organization and structure as well as conservation of many key residues mutated in *LRRK2* PD. Both LRK-1 and LRRK2 contain leucine-rich repeats, a Roc domain, a COR domain, a serine threonine kinase domain, and WD40 repeats (Saha et al. 2009; Sämann et al. 2009). The extent of functional conservation between LRK-1 and LRRK2 is broadly unknown; however, some studies have identified that LRRK2 expression is able to complement *lrk-1* mutant phenotypes related to axonal termination, lysosomal regulation (Kuwahara et al. 2016) and vesicular trafficking (Sakaguchi-Nakashima et al. 2007; Choudhary et al. 2017). In *C. elegans lrk-1* is expressed in various body regions, including the pharynx, head and tail neurons, the distal tip cells, vulval epithelium, and the canal-associated neurons (Sämann et al. 2009). Therefore, the expression pattern of *lrk-1,* specifically expression in the head neurons, allows for potential interaction or synergy of the pathogenic human protein and LRK-1 in our model. Interestingly, a study found that loss of endogenous LRK-1, via *lrk-1(km41),* reduced dopaminergic neurodegeneration induced by overexpression of pathogenic *LRRK2(G2019S)* through adulthood (Yao et al. 2010). Additionally, the same study found that both *lrk-1(km41)* and *lrk-1(km17)* null alleles suppressed the impaired basal slowing

response caused by overexpression of *LRRK2(G2019S)* in dopaminergic neurons, suggesting that LRK-1 contributes to the *LRRK2(G2019S)* mediate neurotoxicity (Yao et al. 2010). Alternatively, given that the *LRRK2(G2019S)* is a toxic gain of function mutation, the loss of *lrk-1* resulting in reduced pathogenic phenotypes may be attributed to a decreased overall dose of active protein. Despite this, limited consideration was given in our study for the potential interplay between human LRRK2 and the *C. elegans* ortholog LRK-1. Future work could be done using the SGC102 strain (Yao et al. 2010), (*lrk-1(km41); lin-15(n765ts)*; *cwrIs722*[*Pdat-1::GFP, Pdat-1::LRRK2(G2019S), lin-15(+)*], expressing pathogenic G2019S human *LRRK2* in a *lrk-1(km41)* mutant background to isolate the microbial impacts on LRRK(G2019S) mediated neurodegeneration in the absence of its neurotoxic synergy with endogenous LRK-1.

Our work primarily focused on characterizing the role of aspartic cathepsins and autophagy in the neuroprotective phenotype; however, exploration of other gene expression changes identified in the RNA sequencing experiments could more clearly define the host response to the microbiota. In the context of the differentially regulated small RNAs, we identified two miRNAs *mir-38* and *mir-51,* as potential candidates for characterization. Currently, strains VC514 and MT14450, available through the Caenorhabditis Genetics Centre (CGC), carry deletions affecting *mir-38* and *mir-51,* respectively. These deletions also affect the expression of additional miRNAs; however, crossing these alleles into the *LRRK2* transgenic background may act as a preliminary and relatively straightforward mechanism for determining the implications of these miRNAs in neuronal health and the neuroprotective phenotype. Additionally, we could observe the

impacts of F29B9.8 knockdown to determine its impacts on neuronal health in *LRRK2* transgenic animals, potentially linking changes in miRNA expression to the expression of protein-coding genes. In the context of the other differentially regulated protein-coding genes, we could conduct an RNAi screen focusing on genes from categories enriched for among the up and down-regulated mRNA to further characterize environmentally responsive host pathways implicated in neuronal health in *LRRK2* transgenic animals.

Identification of the localized intestinal expression of *asp-1* and *asp-8 opens* avenues for further exploration of the cell non-autonomous mechanism underlying the role of these proteins in neuronal health in the context of *LRRK2* transgenic animals. In our study, we identified the ability of *A. viscosus* exposure to improve *LRRK2* mediated autophagic deficits in neurons; however, we did not monitor autophagy in other tissues. A previous study established that in a rotenone-induced model of dopaminergic neurodegeneration, enhancing intestinal autophagy was required for the neuroprotective effects of intestinal activation of the p30 MAPK (PMK-1)/ATF-7 pathway (Chikka et al. 2016). Therefore, monitoring the effects of the neuroprotective bacteria on intestinal autophagy may begin to provide insight into the link between intestinal cells and neurodegeneration. In addition to generating transgenic animals overexpressing aspartic cathepsins pan-neuronally using our developed expression vectors, we can also determine the impacts of intestinal overexpression of aspartic cathepsins on neuronal health. Additionally, identification of the expression patterns of the other differentially regulated aspartic cathepsins would allow us to get a more complete picture of how this class of protease impacts neuronal health in our model.

Our study primarily focused on characterizing host mechanisms implicated in the *A. viscosus* mediated neuroprotection; however, we can also investigate bacterial factors contributing to the neuroprotective phenotype. The production and testing of crude bacterial extracts for protective effects in *LRRK2* transgenic animals may allow us to identify if our phenotype is mediated by a stable bioactive molecule produced by *A. viscosus.* Additionally, identification of species closely related by *A. viscosus* unable to induce neuroprotection may allow for the comparison of bacteria genomes to determine bacteria genes and pathways required for the neuroprotective phenotype. Over the course of our screen, we identified three *Actinomyces* species able to induce neuroprotection. Additionally, phylogenetic analysis determined that *Tidjanibacter massiliensis,* another strain in our library, is evolutionarily close to *Actinomyces. Tidjanibacter massiliensis* was not significantly neuroprotective in the initial screen, making it a potential candidate for comparison with *Actinomyces* to determine bacteria processes underlying the effect of the neuroprotective bacteria.

Overall significance and implications

The population of North America is aging. Projections show that by the year 2050, approximately one-third of the population will be over 60 years of age (United Nations 2019). Thus, age-related disorders like PD present a growing personal and financial burden for Canadians and the healthcare system. Currently treatment options for PD focus on symptom management and do not cure nor slow disease course. Over the last decade, the importance of the microbiome in human health and disease has become increasingly evident with emerging research identifying links between PD progression and

pathogenesis and alterations in composition and activity of the microbiota (T. Shen et al. 2021; Toh et al. 2022); however, the health impact of individual human gut commensals has been largely unexplored. Using our developed protocol, we identified novel human gut commensal bacteria able to influence disease pathogenesis in *LRRK2* transgenic animals. Additionally, we were able to begin characterizing environmentally responsive host genes implicated in neuronal health in the context of a neurodegenerative model. Our work, even in a small way, has contributed to an enhanced comprehension of how the host environment impacts host genetics and the neurodegenerative process. Furthermore, these analyses may aid in pinpointing more effective intervention targets for the development of treatments for PD and may allow for the identification of novel disease-altering bacterial-derived therapeutics targeting aspects of PD pathogenesis.

References

Arumugam, Manimozhiyan, Jeroen Raes, Eric Pelletier, Denis Le Paslier, Takuji Yamada, Daniel R. Mende, Gabriel R. Fernandes, et al. 2011. "Enterotypes of the Human Gut Microbiome." *Nature* 473 (7346): 174–80.

Asikainen, Suvi, Martina Rudgalvyte, Liisa Heikkinen, Kristiina Louhiranta, Merja Lakso, Garry Wong, and Richard Nass. 2010. "Global microRNA Expression Profiling of Caenorhabditis Elegans Parkinson's Disease Models." *Journal of Molecular Neuroscience: MN* 41 (1): 210–18.

Chen, Xi, Yang Hu, Zongze Cao, Qingshan Liu, and Yong Cheng. 2018. "Cerebrospinal Fluid Inflammatory Cytokine Aberrations in Alzheimer's Disease, Parkinson's Disease and Amyotrophic Lateral Sclerosis: A Systematic Review and Meta-Analysis." *Frontiers in Immunology* 9 (September): 2122.

Chikka, Madhusudana Rao, Charumathi Anbalagan, Katherine Dvorak, Kyle Dombeck, and Veena Prahlad. 2016. "The Mitochondria-Regulated Immune Pathway Activated in the C. Elegans Intestine Is Neuroprotective." *Cell Reports* 16 (9): 2399–2414.

Choudhary, Bikash, Madhushree Kamak, Neena Ratnakaran, Jitendra Kumar, Anjali Awasthi, Chun Li, Ken Nguyen, Kunihiro Matsumoto, Naoki Hisamoto, and Sandhya P. Koushika. 2017. "UNC-16/JIP3 Regulates Early Events in Synaptic Vesicle Protein Trafficking via LRK-1/LRRK2 and AP Complexes." *PLoS Genetics* 13 (11): e1007100.

Gaeta, Anthony L., Kim A. Caldwell, and Guy A. Caldwell. 2019. "Found in Translation: The Utility of C. Elegans Alpha-Synuclein Models of Parkinson's Disease." *Brain Sciences* 9 (4). https://doi.org/10.3390/brainsci9040073.

Goya, María Eugenia, Feng Xue, Cristina Sampedro-Torres-Quevedo, Sofia Arnaouteli, Lourdes Riquelme-Dominguez, Andrés Romanowski, Jack Brydon, Kathryn L. Ball, Nicola R. Stanley-Wall, and Maria Doitsidou. 2020. "Probiotic Bacillus Subtilis Protects against α-Synuclein Aggregation in C. Elegans." *Cell Reports* 30 (2): 367–80.e7.

Houthoofd, Koen, Bart P. Braeckman, Thomas E. Johnson, and Jacques R. Vanfleteren. 2003. "Life Extension via Dietary Restriction Is Independent of the Ins/IGF-1 Signalling Pathway in Caenorhabditis Elegans." *Experimental Gerontology* 38 (9): 947–54.

Houthoofd, Koen, Bart P. Braeckman, Isabelle Lenaerts, Kristel Brys, Annemie De Vreese, Sylvie Van Eygen, and Jacques R. Vanfleteren. 2002. "No Reduction of

Metabolic Rate in Food Restricted Caenorhabditis Elegans." *Experimental Gerontology* 37 (12): 1359–69.

Jadiya, Pooja, Manavi Chatterjee, Shreesh Raj Sammi, Supinder Kaur, Gautam Palit, and Aamir Nazir. 2011. "Sir-2.1 Modulates 'Calorie-Restriction-Mediated' Prevention of Neurodegeneration in Caenorhabditis Elegans: Implications for Parkinson's Disease." *Biochemical and Biophysical Research Communications* 413 (2): 306–10.

King, Charles H., Hiral Desai, Allison C. Sylvetsky, Jonathan LoTempio, Shant Ayanyan, Jill Carrie, Keith A. Crandall, et al. 2019. "Baseline Human Gut Microbiota Profile in Healthy People and Standard Reporting Template." *PloS One* 14 (9): e0206484.

Kuwahara, Tomoki, Keiichi Inoue, Vivette D. D'Agati, Tetta Fujimoto, Tomoya Eguchi, Shamol Saha, Benjamin Wolozin, Takeshi Iwatsubo, and Asa Abeliovich. 2016. "LRRK2 and RAB7L1 Coordinately Regulate Axonal Morphology and Lysosome Integrity in Diverse Cellular Contexts." *Scientific Reports* 6 (July): 29945.

Lin, Chin-Hsien, Chieh-Chang Chen, Han-Lin Chiang, Jyh-Ming Liou, Chih-Min Chang, Tzu-Pin Lu, Eric Y. Chuang, et al. 2019. "Altered Gut Microbiota and Inflammatory Cytokine Responses in Patients with Parkinson's Disease." *Journal of Neuroinflammation* 16 (1): 129.

Ma, Liang, Xi Li, Chengyu Liu, Wanyao Yan, Jinlu Ma, Robert B. Petersen, Anlin Peng, and Kun Huang. 2022. "Modelling Parkinson's Disease in C. Elegans: Strengths and Limitations." *Current Pharmaceutical Design* 28 (37): 3033–48.

Migliore, Lucia, and Fabio Coppedè. 2009. "Genetics, Environmental Factors and the Emerging Role of Epigenetics in Neurodegenerative Diseases." *Mutation Research* 667 (1-2): 82–97.

Mulak, Agata, Magdalena Koszewicz, Magdalena Panek-Jeziorna, Ewa Koziorowska-Gawron, and Sławomir Budrewicz. 2019. "Fecal Calprotectin as a Marker of the Gut Immune System Activation Is Elevated in Parkinson's Disease." *Frontiers in Neuroscience* 13 (September): 992.

Qiao, Liyan, Shusei Hamamichi, Kim A. Caldwell, Guy A. Caldwell, Talene A. Yacoubian, Scott Wilson, Zuo-Lei Xie, et al. 2008. "Lysosomal Enzyme Cathepsin D Protects against Alpha-Synuclein Aggregation and Toxicity." *Molecular Brain* 1 (November): 17.

Saftig, Paul, and Judith Klumperman. 2009. "Lysosome Biogenesis and Lysosomal Membrane Proteins: Trafficking Meets Function." *Nature Reviews. Molecular Cell Biology* 10 (9): 623–35.

Saha, Shamol, Maria D. Guillily, Andrew Ferree, Joel Lanceta, Diane Chan, Joy Ghosh, Cindy H. Hsu, et al. 2009. "LRRK2 Modulates Vulnerability to Mitochondrial Dysfunction in Caenorhabditis Elegans." *The Journal of Neuroscience: The Official Journal of the Society for Neuroscience* 29 (29): 9210–18.

Sakaguchi-Nakashima, Aisa, James Y. Meir, Yishi Jin, Kunihiro Matsumoto, and Naoki Hisamoto. 2007. "LRK-1, a C. Elegans PARK8-Related Kinase, Regulates Axonal-Dendritic Polarity of SV Proteins." *Current Biology: CB* 17 (7): 592–98.

Sämann, Julia, Jan Hegermann, Erika von Gromoff, Stefan Eimer, Ralf Baumeister, and Enrico Schmidt. 2009. "Caenorhabditits Elegans LRK-1 and PINK-1 Act Antagonistically in Stress Response and Neurite Outgrowth." *The Journal of Biological Chemistry* 284 (24): 16482–91.

Schröder, Bernd A., Christian Wrocklage, Andrej Hasilik, and Paul Saftig. 2010. "The Proteome of Lysosomes." *Proteomics* 10 (22): 4053–76.

Schwiertz, Andreas, Jörg Spiegel, Ulrich Dillmann, David Grundmann, Jan Bürmann, Klaus Faßbender, Karl-Herbert Schäfer, and Marcus M. Unger. 2018. "Fecal Markers of Intestinal Inflammation and Intestinal Permeability Are Elevated in Parkinson's Disease." *Parkinsonism & Related Disorders* 50 (May): 104–7.

Seidel, Hannah S., and Judith Kimble. 2011. "The Oogenic Germline Starvation Response in C. Elegans." *PloS One* 6 (12): e28074.

Shen, Linjing, Changliang Wang, Liang Chen, and Garry Wong. 2021. "Dysregulation of MicroRNAs and PIWI-Interacting RNAs in a Caenorhabditis Elegans Parkinson's Disease Model Overexpressing Human α-Synuclein and Influence of Tdp-1." *Frontiers in Neuroscience* 15 (March): 600462.

Shen, Ting, Yumei Yue, Tingting He, Cong Huang, Boyi Qu, Wen Lv, and Hsin-Yi Lai. 2021. "The Association Between the Gut Microbiota and Parkinson's Disease, a Meta-Analysis." *Frontiers in Aging Neuroscience* 13 (February): 636545.

Tan, Eng-King, Yin-Xia Chao, Andrew West, Ling-Ling Chan, Werner Poewe, and Joseph Jankovic. 2020. "Parkinson Disease and the Immune System — Associations, Mechanisms and Therapeutics." *Nature Reviews. Neurology* 16 (6): 303–18.

Tcherepanova, I., L. Bhattacharyya, C. S. Rubin, and J. H. Freedman. 2000. "Aspartic Proteases from the Nematode Caenorhabditis Elegans. Structural Organization and Developmental and Cell-Specific Expression of Asp-1." *The Journal of Biological Chemistry* 275 (34): 26359–69.

Toh, Tzi Shin, Chun Wie Chong, Shen-Yang Lim, Jeff Bowman, Mihai Cirstea, Chin-Hsien Lin, Chieh-Chang Chen, Silke Appel-Cresswell, B. Brett Finlay, and Ai Huey

Tan. 2022. “Gut Microbiome in Parkinson’s Disease: New Insights from Meta-Analysis.” *Parkinsonism & Related Disorders* 94 (January): 1–9.

Troemel, Emily R., Stephanie W. Chu, Valerie Reinke, Siu Sylvia Lee, Frederick M. Ausubel, and Dennis H. Kim. 2006. “p38 MAPK Regulates Expression of Immune Response Genes and Contributes to Longevity in C. Elegans.” *PLoS Genetics* 2 (11): e183.

United Nations. 2019. *World Population Ageing 2017 Highlights*. UN.

Vanfleteren, Jacques R., and Bart P. Braeckman. 1999. “Mechanisms of Life Span Determination in Caenorhabditis Elegans☆.” *Neurobiology of Aging* 20 (5): 487–502.

Vozdek, Roman, Peter P. Pramstaller, and Andrew A. Hicks. 2022. “Functional Screening of Parkinson’s Disease Susceptibility Genes to Identify Novel Modulators of α-Synuclein Neurotoxicity in Caenorhabditis Elegans.” *Frontiers in Aging Neuroscience* 14 (April): 806000.

Yao, Chen, Rabih El Khoury, Wen Wang, Tara A. Byrd, Elizabeth A. Pehek, Colin Thacker, Xiongwei Zhu, Mark A. Smith, Amy L. Wilson-Delfosse, and Shu G. Chen. 2010. “LRRK2-Mediated Neurodegeneration and Dysfunction of Dopaminergic Neurons in a Caenorhabditis Elegans Model of Parkinson’s Disease.” *Neurobiology of Disease* 40 (1): 73–81.